Reliability Assessment of Steel Structural Elements in Wind Excited Buildings

J.S. van Hulst

Delft University of Technology

TU Delft

Reliability Assessment

Steel Structural Elements in Wind Excited Buildings

by

J.S. van Hulst

to obtain the degree of

Master of Science
in Civil Engineering
Specialization Steel, Timber and Composite Structures

at the Delft University of Technology,
to be defended publicly on Thursday July 22, 2021 at 9:00 AM.

Student number:	4474392	
Project duration:	November 12, 2020 – July 22, 2021	
Thesis committee:	Prof. dr. M. Veljkovic,	TU Delft, chairman
	Dr. F. Kavoura,	TU Delft
	Prof. dr. ir. M.A.N. Hendriks,	TU Delft
	Prof. dr. ir. R.D.J.M. Steenbergen,	TNO, UGent
	ir. L.C. la Gasse,	TNO

An electronic version of this thesis is available at `http://repository.tudelft.nl/`.

TU Delft

TNO innovation for life

Preface

Dear reader,

This thesis is written as a final work for the degree of Master of Science in *Civil Engineering* for the master track of *Structural Engineering* and specialisation *Steel, Timber and Composite Structures* at the Delft University of Technology. This research into the *Reliability Assessment of Steel Structural Elements in Wind Excited Buildings* is realised in cooperation with the Netherlands Organisation for Applied Scientific Research, TNO.

First, I would like to thank the chairman of my graduation committee, Milan Veljkovic, for his close involvement, enthusiasm and very helpful feedback. His knowledge in the field of steel structures has certainly lifted this study to a higher level. Next, I would like to thank my daily supervisor, Liesette la Gasse, for her very good guidance throughout the whole project. Despite the fact that I had to work completely from home because of the covid situation, I have always found the weekly zoom-meetings very positive and they have certainly led to this final result. Next, I would like to thank the person who actually got me into this subject, Raphaël Steenbergen. A lecture by Raphaël during the course *Probabilistic Design and Risk Management* sparked the idea in me to research something in this field for my Master Thesis. After all, this forms a perfect overlap between my interests in mathematics, statistics and engineering. Next, I would like to thank Florentia Kavoura for her reflections on this study. Furthermore, I would like to thank Max Hendriks for his enthusiasm and guidance during the research. Finally, I would like to thank my colleagues at TNO for their support and interest in my research.

This research is certainly one of my greatest achievements to date and would not have been possible without the wonderful support of my family and friends. In particular, I would like to thank Marit for her trust in me and support throughout the project. Your presence made the home work situation a lot more pleasant. Finally, I would like to express my appreciation to all the people who have contributed to this research over the past months, but also to the people I spent my entire student life with and have many great memories about. It has certainly shaped me into the person I am today.

”Doubt is the origin of wisdom” - René Descartes

J.S. van Hulst
Barendrecht, July 2021

Abstract

One of the basic principles of the design of structures is that they must be sufficiently safe and meet the required reliability requirements. In Eurocode NEN-EN 1990 specific minimum reliability index β values are defined, which depend on a certain reference period and reliability class. In this study, a standard design situation[1] with a minimum reliability index of $\beta = 3.8$ is assumed. To ensure that the structures meet the reliability requirements, partial factors are applied in the Eurocode. The aim is to steer the design to the minimum reliability requirements in a relatively simple way without a complete reliability assessment. Since such a reliability assessment is much more complex and requires more time and knowledge of the engineer. This research investigates how the reliability of a steel main bearing structure in a wind excited building can be determined, taking into account all uncertainties on both the resistance and load side. A new method is developed in which wind tunnel measurements, wind speed models and a finite element model of the building can be directly linked. This is an improvement on recent studies. With this method it is possible to determine the load effects of the wind in specific elements of the building. This can then be used to determine the reliability of the steel main bearing structure in a wind excited building.

First of all, all probabilistic models concerning the resistance side of the reliability assessment are identified by means of an extensive literature study. In this way all material properties and uncertainties are included in the reliability assessment. In addition, wind speed models from the study by la Gasse [23], boundary layer wind tunnel pressure measurements and a FEM of the case study building are used. A wind load effect model quantifies the forces that occur in the structure due to the given wind load (based on the wind tunnel research) on the structure. This wind load effect model consists of several deterministic (ρ_{air}, A_{ref}, h) and stochastic parameters as input; think of basic wind velocity v_{pot} and associated sampling uncertainties S_v, terrain roughness factor $c_r(h_{ref})$, model uncertainty χ_{model} and finally the peak load effects $\hat{C}_X$ and associated sampling uncertainties $S_{\hat{C}_X}$. All these data and models are linked to each other to determine the peak load effects $\hat{C}_X$ and associated sampling uncertainties $S_{\hat{C}_X}$ in various elements of the case study building.

To further use the wind load effects in the reliability assessment, extreme value theory must be applied to determine the extreme value distributions of these peak load effects. It should be taken into account that the extremes extracted from the data are independent and identically distributed. This study has shown that the application of the block method, in combination with the use of the autocorrelation and reversed univariate method - to determine the correct block duration - works very well. A generalized extreme value distribution without the application of a certain threshold value will result in a non-conservative tail of the distribution. Note that this tail is the most important part of the whole distribution and must therefore be described well. In almost all cases, the extremes in the tail are best described by a Gumbel distribution. This distribution is characterised by the straight tail (shape parameter $\xi = 0$) and, in combination with the addition of a certain threshold value, it is the best way to describe the data including the tail. The decision of a good threshold value can be based on a visual approach of the Quantile-Quantile plot (quantiles of the data vs quantiles of the fit). To keep the effects of sampling uncertainties as low as possible, it is recommended to use as large a data set as possible. To quantify the sampling uncertainties, the bootstrap method is used in combination with the variation of the Cook-Mayne fractile. It is clearly visible that when a smaller block duration t can be used and thus more extreme values remain for fitting, the sampling uncertainties become smaller. In addition, the choice of threshold value also influences the size of the sampling uncertainties; with a higher threshold value, the uncertainty will also increase. A good balance must be achieved between describing the data well with a correct threshold value and not making the threshold value too high in order to reduce

---

[1] Consequence class 2 (medium consequences: e.g. residential and office buildings), ultimate limit state design and a reference period of 50 years

the sampling uncertainties.

To demonstrate that the method works, it is applied to a case study building. This case study building is initially designed in a deterministic Eurocode manner. Next, the reliability of a number of elements of the steel main bearing structure is extensively determined. For this particular case study building, it is evident that the design can be further optimised compared to the Eurocode design. For most elements, the reliability is higher than minimum required. In the reliability assessment of the steel bracing (most wind-loaded element) of the building it appears that the wind speed variable v_{pot} has the most influence on the reliability. It is interesting to note that the reliability is lower (conservative) if v_{pot} is described with a type I GEV (Gumbell). It is also noticeable that the roughness factor $c_r(h_{ref})$ in the Eurocode design is a lot higher. Finally, in this particular case study building, it is noticeable that elements dominated by permanent and variable load, G and Q respectively, have a higher design value in the Eurocode. The partial factors $\gamma_G = 1.35$ and $\gamma_Q = 1.5$ are in that case too high. These conclusions relate only to this specific case study building; further research into other buildings with different characteristics and typologies is certainly recommended. In conclusion, this method shows that the possibilities in the field of a reliability-based design are certainly worthwhile for the further optimisation of a structure. And the use of this new method in which all data and models can be linked makes the application of a reliability-based design a lot more efficient, more accurate and therefore more interesting.

Contents

List of Figures xi

List of Tables xvii

List of Symbols xix

1 Introduction 1
- 1.1 Problem description 1
- 1.2 Research question 2
- 1.3 Scope of this research 2
- 1.4 Outline of this report 3

I Literature Review 5

2 Structural Reliability 7
- 2.1 Fundamental theory on structural reliability 7
  - 2.1.1 General 7
  - 2.1.2 Level III methods: Numerical 9
  - 2.1.3 Level II methods: Approximation 10
  - 2.1.4 Level I methods: Semi-probabilistic design 11
  - 2.1.5 Discussion on the different methods 11
- 2.2 Approach in the Eurocodes 12

3 Wind Engineering Fundamentals 15
- 3.1 Basics wind 15
- 3.2 Wind loading chain 16
  - 3.2.1 Wind climate v_b 16
  - 3.2.2 Influence of terrain c_e 17
  - 3.2.3 Aerodynamic coefficients c_f 18
- 3.3 Wind loading approach in the Eurocode 19
  - 3.3.1 Wind climate 19
  - 3.3.2 Influence of terrain 21
  - 3.3.3 Aerodynamic coefficients 22
  - 3.3.4 Dynamic effects 22
- 3.4 Probabilistic modelling of wind loading 23
  - 3.4.1 Cook and Mayne method 25
  - 3.4.2 Davenport's method 26
  - 3.4.3 JCSS Probabilistic Model Code method on wind loads 27
  - 3.4.4 Recent assessment methods 28
  - 3.4.5 Discussion 29

4 Probabilistic Modelling of Extremes 31
- 4.1 Specification sample data 31
- 4.2 Theory on extreme values 32
  - 4.2.1 Univariate theorem 32
  - 4.2.2 Generalised extreme value distribution 32
  - 4.2.3 Methods for estimating high probability quantiles 33

5 Probabilistic Structural Resistance Model 37
- 5.1 Material properties steel 37
- 5.2 Dimensional properties 38
- 5.3 Initial imperfections element 38
  - 5.3.1 Sensitivity analysis of the initial imperfections on a steel element 39

5.4 Model uncertainties . . . 40
5.5 Existing research on reliability analysis steel buildings . . . 42
5.5.1 'Proqua' strategy: example steel office building . . . 42
5.5.2 Discussion on existing research . . . 46

II Method Development 47

6 Methodology of this study 49
6.1 Method overview of recent and current study . . . 49
6.2 Stochastic wind load model . . . 49
6.3 Method overview of the reliability assessment procedure . . . 50

7 Probabilistic Wind Pressure Model 53
7.1 Observations from the wind tunnel data and literature . . . 53
7.2 Formulation of the probabilistic wind pressure model . . . 56
7.3 Remark on fully uncorrelated zones . . . 58

8 Technique for Obtaining Load Effects 61
8.1 Pre-processing measurements wind tunnel test . . . 61
8.2 Finite Element Model . . . 62
8.2.1 FEM Program . . . 62
8.2.2 Details Case Study Building Model . . . 62
8.2.3 Load effects . . . 63
8.3 Probabilistic modelling of extremes load effects . . . 63
8.3.1 Block duration t . . . 64
8.3.2 Fit data to certain distribution . . . 67
8.3.3 Sampling uncertainties . . . 69

9 Reliability Assessment Procedure 73
9.1 Generic assessment procedure . . . 73
9.2 Resistance . . . 74
9.2.1 External beams level 1 and 2 (S18 & S42) . . . 74
9.2.2 Steel bracing (S65) . . . 75
9.2.3 Internal column (S13) . . . 75
9.2.4 External column (S2) . . . 76
9.2.5 Corner column (S1) . . . 78
9.3 Wind loading effect model . . . 80

III Reliability Assessment of the Case Study Building 83

10 Case Study Description 85
10.1 Case study building . . . 85
10.2 Wind tunnel data . . . 87

11 Description Load Effects 89
11.1 Example: Steel bracing (S65) . . . 89
11.1.1 $E_{wind,N}$ . . . 89
11.2 Load effects used in reliability assessment . . . 90
11.3 Comparison load effects time series vs probabilistic wind pressure model . . . 92

12 Reliability Assessment 95
12.1 General information . . . 95
12.2 Reliability assessment steel structural elements . . . 96
12.2.1 External beam level 2 (S42) . . . 98
12.2.2 External beam level 1 (S18) . . . 99
12.2.3 Steel bracing (S65) . . . 100
12.2.4 Internal column (S13) . . . 102
12.2.5 External column (S2) . . . 103
12.2.6 Corner column (S1) . . . 104
12.3 Conclusions . . . 105

13 Discussion 107
13.1 Developed method 107
13.2 Determination load effects 108
13.3 Reliability assessment 108

IV Conclusions and Recommendations 111

Bibliography 119

A Deterministic Design Case Study Building according to the Eurocode 121
A.1 Actions on the building 121
A.1.1 Permanent actions 121
A.1.2 Imposed loads 121
A.1.3 Wind loads 121
A.1.4 Load combinations 125
A.2 Design of the structural elements 128
A.2.1 External beam level 2 128
A.2.2 Internal beam level 2 131
A.2.3 External beam level 1 133
A.2.4 Internal beam level 1 135
A.2.5 Steel bracing 136
A.2.6 Internal column 138
A.2.7 External column 140
A.2.8 Corner column 144
A.2.9 Frame stability 146
A.3 Overview chosen structural elements 147

B Explanation on Coupling SCIA FEM with Python using SCIA OpenAPI 149

C Finite Element Model Case Study Building Figures - Designation of Various Elements 157

D Resistance Model Uncertainties 163

E Tolerances on construction building - NEN-EN 1090-2 [12] 175

F Assessment Procedure: la Gasse and Meinen 183

G Extra Figures - Description Load Effects 185
G.1 External beam level 2 (S42) 185
G.1.1 $E_{wind,M}$ 185
G.2 External beam level 1 (S18) 187
G.2.1 $E_{wind,M}$ 187
G.3 Steel bracing (S65) 189
G.3.1 $E_{wind,N}$ 189
G.4 Internal column (S13) 190
G.4.1 $E_{wind,N}$ 190
G.5 External column (S2) 194
G.5.1 $E_{wind,N}$ 194
G.5.2 $E_{wind,M}$ 195
G.6 Corner column (S1) 196
G.6.1 $E_{wind,N}$ 196
G.6.2 $E_{wind,My}$ 200
G.6.3 $E_{wind,Mz}$ 202

H Analysis Wind Pressures from Wind Tunnel Test - For Making Probabilistic Wind Pressure Model 205

I Reliability Assessment - Additional Input Parameters 207

J Resistance to Combination of Bending Moment and Axial Force 211

List of Figures

2.1 Joint probability density functions . . . 8
2.2 Example of Monte-Carlo simulation . . . 10
2.3 Representative values of variable actions . . . 14

3.1 Fluctuations in wind speed . . . 15
3.2 Spectrum of horizontal wind speed, based on analysis of van der Hoven [8] . . . 16
3.3 Wind loading chain by Davenport . . . 16
3.4 Atmospheric Boundary Layer (ABL) [16] . . . 17
3.5 Vector notation wind-speed components . . . 18
3.6 Action model for wind loads in EN1991-1-4 (Meinen, 2015) . . . 19
3.7 Wind zones in the Netherlands [6] . . . 20
3.8 Wind zones for vertical walls [6] . . . 23
3.9 Reference height z_e depending on h and b, and corresponding velocity pressure profile [6] 24
3.10 Joint PDF yearly extreme wind speeds and hourly extreme pressure coefficients [25] . . 25
3.11 1st and 2nd order joint PDF [25] . . . 26
3.12 Stochastic parameters from Davenport's wind loading chain [9] . . . 27

4.1 Skewness of a certain distribution; on the left a positive skew and on the right a negative skew . . . 32
4.2 The three different distributions; type I (Gumbel), type II (Frèchet) and type III (Reversed Weibull) in both the PDF in normal domain (left) and CDF in the Gumbel domain (right) [25] . . . 33
4.3 Block method [25] . . . 33
4.4 Peak over threshold method [25] . . . 34

5.1 Three types of initial imperfections e, f and ϕ . . . 39
5.2 Frame 1 on the left (rotation and translation fixed boundary conditions) and Frame 2 on the right (rotation free and translation fixed boundary conditions) in study from Kala [20] 40
5.3 Initial sway and bow imperfections in study from Kala [20] . . . 40
5.4 . . . 41
5.5 Steel office building example; general geometry and steel grades of the steel frame [5] . 42
5.6 Conventional models of basic variables for time invariant reliability analyses [5] . . . 43
5.7 Statistical parameters (steel office building) for the FORM-calculation [5] . . . 44
5.8 Plastic calculation of the inner steel beam [5] . . . 44
5.9 Identification of the profile which yields appr. $\beta = 3.8$ for the beam of the inner frame [5] 45
5.10 Plastic calculation of the outer steel beam [5] . . . 45
5.11 Identification of the profile which yields appr. $\beta = 3.8$ for the external column on ground level [5] . . . 46
5.12 Identification of the profile which yields appr. $\beta = 3.8$ for the internal column on ground level [5] . . . 46

6.1 Method overview of the reliability assessment procedure in this study . . . 51

7.1 Pressure points from the wind tunnel test, the used pressure points for the case study building are highlighted in blue . . . 54
7.2 Tributary areas (including the number of the pressure tap) for the pressure taps of interest for the case study building . . . 55
7.3 Probability Density Functions (PDF) for the pressures in wind zone 1 to 7 (side A) . . . 56
7.4 Probability Density Functions (PDF) for the pressures in wind zone 90 to 96 (side B) . . 56

7.5 Probability Density Functions (PDF) for the pressures in wind zone 39 to 45 (side C) . . 56
7.6 Probability Density Functions (PDF) for the pressures in wind zone 128 to 134 (side D) 57
7.7 Probability Density Functions (PDF) for the pressures in wind zone 77 to 86 (Top, run 1) 57
7.8 Probability Density Functions (PDF) for the pressures in wind zone 166 to 175 (Top, run 2) 57
7.9 Covariance matrix of all wind pressure zones 59

8.1 Raw load effect data, as example for M_z beam 42: External beam level 2 $(n = 80.000)$. 64
8.2 Raw load effect data including blocks (for clarity very large block duration $t = 9.26$ minutes) in which maxima are selected, as example for M_z beam 42: External beam level 2 $(n = 80.000)$ 64
8.3 Autocorrelation example, other elements are in Annex Extra Figures - Description Load Effects 65
8.4 Reversed univariate method example for N beam 2; comparison between 10-minute extremes and the 1-second, 10-second and 20-second shifted extremes 66
8.5 Tail behaviour reversed univariate method example for N beam 2; comparison between 10-minute extremes and the 1-second, 10-second and 20-second shifted extremes . . . 67
8.6 Generalized extreme value fit example 68
8.7 Gumbel fit example 68
8.8 Gumbel including threshold value fit example, threshold 3.0 69
8.9 Gumbel including threshold value fit example, threshold 3.8 69
8.10 Q-Q plots; to illustrate the influence of the choice of the threshold value 70
8.11 Bootstrap using GEV distribution example 71
8.12 Bootstrap using Gumbel including threshold distribution example, threshold: 3.0 71
8.13 Bootstrap using Gumbel including threshold distribution example, threshold: 3.8 72
8.14 Bootstrap using Gumbel including threshold distribution example; threshold: 4.4 72

9.1 Plastic calculation of the beams 74

10.1 Case study building dimensions 86
10.2 Plan and side view of the case study building 87
10.3 3d model of the case study building 87

11.1 Autocorrelation and Reversed univariate method plots of N steel bracing (S65), in order to obtain the correct block duration t 90
11.2 Gumbel fit and Bootstrap (threshold value: 0.4) of N steel bracing (S65) ($20s$-extremes) 90
11.3 Gumbel fit and Bootstrap (threshold value: 0.8) of N steel bracing (S65) ($20s$-extremes) (probabilistic wind pressure model) 91
11.4 All raw load effect data for $n = 65,000$ timesteps 92

12.1 Sensitivity factors α^2 of the stochastic variables and β-values of the reliability assessment for external beam level 2 (S42) with IPE240 profile (deterministic Eurocode design). (A) v_{pot}: Type I GEV (Gumbel) and load effects based on timeseries, (B) v_{pot}: Type III GEV (Weibull) and load effects based on timeseries, (1) $\mu_{m_{bending}} = 1.1$, (2) $\mu_{m_{bending}} = 1.0$ 98
12.2 Sensitivity factors α^2 of the stochastic variables and β-values of the reliability assessment for external beam level 1 (S18) with IPE450 profile (deterministic Eurocode design). (A) v_{pot}: Type I GEV (Gumbel) and load effects based on timeseries, (B) v_{pot}: Type III GEV (Weibull) and load effects based on timeseries, (1) $\mu_{m_{bending}} = 1.1$, (2) $\mu_{m_{bending}} = 1.0$ 99
12.3 Sensitivity factors α^2 of the stochastic variables and β-values of the reliability assessment for steel bracing (S65) with steel rod $\phi = 45\ mm$ profile (deterministic Eurocode design). (A) v_{pot}: Type I GEV (Gumbel) and load effects based on timeseries, (B) v_{pot}: Type III GEV (Weibull) and load effects based on timeseries, (C) v_{pot}: Type I GEV (Gumbel) and load effects based on probabilistic wind pressure model, (D) v_{pot}: Type III GEV (Weibull) and load effects based on probabilistic wind pressure model 101

12.4 Sensitivity factors α^2 of the stochastic variables and β-values of the reliability assessment for internal column (S13) with HEA200 profile (deterministic Eurocode design). (A) v_{pot}: Type I GEV (Gumbel) and load effects based on timeseries, (B) v_{pot}: Type III GEV (Weibull) and load effects based on timeseries, (1) $\mu_{m_{buckling}} = 1.2$, (2) $\mu_{m_{buckling}} = 1.0$. 102
12.5 Sensitivity factors α^2 of the stochastic variables and β-values of the reliability assessment for external column (S2) with HEA220 profile (deterministic Eurocode design). (A) v_{pot}: Type I GEV (Gumbel) and load effects based on timeseries, (B) v_{pot}: Type III GEV (Weibull) and load effects based on timeseries, (1) $\mu_{m_{buckling}} = 1.2$ and $\mu_{m_{lat-buckling}} = 1.1755$, (2) $\mu_{m_{buckling}} = 1.0$ and $\mu_{m_{lat-buckling}} = 1.0$ . . . 103
12.6 Sensitivity factors α^2 of the stochastic variables and β-values of the reliability assessment for corner column (S1) with HEA220 profile (deterministic Eurocode design). (A) v_{pot}: Type I GEV (Gumbel) and load effects based on timeseries, (B) v_{pot}: Type III GEV (Weibull) and load effects based on timeseries, (1) $\mu_{m_{interaction}} = 1.3$, (2) $\mu_{m_{interaction}} = 1.0$ 104

A.1 Reference height z_e, depending on h and b, and corresponding velocity pressure profile [6] . . . 122
A.2 Wind pressure zones top view . . . 123
A.3 Wind pressure zones side view for $e \geq d$ [6] . . . 123
A.4 Wind pressure zones for flat roofs [6] . . . 124
A.5 Wind zones in The Netherlands (Dutch National Annex [6]) . . . 125
A.6 Pressure coefficients on walls, wind coming from D . . . 126
A.7 Pressure coefficients on roof, wind coming from the left . . . 126
A.8 Beam A-B on grid 1, level 2 . . . 128
A.9 Beam B-C on grid 1, level 2 . . . 130
A.10 Beam B-C on grid 2, level 2 . . . 131
A.11 Beam A-B on grid 2, level 2 . . . 133
A.12 External beams level 1 . . . 133
A.13 Internal beams level 1 . . . 135
A.14 Most severe wind pressures on building . . . 136
A.15 Axial force in bracing . . . 137
A.16 Internal column . . . 138
A.17 Internal column forces . . . 138
A.18 External column . . . 141
A.19 External column vertical force generates bending moment due to eccentric loading (moment arm) . . . 141
A.20 External column forces . . . 141
A.21 Corner column . . . 144
A.22 Corner column vertical force generates bending moment due to eccentric loading (moment arm) . . . 144
A.23 Corner column forces . . . 145
A.24 Total horizontal forces for the frame stability verification . . . 147
A.25 Displacements due to the total horizontal loads . . . 147

C.1 Render of the Case Study Building in the SCIA FEM . . . 157
C.2 Side view of the Case Study Building in the SCIA FEM, the green areas are the load panels on the building facade . . . 158
C.3 Side view 2 of the Case Study Building in the SCIA FEM, wind load is shown on the left of the building . . . 158
C.4 Top view of the Case Study Building in the SCIA FEM . . . 159
C.5 Element: S42, External Beam Level 2 . . . 159
C.6 Element: S18, External Beam Level 1 . . . 160
C.7 Element: S13, Internal Column . . . 160
C.8 Element: S2, External Column . . . 161
C.9 Element: S1, Corner Column . . . 161
C.10 Element: S65, Bracing . . . 162

F.1 Assessment procedure by la Gasse [23] . . . 183
F.2 Assessment procedure by Meinen [25] . . . 184

G.1 All the load effect data used for external beam level 2 (S42): M_y . . . 185
G.2 Gumbel fit and Bootstrap (threshold value: 0.0) of M_y external beam level 2 (S42) . . . 186
G.3 Autocorrelation and Reversed univariate method plots of M_y external beam level 2 (S42), in order to obtain the correct block duration t . . . 186
G.4 Gumbel fit and Bootstrap (threshold value: 0.0006) of M_y external beam level 2 (S42) ($20s$-extremes) . . . 186
G.5 All the load effect data used for external beam level 2 (S42): M_y (probabilistic wind pressure model) . . . 187
G.6 All the load effect data used for external beam level 1 (S18): M_y . . . 187
G.7 Autocorrelation and Reversed univariate method plots of M_y external beam level 1 (S18), in order to obtain the correct block duration t . . . 188
G.8 Gumbel fit and Bootstrap (threshold value: 0.002) of M_y external beam level 1 (S18) ($20s$-extremes) . . . 188
G.9 All the load effect data used for external beam level 1 (S18): M_y (probabilistic wind pressure model) . . . 188
G.10 All the load effect data used for steel bracing (S65): N . . . 189
G.11 Gumbel fit (threshold 0.0) and Q-Q plot (threshold value: 0.4) of N steel bracing (S65), in order to obtain the correct block duration t . . . 189
G.12 All the load effect data used for steel bracing (S65): N (probabilistic wind pressure model) 190
G.13 All the load effect data used for internal column (S13): N . . . 190
G.14 Gumbel fit (threshold 0.0 and 0.04) of N internal column (S13), in order to obtain the correct block duration t . . . 191
G.15 Q-Q plot (threshold 0.0 and 0.03) of N internal column (S13) . . . 191
G.16 Q-Q Plot (threshold value: 0.04) of N internal column (S13) . . . 191
G.17 Bootstrap (threshold value: 0.0 and 0.04) of N internal column (S13) . . . 192
G.18 Autocorrelation and Reversed univariate method plots of N internal column (S13), in order to obtain the correct block duration t . . . 192
G.19 Gumbel fit and Bootstrap (threshold value: 0.03) of N internal column (S13) ($20s$-extremes) 192
G.20 All the load effect data used for internal column (S13): N ($F = 100$) (probabilistic wind pressure model) . . . 193
G.21 All the load effect data used for external column (S2): N . . . 194
G.22 Autocorrelation and Reversed univariate method plots of N external column (S2), in order to obtain the correct block duration t . . . 194
G.23 Gumbel fit and Bootstrap (threshold value: 0.0) of N external column (S2) ($10s$-extremes) 195
G.24 All the load effect data used for external column (S2): N (probabilistic wind pressure model) . . . 195
G.25 All the load effect data used for external column (S2): M_y . . . 196
G.26 Autocorrelation and Reversed univariate method plots of M_y external column (S2), in order to obtain the correct block duration t . . . 196
G.27 Gumbel fit and Bootstrap (threshold value: 0.004) of M_y external column (S2) ($20s$-extremes) . . . 196
G.28 All the load effect data used for external column (S2): M_y (probabilistic wind pressure model) . . . 197
G.29 All the load effect data used for corner column (S1): N . . . 197
G.30 Gumbel fit (threshold value: 0.2) and Q-Q plot (threshold value: 0.15) of N corner column (S1) . . . 198
G.31 Q-Q plot and Bootstrap (threshold value: 0.2) of N corner column (S1) . . . 198
G.32 Autocorrelation and Reversed univariate method plots of N corner column (S1), in order to obtain the correct block duration t . . . 198
G.33 Gumbel fit and Bootstrap (threshold value: 0.15) of N corner column (S1) ($20s$-extremes) 199
G.34 All the load effect data used for corner column (S1): N (probabilistic wind pressure model) 199
G.35 All the load effect data used for corner column (S1): M_y . . . 200

G.36 Autocorrelation and Reversed univariate method plots of M_y corner column (S1), in order to obtain the correct block duration t . . . 200
G.37 Gumbel fit and Bootstrap (threshold value: 0.005) of M_y corner column (S1) ($10s$-extremes) 201
G.38 All the load effect data used for corner column (S1): M_y (probabilistic wind pressure model) 201
G.39 All the load effect data used for corner column (S1): M_z . . . 202
G.40 Autocorrelation and Reversed univariate method plots of M_z corner column (S1), in order to obtain the correct block duration t . . . 202
G.41 Gumbel fit and Bootstrap (threshold value: 0.003) of M_z corner column (S1) ($20s$-extremes) 203
G.42 All the load effect data used for corner column (S1): M_z (probabilistic wind pressure model) 203

J.1 Visual representation of combined bending moment and axial force on the cross-section 211

List of Tables

2.1 Standardised α values for structures according to the Eurocode 11
2.2 Definition of consequence classes for Standardization [15] 12
2.3 Recommended minimum values for the reliability index β (Ultimate Limit State) [15] . . 13

3.1 Values for κ and n for the different wind zones as input for the factor c_{prob} [6] 20
3.2 Values for the fundamental basic wind velocity $V_{b,0}$ for the different wind zones in the Netherlands [6] 21
3.3 Terrain categories and corresponding terrain parameters in Dutch National Annex [6] . . 21
3.4 Pressure coefficients according to the Dutch National Annex 23
3.5 Random variables occuring in the assessment of the wind loading [27] 28

4.1 Comparison between both methods; Block Method & Peak over Threshold Method [25] 35

5.1 Mean and standard deviation material properties structural steel (rolled sections) [5][28] 38
5.2 Correlation matrix material properties structural steel (rolled sections) [28] 38
5.3 Mean and standard deviation dimensional properties [5] 38
5.4 Mean and standard deviation initial imperfections element [28] 39
5.5 Load effect model uncertainties [28] 41
5.6 Resistance model uncertainties [28] 42

10.1 Wind tunnel data details [25] 88

11.1 Load effects results (based on time series of wind pressures), to be used in the reliability assessment 91
11.2 Load effects results (based on probabilistic model of wind pressures), to be used in the reliability assessment 92

12.1 Different types of reliability analyses, including indication for in the further analyses below in this chapter 96
12.2 Input variables, distribution types and associated parameters regarding load side of the reliability assessment of the case study building 97
12.3 Input variables, distribution types and associated parameters regarding resistance side of the reliability assessment of the case study building 98
12.4 Optimisation of profile for External beam level 2 (S42) based on reliability assessment including both probabilistic action and resistance models 99
12.5 Optimisation of profile for External beam level 1 (S18) based on reliability assessment including both probabilistic action and resistance models 100
12.6 Optimisation of profile for Steel bracing (S65) based on reliability assessment including both probabilistic action and resistance models 100
12.7 Design values (steel bracing) based on reliability assessments in comparison with design values based on deterministic Eurocode design 101
12.8 Optimisation of profile for Internal column (S13) based on reliability assessment including both probabilistic action and resistance models 102
12.9 Optimisation of profile for External column (S2) based on reliability assessment including both probabilistic action and resistance models 103
12.10 Optimisation of profile for Corner column (S1) based on reliability assessment including both probabilistic action and resistance models 104
12.11 Design values (corner column) based on reliability assessments in comparison with design values based on deterministic Eurocode design 105

A.1 External pressure coefficients for the facade and roof zones 123
A.2 Calculation of the peak velocity pressure $q_p(z)$ for all relevant heights z 126
A.3 Wind pressures kN/m^2 over height on facade (A - E) and roof (F - I) zones 127
A.4 Reduction factors ψ 127
A.5 Description, type and value of the loads 127
A.6 Forces in external column for bottom and top part 140
A.7 Forces in corner column for bottom and top part 145
A.8 Overview chosen structural elements and related unity checks 148

C.1 Designation of various elements - used in the further analysis - in the FEM 158

H.1 Analysis of wind pressures and associated distribution type, based on values of skewness and kurtosis 206

I.1 Input for the reliability analyses of External beam level 2 (S42) 207
I.2 Input for the reliability analyses of External beam level 1 (S18) 207
I.3 Input for the reliability analyses of Steel bracing (S65) 207
I.4 Input for the reliability analyses of Internal column (S13) 208
I.5 Input for the reliability analyses of External column (S2) 208
I.6 Input for the reliability analyses of Corner column (S1) 209

List of Symbols

List of Latin symbols

Symbol	Description	Unit
A	Area	m^2
A_{ref}	Reference area	m^2
c_d	Dynamic factor	-
c_{dir}	Directional factor	-
c_e	Terrain roughness correction factor	-
c_g	Gust correction factor	-
c_o	Orography factor	-
c_{pe}	External pressure coefficient	-
c_{pi}	Internal pressure coefficient	-
c_{prob}	Probability factor	-
c_r	Terrain roughness factor	-
c_s	Size factor	-
c_{season}	Seasonal factor	-
$\hat{C}_X$	Peak load effect coefficient (1-hour extremes)	-
e	Average eccentricity	m
E	Young’s modulus	N/m^2
E_d	Design value of effect of actions	-
f	Out of straightness	m
$f_S(x)$	Importance sampling probability distribution function	-
f_y	Yield strength steel	N/m^2
f_u	Ultimate tensile strength steel	N/m^2
F	Action	N
F_d	Design value of an action	N
F_k	Characteristic value of an action	N
F_{rep}	Representative value of an action	N
F_w	Resultant wind force	N
$F_{w,e}$	External wind force	N
$F_{w,i}$	Internal wind force	N
G	Permanent action	-
G_d	Design value of a permanent action	N
G_k	Characteristic value of a permanent action	N
h	Height of the building	m

Symbol	Description	Unit
I	Second moment of area	m^4
I_v	Turbulence intensity	-
k_r	Terrain factor	-
$m_{bending}$	Model uncertainty related to bending moment capacity	-
$m_{buckling}$	Model uncertainty related to column buckling	-
m_i	Model uncertainty related to live or imposed load	-
$m_{interaction}$	Model uncertainty related to interaction of bending and compression	-
$m_{lat-buckling}$	Model uncertainty related to lateral torsional buckling	-
N	Amount of simulations in a Monte Carlo analysis	-
N_f	Amount of failures in Monte Carlo analysis	-
P	Relevant representative value of a prestressing action	-
P_f	Probability of failure	-
$P_{reliable}$	Reliability of structure	-
q_p	Peak velocity pressure	N/m^2
Q	Variable action	-
Q_d	Design value of a variable action	N
Q_k	Characteristic value of a variable action	N
R	Basic variable resistance of structure in limit state function	-
R_d	Design value of the resistance	-
R_k	Characteristic value of the resistance	-
R_{xx}	Autocorrelation function	-
S	Basic variable solicitation (load) on structure in limit state function	-
$S_{\hat{C}_X}$	Sampling uncertainties of load effect model	-
S_v	Sampling uncertainties of basic wind velocity model	-
T_{ref}	Reference time	s
u_*	Shear velocity	m/s
U	Threshold value in peak over threshold method	-
v	Poisson's ratio	-
$\overline{v}$	Average wind speed	m/s
$\tilde{v}$	Turbulent component of the wind speed	m/s
$\overline{v}(z)$	Mean wind speed (in x-direction) at height z	m/s
$v_{b,0}$	Fundamental value of the basic wind velocity	m/s
v_m	Mean wind velocity	m/s
V	Coefficient of variation (COV)	-
W	Section modulus	m^3
w_e	External wind pressure	N/m^2
w_i	Internal wind pressure	N/m^2
X_d	Design value of a material property	-
X_k	Characteristic value of a material property	-
Z	Limit state function	-
z_e	Reference height	m
z_{min}	Minimum height	m
z_{max}	Maximum height	m
z_0	Roughness length	m

List of Greek symbols

Symbol	Description	Unit
α_i	Sensitivity factors	-
$\hat{\alpha}_X$	Unbiased sample skewness	-
β	Reliability index	-
χ_{model}	Model uncertainty factor	-
ϵ	Strain material	-
γ	Partial factor (safety or serviceability)	-
γ_f	Partial factor for actions, which takes account of the possibility of unfavourable deviations of the action values from the representative values	-
γ_F	Partial factor for actions, also accounting for model uncertainties and dimensional variations	-
γ_g	Partial factor for permanent actions, which takes account of the possibility of unfavourable deviations of the action values from the representative values	-
γ_G	Partial factor for permanent actions, also accounting for model uncertainties and dimensional variations	-
γ_m	Partial factor for a material property	-
γ_M	Partial factor for a material property, also accounting for model uncertainties and dimensional variations	-
γ_Q	Partial factor for variable actions, also accounting for model uncertainties and dimensional variations	-
κ	Von Karman constant = 0.4	-
λ_f	Frequency scale	-
λ_g	Geometric scale	-
λ_t	Time scale	-
λ_v	Wind speed scale	-
μ	Mean of basic variable	-
μ	Location parameter (GEV)	-
Φ	Standard normal distribution	-
ϕ	Out of plumbness	rad
ψ_0	Factor for combination value of a variable action	-
ψ_1	Factor for frequent value of a variable action	-
ψ_2	Factor for quasi-permanent value of a variable action	-
ρ_{air}	Air density	kg/m^3
σ	Standard deviation of basic variable	-
σ	Scale parameter (GEV)	-
σ_v	Standard deviation of the turbulence	m/s
ξ	Reduction factor	-
ξ	Shape parameter (GEV)	-

List of abbreviations

Symbol	Description
ABL	Atmospheric Boundary Layer
ECDF	Empirical Cumulative Distribution Function
FEM	Finite Element Model
FORM	First Order Reliability Method
GEV	Generalized Extreme Value
GRF	Gust Response Factor
MLE	Maximum Likelihood Estimator
SLS	Serviceability Limit State
ULS	Ultimate Limit State

1

Introduction

One of the key challenges of the current society is the exponential increase in urban population worldwide. The expectations are that in 2030, about 60 percent of the world population will be living in urban areas. And if the trend continues in that way, this percentage will reach 80 percent in 2050 [1]. In order to accommodate these large number of people, in cities which are limited to expand in horizontal direction, the only possible way is to go up. A direct consequence of this, is the increased demand for high-rise buildings. These high-rise buildings are subjected to severe wind forces and it is these wind forces that largely dominate the design of the structural system. In order to optimise the structural system, thorough understanding of the wind forces and the response on the structural system is necessary.

1.1. Problem description

The design of the structural system of high-rise buildings is influenced by wind-related aspects. These wind forces on the building have a stochastic character and lead to uncertainties in the description of the loads S. Also the structural resistance R is not fully deterministic and thus introduces uncertainties in the design. The safety of the structure must always be taken into account during this design process. In order to assess the safety of the structure, minimum reliability requirements are formulated as the minimum reliability index β in Eurocode NEN-EN 1990. These reliability levels - specified in the Eurocode - will make sure that the design and execution of the structure is able to withstand the applied loads on it during its intended working life, with a specified probability of structural failure. The reliability index β is a direct measure of the failure probability of the structure. The Eurocode deals with the uncertainties in the loading and resistance part by applying partial factors. This in itself does not say anything about the reliability, but it does guide the design towards certain minimum requirements. This is a faster and easier – and thus practical – approach to assess the structural reliability, however, research by Meinen [25] and la Gasse [23] shows that it is unclear if the approach guarantees sufficient reliability levels for wind loaded structures.

This research focuses on the design and reliability of a steel main bearing structure. In order to optimise the design of the steel structural system, a good understanding between the wind pressures on the building and the reaction forces in the structure is needed, while keeping all the uncertainties in mind. Already a lot of research focussed on probabilistic wind force descriptions. Ever since Davenport formulated his wind loading chain, better probabilistic models have emerged over the years. The uncertainties have been determined and taken into account more and more accurately, such as by Cook and Mayne, Davenport himself, JCSS Probabilistic Model Code and more recent studies. Many researchers have also looked at the design of structures loaded by the wind from a reliability viewpoint. However, less is known of the load effects in specific elements of the steel structural system. This research will focus on this topic and investigate what the failure probability of the governing steel columns and beams on different locations in wind excited buildings is. In this research, a method is developed that evaluates the reliability of elements in a wind-loaded steel main bearing structure, describing both the wind load and the strength in a fully probabilistic way, and also makes direct use of wind speed and wind tunnel measurements. The building is also completely modelled, including all structural elements, in a 3D finite element model (FEM). This is a step forward compared to other studies in which the analysis is mainly done on element level and in which the interactions in the structure and the more intricate behaviour are not always included. This study gives an insight in the level of reliability and also which elements in this case study building are the most reliable or unreliable. This study is only a small part of the larger quest for the most optimal design of buildings; designing buildings in such an efficient and economic way (minimizing resources) while still complying with the current reliability standards.

1.2. Research question

In order to carry out the research, first of all a main research question is formulated. The main research question of this Master Thesis is:

> *”How can the reliability of the steel structural system of wind excited buildings be assessed, based on probabilistic models accounting for uncertainties in wind forces and resistance, resulting in failure probabilities on element level?”*

In order to decompose this main research question in a thorough and structured manner, a number of sub-questions are formulated. Each of these sub-questions relates to a particular part of this research. If a satisfactory answer can be formulated to all these sub-questions, this will contribute to answering the main research question.

- How can a probabilistic model of the resistance part be made to account for all the uncertainties in the material and the structural behaviour?
- How can a wind load effect model be incorporated into the reliability assessment procedure?
- How can the reliability assessment procedure be linked with a finite element model?
- Which reliability method (such as Monte Carlo, FORM, etc.) is best suited for the analysis?
- How do the reliability values compare to the target reliability of $\beta = 3.8$ according to the Eurocode for this type of structure?

1.3. Scope of this research

As it is not feasible to include all possible scenarios and aspects that play a role in reality in the study, the scope of the study is elaborated first. What issues are included and what issues are explicitly not considered? The scope of this research is as follows:

- The reliability assessment of steel buildings, which is the topic of this research, is based on Ultimate Limit State (ULS) design, a reference period of 50 years and consequence class 2.
- Global failure of the steel structural elements in the main bearing structure is of focus in this research.
- It is assumed that the building is prone to wind forces, imposed loads (office, class b) and its own weight. Wind forces are considered the dominant loading. Only the dominant wind direction, which results in wind pressures on all facades and roof of the building, is included in this study.
- Connections are not designed in great detail. It is only assumed that the connections are hinged or rigid, a detailed design of these connections is omitted.
- The influence of the surrounding buildings on the wind characteristics for the design of the case study building are not considered in this study.
- The reliability assessment is based on a specific case study building which is designed according to the regulations in the Eurocode.

1.4. Outline of this report

To make the structure of the report clear as possible for you - as the reader - an outline of the report is given here. *Part I: Literature Review* contains the necessary information that is used as background knowledge to carry out this research. *Part II: Method Development* is about the development of the reliability assessment procedure and all aspects that are involved are central. In *Part III: Reliability of the Case Study Building*, the reliability assessment procedure is applied to a specific case study building. Finally, in *Part IV: Conclusions and Recommendations*, the conclusions and recommendations based on this study are formulated.

Part I: Literature Review

In *Chapter 2: Structural Reliability*, the basic knowledge of the reliability of structures is explained, both general concepts and the various reliability levels, as well as the approach in the Eurocode. This chapter is the basis for all further analyses in the domain of reliability. Then in *Chapter 3: Wind Engineering Fundamentals*, all aspects of wind engineering are discussed. First the wind phenomenon is explained and the physical aspects on the basics of the wind loading chain are explained. This chapter also shows how wind loading is included in the Eurocode. Finally, the probabilistic modelling of the wind is of focus. Next, in *Chapter 4: Probabilistic Modelling of Extremes*, it is explained how extreme values can be modelled and which methods are possible. This knowledge is used to fit the extreme values of the normalized load effects to an extreme value distribution. *Chapter 5: Probabilistic Structural Resistance Model* deals with the uncertainties that occur on the side of material and structural resistance. This results in a probabilistic structural resistance model that in combination with the probabilistic load effect model, can evaluate the reliability of the structure in a full probabilistic way. Also the state-of-the-art in the field of reliability analysis steel buildings is discussed.

Part II: Method Development

Part 2 of this report begins with *Chapter 6: Methodology of this study*, which explains the methodology of this research; how it continues from recent research and in what ways this research is different and contributes to scientific improvement. *Chapter 7: Probabilistic Wind Pressure Model* is dedicated to the creation of a probabilistic wind pressure model. Also the influence of the dependencies between different zones is discussed. Next, *Chapter 8: Technique for Obtaining Load Effects* describes the technique that is used to obtain the load effects. All necessary steps and also the probabilistic modelling of the extreme load effects is discussed. Finally, the reliability assessment procedure is explained in *Chapter 9: Reliability Assessment Procedure*. All aspects that are involved are highlighted. Also, the various failure mechanisms and corresponding limit state functions are defined for the various elements. Furthermore, the wind loading effect model is described.

Part III: Reliability of the Case Study Building

Chapter 10: Case Study Description gives a general description of the case study on which the reliability analysis is carried out. Also the wind tunnel data is explained. After this, in *Chapter 11: Description Load Effects*, the load effects for the various elements are determined, both for the timeseries and for the probabilistic model of the wind pressures. In *Chapter 12: Reliability Assessment* the reliability assessment is performed. For the different elements, several types of analyses are performed, whereby different variations are possible. Also all input parameters are explained. Finally, in *Chapter 13: Discussion* a discussion on the developed method in this study and also the results of the reliability assessment is given.

Part IV: Conclusions and Recommendations

This part contains the main conclusions of this study as well as recommendations for future research.

I

Literature Review

2

Structural Reliability

This chapter focuses on structural reliability and provides a general introduction to the subject. This chapter can be considered as background theory, for the completeness of this report and for clarification for people who have less knowledge of reliability, this chapter will still give useful basic insights.

The design of new structures always have to satisfy the required safety levels in an economic and optimised way. These safety - or in other words - reliability levels specified in the Eurocode, will make sure that the design and execution of the structure is able to withstand the applied loads on it during its intended working life, with a specified (very small or negligible) probability of structural failure. A widely used definition of the term 'reliability' is provided in the ISO 2394 [29] document and is stated as follows: *"ability of a structure or structural member to fulfil the specified requirements, during the working life, for which it has been designed"*. A distinction is made between different reliability level requirements, based on the use of the structure, type of structure and intended working life. The first part of this chapter Fundamental theory on structural reliability, will provide the basic knowledge on structural reliability including mathematical statistics and probabilistic concepts. The second part of this chapter Approach in the Eurocodes, goes into more detail on the reliability principles used in the Eurocodes.

This knowledge can then be used in this research; how to properly apply the theory in a reliability assessment? And also, which method is most suitable for this research? A discussion on the most suitable method for this study is also included in section Discussion on the different methods.

2.1. Fundamental theory on structural reliability

2.1.1. General

The essence of structural reliability analysis is to formulate a certain failure probability P_f for a specific structure. For each structure - or looking at element level - specific boundary-, loading-, geometrical-, material- and other conditions hold. Therefore for each case the failure probability P_f is different. A distinct failure mechanism is investigated in the so-called *Limit State Function* Z:

$$Z = R - S \tag{2.1}$$

Failure will take place when the resistance of the structure R is lower than the applied load (or in other words called *Solicitation*). This limit state function is based on basic variables for the structural resistance R and loads S. These basic variables and also the physical models describing these basic variables are subject to uncertainties; therefore these variables are not described in a deterministic, but in a stochastic manner. For each basic variable a specific distribution (e.g. normal-, lognormal-, Gumbel-, extreme value distribution) and accompanying parameters is formulated. Then the failure probability $P_f = P(Z < 0)$ is calculated using one of the available methods. The failure probability is the volume under the curve (in the case of $n = 2$ basic variables) in the unsafe region ($Z < 0$) of the combined probability density functions in figure 2.1a and visually for another example in figure 2.1b.

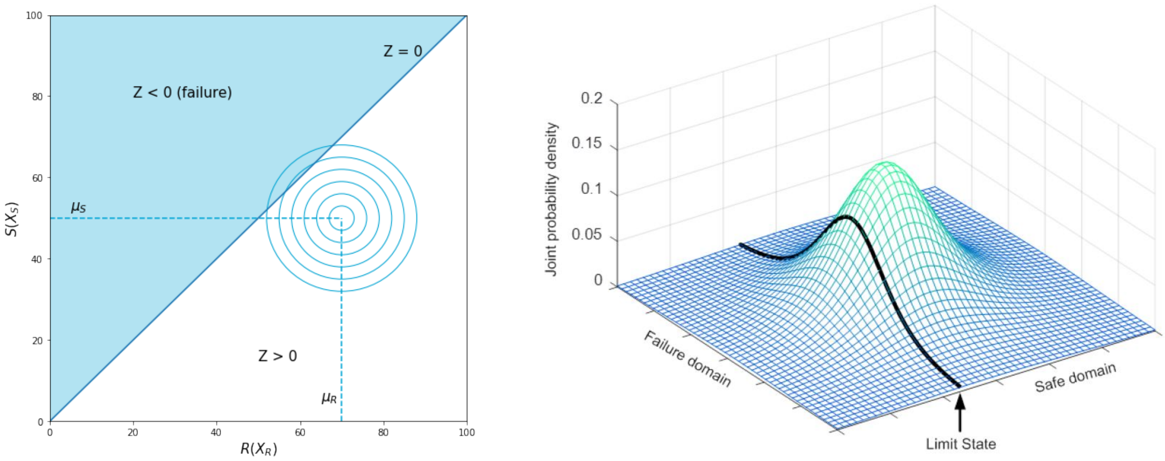

(a) Limit state function in two dimensions

(b) Example of joint probability density function in 3D with specified limit state including failure and safe domain [19]

Figure 2.1: Joint probability density functions

The example in figure 2.1a only deals with 2 stochastic variables, in general, the following integral gives the failure probability explicitly:

$$P_f = \int_{Z<0} f_{\underline{x}}(\underline{x})d\underline{x} \tag{2.2}$$

The opposite of the failure probability is the reliability of the structure and is formulated as follows:

$$P_{reliable} = P(Z > 0) = 1 - P_f \tag{2.3}$$

Instead of speaking in terms of failure probabilities P_f, the *reliability index* β is used to quantify the reliability of structures. The reliability index β and the failure probability P_f are related by the cumulative distribution function of the standard Normal distribution Φ:

$$\beta = -\Phi^{-1}(P_f) \tag{2.4}$$

There are several different methods to determine the failure probabilities. These methods are characterised into different levels:

- Level IV methods: Risk-based
- Level III methods: Numerical
- Level II methods: Approximation
- Level I methods: Semi-probabilistic design
- Level 0 methods: Deterministic

Level IV methods (risk-based) are very comprehensive methods where the consequences of failure are also taken into account. These consequences are expressed in terms of costs. The reliability of the structure is measured in terms of the risk, where the definition of risk (*risk = consequence x probability of failure*) is used.

In level 0, or specifically deterministic methods, the structures are analysed based on deterministic values. The uncertainties in the basic variables for the resistance of the structure R and the load S are not considered. The verification uses one (empirical) global safety factor γ:

$$R_{nom} \geq \gamma \cdot S_{nom} \tag{2.5}$$

The other methods, ranging from level III to I, are discussed in more detail in the following sections.

2.1.2. Level III methods: Numerical

Level III methods are based on numerical techniques to evaluate the integral in equation 2.2 explicitly. It depends on the number of basic variables, the dependency between these basic variables, the associated distribution type and also whether the limit state function is linear or nonlinear, if numerical integration is efficient to use or not.

For the standard case of independent normally distributed random variables in a linear limit state function, the analysis is fairly simple. The variable $Z = R - S$ is also normally distributed with the following parameters (μ is the mean and σ is the standard deviation):

$$\mu_Z = \mu_R - \mu_S \tag{2.6}$$

$$\sigma_Z = \sqrt{\sigma_R^2 + \sigma_S^2} \tag{2.7}$$

The probability of failure P_f is determined using the standard normal distribution (Φ):

$$P_f = P(Z < 0) = \Phi\left(\frac{0 - \mu_Z}{\sigma_Z}\right) = \Phi(-\beta) \tag{2.8}$$

The reliability index β is defined as the distance between the mean of Z μ_Z and value of $Z = 0$ with a standard deviation of σ_Z:

$$\beta = \frac{\mu_Z}{\sigma_Z} \tag{2.9}$$

In the general case, where the basic variables are not necessarily normal distributed and the limit state function is nonlinear, numerical integration can be used to determine the failure probability. Recognise that the failure probability for the case of $n = 2$ basic variables, resembles the volume under the curve at the unsafe side of the joint probability density function. This analogy also holds for $n > 2$ basic variables, only then the failure probability is not the volume but a higher order shape.

The volume under the joint probability density function at the unsafe side ($Z < 0$), is calculated using equation 2.2, this can be written in exact form as follows:

$$P_f = \int_{-\infty}^{+\infty} \left(f_R(r) \int_{S=r}^{+\infty} f_S(s) ds \right) dr \tag{2.10}$$

This integral can also be solved numerically by dividing the volume in small boxes and adding these together:

$$P_f = \sum_i \sum_j f_{R,S}(r_i, s_j) \Delta r \Delta s \tag{2.11}$$

In order to solve this integral for larger number of stochastic variables, a huge amount of computational power is necessary, since the number of integration steps increases exponentially with regard to the number of stochastic variables. For these cases the Monte-Carlo simulation method - in which random samples are generated - is very efficient to use. Then for each random sample, the limit state function is checked and when $Z < 0$, a counter N_f (representing the amount of failures) increases (see also figure 2.2a). If this procedure is performed N times, or in theory approaches $N \longrightarrow \infty$, than the failure probability is:

$$P_f = \frac{N_f}{N} \tag{2.12}$$

For situations where very low probabilities of failure are present, the number of required simulations N to get a sufficient amount of N_f and thus accurate result, will increase rapidly. Therefore a specific technique, called *importance sampling*, is invented to increase the amount of failures N_f for the same

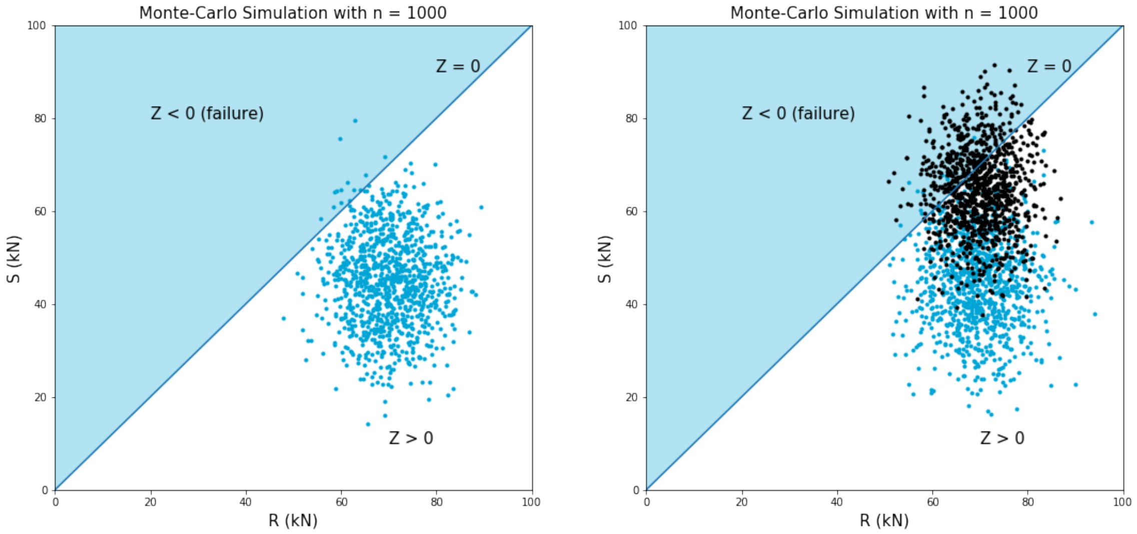

(a) Example of Monte-Carlo simulation with $n = 1000$ samples

(b) Example of using Importance sampling (black dots) in a Monte-Carlo simulation with $n = 1000$ samples

Figure 2.2: Example of Monte-Carlo simulation

amount of simulations N (see also figure 2.2b and compare this with the original Monte-Carlo simulation in figure 2.2a). Together with the importance sampling probability distribution function $f_S(x)$, the probability of failure can be calculated as follows:

$$P_f = \frac{N_f}{N}\frac{f_{\underline{X}}(\underline{x})}{f_S(\underline{x})} \tag{2.13}$$

2.1.3. Level II methods: Approximation

The level II method approximates the failure probability. Nonlinear limit state functions are linearized in a specific point - also called the *design point* - and all the stochastic variables are considered normally distributed, even when this is not the case. The accuracy of the approximation obtained by this level II method, highly depend on the exact linearization with the associated design point and also on the fitted normal distribution for the non-normally distributed stochastic variables. This method is also called the First Order Reliability Method (FORM).

The linearization of the nonlinear limit state function is done at the design point. Hasofer and Lind [18] described that the reliability index β is equal to the shortest distance from the origin to the surface described by $Z = 0$ in the space of the normalised basic variables. This definition always hold, also for nonlinear limit state functions. Determine the design point - where the limit state function is linearised - in such a way that the distance from the origin in the space of normalised basic variables tangent to the linearization is minimised. This is in accordance with our intuition; a larger value of β result in a smaller volume under the joint probability density function and thus in a more reliable system.

In the case of a linear limit state function $Z = a_1X_1 + a_2X_2 + ... + a_nX_n + b$, the mean μ_Z and standard deviation σ_Z are determined as follows:

$$\mu_Z = a_1\mu_{X_1} + a_2\mu_{X_2} + ... + a_n\mu_{X_n} + b \tag{2.14}$$

$$\sigma_Z = \sqrt{\sum_{i=1}^{n}\sum_{j=1}^{n} a_i a_j Cov(X_i, X_j)} \tag{2.15}$$

For nonlinear limit state functions Z, linearization based on Taylor expansion is used. The most accurate results are obtained for linearisations in the design point. Finding this design point $(X_1^*, X_2^*, ..., X_n^*)$ is an iterative procedure. A good first estimate for the design point is using the mean values, then the mean μ_Z and standard deviation σ_Z are determined as follows:

$$\mu_Z = Z(X_1^*, X_2^*, ..., X_n^*) + \sum_{i=1}^{n} \left(\frac{\partial Z}{\partial X_i}\right)(\mu_{X_i} - X_i^*) \tag{2.16}$$

$$\sigma_Z = \sqrt{\sum_{i=1}^{n} \left(\frac{\partial Z}{\partial X_i}\right)^2 \sigma_{X_i}^2} = \sum_{i=1}^{n} \alpha_i \frac{\partial Z}{\partial X_i} \sigma_{X_i} \tag{2.17}$$

Where α_i are the sensitivity factors, which are very useful and give a direct insight in the influence of the standard deviation of a certain basic variable to the reliability index. A property of the sensitivity factors is: $\alpha_1^2 + \alpha_2^2 + ... + \alpha_n^2 = 1$. The sensitivity factor α_i is defined as follows [1]:

$$\alpha_i^2 = \frac{a_i^2 \sigma_i^2}{\sigma_Z^2} \tag{2.18}$$

α is negative for load parameters and positive for resistance parameters. Based on the values of β and α a new design point can be determined. If the β and thus also the solution converges to a single point, then the actual design point is found. A new guess for the design point is determined using the following formula:

$$X_i^* = \mu_{Xi} - \alpha_i \beta \sigma_{Xi} \tag{2.19}$$

2.1.4. Level I methods: Semi-probabilistic design

Level I methods are based on regulations by for instance the Eurocode. The α factors are standardised for both the strength and load parameters and also whether this is dominant or non-dominant on the structure. The standardised α values are in table 2.1. Using partial factors for both the material properties and the loads, a verification is performed:

$$\frac{R_k}{\gamma_R} > \gamma_S \cdot S_k \tag{2.20}$$

	Load	Resistance
Dominant variable	$\alpha_S = -0.7$	$\alpha_R = 0.8$
Non-dominant variable	$\alpha_S = -0.28$	$\alpha_R = 0.32$

Table 2.1: Standardised α values for structures according to the Eurocode

The design values for the strength and load parameters are determined as:

$$\text{Strength} \longrightarrow R_d = \mu_R - \alpha_R \beta_t \sigma_R \tag{2.21}$$

$$\text{Load} \longrightarrow S_d = \mu_S - \alpha_S \beta_t \sigma_S \tag{2.22}$$

2.1.5. Discussion on the different methods

Various methods are discussed above, ranging from level IV to level 0 methods. Which method is ultimately the best to use in this study depends on a number of factors. In particular, level III and level II methods, Monte Carlo simulation and FORM respectively, are possible candidates.

---

[1] note the difference between α (alpha) and a (a)

The first method we consider is the Monte Carlo method. This method performs a large number of simulations, and if failure occurs, this will be reported. Eventually, the failure probability can be determined in this way. The major disadvantage of this method is that it is pretty computationally heavy and has to run for quite a long time to get results. A second disadvantage is that the specific influence of certain factors cannot be determined (however, possible using specific software). This is however the case in the other method: FORM. The great advantage of FORM is that, based on the sensitivity factors, it can be determined how large the contribution of specific factors is. This provides a lot of insight into the reliability at a detailed level. The FORM method also converges quite quickly, which makes it computationally more efficient than Monte Carlo. Therefore, the FORM method is used in this study.

2.2. Approach in the Eurocodes

The main principle of the Eurocode is to achieve a structure with sufficient strength, serviceability and durability. The structural reliability approach in the Eurocode is based on different classes which results from specific consequences of failure and the vulnerability of structures to hazards. These classes are used to define certain partial factors for both actions and resistance parameters. In that way, the structural reliability classification is represented by β (reliability) indexes which takes into account accepted or assumed statistical variability in action effects and also resistances and model uncertainties [15].

The Eurocode provides a basic classification of structures according to the consequences - for human life, economy, society and the environment - which might occur due to a failure. These classes are called the *'consequence classes'* and are in table 2.2. Currently, the structural reliability is on member level (so each member need to fulfil the requirements) and not on global - or in other words - building level. Therefore the structural reliability of the complete structure is lower (higher probability of failure P_f due to the series system and thus lower β). The consequence classes can be coupled to the *'reliability classes'* from table 2.3. Based on this table the minimum reliability index β is determined. When designing a structure using the general Eurocode approach (with the partials factors) from EN1991 to EN1999, the structure will be more reliable than the minimum specified reliability level β from table 2.3 depending on the reliability class and reference period. This reference period, also called design lifetime of the structure, differs for each type of structure. Roughly speaking, this design lifetime is between 2 and 100 years respectively for temporary structures or monumental buildings, bridges and civil engineering construction works. However, a reference period of one year may also be useful if, for example, the load distribution functions and the reliability requirement are derived from it.

Consequences Class	Description	Examples of building and civil engineering works
CC3	**High** consequence for loss of human life, or economic, social or environmental consequences **very great**	Grandstands, public buildings where consequences of failure are high (e.g. a concert hall)
CC2	**Medium** consequence for loss of human life, or economic, social or environmental consequences **considerable**	Residential and office buildings, public buildings where consequences of failure are medium (e.g. an office building)
CC1	**Low** consequence for loss of human life, or economic, social or environmental consequences **small or negligible**	Agricultural buildings where people do not normally enter (e.g. storage buildings), greenhouses

Table 2.2: Definition of consequence classes for Standardization [15]

The Eurocode uses the partial factor method in order to design structures with a sufficient reliability

Reliability Classes (RC)	Minimum reliability index β	
	1 year reference period	50 year reference period
RC3	5.2	4.3
RC2	4.7	3.8
RC1	4.2	3.3

Table 2.3: Recommended minimum values for the reliability index β (Ultimate Limit State) [15]

level. The partial factors are determined based on reliability-based methods and calibration. All the basic variables - actions, resistances and geometrical properties - are converted into design values using partial factors γ and combination factors ψ.

Several types of uncertainties are dealt with in the partial factors. γ_F is the combination of γ_f which deals with the uncertainty in representative values of actions and γ_{Sd} which is related to the model uncertainty in actions and the associated action effects. Related to the resistance of the material is the partial factor γ_M, which is based on γ_{Rd} which deals with the model uncertainty in the structural resistance and γ_m which is related to the uncertainty in the material properties. The ψ factors (ψ_0, ψ_1 and ψ_2) are respectively related to the combination -, frequent - and quasi-permanent value of a variable action.

According to the Eurocode, the structure needs to be verified using both the *ultimate limit state (ULS)* and the *serviceability limit state (SLS)*. The ultimate limit state verifies if the resistance capacity of the structure can withstand the action effects (e.g. loss of static equilibrium, fracture or excessive deformation of (some parts of) the structure, fatigue, collapse, instability such as (lateral) buckling) and the serviceability limit state checks if the structure is capable to function under normal use (e.g. performance of the structure, comfort of the users, visually alright). Two types of SLS can be distinguished: irreversible and reversible. In the first case, the design criteria are similar to those of ULS.

If there are variable actions, the characteristic values Q_k shall be used. This corresponds to a high or low quantile value, resulting in a low or high probability of exceedence respectively. This characteristic value Q_k of a variable action is in most cases described in the Eurocode as the value that occurs with a probability of exceedence of 2% during one year, which corresponds to a return period of 50 years. By using characteristic values in combination with partial safety factors γ and combination -, frequent - and quasi-permanent factors ψ, different reliability levels are realized (see figure 2.3).

- Combination value ψ_0: if there is a co-occurrence of extreme values of various independent variable actions
- Frequent value ψ_1: In the case of buildings, an exceedence probability of 1% is often considered
- Quasi-permanent value ψ_2: In this case, the value that is exceeded in 50% of cases is often taken. Instead of the quasi-permanent value, the average value could also be used

The general check for ULS design is in equation 2.23 or alternatively using the less favourable from equation 2.24a or 2.24b. These formulas 2.24a and 2.24b may only be used for STR and GEO limits[2]. In these formulas, "+" means 'to be combined with', $\sum$ implies 'the combined effect' and ξ is a reduction factor for unfavourable permanent actions.

$$\frac{R_k}{\gamma_M} \geq E_d = \sum_{j\geq 1} \gamma_{G,j} G_{k,j} \text{ "+" } \gamma_P P \text{ "+" } \gamma_{Q,1} Q_{k,1} \text{ "+" } \sum_{i>1} \gamma_{Q,i} \psi_{0,i} Q_{k,i} \tag{2.23}$$

---

[2] STR: *"Internal failure or excessive deformation of the structure or structural members, including footings, piles, basement walls, etc., where the strength of construction materials of the structure governs"*; GEO: *"Failure or excessive deformation of the ground where the strengths of soil or rock are significant in providing resistance"* [15]

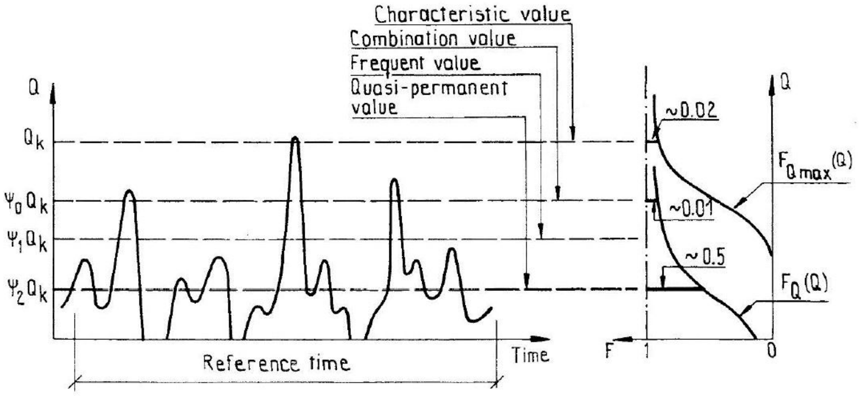
Characteristic value
Combination value
Frequent value
Quasi-permanent value
Q
Q_k
ψ0 Qk
ψ1 Qk
ψ2 Qk
Reference time
Time
~0.02
~0.01
~0.5
F_Qmax(Q)
F_Q(Q)
F
1
0
Q

Figure 2.3: Representative values of variable actions

$$\frac{R_k}{\gamma_M} \geq E_d = \sum_{j\geq 1} \gamma_{G,j} G_{k,j} \text{ "+" } \gamma_P P \text{ "+" } \gamma_{Q,1}\psi_{0,1} Q_{k,1} \text{ "+" } \sum_{i>1} \gamma_{Q,i}\psi_{0,i}Q_{k,i} \tag{2.24a}$$

$$\frac{R_k}{\gamma_M} \geq E_d = \sum_{j\geq 1} \xi\gamma_{G,j} G_{k,j} \text{ "+" } \gamma_P P \text{ "+" } \gamma_{Q,1} Q_{k,1} \text{ "+" } \sum_{i>1} \gamma_{Q,i}\psi_{0,i}Q_{k,i} \tag{2.24b}$$

3

Wind Engineering Fundamentals

This chapter focuses on the wind engineering basic knowledge. Section Basics wind will first focus on the basic principles and description of the wind. How can the irregular character of the wind be described in such a way that further analyses can be done with it? Then, in section Wind loading chain, Davenport's wind loading chain, containing all relevant parameters for modelling the wind load, is discussed. Next, the method for determining the wind load according to the Eurocode is described in section Wind loading approach in the Eurocode. Finally, the modelling of the wind load in a probabilistic way is described in section Probabilistic modelling of wind loading.

As this research focuses on wind excited buildings, it is very useful to understand the theory of wind engineering - from the basic knowledge, to the methods in the Eurocode and even the probabilistic models described in the literature. Not all aspects covered in this chapter will be used directly in this research, but the theory is included for the sake of completeness.

3.1. Basics wind

Wind is a natural phenomenon in which air particles move in the atmosphere due to the presence of horizontal air pressure differences. The resulting force and direction of these air currents - or also called wind - is influenced by the earth's rotation and friction with the earth's surface.

In figure 3.1 it is shown that the speed of the wind has a random character. For a certain reference period (not the same as the reference period regarding reliability in the previous chapter), often between 10 minutes and 1 hour, an average wind speed $\overline{v}$ can be determined which results in a long-term distribution. In addition, it can be seen that the wind shows a second type of variation $\tilde{v}$, which is of a faster nature and can be assigned to the short-term distribution. These rapid fluctuations around the average can be attributed to the turbulent nature of the wind itself.

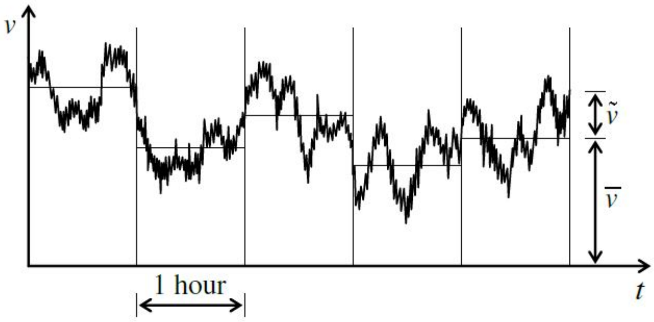

Figure 3.1: Fluctuations in wind speed

Van der Hoven [34] has been able to compile a power spectrum (see figure 3.2) of the horizontal wind speeds in the frequency range of 0.0007 to 900 cycles per hour based on many measurements. This power spectrum shows the contribution of oscillations with continuously changing frequencies to the variance of the wind speed. A number of important things can be deduced from this figure. Firstly, a clear peak can be seen around a frequency of 100 hours (around 4 days). This macro-meteorological peak is related to the development of the larger weather systems in the atmosphere. Secondly, there is the micro-meteorological peak, which takes place in the higher frequency regions and has to do with the mechanically generated turbulence of the atmospheric boundary layer. The last observation is the spectral gap present between the two peaks mentioned above. In this area there is little variation, therefore the above mentioned reference period between 10 minutes and 1 hour show similar results due to the spectral gap. Since both peaks lie in different parts of the frequency spectrum, they may be taken as statistically independent. Therefore the wind speed $v(t)$ can be formulated using the mean wind speed $\overline{v}_{T_{ref}}$ over a reference time T_{ref} and the micro-meteorological fluctuations $\tilde{v}(t)$:

$$v(t) = \overline{v}_{T_{ref}} + \tilde{v}(t) \tag{3.1}$$

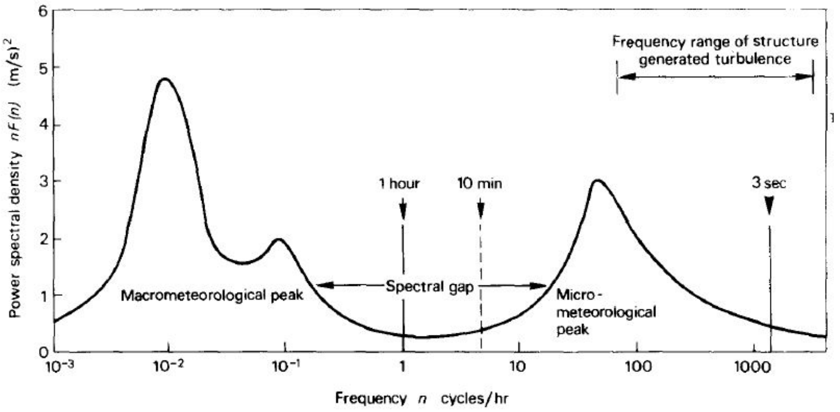

Figure 3.2: Spectrum of horizontal wind speed, based on analysis of van der Hoven [8]

3.2. Wind loading chain

Davenport [10] has developed the wind loading chain (figure 3.3) in which all aspects that influence the modelling of the wind are included. The resulting wind load effect on a structure consist of the local wind climate, terrain aspects, aerodynamic influence, dynamic effects and criteria to assess the predicted loads and responses of the structure. It is in the form of a chain, since the weakest link of the system determines the eventual result. And also the placement of the several chains indicate the dependencies between the different elements.

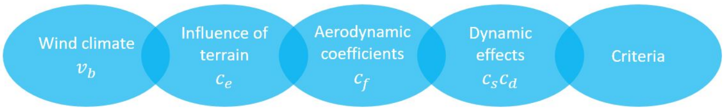
Wind climate v_b
Influence of terrain c_e
Aerodynamic coefficients c_f
Dynamic effects $c_s c_d$
Criteria

Figure 3.3: Wind loading chain by Davenport

3.2.1. Wind climate v_b

Davenport's wind loading chain starts with the wind climate link. This wind climate is not the same all over the world, regional differences can be distinguished. The specific wind climate stems from the differences in earth solar heating. In addition, a number of natural phenomena play a role in the wind climate, such as horizontal pressure gradient force, Coriolis force on the earths rotation, the centrifugal force and frictional forces due to geographical characteristics. The interaction between all these forces results in various weather patterns, in which these can occur both on a large scale in the form of larger global weather systems, but also on a smaller scale as is the case, for example, with tornadoes or thunderstorms. In addition, after observing the wind climate, it turns out that it is not the same all year round. There are changes in the wind climate during the seasons. Finally, it is good to realise that the wind does not occur equally often from all directions; varying per region, some wind directions occur more often and also result in higher wind speeds. This is useful knowledge for the design of tall buildings, for example.

3.2.2. Influence of terrain c_e

The next link in Davenport's wind loading chain deals with the influence of the terrain. Wind is, as it were, a medium that 'flows' over the surface of the earth, and since they make contact with each other on the earth's surface, a frictional force is exerted on the wind. Observation of wind speeds over the height above the earth's surface shows that the higher you go, the higher the wind speed, due to the lesser presence of the frictional force at that height. This results in an atmospheric boundary layer (ABL) (see figure 3.4) with an average wind speed that increases with height.

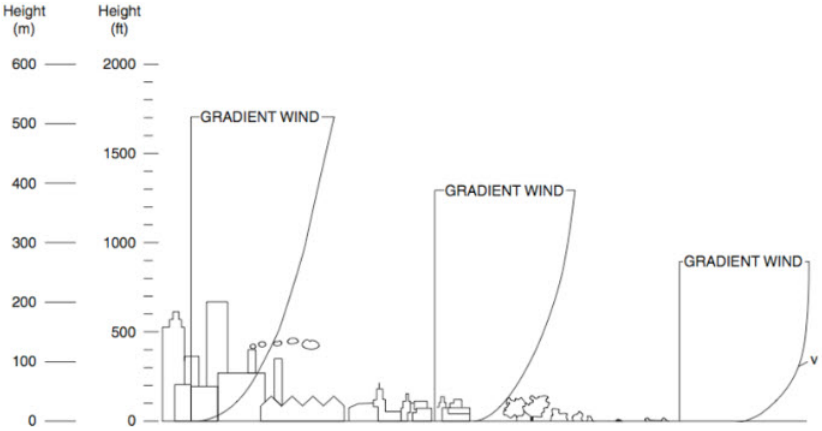

Figure 3.4: Atmospheric Boundary Layer (ABL) [16]

Figure 3.4 shows that the rougher the terrain, for example due to more and/or larger buildings, the greater the frictional forces on the wind and thus the more the wind profile changes over height such that the gradient wind only occurs at a higher altitude. Above the ABL, the wind travels at an almost constant speed, but in the ABL turbulence of the wind occurs. This turbulence makes the determination of a design wind load, at heights where we are interested in for the design of buildings, a lot more difficult. The distance in the landscape that affects wind characteristics is also called the wind fetch length.

There are 4 different influences that can be distinguished:

- Atmospheric instabilities: Such as the temperature distribution in the surface layer, which influence the wind profile too. These are so small for the wind load that they do not play a significant role.
- The roughness of the upwind terrain: This affects the magnitude of the frictional forces on the wind and is described by the roughness length z_0. This is determined over the distance that affects the wind characteristics; the wind fetch length.
- The terrain orography: This is due to the variation in the relief of the landscape, such as mountains and hills, which results in a vertical flow of the wind. This will also change the average wind speed.
- The effect of neighboring structures: How the wind behaves also depends on the buildings around it. The buildings interact with the wind so the wind would flow in a different way than if the buildings were not there. Since the same amount of wind still wants to go from a to b, despite the presence of obstructions in the form of buildings, the wind will be squeezed between the buildings and the wind speed will increase.

The average wind speed profile over the height can theoretically be described by a logarithmic function (see equation 3.2). The roughness of the landscape plays a major role here. In section Wind loading approach in the Eurocode it can be seen that this formula is slightly different in Eurocode EN 1991-1-4.

$$\overline{v}(z) = \frac{u_*}{\kappa} ln\left(\frac{z-d}{z_0}\right) \tag{3.2}$$

With:

$\overline{v}(z)$ = mean wind speed (in x-direction) at height z $[m/s]$
κ = Von Karman constant = 0.4 [-]
d = average height of the buildings $[m]$
u_* = shear velocity $[m/s]$
z = height above the surface of the earth $[m]$
z_0 = measure for the roughness of the terrain (roughness length) $[m]$

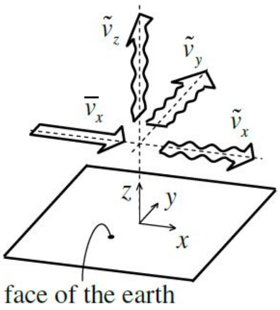

Figure 3.5: Vector notation wind-speed components

A vector notation is used to describe the wind flow (see equation 3.3 and figure 3.5). Here the x-axis is in the direction of the wind flow, this direction is also called the longitudinal direction. Both the average wind speed and the turbulent component are distinguished. In addition, there is also the z-axis which is perpendicular to the surface of the earth and the y-axis which is normal to the x- and z-axis, which only contain the turbulent component of the wind.

$$\underline{v}(x,t) = \begin{bmatrix} v_x(t) \\ v_y(t) \\ v_z(t) \end{bmatrix} = \begin{bmatrix} \overline{v}_x + \tilde{v}_x(t) \\ \overline{v}_y + \tilde{v}_y(t) \\ \overline{v}_z + \tilde{v}_z(t) \end{bmatrix} \tag{3.3}$$

3.2.3. Aerodynamic coefficients c_f

The third link in Davenport's wind loading chain is for the aerodynamic coefficients. These aerodynamic coefficients are expressed in the form of a force or pressure coefficient. The definition of these coefficients is the ratio between the local mean or peak pressure at the facade and the global mean wind pressure q that occurs for the building. The values are not the same for the whole building, but will be different for each specific point on the facade. This also has to do with the type of wind flow around the building.

These pressure coefficients also depend on the reference time. The large peaks in wind load are usually of short duration, so if the coefficients are based on longer time measurements, the coefficients will be lower than if only the short duration peaks are considered.

It is not efficient to determine a pressure coefficient for every point on the facade of a building. What is often done is to determine a pressure coefficient for a certain area A_{ref}. The peaks in wind pressure on the facade never occur all at once over the entire facade, therefore a space-averaging effect is present for a certain A_{ref}. This effect is bigger for a larger A_{ref}, in which the pressure coefficient will be lower due to the absence of full correlation between the pressures on the various places on the facade.

3.3. Wind loading approach in the Eurocode

In this section it is explained how the theoretical models for describing the wind - as explained above using davenport's loading chain - have been translated into clear procedures in Eurocode EN1991-1-4. All aspects that influence the wind and the resulting forces on structures are included in the Eurocode. The EN1991-1-4 wind load model is summarised in figure 3.6.

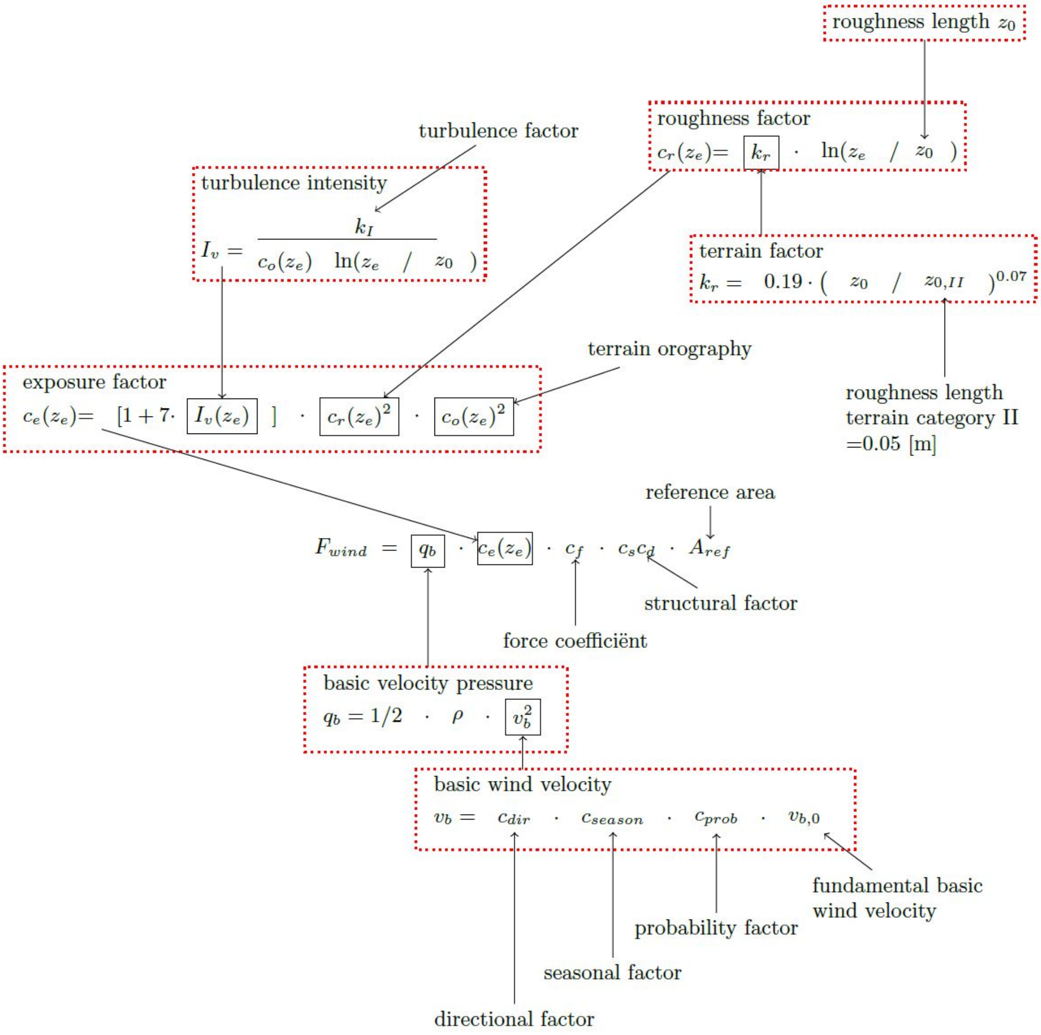
roughness length z_0
turbulence factor
roughness factor
$c_r(z_e) = \boxed{k_r} \cdot \ln(z_e \;/\; z_0\;)$
turbulence intensity
$I_v = \frac{k_I}{c_o(z_e)\;\ln(z_e\;/\;z_0\;)}$
terrain factor
$k_r = 0.19 \cdot (\;z_0\;/\;z_{0,II}\;)^{0.07}$
terrain orography
roughness length
terrain category II
=0.05 [m]
exposure factor
$c_e(z_e) = [1 + 7 \cdot \boxed{I_v(z_e)}\;] \cdot \boxed{c_r(z_e)^2} \cdot \boxed{c_o(z_e)^2}$
reference area
$F_{wind} = \boxed{q_b} \cdot \boxed{c_e(z_e)} \cdot c_f \cdot c_s c_d \cdot A_{ref}$
structural factor
force coefficiënt
basic velocity pressure
$q_b = 1/2 \cdot \rho \cdot \boxed{v_b^2}$
basic wind velocity
$v_b = c_{dir} \cdot c_{season} \cdot c_{prob} \cdot v_{b,0}$
fundamental basic
wind velocity
probability factor
seasonal factor
directional factor

Figure 3.6: Action model for wind loads in EN1991-1-4 (Meinen, 2015)

3.3.1. Wind climate

The specific wind climate at a given location is described in the Eurocode by the basic wind velocity v_b. This basic wind velocity v_b is defined as a function of wind direction including seasonal variations at a height of 10 m above the ground of a certain terrain which corresponds to a terrain category II ($z_0 = 0.05$ in that case). The mean wind velocity v_m is then based on the basic wind velocity and the terrain roughness and orography.

Air density ρ_{air}

What also depends on regional characteristics like altitude, temperature and barometric pressure is the air density ρ_{air}. In the Dutch National Annex a value of $\rho_{air} = 1.25\; kg/m^3$ is recommended.

Directional factor c_{dir}

The directional factor c_{dir} deals with the wind directionality. The factor c_{dir} is a ratio of a characteristic wind speed in a particular direction, divided by the characteristic wind speed irrespective of the wind direction. The Eurocode recommends a value of $c_{dir} = 1.0$ and also in the Dutch National Annex it is stated that $c_{dir} = 1.0$ has to be chosen.

Seasonal factor c_{season}

The seasonal factor c_{season} deals with the changes of the wind characteristics during the different seasons. The factor c_{season} is a ratio of a characteristic wind speed in a specific season, divided by the characteristic wind speed which occurs over all seasons. The Eurocode recommends a value of $c_{season} = 1.0$ and also in the Dutch National Annex it is stated that $c_{season} = 1.0$ has to be chosen.

Probability factor c_{prob}

The basic values, for instance the basic wind velocity v_b, is a characteristic value with a corresponding annual probability of exceedence of 0.02 (equivalent to a return period of 50 years). In order to define wind characteristics for a different reference period than the standard 50 years, the basic wind velocity v_b can be multiplied by the probability factor c_{prob} (given in equation 3.4 with corresponding values depending on the wind zone in table 3.1).

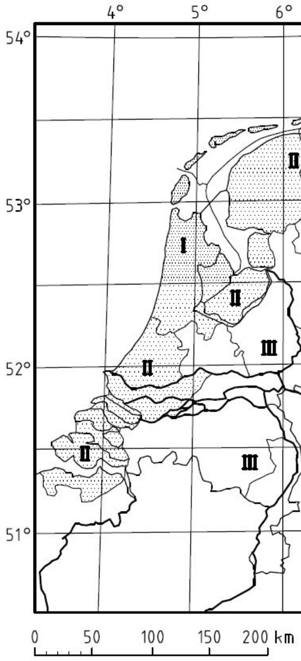

Figure 3.7: Wind zones in the Netherlands [6]

$$c_{prob} = \left(\frac{1 - \kappa \cdot ln(-ln(1-p))}{1 - \kappa \cdot ln(-ln(0.98))} \right)^n \tag{3.4}$$

Wind zone	I	II	III
κ	0.2	0.234	0.281
n	0.5	0.5	0.5

Table 3.1: Values for κ and n for the different wind zones as input for the factor c_{prob} [6]

Fundamental basic wind velocity $v_{b,0}$

The fundamental value of the basic wind velocity, $v_{b,0}$, is the characteristic 10 minutes mean wind velocity with a return period of 50 years, irrespective of wind direction and time of year, at 10 m above ground level in open country terrain with low vegetation such as grass and isolated obstacles with separations of at least 20 obstacle heights [6]. These values are specified in the Dutch National Annex. Three wind zones are defined in the Netherlands (see figure 3.7), the corresponding values for $v_{b,0}$ are given in table 3.2.

Wind zone	I	II	III
$v_{b,0}$ $[m/s]$	29.5	27	24.5

Table 3.2: Values for the fundamental basic wind velocity $V_{b,0}$ for the different wind zones in the Netherlands [6]

3.3.2. Influence of terrain

The specific terrain characteristics that influence the wind are described in the Eurocode by various factors. All these factors will be briefly discussed here.

Roughness factor $c_r(z)$

The roughness factor $c_r(z)$ refers to the change in mean wind speed over a height z and corrects directly for the terrain roughness z_0. This factor is useful in the case where the terrain and reference height relevant for the design of a particular structure deviate from the standard reference height of $z_{ref} = 10\ m$ and terrain roughness $z_{0,II} = 0.05\ m$. The corresponding formulas - also based on the Dutch National Annex - are in equations 3.5, 3.6 and in table 3.3.

$$\begin{aligned} c_r(z) = k_r \cdot ln\left(\frac{z}{z_0}\right) \quad & \text{for} \quad z_{min} \leq z \leq z_{max} \\ c_r(z) = c_r(z_{min}) \quad & \text{for} \quad z \leq z_{min} \end{aligned} \tag{3.5}$$

$$k_r = 0.19 \cdot \left(\frac{z_0}{0.05}\right)^{0.07} \tag{3.6}$$

With:

z_0 = Roughness length $[m]$
k_r = Terrain factor depending on the roughness length z_0 [-]
$z_{0,II}$ = $0.05\ m$ (terrain category II) $[m]$
z_{min} = Minimum height $[m]$
z_{max} = $200\ m$ $[m]$

	Terrain category	z_0 [m]	z_{min} [m]
0:	Sea or coastal area	0.005	1
II:	unbuilt area	0.2	4
III:	built area	0.5	7

Table 3.3: Terrain categories and corresponding terrain parameters in Dutch National Annex [6]

Roughness length z_0

The roughness length z_0 is a factor used to characterise the terrain roughness. In the Netherlands, a distinction is made between three different categories. The roughness length z_0 is also different for each of these categories (see table 3.3).

Terrain orography c_o

How the orography of the landscape affects the wind characteristics is included in the terrain orography factor c_o [-]. These effects can be neglected if the average slope of the upwind terrain is less than 3 degrees. This upwind terrain applies over a distance of 10 times the height of the isolated orographic feature.

If the orographic characteristics of the land, like mountains or hills, increase the wind speed to such an extent that it is 5% faster than if there had been no hills, for example, then these effects must be included in the orography factor c_o. The calculation method for factor c_o is described in Appendix A3 of EN 1991-1-4.

Gust amplification factor $[1 + 7I_v(z)]$

As shown in figure 3.1 at the beginning of this chapter, the wind has an irregular character. If the wind were not influenced by the terrain, it would 'flow' much more smoothly, but the terrain influences the turbulence of the wind. This causes an occasional peak load on a structure for a short time. Using the gust factor approach, in which the mean wind pressure for a characteristic wind velocity is multiplied by another factor, these peak loads can be modelled. This factor that represents the short-term fluctuations is equal to:

$$1 + 7 \cdot I_v(z) \tag{3.7}$$

In this formula $I_v(z)$ [-] is the turbulence intensity at a height z and is defined as the ratio between the standard deviation of the turbulence σ_v $[m/s]$ and the mean wind speed $v_m(z)$ $[m/s]$.

3.3.3. Aerodynamic coefficients

The external pressure coefficients c_p [-] indicate to what extent the pressures measured directly on the facade deviate from the undisturbed dynamic pressure due to the mean wind velocity v_m at a distance in front of the building. These wind-structure interactions are contained in the pseudo-steady pressure coefficients. In the standards presented in EN1991-1-4 four orthogonal directions are considered ($0°$, $90°$, $180°$ and $270°$).

The external pressures are given both for a loaded area of $A = 1\ m^2$ and $A = 10\ m^2$, with $c_{pe,1}$ and $c_{pe,10}$ respectively. In case of local effects, $c_{pe,1}$ shall be used and for overall wind loading the $c_{pe,10}$ value has to be used. In this report the $c_{pe,10}$ values is used, since the design of the overall load bearing structure is of main focus. The values as described in the Dutch National Annex are listed in table 3.4. Some values depend on the h/d ratio, in other words the height-over-width ratio. If a value for h/d is not directly mentioned in the table, linear interpolation can be applied. The different zones on the surface of the building are illustrated in figure 3.8. Zone D and E are located respectively on the windward and leeward side of the building, in addition both side walls are subdivided into zones A, B and C. The specific dimensions of these zones are determined by parameter e, which is the smallest of b or $2h$.

In addition, figure 3.9 shows how the reference height z_e, depending on the specific values for h and b, results in a velocity pressure profile over the height of the building. In case the building is lower than its width ($h \leq b$), a constant pressure is calculated with a reference height z_e of h. If the height of the building is between 1 and 2 times its width ($b < h \leq 2b$), a 2-zone velocity pressure profile is calculated over the height with both a z_e at height b and height h. Finally, it is possible that the building is higher than 2 times its width ($h > 2b$), in which case the velocity pressure profile will consist, at the bottom and at the top, of an area of b high with, in between, an area divided into $(h - 2b)/h_{strip}$ areas with a height of h_{strip} each.

3.3.4. Dynamic effects

The dynamic effects of the wind on the structure are included in the Eurocode in the factor $c_s c_d$ [-]. The factor c_s (size factor) includes the effects of the non-simultaneous occurrence of peak wind pressures on the facades and the factor c_d (dynamic factor) includes the effects of the vibrations of the structure due to the present turbulence of the wind.

Zone	A	B	C	D	E
h/d	$c_{pe,10}$	$c_{pe,10}$	$c_{pe,10}$	$c_{pe,10}$	$c_{pe,10}$
5	-1.2	-0.8	-0.5	+0.8	-0.7
1	-1.2	-0.8	-0.5	+0.8	-0.5

Table 3.4: Pressure coefficients according to the Dutch National Annex

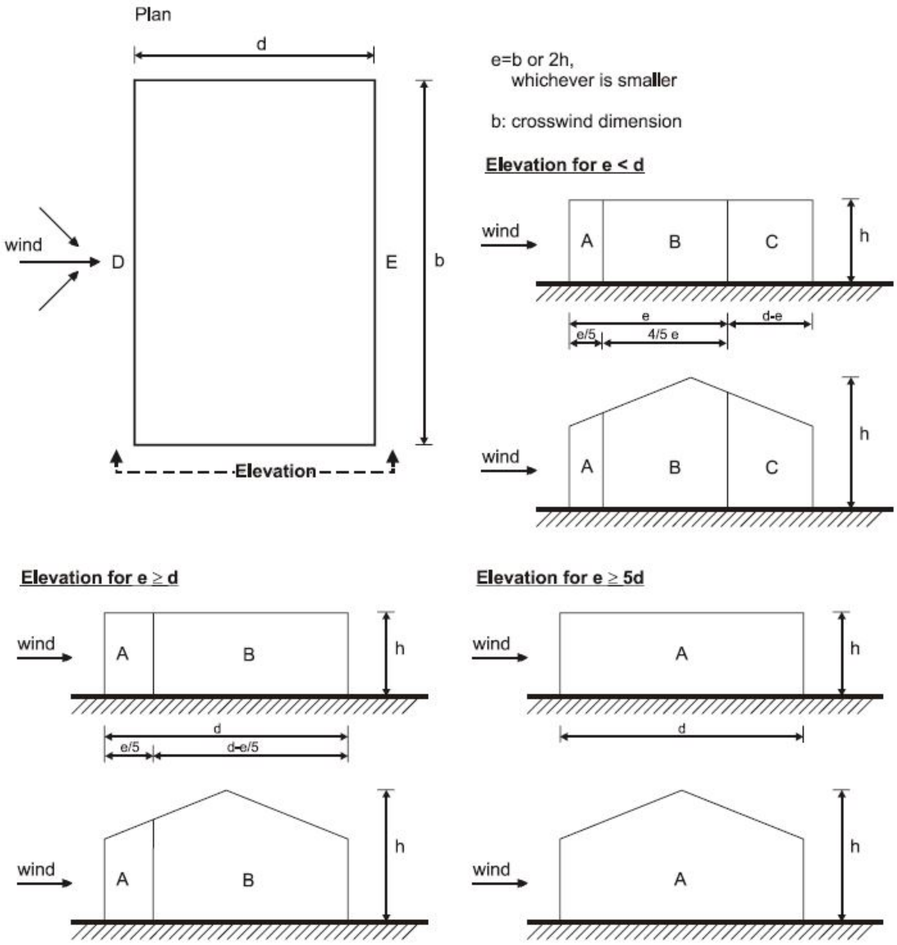
Plan
d
wind
D
E
b
Elevation
e=b or 2h,
whichever is smaller
b: crosswind dimension
Elevation for e < d
wind
A
B
C
h
e
d-e
e/5
4/5 e
Elevation for e ≥ d
e/5
d-e/5
Elevation for e ≥ 5d

Figure 3.8: Wind zones for vertical walls [6]

The value for c_sc_d does not need to be determined in all cases, e.g. a value of $c_sc_d = 1.0$ may be taken if the building height is below 15 m, this also applies if the natural frequency of the facade or roof elements is higher than 5 Hz, if a framed building has specific dimensions for the structural walls or if it meets certain conditions in the case of chimneys. In all other cases the value for c_sc_d should be determined according to a detailed procedure in the Eurocode. How exactly this works can be found in the Eurocode.

3.4. Probabilistic modelling of wind loading

This section focuses on the probabilistic modelling of wind loads. In the past, several researchers have thought about this, which has resulted in different models. These different models and also the thought process behind them is discussed in this section. How are the different parameters related to the wind load taken into account? What uncertainties lie at the origin of this? Based on all this knowledge, an

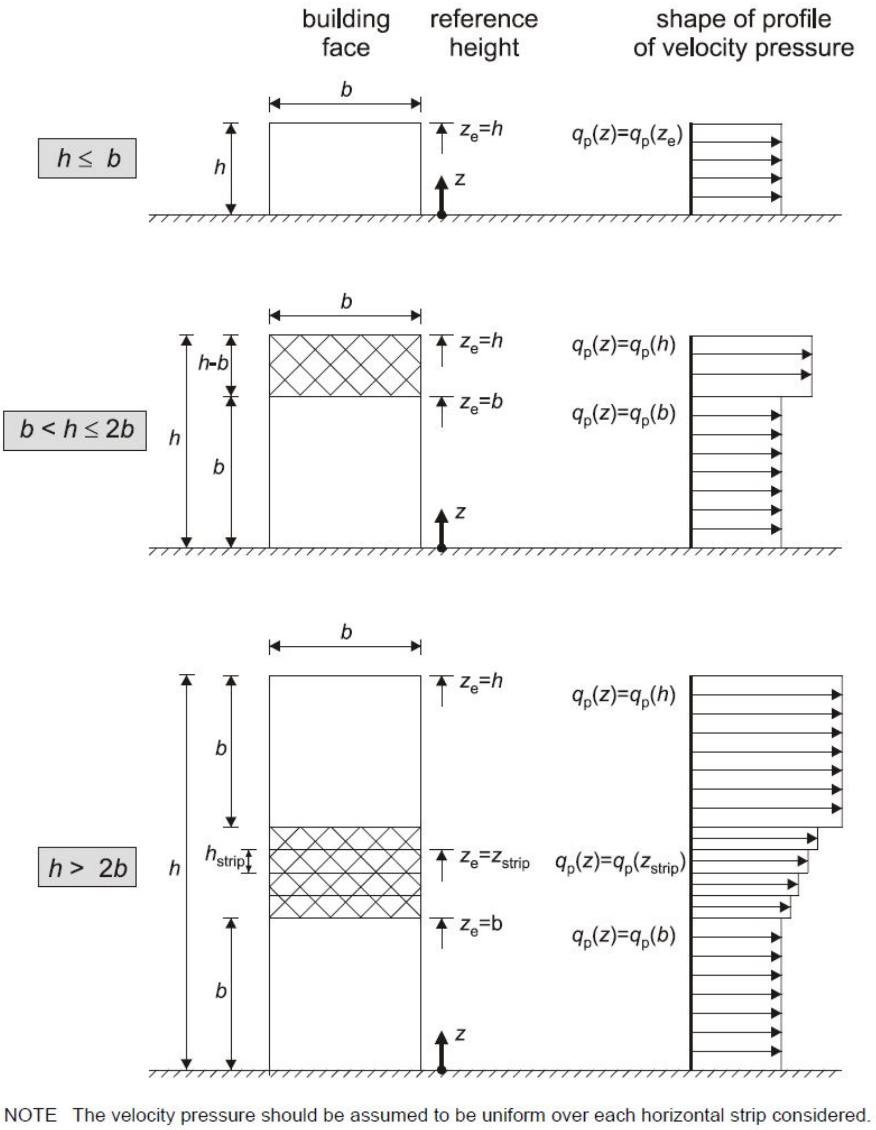
building face
reference height
shape of profile of velocity pressure
h ≤ b
b
h
z_e=h
z
q_p(z)=q_p(z_e)
b < h ≤ 2b
h-b
z_e=b
q_p(z)=q_p(h)
q_p(z)=q_p(b)
h > 2b
h_strip
z_e=z_strip
q_p(z)=q_p(z_strip)
NOTE The velocity pressure should be assumed to be uniform over each horizontal strip considered.

Figure 3.9: Reference height z_e depending on h and b, and corresponding velocity pressure profile [6]

explanation of the applicability in this research will follow at the end of this section.

From the moment Davenport formulated his wind loading chain - see also section Wind loading chain - great strides have been made in wind engineering research. Initially, the uncertainties were not so extensively incorporated in the models. However, with time, uncertainties were introduced into the models and this led to Davenport's gust-factor approach. Using the mean wind speed with a certain standard deviation and a gust response factor (GRF), peak values can be obtained. This gust factor approach only relates to the wind speed, later new methods were developed such as the Cook and Mayne method (see section Cook and Mayne method), which include uncertainties for both wind speed and pressure coefficients in a joint effect. Davenport also described a full-probabilistic model that states that the wind loading parameters are subjected to uncertainties, see section Davenport's method. However, a probabilistic description of these uncertainties is not provided. A newer model formulated by the JCSS Probabilistic Model Code, in section JCSS Probabilistic Model Code method on wind loads, does provide probabilistic descriptions for these uncertainties, however, these are still of an approximate nature. Finally, recent research by, for example, Meinen and la Gasse complements the models of Cook and Mayne and Davenport, see section Recent assessment methods. These include better stochastic modelling of extreme wind speeds, extreme pressure coefficients and other stochastic inputs. This method should also be able to provide a probabilistic description of the wind loads for longer return periods than Cook and Mayne's method.

3.4.1. Cook and Mayne method

The method of Cook and Mayne is a full probabilistic procedure for the determination of the wind load. The wind load is determined by the joint probability density function of the independent variables wind speed and aerodynamic coefficients. The general equation for the wind load is:

$$X = \frac{1}{2} \cdot \rho_{air} \cdot V^2 \cdot C \cdot A \tag{3.8}$$

With:

X = Wind load $[kN]$
V = Mean wind speed $[m/s]$
C = Peak pressure coefficient [-]
A = Reference area $[m^2]$

This factor V only includes the macro-meteorological peak - with an averaging time of $T = 1$ hour - and C includes both the wind-structure interaction and the micro-meteorological behaviour. This method aims to answer the following question; what is the value of the aerodynamic coefficient that results in a wind load with return period N, given a wind speed with the same return period N [7]? The joint probability density function (PDF) of the peak wind load can be used to answer this question. Since V and C are statistically independent, the joint PDF can be determined by the product of the individual PDFs:

$$f_{V,C}(V, C) = f_V(V) \cdot f_C(C) \tag{3.9}$$

From this the probability of exceedence of the wind load $X(N)$ with return period N can be determined in equations 3.10 and 3.11 [21]. This can also be visualised in figure 3.10, showing the joint PDF of the yearly extreme wind speeds and hourly extreme pressure coefficients. For both the annual-maximum hourly-mean wind speed and the peak loading coefficient a Type I GEV distribution is used, more explanation on these distributions can be found in Chapter 4: Probabilistic Modelling of Extremes.

$$P(X > X(N)) = \int_{V=0}^{\infty} f_V(V) \int_{C_{lim}}^{\infty} f_C(C) dC dV \tag{3.10}$$

$$C_{lim} = \frac{V(N)^2 C(N)}{V^2} \tag{3.11}$$

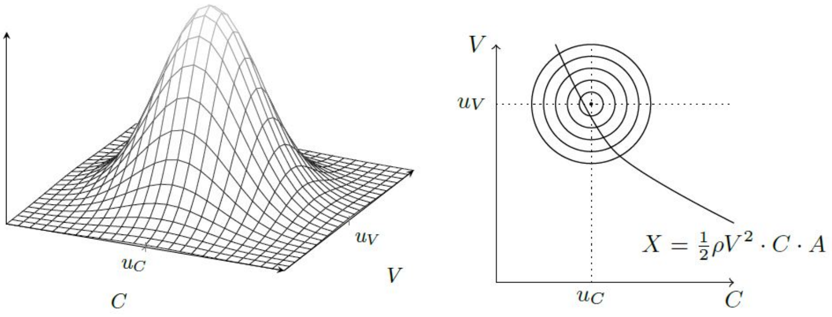

Figure 3.10: Joint PDF yearly extreme wind speeds and hourly extreme pressure coefficients [25]

Initially, only the 1st order effects were included in the above process. These 1st order effects are based on the governing annual-maximum hourly-mean wind speed and the maximum loading coefficient. However, it could also happen that the second highest wind speed in combination with a relatively

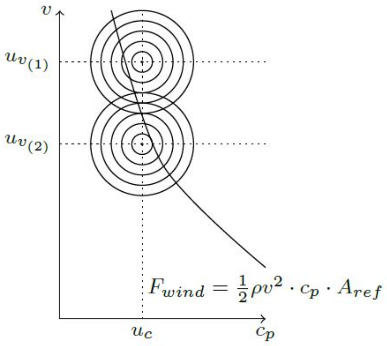

Figure 3.11: 1st and 2nd order joint PDF [25]

large peak loading can lead to governing load values (figure 3.11). To take this into account and prevent underestimation, a few corrections have been added. Research by Cook and Mayne shows that corrections up to the 5th order are good enough for design applications.

Depending on the quality of the wind speed and loading coefficient data, the results may be different. As the data is fitted to a type I GEV, the quality of the results depends on the accuracy of the fit. Cook and Mayne also found that the parent distribution of the dynamic pressure converges to the Type I GEV faster than the parent distribution of the wind speeds. Two different methods; 'q-c method' and the 'V-c method', can then be compared. If the dynamic pressure data can be fitted better than the wind speed data, it appears that the 'V-c method' overestimates and the 'q-c method' generates a correct result. In other words, the 'V-c method' is more conservative and therefore also advisable if it is not clear to what extent the dynamic pressure fits.

Finally, Cook made a simplified model in 1990. First, the sensitivity of the variation in the parameters was tested, which showed a small dependence between the return period and a small range of fitted distribution parameters. Based on this, a 'Cook-Mayne coefficient' was defined, resulting in a standard design value for peak loading. In the UK, this design value corresponds to the 0.78-fractile of the peak loading coefficient data.

3.4.2. Davenport's method

Davenport also developed a method to determine the reliability of wind loading. Davenport, also known for his wind loading chain, uses this chain and states that all the individual elements have uncertainties. The wind pressure can be determined as follows:

$$p = q \cdot c_e \cdot c_p \cdot c_g \tag{3.12}$$

With:

p = Wind pressure [N/m^2]
q = Dynamic pressure [N/m^2]
c_e = Terrain roughness correction factor [-]
c_p = Mean pressure coefficient [-]
c_g = Gust correction factor [-]

Davenport assumes that all elements contain uncertainties and also describes a model uncertainty factor μ. This factor corrects for deviations between the specified and actual wind load. A first estimate for this model uncertainty according to Davenport is approximately $V_\mu = 0.14$.

In addition, Davenport assumes that all variables are stochastic, with a certain mean and coefficient of variation (see figure 3.12). Assuming that the parameters are statistically independent, the mean wind load and variability can be determined with equations 3.13 and 3.14. These can also be described as the ratio of the mean to specified value, see equation 3.15.

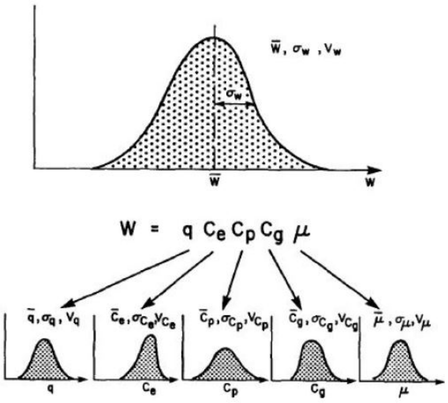

Figure 3.12: Stochastic parameters from Davenport's wind loading chain [9]

$$\overline{p} = \overline{q} \cdot \overline{c_e} \cdot \overline{c_p} \cdot \overline{c_g} \cdot \overline{\mu} \tag{3.13}$$

$$(1 + COV_p^2) = (1 + COV_q^2) \cdot (1 + COV_{c_e}^2) \cdot (1 + COV_{c_p}^2) \cdot (1 + COV_{c_g}^2) \cdot (1 + COV_{\mu}^2) \tag{3.14}$$

$$\frac{\overline{p}}{(p)_s} = \frac{\overline{q}}{(q)_s} \cdot \frac{\overline{c_e}}{(c_e)_s} \cdot \frac{\overline{c_p}}{(c_p)_s} \cdot \frac{\overline{c_g}}{(c_g)_s} \cdot \overline{\mu} \tag{3.15}$$

Davenport also defined a full probabilistic method for determining the structural reliability of wind loaded buildings, based on the second moment reliability theory with wind load uncertainty factors. This theory firstly assumes that the stochastic variables in the limit state function are determined by a first and second moment, or respectively mean value and standard deviation. Secondly, this theory is based on the Central Limit Theorem; the combination (sum or product) of independent stochastic variables will result in a normal or log-normal distribution, even if the underlying distributions are not normal or log-normal.

Finally, Davenport uses the safety factor approach to deal with these uncertainties. How this method works exactly is described in Davenport [9] and Meinen [25].

3.4.3. JCSS Probabilistic Model Code method on wind loads

In addition, the Joint Committee on Structural Safety (JCSS), which deals with structural risk and reliability, also made a probabilistic model of the wind loads. This can be found in *'part 2: loads, chapter 13 wind'* [27]. Davenport's wind loading chain is also in this method the fundamental basis. For the wind forces per unit area on a structure two categories are distinguished. Like Davenport, the JCSS assumes that all parameters affecting wind forces on structures contain uncertainties. For the mean $\overline{w}$ and coefficient of variation COV of the wind forces the following equations can be applied. It is assumed that the variables are uncorrelated. For these parameters, in general, a lognormal distribution according to JCSS can be used. The mean-to-specified values and the coefficient of variation of these parameters are given in table 3.5.

- Small rigid structures:

$$w = c_a \cdot c_g \cdot c_r \cdot \overline{Q}_{ref} = c_a \cdot c_e \cdot \overline{Q}_{ref} \tag{3.16}$$

$$\overline{w} = \overline{c_a} \cdot \overline{c_e} \cdot \overline{\overline{Q}_{ref}} \tag{3.17}$$

$$COV_w^2 = COV_{c_a}^2 + COV_{c_e}^2 + COV_{Q_{ref}}^2 \tag{3.18}$$

- Large rigid structures and dynamically sensitive structures (natural frequency < 1 Hz):

$$w = c_d \cdot c_a \cdot c_g \cdot c_r \cdot \overline{Q}_{ref} = c_d \cdot c_a \cdot c_e \cdot \overline{Q}_{ref} \tag{3.19}$$

$$\overline{w} = \overline{c_d} \cdot \overline{c_a} \cdot \overline{c_e} \cdot \overline{\overline{Q}_{ref}} \tag{3.20}$$

$$COV_w^2 = COV_{cd}^2 + COV_{ca}^2 + COV_{ce}^2 + COV_{Qref}^2 \tag{3.21}$$

With:

$\overline{Q}_{ref}$ = Reference (mean) velocity pressure $[N/m^2]$
c_a = Aerodynamic shape factor [-]
c_g = Gust factor [-]
c_r = Roughness factor [-]
c_d = Dynamic factor [-]
c_e = Exposure factor $(c_g \cdot c_r)$ [-]

Variable	$\frac{\text{Mean}}{\text{Specified}}$	COV
$\overline{Q}_{ref}$	0.8	0.2 - 0.3
c_r	0.8	0.1 - 0.2
c_a (pressure coefficients)	1.0	0.1 - 0.3
c_a (force coefficients)	1.0	0.1 - 0.15
c_g	1.0	0.1 - 0.15
c_d	1.0	0.1 - 0.2

Table 3.5: Random variables occuring in the assessment of the wind loading [27]

3.4.4. Recent assessment methods

Meinen's research [25] has attempted to extend the method of both Cook and Davenport in the form of a full probabilistic assessment procedure of façade elements loaded by wind. Here the wind direction dependent component is also included in the analysis. In this full probabilistic assessment both the load and the resistance part are included in the reliability analysis. However, the resistance part is included in a simplistic form. The scheme for this assessment procedure is shown in appendix Assessment Procedure: la Gasse and Meinen. The wind load model is formulated in equation 3.22.

In la Gasse's research [23], a complete probabilistic assessment procedure is developed in which dynamically sensitive buildings are addressed. All uncertainties regarding the wind climate, dynamic response, global pressure effects and resistance are included. The results of the case study show that the uncertainties in the wind speed have the largest influence on the derived reliability levels.

$$S(z, \theta_i) = \frac{1}{2} \cdot \rho_{air} \cdot v_{1hr,N}(\theta_i)^2 \cdot S_v(\theta_i)^2 \cdot c_r(z, \theta_i)^2 \cdot \hat{c}_{pe,1hr}(\theta_i) \cdot A_{ref} \cdot \chi_{model} \tag{3.22}$$

With:

$S(z,\theta_i)$ = Direction dependent N-yearly extreme wind loads
θ_i = Incident wind direction [-]
$v_{1hr,N}(\theta_i)$ = Direction dependent N-yearly extreme hourly-mean wind speed at height $z_{ref} = 10\ m\ [m/s]$
S_v = Direction dependent factor considering sampling uncertainties of basic wind velocity modelling [-]
$c_r(\theta_i)$ = Direction dependent roughness factor correcting for height z [-]
$\hat{c}_{pe,1hr}(\theta_i)$ = Direction dependent hourly extreme peak external pressure coefficient [-]
A_{ref} = Reference area façade element $[m^2]$
χ_{model} = Model uncertainty factor [-]

3.4.5. Discussion

The different methods described above clearly show the process of increasingly sophisticated models. One model serves as input for the next with some additions here and there. This is all to describe the reality and also to include the uncertainties in the wind loading as well as possible. Cook and Mayne included both the uncertainties in the extreme wind speeds and the extreme pressure coefficients in a probabilistic way. All other uncertainties that occur in the other parameters are not included. However, Davenport noted that these uncertainties of all parameters are indeed important and should therefore be included. However, he did not describe them in a probabilistic way. These uncertainties are subsequently described - in an approximate manner - in the JCSS Probabilistic Model Code. More recent research, such as that of Meinen and la Gasse [25] [23], has resulted in better probabilistic descriptions of certain parameters and also a stochastic wind loading model. It is worth noting, however, that the buildings in these studies were described in a relatively simple manner. This is in contrast to this research, where the building - including all structural elements, supports, connections, etc. - is fully modelled in a 3D finite element model. In this way, the construction is included in this research in a more realistic and detailed way. Also the strength of the material and of the elements is included in a more detailed way in the full probabilistic descriptions. Also other aspects related to the specific failure mechanisms, like moment resistance and buckling resistance are included in the reliability assessment.

4

Probabilistic Modelling of Extremes

Describing the wind speeds and wind load effects in a stochastic load model requires the modelling of extremes. Therefore, this chapter provides the necessary theory on the probabilistic modelling of extreme values, which can then be used further in this research.

When it comes to the ultimate limit cases, we are often not so much interested in the averages of the data or the events that occur regularly, but rather in the cases that only occur in a small number of situations and lead to extreme values. These extreme values take place in the tail of the distribution function, i.e the highest probability fractiles in the cumulative distribution function. Therefore, this chapter focuses on the probabilistic modelling of extremes. How can we properly study and describe the maxima or minima (depending on the type of variable we are interested in) of a certain effect? For those cases we can use extreme value distributions.

4.1. Specification sample data

The sample data, which contains the measurements of a certain variable, is the input that serves in the description of an extreme value distribution. In general, this data contains N values, which can be placed in ascending order according to their magnitude:

$$\vec{X}_N = X_{(1)}, X_{(2)}, \dots, X_{(N)} \tag{4.1}$$

The sample data can be characterised using a number of parameters. The mean of the data can be described by the sample mean $\hat{\mu}_X$, the spread of a variable by the sample standard deviation $\hat{\sigma}_X$ or the coefficient of variation $\hat{V}_X$ and finally by the unbiased sample skewness $\hat{\alpha}_X$. See also the definitions for these parameters in equations 4.2 to 4.5. The skewness of the data can be zero, positive or negative (see also figure 4.1) and indicates the degree of asymmetry of the sample data.

$$\hat{\mu}_X = \frac{1}{N}\sum_{i=1}^{N} X_i \tag{4.2}$$

$$\hat{\sigma}_X = \sqrt{\frac{1}{N-1}\sum_{i=1}^{N}(X_i - \hat{\mu}_x)^2} \tag{4.3}$$

$$\hat{V}_X = \frac{\hat{\sigma}_X}{\hat{\mu}_X} \tag{4.4}$$

$$\hat{\alpha}_X = \frac{N^2}{(N-1)(N-2)} \cdot \frac{1}{N\hat{\sigma}_X^3}\sum_{i=1}^{N}(X_i - \hat{\mu}_x)^3 \tag{4.5}$$

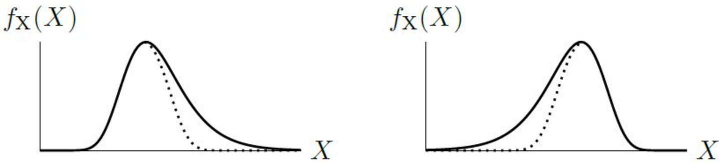

Figure 4.1: Skewness of a certain distribution; on the left a positive skew and on the right a negative skew

However, there are some requirements for using the data to describe an extreme value distribution. First of all, the data must be identically distributed, i.e. the deviations caused by the presence of sampling and observation errors must be reduced. The second requirement is that the data must be statistically independent, which means that the measurements do not depend on or influence each other.

4.2. Theory on extreme values

There are various models that are used to fit the extremes, which model gives the best result and what suitable parameters should be chosen, can be determined using extreme value theory. The foundation of this theory is based on the fact that the data satisfies the above conditions; independent and identically distributed sample data.

4.2.1. Univariate theorem

The univariate theorem is a convenient method that can be used if $\vec{X}_N = X_{(1)}, X_{(2)}, ..., X_{(N)}$ are independent and identically distributed random variables with a cumulative distribution function F.In that case, the extreme values in a period of time T can be derived from the extreme values that occur in a period of time t. This is very useful when there is only a limited amount of data and this has to be scaled to the T-extremes. The theory is formulated in the following equations:

$$P(X \leq \hat{X})_T = P(X \leq \hat{X})_t^{T/t} \tag{4.6}$$

$$F_T(X) = F_t(X)^{T/t} \tag{4.7}$$

4.2.2. Generalised extreme value distribution

The extreme value distributions, both for maxima as well as minima, are classified in three categories: type I (Gumbel), type II (Frèchet) and type III (reversed Weibull). The Fisher-Tippett-Gnedenko theorem [14] [17] says that if the distribution of a normalised maximum converges, the limit distribution is part of the generalised extreme value distribution and not of anything else. The cumulative distribution function of the generalised extreme value distribution is formulated as follows:

$$F_X(X) = exp\left(-\left(1 + \xi\left(\frac{X-\mu}{\sigma}\right)\right)^{-1/\xi}\right) \tag{4.8}$$

Three parameters are used in this model. $\xi \in \mathbb{R}$ is the shape parameter, which describes the behaviour of the distribution in the tail; $\mu \in \mathbb{R}$ is the location parameter, which takes care of the translation of the complete distribution and finally there is $\sigma > 0$ the scale parameter, which describes the statistical dispersion of the distribution. Based on the shape parameter ξ, three types of distributions - as also mentioned above - can be distinguished. The three types can also be seen in both the normal domain and the Gumbel domain in Figure 4.2.

- Type I: Gumbel distribution, in the case that $\xi = 0$. The general formula from equation 4.8 can be replaced by the following definition, if $\xi \longrightarrow 0$ in the limit:

  $$F_X(X) = exp\left(-exp\left(-\frac{X-\mu}{\sigma}\right)\right) \tag{4.9}$$

  The possible range of the values of $X \in (-\infty, \infty)$.

- Type II: Frèchet distribution, in the case that $\xi > 0$. In this case, there is a minimum value of the probability density function that X can adopt: $X > \mu - \frac{\sigma}{\xi}$

- Type III: Reversed Weibull distribution, in the case that $\xi < 0$. In this case, there is a maximum value of the probability density function that X can adopt: $X < \mu + \frac{\sigma}{-\xi}$

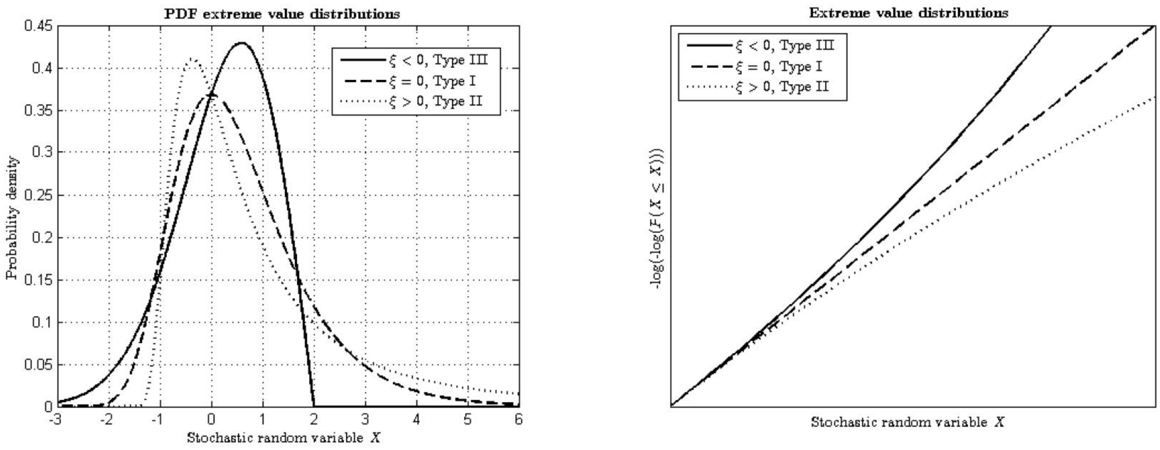

Figure 4.2: The three different distributions; type I (Gumbel), type II (Frèchet) and type III (Reversed Weibull) in both the PDF in normal domain (left) and CDF in the Gumbel domain (right) [25]

4.2.3. Methods for estimating high probability quantiles

Two different methods can be distinguished in the literature for determining which values should be chosen from the sample data, so that the high probability quantiles can be described properly. These two methods, the *Block Method* and the *Peak over Threshold Method*, are explained in more detail below and they are also compared in order to make a good decision about which method to use in this study.

Block method

In the Block Method, time is divided into blocks of a duration of time t (see figure 4.3). For each of these blocks of time, the maximum (or minimum) value will be used, then with these values one of the three extreme value distributions will be fitted to this data. Finally, using the univariate theorem, the extreme values for a longer reference period can be calculated.

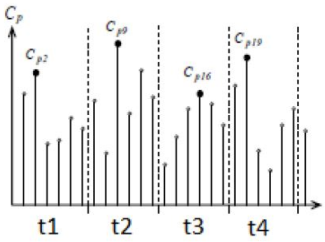

Figure 4.3: Block method [25]

One of the difficulties in applying the Block Method is choosing the correct block duration t. The number of extreme values that can be extracted from a data sample in the total time is: $N = \frac{T_{tot}}{t}$. Since for applying the various theories in this field the data must be statistically independent, the block duration t must be such that it results in statistically independent extremes. However, if the block duration t is too large, this will result in a smaller number of N extremes, which only increases the sampling uncertainties on this small amount of data. Applying time laps is also a way of preserving statistical independence.

Peak over threshold method

The second method, the Peak over threshold method, assumes a certain threshold U (see figure 4.4). All values over the entire time period that are above this threshold U (or below in case of a minimum) are included in the follow-up analyses for determining the extreme value distribution.

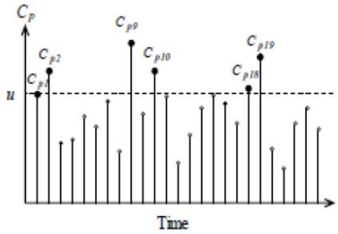

Figure 4.4: Peak over threshold method [25]

The difficulty in this method lies in the correct choice of threshold U ; if a too high value is chosen for threshold U, it may happen that too few data points are left for the follow-up analyses. In that case, there is a chance that sampling uncertainties occur due to the small amount of data. The Pickands-Balkema-de Haan theory [3] [30] shows that for such a threshold U that most of the underlying distributions, the normalized cumulative excess distribution function $F_U(X)$ converges to the Generalized Pareto Distribution (GPD).

$$F_U(X) \longrightarrow GPD(X|U,\sigma,\xi), \quad \text{as } U \longrightarrow \infty \tag{4.10}$$

In other words: a too low choice for the threshold value U, will result in a too large amount of data points, which also do not all have a Poisson arrival rate and therefore do not converge to the GPD asymptote. In that case, an incorrect distribution may be taken as the true distribution.

Since all values above a certain threshold U are included, it can happen that data points that are close to each other in time are selected, which means that the independency in the data cannot be guaranteed. Therefore, the data that remains after applying the threshold value must always be checked for the presence of dependency. If that is the case, they must first be de-clustered.

Comparison between methods and decision for this study

Meinen's study [25] contains a detailed comparison between the two methods. The main points that can be deduced from this are in table 4.1.

Regarding the selection of the extreme values, there is a chance that the relatively high values are not included in the block method. This is not the case for the peak over threshold method. However, the peak over threshold method is more complex to ensure that all extreme values are statistically independent of each other. This is easier to achieve in the block method. Another important point concerns the robustness, in other words, the consequences of certain decisions on the end result. The peak over threshold method is quite sensitive to the choice of the threshold value U and separation technique to get statistical independent data. In this respect, the block method is more robust, although the choice of the block duration can also influence the results, but a block duration is chosen that yields the most extreme values and therefore the least sampling uncertainties. Based on all these observations, it is decided to use the block method in this research.

	Block Method	Peak over Threshold Method
Selected extreme values	Possible loss of information; because there is a possibility that the 2nd highest value in block 1 $X_{(1,2)}$, which is also statistically independent of the 1st highest value in block 1 $X_{(1,1)}$, is higher than the highest value in block 2 $X_{(2,1)}$.	Gives better observation of the extremes, since all the k (independent) highest extremes $X_{(1)}, ..., X_{(k)}$ are taken into account.
Obtaining statistical independent sample data	Relatively easy to guarantee statistical independency by selecting large block-duration t and use of time laps.	More effort-full to obtain statistical independency, since the obtained extremes might need to be de-clustered (way of declustering often topic of concern).
Dealing with inhomogeneities	If sample data *covers* all underlying mechanisms: can deal with inhomogeneities within blocks, if covered in a representative way. If sample data *not covers* all underlying mechanisms: not able to detect and allow for inhomogeneities.	If sample data *covers* all underlying mechanisms: mechanisms should be modelled separately, accounting for probability of each mechanism. If sample data *not covers* all underlying mechanisms: mechanisms should be modelled separately, accounting for probability of each mechanism.
Robustness (consequence of choices)	Consequences of for instance too short block-duration t not that significant.	The consequences of choices regarding the threshold value U and minimum separation are significant, a too low threshold value can even lead to a totally wrong extreme value distribution.
Sampling uncertainties	A too large block-duration t leads to fewer data points in the extreme value distribution and thus to larger sampling uncertainties.	A threshold value U that is too high leads to fewer data points in the extreme value distribution and thus to greater sampling uncertainties.

Table 4.1: Comparison between both methods; Block Method & Peak over Threshold Method [25]

5

Probabilistic Structural Resistance Model

In a perfect world, models and reality would be one to one related to each other, however, this utopic world does not exist. It is therefore necessary to understand the differences between theory, corresponding models and real-life. Probabilistic models are formulated in order to coop with these uncertainties. In addition, the material also contains an intrinsic uncertainty that affects its modelling. The manufacture of the material plays a major role in this. This chapter deals with the uncertainties of the resistance - material - side of the structure. Specifying these uncertainties and setting up a probabilistic structural resistance model is required to determine, in combination with a probabilistic load effect model, the reliability of the structure in a full probabilistic way. In the first part of this chapter Material properties steel, probabilistic models for the steel material properties are described. Followed by probabilistic models regarding dimension, initial imperfections of elements and model uncertainties in respectively section Dimensional properties, Initial imperfections element and Model uncertainties. Most of the information in this chapter is based on the *JCSS (Joint Committee on Structural Safety) Probabilistic Model Code Part 3: Material Properties* document [28]. Finally, existing research related to reliability analysis of steel buildings is discussed in section Existing research on reliability analysis steel buildings. This knowledge can then be used for the current research.

5.1. Material properties steel

The material properties of structural elements, such as steel, are based on a mathematical model and random variables. These models and variables are determined from experience and (standardised) tests. The material properties which are of consideration in the probabilistic model are; yield strength f_y, ultimate tensile strength f_u, modulus of elasticity E, Poisson's ratio v and ultimate strain ϵ_u. A probabilistic model is based on standard mill tests or values given in material specifications.

The random variables (f_y,f_u,E,v,ϵ_u) can be specified with a specific mean value μ_X and standard deviation σ_X (see table 5.1). The correlations between the variables are mentioned in table 5.2. These values hold for static loading and for steel grades and quality given in EN 1990 [15] with yield strength f_y up to 380 MPa. The variation in yield strength is mainly caused by the chemical composition and rolling conditions.

---

[1] $\alpha = 1.05$ for webs of hot rolled sections and $\alpha = 1.0$ otherwise. u is a factor related to the fractile of the distribution used in describing the distance between the code specified or nominal value and the mean value. u (for steel produced according to EN standards) in range of -1.5 to -2.0. For constant C a value of 20 MPa is recommended.

[2] k_s in interval between 2 to 2.5 depending on execution control (2 for mills which do not regularly control the quality and 2.5 for efficient quality control) [5]

[3] Value of κ between 1.1 and 1.5 depending on type of steel (quenched and tempered steel: κ = 1.1, low alloy steel: κ = 1.4, structural carbon steel: κ = 1.5)

Variable	Distribution type	Mean μ_X	Standard deviation σ_X
f_y (version 1)	Log-normal	$f_{y,k} \cdot \alpha \cdot exp(-u \cdot v) - C$ [1]	0.07 μ_X
f_y (version 2)	Log-normal	$f_{y,k} + k_s \cdot \sigma$ [2]	0.08 μ_X
f_u	Log-normal	$\kappa\mu_{f_y}$ [3]	0.05 μ_X
E	Log-normal	E_k	0.03 μ_X
v	Log-normal	v_k	0.03 μ_X
ϵ_u	Log-normal	$\epsilon_{u,k}$	0.06 μ_X

Table 5.1: Mean and standard deviation material properties structural steel (rolled sections) [5][28]

	f_y	f_u	E	v	ϵ_u
f_y	1	0.75	0	0	-0.45
f_u		1	0	0	-0.60
E			1	0	0
v				1	0
ϵ_u					1

Table 5.2: Correlation matrix material properties structural steel (rolled sections) [28]

5.2. Dimensional properties

In table 5.3 the distribution type, mean value and standard deviation regarding the dimensional properties for IPE profiles, L-sections and rods is shown. For a general structure it can be assumed that most of the profiles are produced at one specific company, therefore the production process is quite similar for most of the beams and columns of the structure. Based on that knowledge a positive correlation between the material properties and also the dimensional properties between the steel profiles is assumed. A correlation value of $\rho = 1.0$ is conservative and safe to use [5].

Variable	Distribution type	Mean μ_X	Standard deviation σ_X
A, W, I (IPE profiles)	Normal	$0.99X_{nom}$	$0.01 - 0.04\mu_X$
A, W, I (L-sections, rods)	Normal	$1.02X_{nom}$	$0.01 - 0.02\mu_X$

Table 5.3: Mean and standard deviation dimensional properties [5]

5.3. Initial imperfections element

In theory - elements and specific columns - are assumed to be perfectly vertical, completely straight and without any initial sway. However, this is not the case in reality. In reality three types of initial imperfections can be identified; average eccentricity e, initial curvature f and out of plumbness ϕ (see figure 5.1). These initial imperfections lead to differences in the theoretical and actual resistance capacity of the element.

The stochastic parameters for these initial imperfections are in table 5.4. It is assumed that these initial imperfections are independent variables. The dependency between several columns in one structure is modelled in the following way according to the *JCSS document* [28]. The average eccentricity e and initial curvature f of the columns are considered being uncorrelated in the structure, however, for the

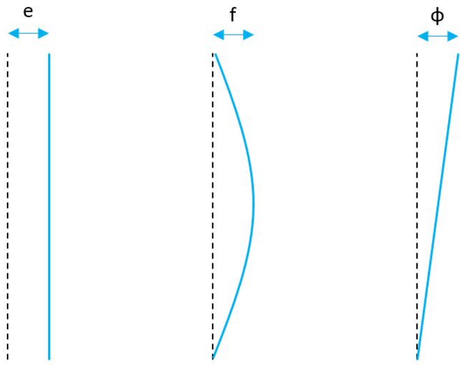

Figure 5.1: Three types of initial imperfections e, f and ϕ

out of plumbness ϕ it is recommended to use a correlation of $\rho(\phi_i, \phi_j) = 0.5$ for two columns on the same floor and $\rho(\phi_i, \phi_j) = 0$ for two columns on different floors.

5.3.1. Sensitivity analysis of the initial imperfections on a steel element

Elishakoff et al. [11] came to the conclusion that the deviation in the initial deflection have significant effects on the probability distribution of the buckling load and also on the reliability of the column [11]. The study, in which a finite column on a non-linear elastic foundation was examined for the normative buckling load, showed that the buckling load is sensitive to the initial deflections. It is therefore very important to include this aspect in this study, as it has a contribution to the ultimate failure probability of a certain element. There are several ways to include this aspect in the reliability analysis, one is to include it in a general model uncertainty, another is to include it directly in the model.

Variable	Distribution type	Mean μ_X	Standard deviation σ_X
e	Normal	0	$L/1000$
f	Normal	0	$L/1000$
ϕ	Normal	0	$0.0015\,rad$

Table 5.4: Mean and standard deviation initial imperfections element [28]

In the study by Kala [20], the sensitivity and statistical characteristics of the load-carrying capacity of a steel portal frame were examined. The two extreme boundary cases are modelled in Frame 1 and Frame 2 (see Figure 5.2). It also looked at how the elements influence each other and how this directly affects the load-carrying capacity. In addition, the initial imperfections - think of material properties imperfections, dimensional properties, but also of eccentricities of the element such as initial curvature or bow imperfection f (noted in the study with a δ_1 and δ_2, see figure 5.3) and the out of plumbness ϕ (noted in the study with a θ_1 and θ_2, see figure 5.3) - have been investigated.

For the global sensitivity analysis of the two portal frames, the Sobol' decomposition method was used. This method shows the specific influence of various input parameters on the monitored output. In this case, the imperfections are the input parameters in the form of stochastic variables and the measured output is the load-carrying capacity.

The Sobol' first-order and second-order sensitivity index are formulated in equations 5.1 and 5.2. S_i indicates how much effect a certain input random variable X_i has on the output. S_{ij} $(i \neq j)$ is the second-order sensitivity index and indicates the effect of the interaction between a pair of input parameters (X_i and X_j). The great advantage of the Sobol' method over the normal sensitivity analysis is that the

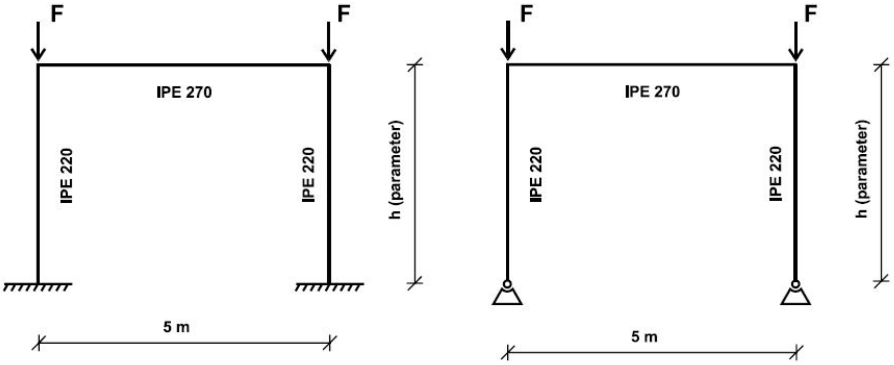

Figure 5.2: Frame 1 on the left (rotation and translation fixed boundary conditions) and Frame 2 on the right (rotation free and translation fixed boundary conditions) in study from Kala [20]

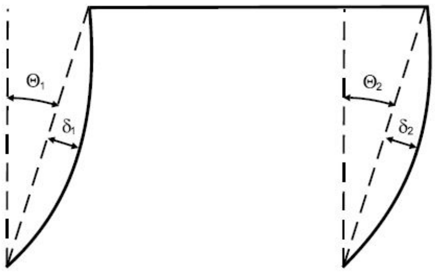

Figure 5.3: Initial sway and bow imperfections in study from Kala [20]

interaction between the different terms in the higher powers is also included in the analysis.

$$S_i = \frac{V(E(Y|X_i))}{V(Y)} \tag{5.1}$$

$$S_{ij} = \frac{V(E(Y|X_i, X_j))}{V(Y)} - S_i - S_j \tag{5.2}$$

The results for the 2 different frames are shown in figure 5.4a and 5.4b. All included input parameters and the corresponding Sobol' sensitivity are plotted against the non-dimensional slenderness $\overline{\lambda}$. Both figures show a similar behaviour. The imperfection out of plumbness correspond to variables S_{21} and S_{22} in the figures. These show a clear peak in the region of $\overline{\lambda} = 1.0$, they have a great impact on the load-carrying capacity of the structure. The other geometrical imperfection that was taken into account, the initial curvature δ, is in variables S_7 and S_{20}. It does not show a clear spike over the whole range of $\overline{\lambda}$ and therefore only contributes to a small extent to the load-carrying capacity of the structure. What is also noticeable is that for a small value of lambda, especially S_6 and S_{19} - these variables relate to the yield strength f_y of the two columns - have a large contribution to the output of the model. However, this influence diminishes again for a larger value of lambda. If such a large value for the non-dimensional slenderness lambda is considered, it can be seen that it is mainly S_5 and S_{18} that have a large contribution. These variables are related to the Young's modulus E of both columns.

5.4. Model uncertainties

The models described above are capable of predicting the behaviour of the structure at a reasonably good level, but there will still be discrepancies between the mathematical models and experiments performed in real life. Differences between the results from the mathematical formulations and reality may be due to the lack of certain characteristics of the material, simplifications in the mathematical formulations, overlooked interactions of certain elements, questionable boundary conditions, imperfections, etc. Therefore model uncertainties are formulated to coop with these errors. These model uncertainties are derived based on the differences between the observed values during experiments or on real

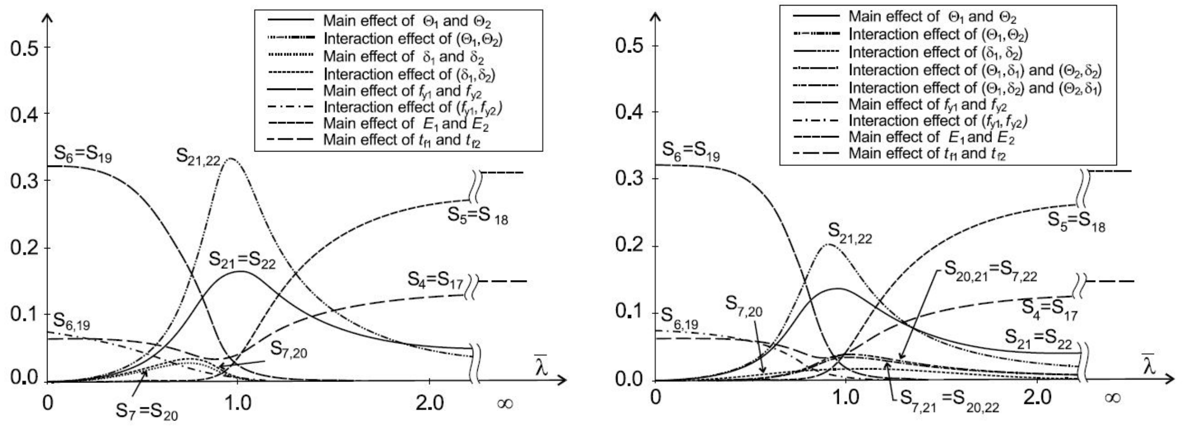

(a) Sobol's sensitivity indices of Frame 1 vs. non-dimensional slenderness $\bar{\lambda}$ [20]

(b) Sobol's sensitivity indices of Frame 2 vs. non-dimensional slenderness $\bar{\lambda}$ [20]

Figure 5.4

structures and model values.

There are several categories for the model uncertainties; load effect uncertainties and resistance uncertainties. The load effect uncertainties deal with for instance 3d-effects, inhomogenities, interactions, boundary effects, simplification of connection behaviour, imperfections, etc. This will also depend on the type of structure. The resistance uncertainties on the other hand, deal with for instance the visco-elastic properties of the material, elastic-plastic model, yield condition, hardening and softening behaviour, thermal properties, etc.

The *JCSS* document [28] provides recommended probabilistic models for the model uncertainties. The models regarding the load effect uncertainties are in table 5.5 and for the resistance uncertainties are in table 5.6. In annex Resistance Model Uncertainties a complete overview of all the model uncertainties regarding the resistance of steel structures is shown. These models are based on the background documentation of *Eurocode 3*.

Load effect	Distribution type	Mean μ_X	Standard deviation σ_X
Moments in frames	Log-normal	1.0	$0.10\mu_X$
Axial forces in frames	Log-normal	1.0	$0.05\mu_X$
Shear forces in frames	Log-normal	1.0	$0.10\mu_X$
Moments in plates	Log-normal	1.0	$0.20\mu_X$
Forces in plates	Log-normal	1.0	$0.10\mu_X$
Stresses in 2D solids	normal	0.0	$0.05\mu_X$
Stresses in 3D solids	normal	0.0	$0.05\mu_X$

Table 5.5: Load effect model uncertainties [28]

---

[4] Including effects due to normal and shear forces

Model type	Distribution type	Mean μ_X	Standard deviation σ_X
Bending moment capacity [4]	Log-normal	1.0	$0.05\mu_X$
Shear capacity	Log-normal	1.0	$0.05\mu_X$
Welded connection capacity	Log-normal	1.15	$0.15\mu_X$
Bolted connection capacity	Log-normal	1.25	$0.15\mu_X$

Table 5.6: Resistance model uncertainties [28]

5.5. Existing research on reliability analysis steel buildings

Several studies have been conducted on the reliability analysis of steel buildings. These studies and the methodologies used in them can serve as a useful basis for this research. One of those researches that deals extensively with a complete reliability analysis of steel buildings is *'Probabilistic quantification of safety of a steel structure highlighting the potential of steel versus other materials'* (in this research abbreviated to *'Proqua'*) [5].

5.5.1. 'Proqua' strategy: example steel office building

First, a steel office building is designed based on the Eurocode standards (deterministic design). This building is further used for the reliability analysis. The results of this analysis tell us something about the reliability of the building by using the Eurocode standards. Next the building is (probabilistic) re-designed and optimized for a reliability index $\beta = 3.8$.

The design of the building is shown in figure 5.5. A probabilistic analysis is performed for the steel beams and columns at the ground level. The columns at ground level are chosen because here the axial forces are the largest due to the weight of the structure above. Based on the corresponding resistance functions of the various elements, the limit state functions are derived. The statistical parameters used in the FORM analysis are shown in figure 5.7.

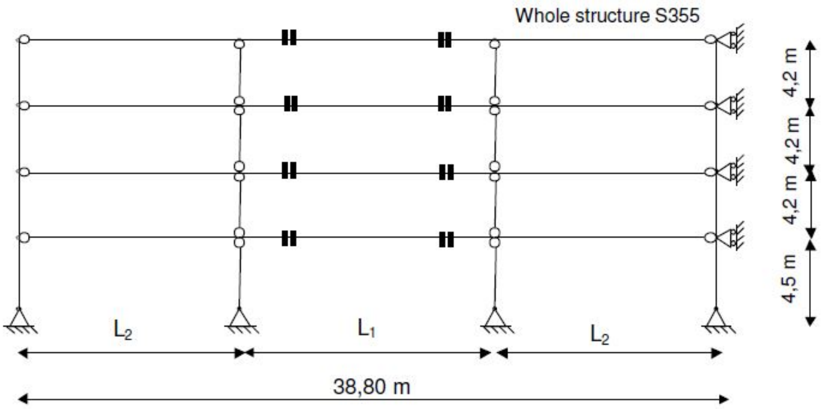

Figure 5.5: Steel office building example; general geometry and steel grades of the steel frame [5]

For beams the plastic bending resistance is calculated as follows:

$$M_{pl,y} = f_y \cdot W_{pl,y} \tag{5.3}$$

Buckling about the strong axis, with dimensionless slenderness $\bar{\lambda}$ and factor $\alpha = 0.34$ for buckling curve a, gives the reduction factor χ:

$$\chi = \frac{1}{\theta + \sqrt{\theta^2 - \bar{\lambda}^2}} \tag{5.4}$$

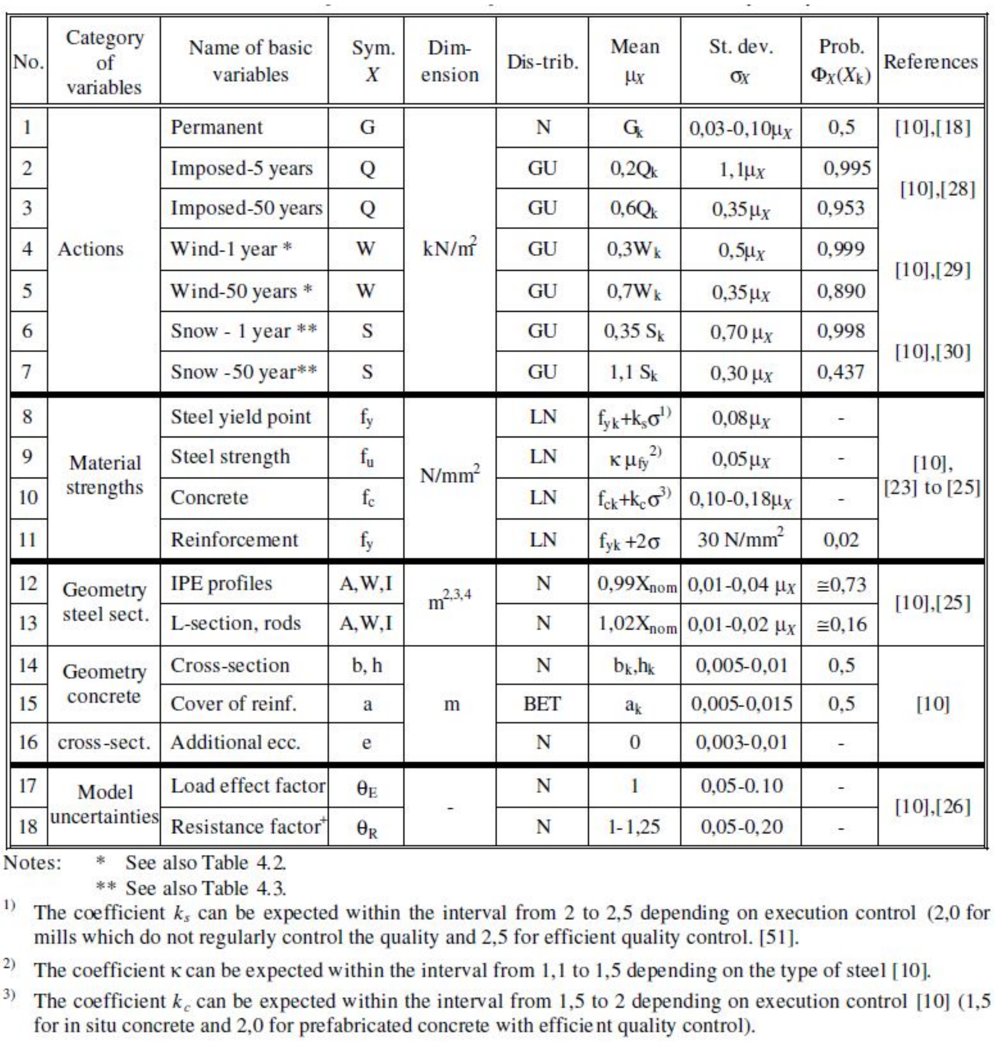

No.	Category of variables	Name of basic variables	Sym. X	Dim-ension	Dis-trib.	Mean μ_X	St. dev. σ_X	Prob. $\Phi_X(X_k)$	References
1	Actions	Permanent	G	kN/m²	N	G_k	0,03-0,10μ_X	0,5	[10],[18]
2		Imposed-5 years	Q		GU	0,2Q_k	1,1μ_X	0,995	[10],[28]
3		Imposed-50 years	Q		GU	0,6Q_k	0,35μ_X	0,953	
4		Wind-1 year *	W		GU	0,3W_k	0,5μ_X	0,999	[10],[29]
5		Wind-50 years *	W		GU	0,7W_k	0,35μ_X	0,890	
6		Snow - 1 year **	S		GU	0,35 S_k	0,70 μ_X	0,998	[10],[30]
7		Snow -50 year**	S		GU	1,1 S_k	0,30 μ_X	0,437	
8	Material strengths	Steel yield point	f_y	N/mm²	LN	$f_{yk}+k_s\sigma^{1)}$	0,08μ_X	-	[10], [23] to [25]
9		Steel strength	f_u		LN	$\kappa\,\mu_{fy}^{2)}$	0,05μ_X	-	
10		Concrete	f_c		LN	$f_{ck}+k_c\sigma^{3)}$	0,10-0,18μ_X	-	
11		Reinforcement	f_y		LN	$f_{yk}+2\sigma$	30 N/mm²	0,02	
12	Geometry steel sect.	IPE profiles	A,W,I	$m^{2,3,4}$	N	0,99X_{nom}	0,01-0,04 μ_X	≅0,73	[10],[25]
13		L-section, rods	A,W,I		N	1,02X_{nom}	0,01-0,02 μ_X	≅0,16	
14	Geometry concrete cross-sect.	Cross-section	b, h	m	N	b_k,h_k	0,005-0,01	0,5	[10]
15		Cover of reinf.	a		BET	a_k	0,005-0,015	0,5	
16		Additional ecc.	e		N	0	0,003-0,01	-	
17	Model uncertainties	Load effect factor	θ_E	-	N	1	0,05-0.10	-	[10],[26]
18		Resistance factor⁺	θ_R		N	1-1,25	0,05-0,20	-	

Notes: * See also Table 4.2.
** See also Table 4.3.

[1)] The coefficient k_s can be expected within the interval from 2 to 2,5 depending on execution control (2,0 for mills which do not regularly control the quality and 2,5 for efficient quality control. [51].

[2)] The coefficient κ can be expected within the interval from 1,1 to 1,5 depending on the type of steel [10].

[3)] The coefficient k_c can be expected within the interval from 1,5 to 2 depending on execution control [10] (1,5 for in situ concrete and 2,0 for prefabricated concrete with efficient quality control).

Figure 5.6: Conventional models of basic variables for time invariant reliability analyses [5]

$$\theta = 0.5 \cdot \left(1 + \alpha\left(\bar{\lambda} - 0.2\right) + \bar{\lambda}^2\right) \tag{5.5}$$

$$\frac{N_E}{\chi N_{pl,R}} + \frac{k_y M_E}{M_{pl,R}} \leq 1.0 \tag{5.6}$$

For the k_y factor, a conservative value of $k_y = 1.5$ is chosen.

Figure 5.6 shows the conventional models for the basic variables used for the analyses. On the basis of a lot of literature research, models with corresponding parameters have been established for the various basic variables (on the strength side as well as on the load side).

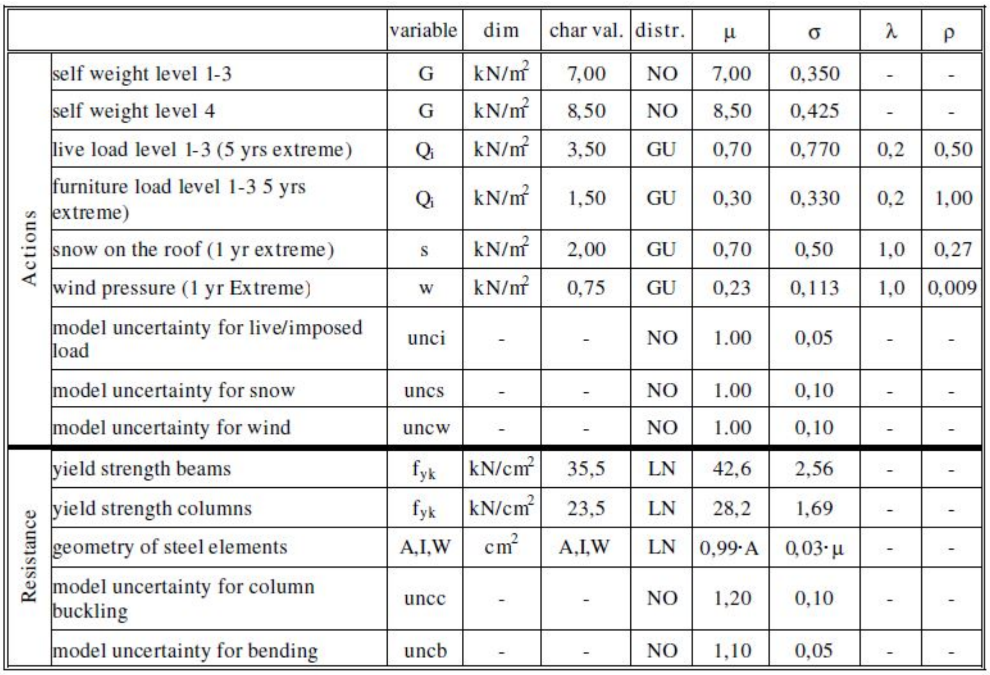

		variable	dim	char val.	distr.	μ	σ	λ	ρ
Actions	self weight level 1-3	G	kN/m^2	7,00	NO	7,00	0,350	-	-
	self weight level 4	G	kN/m^2	8,50	NO	8,50	0,425	-	-
	live load level 1-3 (5 yrs extreme)	Q_i	kN/m^2	3,50	GU	0,70	0,770	0,2	0,50
	furniture load level 1-3 5 yrs extreme)	Q_i	kN/m^2	1,50	GU	0,30	0,330	0,2	1,00
	snow on the roof (1 yr extreme)	s	kN/m^2	2,00	GU	0,70	0,50	1,0	0,27
	wind pressure (1 yr Extreme)	w	kN/m^2	0,75	GU	0,23	0,113	1,0	0,009
	model uncertainty for live/imposed load	unci	-	-	NO	1.00	0,05	-	-
	model uncertainty for snow	uncs	-	-	NO	1.00	0,10	-	-
	model uncertainty for wind	uncw	-	-	NO	1.00	0,10	-	-
Resistance	yield strength beams	f_{yk}	kN/cm^2	35,5	LN	42,6	2,56	-	-
	yield strength columns	f_{yk}	kN/cm^2	23,5	LN	28,2	1,69	-	-
	geometry of steel elements	A,I,W	cm^2	A,I,W	LN	0,99·A	0,03·μ	-	-
	model uncertainty for column buckling	uncc	-	-	NO	1,20	0,10	-	-
	model uncertainty for bending	uncb	-	-	NO	1,10	0,05	-	-

Figure 5.7: Statistical parameters (steel office building) for the FORM-calculation [5]

Steel beam inner frame

For the internal beams, the plastic calculation can be formulated as follows:

$$\delta A = W_{pl,y} \cdot f_y \cdot 4 \cdot \theta - p \cdot B \cdot \frac{1}{4} \cdot l^2 \cdot \theta = 0 \tag{5.7}$$

This equation is based on the fact that plastic hinges occur in the beam (see figure 5.8). Then, using virtual work, moments times a rotation and forces times a displacement are applied. The rotation θ can then be divided out of the equation. In this equation, p is a general uniformly distributed load, B is the frame spacing and l is the beam length. If for p the relevant loads are introduced and also the uncertainties (unc) are taken into account, the following equation arises:

$$\delta A = W_{pl,y} \cdot f_y \cdot uncb - (Q_i \cdot unci + Q_1 \cdot unc1 + G) \cdot B \cdot \frac{1}{16} \cdot l^2 = 0 \tag{5.8}$$

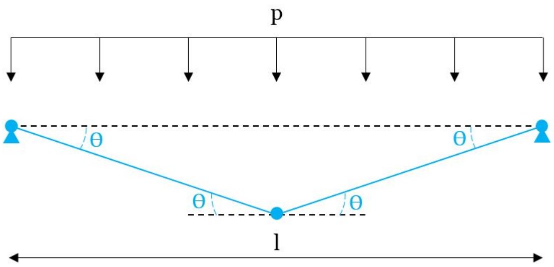

Figure 5.8: Plastic calculation of the inner steel beam [5]

Using this equation, an iterative FORM calculation is performed, in which the inputs (different profiles) are tested on their reliability. The goal is to find the profile which results in a reliability just above the target reliability of $\beta = 3.8$. This is shown in figure 5.9.

Steel beam outer frame

For the steel beam in the outer frame, the same procedure applies as for the inner frame, but now the beam is not rigidly connected on both sides, but there is a hinge on one side. The plastic calculation

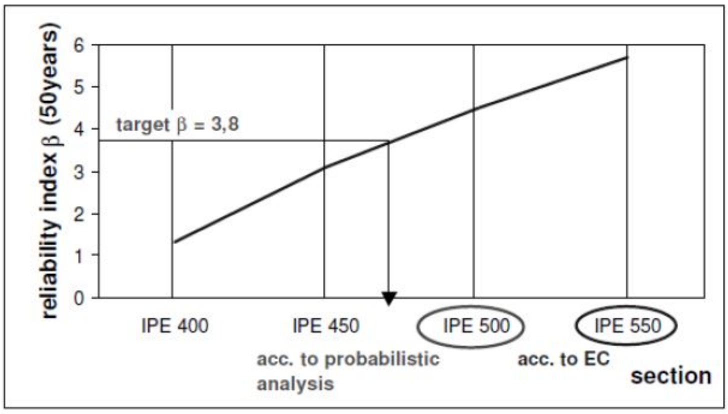

Figure 5.9: Identification of the profile which yields appr. $\beta = 3.8$ for the beam of the inner frame [5]

is therefore also slightly different. Figure 5.10 shows that now only 3 θ's are present. The equations therefore look like this:

$$\delta A = W_{pl,y} \cdot f_y \cdot 3 \cdot \theta - p \cdot B \cdot \frac{1}{4} \cdot l^2 \cdot \theta = 0 \tag{5.9}$$

$$\delta A = W_{pl,y} \cdot f_y \cdot uncb - (Q_i \cdot unci + Q_1 \cdot unc1 + G) \cdot B \cdot \frac{1}{12} \cdot l^2 = 0 \tag{5.10}$$

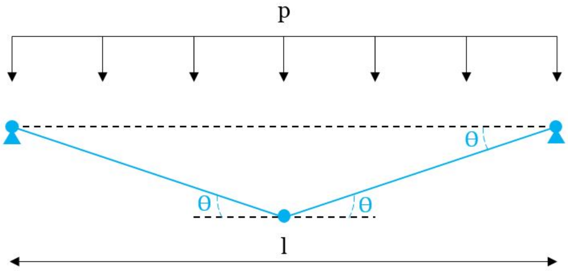

Figure 5.10: Plastic calculation of the outer steel beam [5]

In the same way as for the inner frame beam, an iterative FORM can be done to determine the best profile that just meets target reliability.

External steel columns

The external columns (on the outer boundary of the building) are loaded by normal forces such as own weight, live load, furniture loads etc., but also by moments generated by the wind load. The occurring normal force and moment in the column can be formulated as follows:

$$N_E = \frac{M_{pl,R}}{l} + \left(\sum Q_i \cdot unci + \sum Q_1 \cdot unc1 + \sum G + s \cdot uncs\right) \cdot \frac{l}{2} \cdot B \tag{5.11}$$

$$M_E = 0.076 \cdot w \cdot uncw \cdot B \cdot H \tag{5.12}$$

This factor 0.076 accounts for the calculation of bending.

The $M - N$-interaction is formulated as follows:

$$\frac{N_E}{\chi A f_y} + \frac{1.5 M_E}{W_{pl} f_y} = 0 \tag{5.13}$$

In the same way as for the beams, an iterative FORM can be done to determine the best profile that just meets target reliability, see figure 5.11.

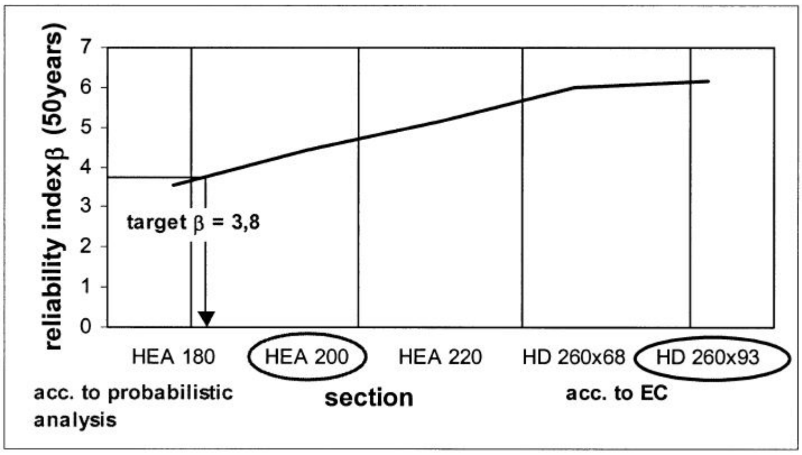

Figure 5.11: Identification of the profile which yields appr. $\beta = 3.8$ for the external column on ground level [5]

Internal steel columns

The internal columns are loaded symmetrically, i.e. only an axial force will occur in the column:

$$N_E = \frac{M_{pl,R}}{l} + \left(\sum Q_i \cdot unci + \sum Q_1 \cdot unc1 + \sum G + s \cdot uncs\right) \cdot \frac{l}{2} \cdot B \tag{5.14}$$

In the same way as for the external columns, an iterative FORM can be done to determine the best profile that just meets target reliability, see figure 5.12.

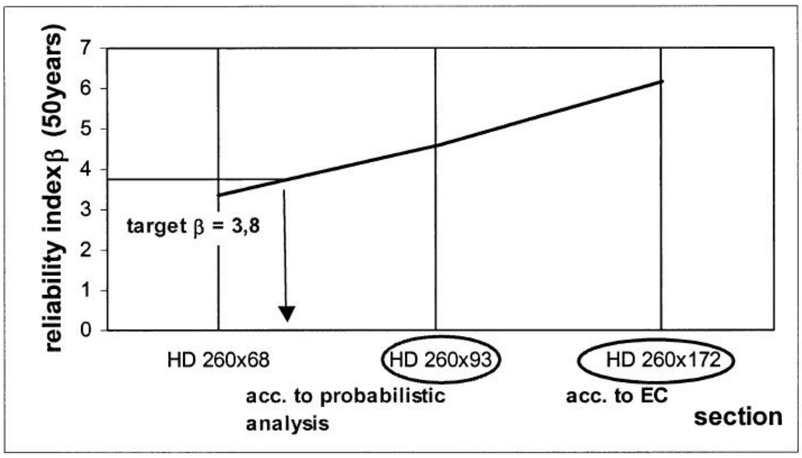

Figure 5.12: Identification of the profile which yields appr. $\beta = 3.8$ for the internal column on ground level [5]

5.5.2. Discussion on existing research

This 'proqua' study gives a clear impression of how a reliability assessment on for example a steel building can be performed. Therefore this study is also used as a basis for the current study. However there are improvements compared to this 'proqua' research. Especially in the field of wind load, the effects of the wind load are examined in a much more precise way in this study. The 'proqua' research assumes a relatively simple description for the wind pressures and the effects of the wind on certain elements is determined in a simple manner. Whereas this research, through a full coupling between both wind speed models, wind tunnel measurements, finite element model of the building, the exact effects of the wind in certain element is determined and so called wind load coefficients are defined.

II

Method Development

6

Methodology of this study

This chapter explains the methodology of this research and describes recent research on which this research builds and in which way this research incorporates new aspects. Also the stochastic wind load model, which is used in this research, is discussed in this chapter. Finally, a method overview of the reliability assessment procedure is given.

6.1. Method overview of recent and current study

The method used in the previous studies by Meinen [25] and la Gasse [23] to which this study precedes is shown in Annex Assessment Procedure: la Gasse and Meinen. In Meinen's [25] research, a full-probabilistic reliability assessment procedure is made for wind-loaded facade elements, which can be used on a local scale and for static response. Also the specific orientation of the building in relation to the incoming wind is taken into account. Next, in the research of la Gasse [23] a full-probabilistic reliability assessment procedure is made for the global response of the main bearing structure of dynamiccaly sensitive buildings subjected to wind loading. Hereby the alongwind response in the foundation of a slender high-rise building with a concrete core main bearing structure is examined.

In this study, a full-probabilistic reliability assessment procedure is developed that can determine the reliability of various steel elements in the steel main load-bearing structure of a wind-loaded building. Full probabilistic models are made for both the strength side and the load side. The probabilistic modelling of the wind load on the building, including all related uncertainties, is also considered extensively. The probabilistic resistance model contains both stochastic models related to the strength of the material, but also models related to the strength of the element itself and the specific failure mechanisms involved. Another big step forward is that the modelling of the building is much more detailed and realistic than in most current studies. This makes it possible to specifically investigate the effects of the wind in each element through a combination of wind speed models, wind tunnel measurements and a finite element model. More explanation of this newly developed method and how to link the various components can be found in Annex Explanation on Coupling SCIA FEM with Python using SCIA OpenAPI.

6.2. Stochastic wind load model

In this study, a wind load model is used, in which almost all parameters are described in a stochastic way. In other words, all uncertainties associated with describing wind forces are included in this model. In this way, an attempt is made to approach reality as closely as possible, and to model this complex phenomenon, 'wind', in the best possible way. To include the effects of wind on the building in specific elements in the reliability assessment, this wind loading effect model is formulated. A distinction is made between effects in the domain of moment, normal force and shear force. The basis of this wind loading effect model is the Davenport's wind loading chain and also the model as used in the Eurocode. The wind loading chain presented here is in accordance with the recent investigations by Meinen [25] and la Gasse [23]. All aspects and associated uncertainties affecting wind loading are included.

$$\text{Moment} \longrightarrow E_{wind,M} = \frac{1}{2} \cdot \rho_{air} \cdot v_{pot}^2 \cdot S_v^2 \cdot c_r(h_{ref})^2 \cdot \hat{c}_M \cdot S_{\hat{C}_M} \cdot A_{ref} \cdot h \cdot \chi_{model} \tag{6.1}$$

$$\text{Normal force} \longrightarrow E_{wind,N} = \frac{1}{2} \cdot \rho_{air} \cdot v_{pot}^2 \cdot S_v^2 \cdot c_r(h_{ref})^2 \cdot \hat{c}_N \cdot S_{\hat{C}_N} \cdot A_{ref} \cdot \chi_{model} \tag{6.2}$$

$$\text{Shear force} \longrightarrow E_{wind,V} = \frac{1}{2} \cdot \rho_{air} \cdot v_{pot}^2 \cdot S_v^2 \cdot c_r(h_{ref})^2 \cdot \hat{c}_V \cdot S_{\hat{C}_V} \cdot A_{ref} \cdot \chi_{model} \tag{6.3}$$

With:

ρ_{air} = Air density [kg/m^3]
v_{pot} = Basic wind velocity: t minute mean wind speeds at $z = 10$ m and for terrain roughness $z_{0,ref}$ m [m/s]
S_v = Sampling uncertainties of basic wind velocity model [-]
$c_r(h_{ref})$ = Terrain roughness factor at the reference height of the structure h_{ref} correcting for $z_{0,ref}$ m [-]
$\hat{c}_X$ = Peak load effect coefficient (1-hour extremes) [-]
$S_{\hat{C}_X}$ = Sampling uncertainties of load effect model [-]
A_{ref} = Area of the facade of the building [m^2]
h = Height of the building [m]
χ_{model} = Model uncertainty factor [-]

See section Wind loading effect model in Chapter 9: Reliability Assessment Procedure for a more detailed description of all parameters in this stochastic wind load model.

6.3. Method overview of the reliability assessment procedure

A method overview of the reliability assessment procedure in this study is given in figure 6.1. The diagram shows in broad outline how the reliability of certain elements of the steel main bearing structure in a wind-loaded building can ultimately be determined. Firstly, boundary layer wind tunnel measurements of pressures on the façade of a scale model in a wind tunnel, carried out at TNO, are used in this research. It is worth noting that the case study building, which is the focus of the reliability assessment in this research, is related to the dimensions of this scale model in the wind tunnel. More explanation about this can be found in Chapter 10: Case Study Description.

Next the diagram shows two different steps; (1) timeseries approach and (2) probabilistic wind pressure model approach. In method (1) the wind pressures as determined in the wind tunnel research are used directly, after which certain pre-processing steps are gone through, resulting in a series of wind load configurations on the building that are sent to the FEM one by one. An alternative way (2) which is investigated in this research, is to make a probabilistic wind pressure model based on the raw wind tunnel data. Here the wind tunnel data is used to make stochastic models for all wind zones on the building, including the correlation between the different zones. Next, this probabilistic wind pressure model can be used to generate wind pressures on the building and these are then sent to the FEM. More information about this probabilistic wind pressure model can be found in Chapter 7: Probabilistic Wind Pressure Model.

In this research, a method is developed that in this case allows the wind tunnel data to be directly linked to a finite element model, after which the results can be further processed. A total of k number of wind load configurations on the building are sent to FEM one by one. The link between the wind tunnel data and the resulting wind pressures on the building in a Python module and the FEM of the building in SCIA Engineer, is achieved by means of a link via SCIA OpenAPI. Next a linear calculation is executed in SCIA Engineer. For all elements that are investigated further in the reliability assessment, the governing internal forces are determined and these are subsequently normalised. When all calculations are done, all normalised load effects C_M, C_N, C_V are stored in a large database.

Next, it is necessary to determine probabilistic models of the extremes of these load effects. Therefore, extreme value analysis (see Chapter 4: Probabilistic Modelling of Extremes) is applied to create these models. The uncertainties associated with the modelling of these load effects are also quantified. The entire process of determining these load effects and creating a probabilistic model of extremes of these load effects can be found in Chapter 8: Technique for Obtaining Load Effects.

In addition, it is necessary to include all other parameters that influence reliability in the full-probabilistic reliability assessment. Thus probabilistic models for v_{pot} and S_v, based on the research of la Gasse [23], are included in the analyses. Furthermore, an extensive literature study is performed, in which probabilistic models for the strength of the material and also of the element itself are formulated. In this way, an attempt is made to include all possible uncertainties that influence the reliability in the full-probabilistic reliability assessment.

Based on the deterministic Eurocode design of the case study building, the governing failure mechanisms for the various elements are determined. Subsequently, the limit state functions $Z = R - S$ are defined. Finally, for each element, the limit state function including all probabilistic models are combined in a reliability analysis - performed in a python module with the TNO 'Prob Toolbox' - which results in the reliability index β and the sensitivity factors α.

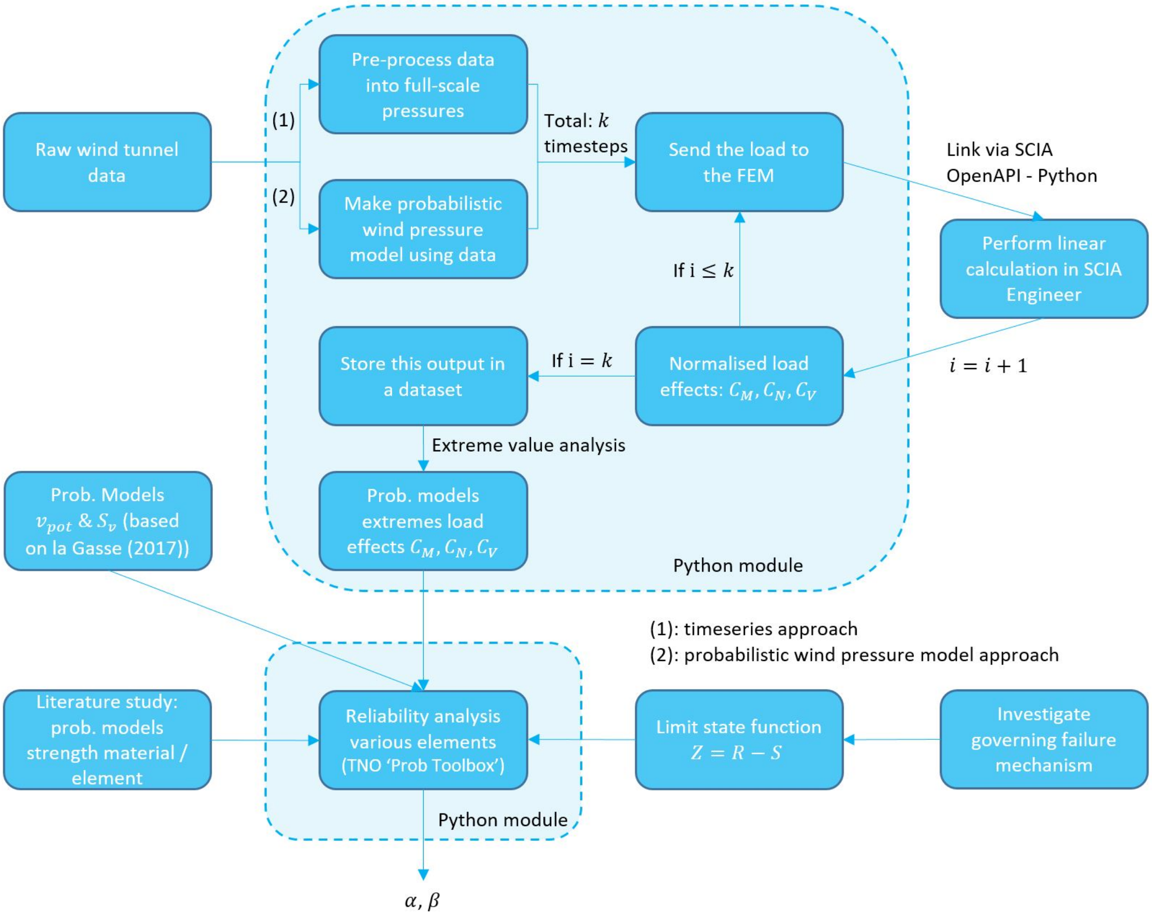
Raw wind tunnel data
(1)
(2)
Pre-process data into full-scale pressures
Make probabilistic wind pressure model using data
Total: k timesteps
Send the load to the FEM
Link via SCIA OpenAPI - Python
Perform linear calculation in SCIA Engineer
If i ≤ k
$i = i + 1$
Store this output in a dataset
If i = k
Normalised load effects: C_M, C_N, C_V
Extreme value analysis
Prob. models extremes load effects C_M, C_N, C_V
Python module
Prob. Models v_{pot} & S_v (based on la Gasse (2017))
(1): timeseries approach
(2): probabilistic wind pressure model approach
Literature study: prob. models strength material / element
Reliability analysis various elements (TNO 'Prob Toolbox')
Limit state function $Z = R - S$
Investigate governing failure mechanism
Python module
α, β

Figure 6.1: Method overview of the reliability assessment procedure in this study

7

Probabilistic Wind Pressure Model

This chapter is dedicated to the development of a probabilistic wind pressure model. This model can then be used to generate the wind pressures on the building in the FEM. For the development of this model also the dependencies between the different wind zones have to be taken into account. In the reliability analysis the two different methods are investigated; firstly the wind pressures are generated directly as a time series based on the wind tunnel data and the second variant based on samples from this wind pressure model. Then also the two different variants are compared. Why is this useful to investigate? If it is possible to make a probabilistic wind pressure model - which can simulate the wind pressures on the facades and top of the building - in such a way that it results in the same reliability analysis results, this offers many advantages. To perform the reliability analysis one does not need the whole big data set from the wind tunnel, but only a relatively simple model which simulates these pressures. An additional advantage is that this relatively simple model can easily be implemented in the reliability analysis itself. This can be particularly useful if a non-linear calculation is performed and the reliability assessment is in the calculation itself. It is good to note that obtaining the wind tunnel data is quite time consuming and costly. If with only a small amount of data a probabilistic model could be made, this also has advantages in this aspect.

First, in section Observations from the wind tunnel data and literature, some observations based on the wind tunnel data are discussed. In addition, some points described in the literature are discussed. Subsequently, in section Formulation of the probabilistic wind pressure model the construction of the probabilistic wind pressure model is addressed.

7.1. Observations from the wind tunnel data and literature

In the wind tunnel, a scale model of a building is exposed to wind. This model is on a scale of $\lambda_g = 1 : 250$ and has the dimensions $0.48\ x\ 0.12\ m$. For this research only the upper 8 meters (full scale) of the building are of interest (a full explanation of why this is chosen can be found in Chapter 10: Case Study Description). On this scale model there are pressure taps that measure the pressure at that point on the building. It can be assumed that these pressures apply over a certain area around this pressure tap, these areas are also called the tributary areas. For the facades of the case study building (side A - D) 28 different pressure taps and corresponding tributary areas, or wind pressure zones can be defined on the case study building. Also 20 pressure taps on top of the building are taken into account in this research. The names, locations and zones of the different pressure taps used in this research - and also part of this probabilistic wind pressure model - are shown in figures 7.1 and 7.2.

The wind tunnel data used in this research contains 2,260,992 number of pressure measurements for each pressure tap. This data can be used to create a probabilistic wind pressure model. This model describes all characteristics of the different wind pressure zones and also takes into account the correlations between the different wind zones. Subsequently, wind loads on the building can be generated based on this model. In this way, the wind tunnel data will not be used directly as time series in the analysis, but this probabilistic wind pressure model will serve as input for the analysis. The big advan-

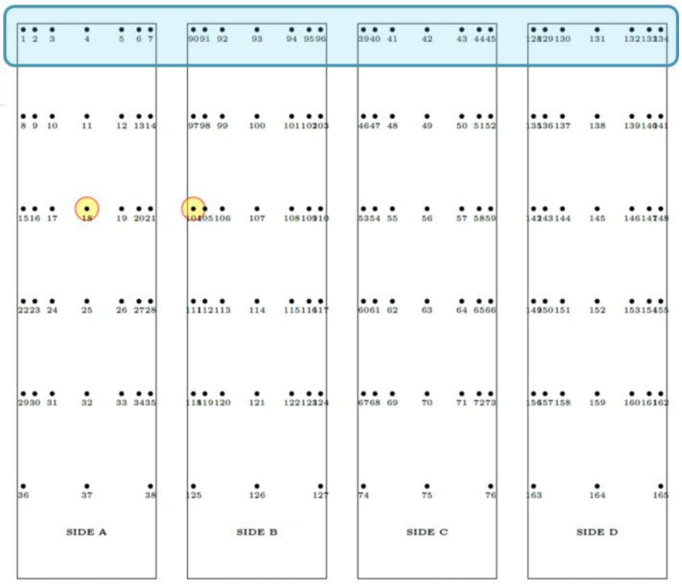

(a) Side A (b) Side B (c) Side C (d) Side D

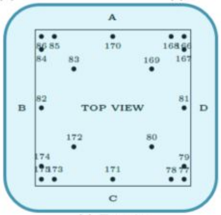

(e) Top view

Figure 7.1: Pressure points from the wind tunnel test, the used pressure points for the case study building are highlighted in blue

tage of this is that this relatively simple model can easily be implemented in other analyses, think for example of a non-linear calculation where the model of the wind pressures is directly in the reliability analysis. This is not possible in the case of a time series of pressures directly from the wind tunnel. The only disadvantage of making a probabilistic wind pressure model is that it requires extra work compared to the method with the time series of pressures directly from the wind tunnel test.

Based on this data, a certain stochastic distribution with corresponding parameters can be defined for each of these wind pressure zones. In addition, the correlation between the different zones must also be taken into account in the model. A probability density function can be created for each wind zone, see figures 7.3 to 7.8. In order to approach reality as closely as possible and get the best results, the basis of the probabilistic model must be right; that is, the choice of the type of distribution.

Several studies [22][31][32][35] have addressed the modelling of wind pressures on a building. They have also looked at the stochastic characteristics for describing these wind pressures. It can be concluded that there can be two types of wind pressure regions on a building; namely a Gaussian (Normal) wind pressure effect and a non-Gaussian effect. The regions characterised by a Gaussian wind pressure effect are mainly flat surfaces, or surfaces where the fluctuations play a lesser role. This in comparison to the other regions; the non-Gaussian, these are mainly in areas where fluctuations or separated and reattached flows occur. These non-Gaussian wind pressure effects can be modelled as stochasts with a log-normal or Weibull distribution. Figure 7.3, for example, shows that the tail is greater on the right than on the left. It is therefore relatively more frequent that higher values occur. It is also not entirely surprising that the log-normal or Weibull distributions are used for modelling the wind pressures on the building, since the wind speed distribution which forms the basis for the wind pressures on the building is also often described by a Weibull distribution.

In order to be able to determine from the wind tunnel data whether a certain zone has a Gaussian or

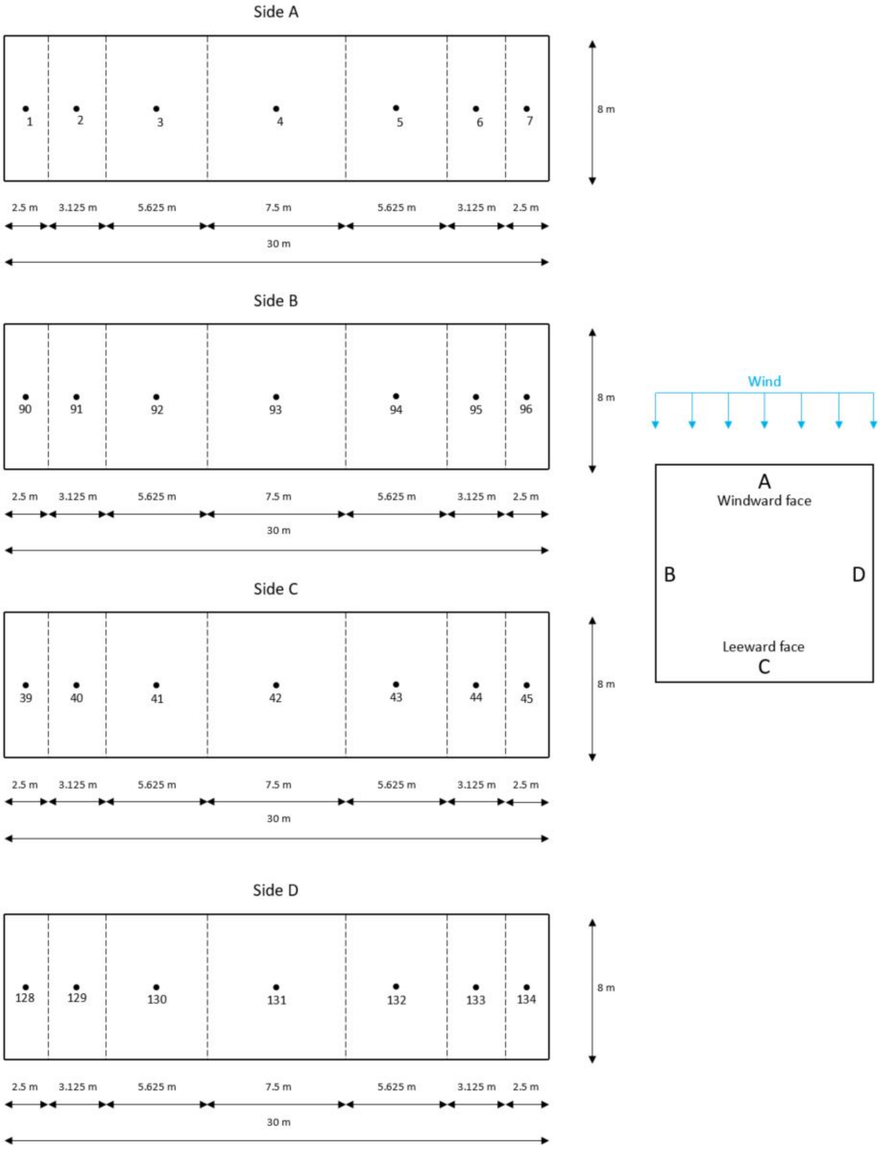
Side A
1
2
3
4
5
6
7
Side B
90
91
92
93
94
95
96
Side C
39
40
41
42
43
44
45
Side D
128
129
130
131
132
133
134
2.5 m
3.125 m
5.625 m
7.5 m
5.625 m
3.125 m
2.5 m
30 m
8 m
Wind
A
Windward face
B
D
Leeward face
C

Figure 7.2: Tributary areas (including the number of the pressure tap) for the pressure taps of interest for the case study building

non-Gaussian wind pressure effect, a few characteristics of the data can be examined more closely. The research of Kumar and Stathopoulos [22] indicates that a stochastic wind pressure in which the absolute value of the skewness (degree of asymmetry in the probability distribution function) and kurtosis (indicates the extent to which the data is heavy-tailed or light-tailed with respect to a normal distribution) are relatively lower than 0.5 and 3.5 can be seen as a Gaussian process. If the data does not meet this requirement, it should be modelled with a non-Gaussian, such as log-normal or Weibull distribution.

All parameters such as mean, standard deviation, skewness and kurtosis of the wind zones used in this study can be found in Annex Analysis Wind Pressures from Wind Tunnel Test - For Making Probabilistic Wind Pressure Model. It also indicates which distribution should be used for the various zones. This shows that almost all wind pressure zones are log-normally distributed. An explanation for this can be found in figure 7.1 which shows the location of the various pressure taps in the wind tunnel test. Most of the pressure points used in this research on the case study building (highlighted in blue) are located close to the edges of the building. Therefore, these are not very stable zones and fluctuations play an important role.

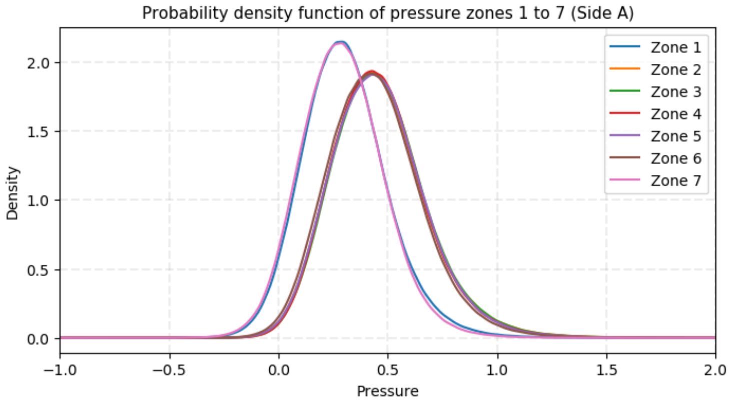

Figure 7.3: Probability Density Functions (PDF) for the pressures in wind zone 1 to 7 (side A)

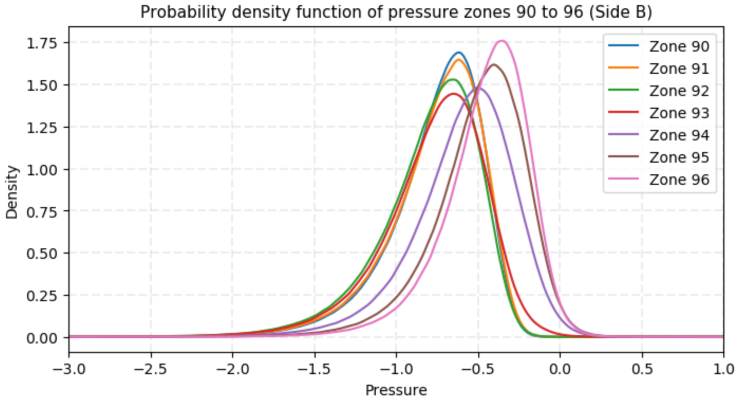

Figure 7.4: Probability Density Functions (PDF) for the pressures in wind zone 90 to 96 (side B)

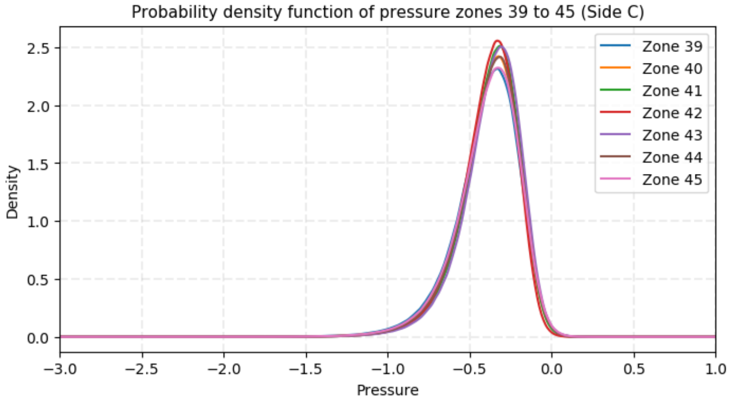

Figure 7.5: Probability Density Functions (PDF) for the pressures in wind zone 39 to 45 (side C)

7.2. Formulation of the probabilistic wind pressure model

The different wind pressure zones across the facade cannot be considered as individual elements that stand alone. There is a certain correlation between the different zones. In order to make the probabilistic wind pressure model as accurate as possible, these dependencies must also be included in the modelling.

Suppose that in wind zone 1 a relatively high wind pressure is measured, then it is very unlikely that directly next to it in wind zone 2 a very low wind pressure is measured. The wind pressures on the

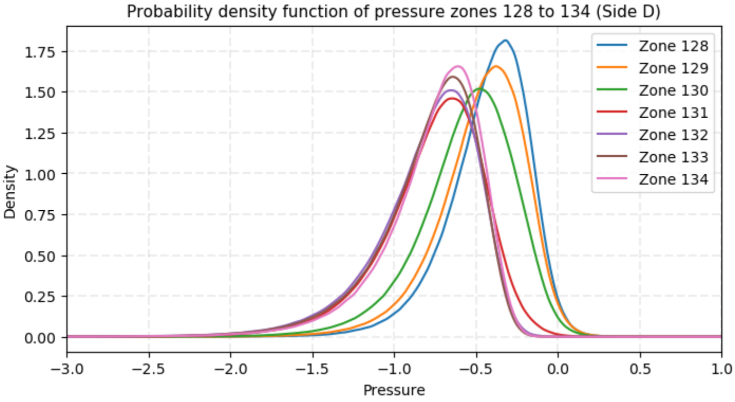

Figure 7.6: Probability Density Functions (PDF) for the pressures in wind zone 128 to 134 (side D)

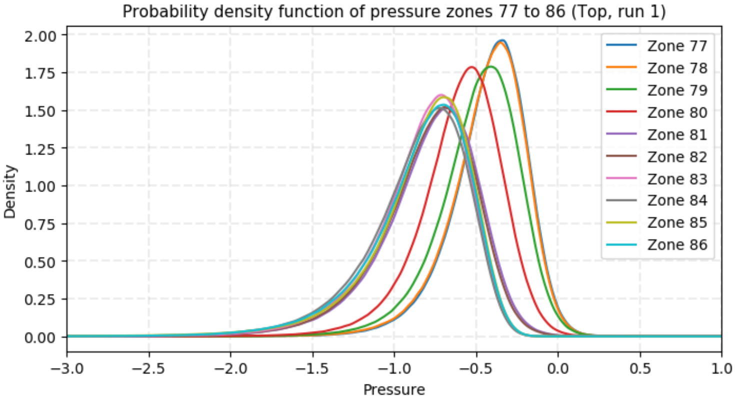

Figure 7.7: Probability Density Functions (PDF) for the pressures in wind zone 77 to 86 (Top, run 1)

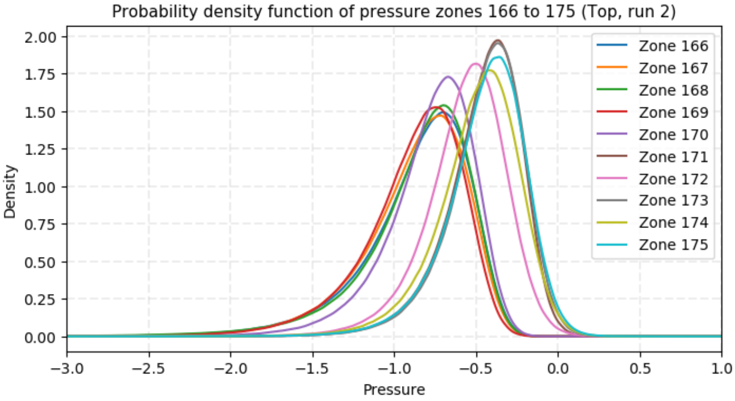

Figure 7.8: Probability Density Functions (PDF) for the pressures in wind zone 166 to 175 (Top, run 2)

facade smoothly flow into each other. As the distance between two wind zones increases, the dependence, or correlation, becomes smaller. This phenomenon of correlations is investigated on the basis of the entire data set. Wind zones that are directly next to each other have a high correlation and zones that are further apart have a smaller correlation. The correlation between two variables X and Y can be calculated as follows:

$$\rho_{X,Y} = corr(X,Y) = \frac{cov(X,Y)}{\sigma_X \cdot \sigma_Y} = \frac{E[(X-\mu_X)(Y-\mu_Y)]}{\sigma_X \cdot \sigma_Y} \quad (-1.0 \leq \rho_{X,Y} \leq 1.0) \tag{7.1}$$

On the basis of the investigation of the data and the types of distributions involved (see also Annex

Analysis Wind Pressures from Wind Tunnel Test - For Making Probabilistic Wind Pressure Model), a probabilistic wind pressure model can be created. Almost all zones can be modelled with a lognormal distribution, only one zone (zone 7) can be classified as a normal distribution. To create the model, a few transformations are performed on the data. Firstly, the lognormal distributions can be transformed into normal distributions[1]:

$$X \sim \text{log-normal}(\cdot) \longrightarrow e^X \sim \text{normal}(\cdot) \tag{7.2}$$

The great advantage of transforming to all normal distributions is that now a multivariate normal distribution can be used. The multivariate normal distribution is the multidimensional version of the normal one-dimensional distribution, and in this case one of the 48th order (48 zones in this model). Whereas the normal distribution is defined by the mean and standard deviation, the multivariate normal distribution is defined by the mean and covariance matrix. This covariance matrix indicates how dependent two variables are on each other. Therefore it is necessary to calculate the covariance matrix of the wind pressure data. The covariance matrix of the pressures in the different zones is shown in figure 7.9.

This covariance matrix shows all possible covariances between all 48 zones. To make the picture as clear as possible, the degree of covariance is indicated by colour coding. What is also remarkable here is that a kind of chessboard can be seen, where zones are totally independent. This has purely to do with the manner in which the wind tunnel data is obtained. Side A, C and Top (run 1) were measured simultaneously, after which the scale model was rotated in the wind tunnel and the measurements for side B, D and Top (run 2) were subsequently determined. This explains the uncorrected data between the different zones.

The covariance is almost similar to the correlation and is calculated as follows:

$$\sigma_{X,Y} = cov(X,Y) = E[(X-\mu_X)(Y-\mu_Y)] \tag{7.3}$$

Now, instead of the time series of pressures, this probabilistic wind pressure model can be used. From this multivariate normal distribution, one sample can be executed each time. Also the dependencies between the different zones are taken into account.

7.3. Remark on fully uncorrelated zones

As explained at the end of the previous section, a kind of chessboard pattern is clearly visible in the covariance matrix (figure 7.9) of the wind tunnel data. As explained above, this is due to the way the wind pressure measurements are determined in the wind tunnel. Pressure measurements are not conducted simultaneously on all surfaces of the scale model in the wind tunnel, but this is done in 2 separate experiments in the wind tunnel. Later, however, all wind tunnel data are combined in one large data file. By doing so, the correlation between all zones is not taken into account in this wind tunnel research and this affects the analyses in this research. This affects both the timeseries approach and the probabilistic wind pressure model approach.

It is very logical that when a relatively high wind pressure occurs at the front of the building (side A), the pressures on the sides of the building (side B and D) will also be relatively high. As a result, the total wind loads on the building will be higher than what is currently assumed in the case of uncorrelation between side A and B-D for example. So it is very good to keep this observation in mind, because this will eventually also influence the reliability assessment results. Since the wind tunnel data does not contain all correlations, the wind load on the building is probably underestimated, which makes it very likely that the reliability of the various elements will be on the higher side.

---

[1] However, this step was not performed for wind zone 7 as it is already normally distributed

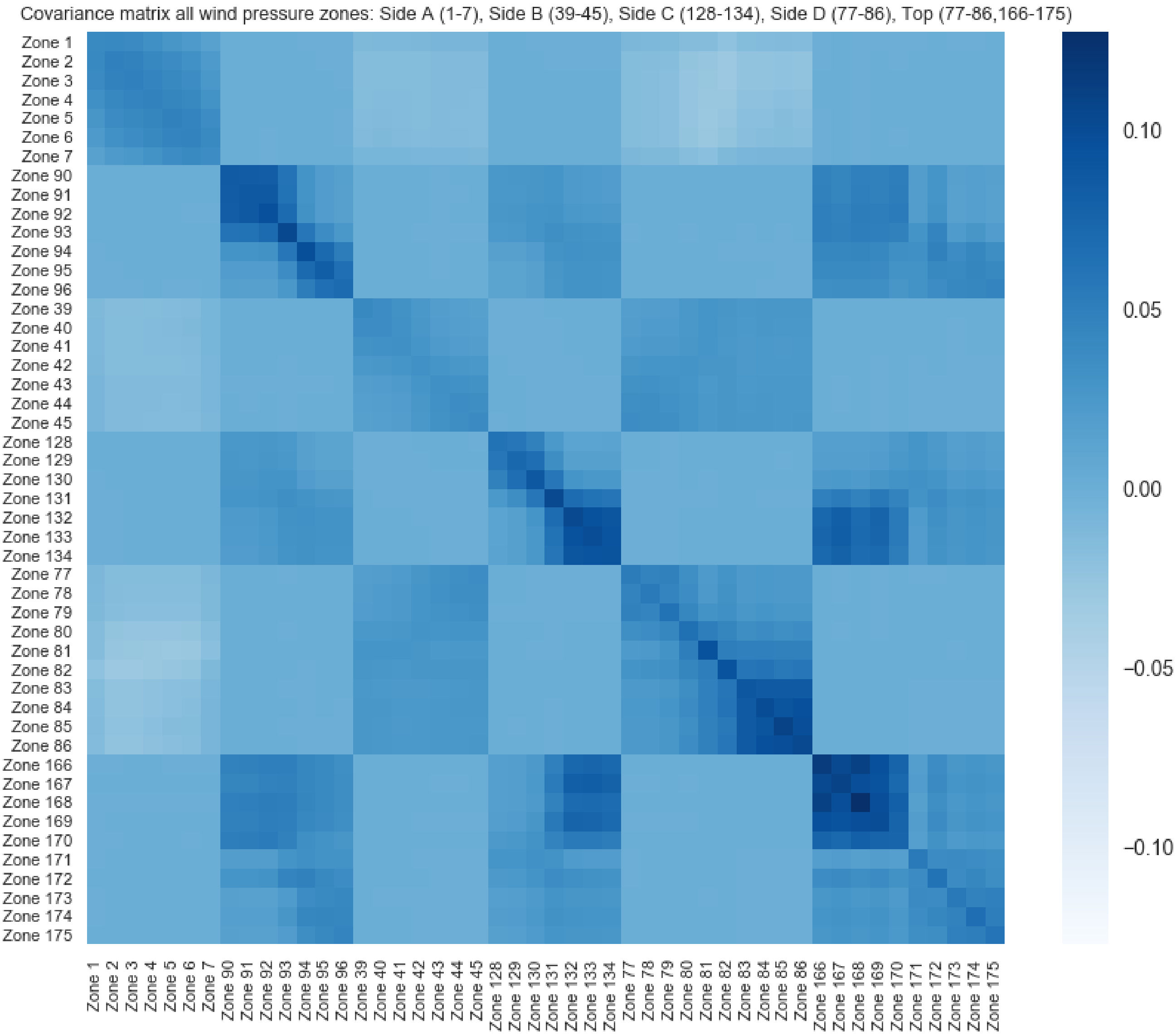

Figure 7.9: Covariance matrix of all wind pressure zones

8

Technique for Obtaining Load Effects

This chapter focuses on the determination of the load effects. These load effects indicate how the internal forces in each specific element of the case study building varies with a time series or probabilistic model of the wind load. To determine these load effects, pressure measurements from the boundary layer wind tunnel test are used. To be able to use these measurements in an adequate way on the case study building, the first section Pre-processing measurements wind tunnel test shows how a number of pre-processing steps must be performed. After these measurements are converted into representative pressures, they are used in the FEM. Everything about the FEM can be found in section Finite Element Model. Finally, in section Probabilistic modelling of extremes load effects, the probabilistic modelling of extremes load effects is described.

8.1. Pre-processing measurements wind tunnel test

The raw wind tunnel data and its characteristics are provided in Wind tunnel data in Chapter 10: Case Study Description. In the wind tunnel test, pressure measurements are performed on a certain scale model building. This model has many pressure taps in which the pressures are measured. The area over which such a pressure measurement is valid is called the tributary area and is a rectangular area surrounding the pressure tap. The way the pressure of the pressure tap measurement is used for the whole tributary area is by definition not very accurate, because the pressures over a certain distance (even within the same tributary area) are not fully correlated. The correlation of pressures decreases with increasing distance between two given points. Normally this discrepancy is solved by applying the aerodynamic admittance, however in the case of wind tunnel data a moving average filter is frequently used which filters the high frequency variations out of the data. These high frequency variations have a low correlation over the tributary surface and are therefore filtered. Decay constants C_r play a role in the formulation of the aerodynamic admittance. What the value for this constant should be differs quite a bit in the literature. To determine these decay constants it is necessary to check the root-coherence of the pressure measurements against Davenport's exponential decay function.

Both the aerodynamic admittance and the moving average filter are low-pass filters, where only incoming signals below a certain limiting frequency are taken into account. In this way, the faster fluctuations consisting of smaller gusts, which only have a minor influence on a large element, are filtered out of the data. The moving average filter, as the name implies, filters over a certain time window and moves it over the time series of wind tunnel data. Since this method should result in a similar behaviour as would occur with the aerodynamic admittance method, the moving average filter must be implemented correctly. In the research by la Gasse [23], a detailed description is given of how the moving average filter yields the best results. The same method is used in this study with, in addition, the same configuration for the moving average filter and the associated averaging constant value $C_T = 1.5$. This averaging time constant C_T should be chosen such that the moving average filter corresponds to the aerodynamic admittance. Since this value shows great similarities with the aerodynamic admittance in the frequency range of interest [23], this value of $C_T = 1.5$ is chosen.

In addition, the necessary factors are introduced to correct the relationship between the scale model in the wind tunnel and the actual building in full scale:

$$\text{Geometric scale} \longrightarrow \lambda_g = \frac{h_{wt}}{h_{fs}} \tag{8.1}$$

$$\text{Wind speed scale} \longrightarrow \lambda_v = \frac{v_{wt}}{v_{fs}} \tag{8.2}$$

$$\text{Time scale} \longrightarrow \lambda_t = \frac{1}{\lambda_g \cdot \lambda_v} \tag{8.3}$$

$$\text{Frequency scale} \longrightarrow \lambda_f = \frac{1}{\lambda_t} \tag{8.4}$$

With:

h_{wt} = Height wind tunnel model $[m]$
h_{fs} = Height full scale model $[m]$
v_{wt} = Resulting average wind speed at top building in wind tunnel $[m/s]$: $v_{wt} = \sqrt{\frac{\mu_{P_{ref}}}{0.5 \cdot \rho_{air}}}$
$\mu_{P_{ref}}$ = Mean reference pressure $[N/m^2]$
v_{fs} = Mean wind speed at top building in full scale $[m/s]$: $v_{fs} = 0.19 \cdot \frac{z_0}{z_{0,II}}^{0.07} \cdot log(\frac{h_{fs}}{z_0}) \cdot v_{pot}$
v_{pot} = Potential wind speed $[m/s]$

8.2. Finite Element Model

In order to determine the behaviour of the case study building and the associated paired distributions of forces in the various elements, a FEM is used. All structural elements, connections, supports and loads are included so that the model approaches the actual situation.

8.2.1. FEM Program

There are several FEM programs available, for this research however SCIA Engineer is used. This program offers all facets necessary for this research and in addition SCIA Engineer can be linked with various programming languages (such as Python, C#, VBA, etc.) by means of the SCIA OpenAPI module[1]. In this way it is possible to adjust for instance model data or loads through a script and perform linear calculations in SCIA Engineer for a large amount of iterations. Also all results such as internal forces, stresses or displacements can be retrieved through the programming script. In this study, the time series of wind pressures or the probabilistic wind pressure model are applied to a large number of time steps, after which all relevant governing internal forces are stored in a database.

8.2.2. Details Case Study Building Model

The case study building, as calculated based on the Eurocode, is modelled in SCIA Engineer. This model includes all structural elements, connections, supports and loads. In order to be able to place the wind loads on the building's facade, several load panels have been added to the model. Subsequently, surface loads can be placed on these load panels. Figures and renders of the building in the FEM and also the designation of the various elements which are of focus in the further reliability analysis, are in Appendix Finite Element Model Case Study Building Figures - Designation of Various Elements. Furthermore, all surfaces of the building (side A - D and top) are included in this study and all have wind pressures acting on it.

---

[1] See also the documentation of the SCIA OpenAPI module: `https://help.scia.net/api/19.1.0031/index.html` (pay close attention to the correct version). Also, examples for the use of this module for various programming languages can be found at: `https://github.com/scia-garage`

8.2.3. Load effects

By means of the analyses in the SCIA FEM, the construction is calculated for a large number of time steps. Subsequently, for each element that is investigated further, the governing moments or forces in that element are stored for that specific time step. In order to be able to use these load effects for other cases as well, where, for example, the wind speed is different, the load effects must be normalised. These load effects are also normalised in such a way that a dimensionless factor remains. The advantage of making these load effects dimensionless is that they can then easily be used for other cases as well.

$$\text{Moment} \longrightarrow C_M = \frac{M}{\frac{1}{2} \cdot \rho_{air} \cdot v_{pot}^2 \cdot c_r(h_{ref})^2 \cdot A_{ref} \cdot h} \tag{8.5}$$

$$\text{Normal force} \longrightarrow C_N = \frac{N}{\frac{1}{2} \cdot \rho_{air} \cdot v_{pot}^2 \cdot c_r(h_{ref})^2 \cdot A_{ref}} \tag{8.6}$$

$$\text{Shear force} \longrightarrow C_V = \frac{V}{\frac{1}{2} \cdot \rho_{air} \cdot v_{pot}^2 \cdot c_r(h_{ref})^2 \cdot A_{ref}} \tag{8.7}$$

With:

M = Moment in certain element $[Nmm]$
N = Normal force in certain element $[N]$
V = Shear force in certain element $[N]$
ρ_{air} = Air density $[kg/m^3]$
v_{pot} = Basic wind velocity $[m/s]$
$c_r(h_{ref})$ = Terrain roughness factor at the reference height of the structure h_{ref} correcting for $z_{0,ref}$ m [-]
A_{ref} = Reference area (in this study: area of the facade of the building $30 \cdot 8\, m$) $[m^2]$
h = Height (in this study: height of the building $8\, m$) $[m]$

8.3. Probabilistic modelling of extremes load effects

After a large number of time steps are calculated, the normalised load effects can be plotted for a certain element and type of internal force. An example of this is shown in figure 8.1. It is evident that the load effects have a certain spread and variation in time.

In addition, a distinction is made between positive and negative behaviour, in other words, the sign of the load effect. It may happen that the wind load is such (for example, suction instead of pressure in a certain area) that the governing internal force is no longer positive but negative. For this reason it is decided to first make a distinction between positive and negative behaviour. Then, for example for the data in figure 8.1, the extreme values can be determined. How this is done exactly is explained below.

To be able to further use the various load effects in the reliability analysis, the extreme values of these data have to be modelled. In chapter 4: Probabilistic Modelling of Extremes the theory of modelling the extreme value distribution can be read. The main principles mentioned there are also applicable here; the data used for fitting an extreme value distribution should be independent and identically distributed. To obtain extreme data points, the block method is used, in which the sample data is divided into parts of blocks of duration t, in which each block extracts an extreme value. This is also visible in figure 8.2.

In order to have as many extreme values as feasible to fit the extreme value distribution, it is necessary to collect as much load effects data as possible. A disadvantage of generating this data is that it requires quite a lot of computing power and time per iteration. On average, it takes about 9 seconds per iteration, which means that performing $n = 10,000$ iterations takes about 25 hours to compute. Therefore, a

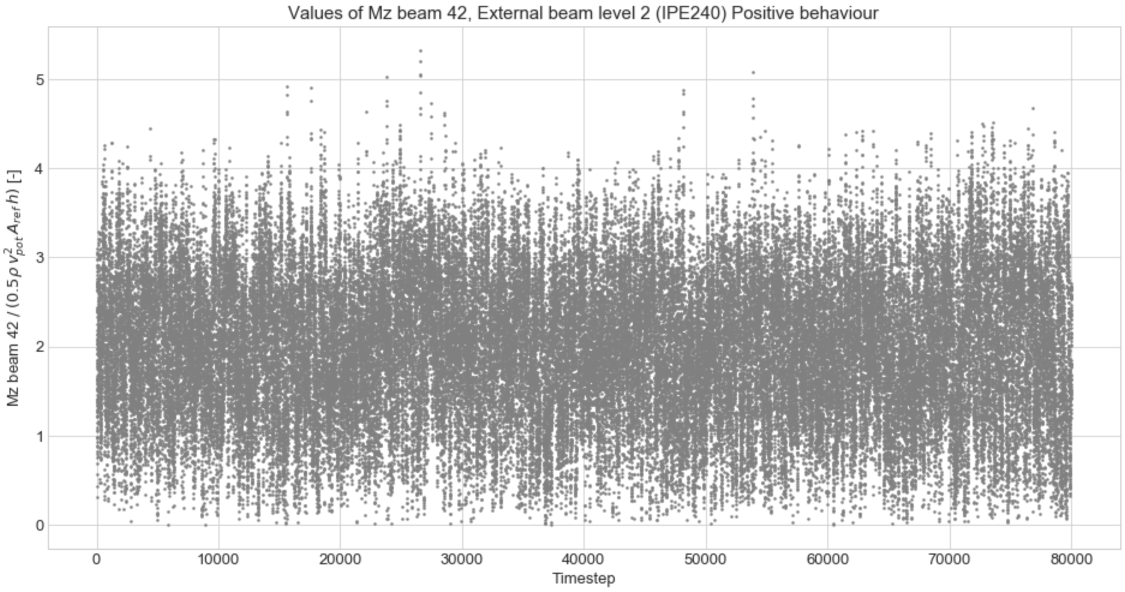

Figure 8.1: Raw load effect data, as example for M_z beam 42: External beam level 2 ($n = 80.000$)

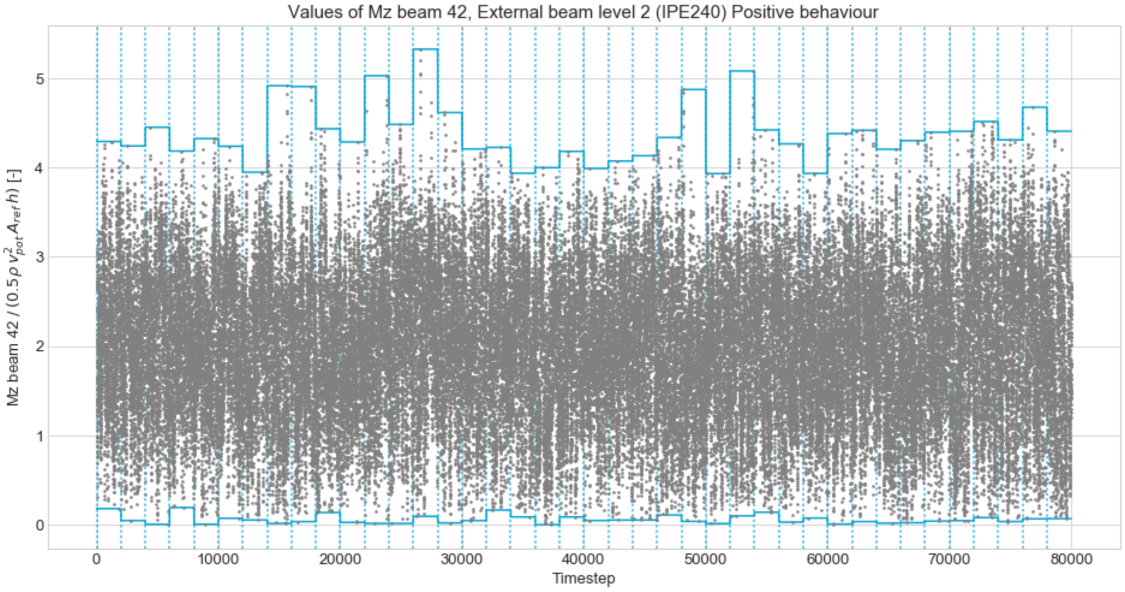

Figure 8.2: Raw load effect data including blocks (for clarity very large block duration $t = 9.26$ minutes) in which maxima are selected, as example for M_z beam 42: External beam level 2 ($n = 80.000$)

trade-off has to be made between performing more iterations, which results in more usable data points to fit the extreme value distribution (this does, however, take more time), but because of the larger amount of data, the statistical and sampling uncertainties in the extreme value distribution of the load effects decreases.

8.3.1. Block duration t

For the determination of a correct block duration t, various methods can be used such as the auto-correlation method or the reversed univariate method. These methods are described below. First, an initial estimate for the block duration t will be given. This gives a first good impression of what the block duration will approximately be.

First estimate block duration t

It is useful to be able to give a first estimate for the block duration t based on existing research. In the research by Meinen [25], a block duration of $t = 10\ s$ is chosen. This research concerns wind-loaded facade elements of a relatively small scale. Another study by la Gasse [23], looking at a larger scale, has a block duration $t = 20\ s$. Since these values give a good idea of how large the block duration should be in order to obtain independent data, a block duration of $t = 20s$ was chosen as a conservative initial guess for this study. By choosing a larger block duration, the requirement for static independent data can be met.

Autocorrelation method

The autocorrelation method, uses signal autocorrelation to determine the extent to which measurements are dependent on each other [24]. This can then be used to choose an appropriate block duration t that results in statistical independency. The autocorrelation function indicates the extent to which the values of measurements depend on other values at another moment in time. The autocorrelation function can be described as follows:

$$R_{xx}(\tau) = \frac{E[(x(t) - \mu_x)(x(t+\tau) - \mu_x)]}{\sigma_x^2} = R_{xx}(-\tau) \tag{8.8}$$

Containing $x(t)$ and corresponding mean μ_x, standard deviation σ_x and additionally the time lag $\tau = t_1 - t_2$. Finally, it may be assumed that the values are independent for an autocorrelation smaller than $R_{xx}(t) \leq 0.2$ [-]. This threshold value gives a good indication, but does not provide solid proof.

Figure 8.3 shows an example of an autocorrelation function. For every 10 consecutive minutes the autocorrelation is determined and plotted, this yields 37 of autocorrelation functions. This 10-minute time lag will ensure that the data is independent of each other. In this example a block duration $t = 10s$ is chosen. This choice of block duration will result in statistically independent extreme samples for determining the extreme value distribution.

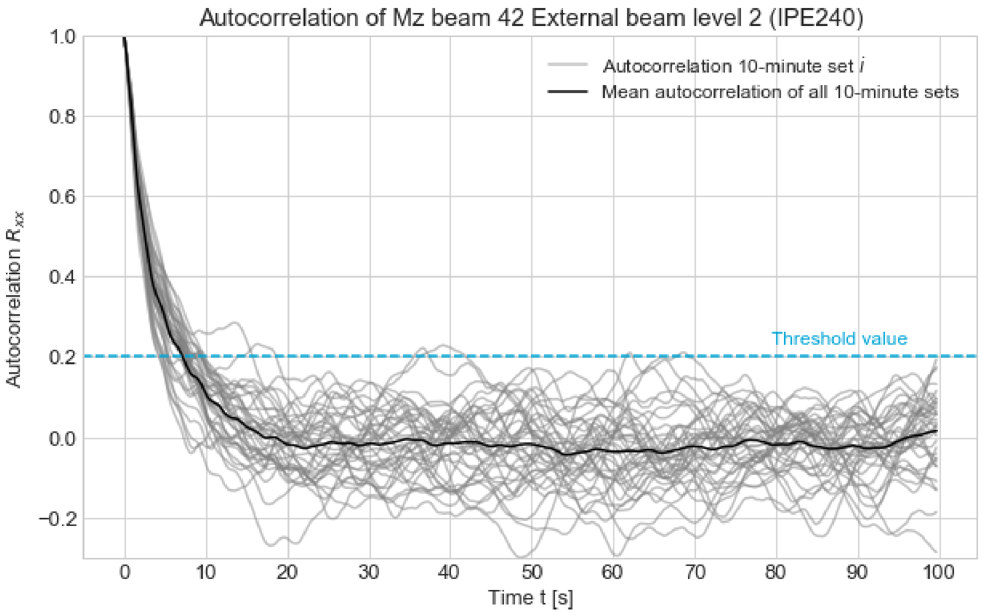

Figure 8.3: Autocorrelation example, other elements are in Annex Extra Figures - Description Load Effects

Reversed univariate method

Meinen [25] proposed a different method, namely the reversed univariate method. This is based on the normal univariate theory, which says that if the t-extreme values are identically distributed, statistically independent and it is the case that $T = N \cdot t$, then in that situation the univariate theory holds. If this reasoning is reversed; if the univariate theorem holds, then the t-extreme values are identically distributed and statistically independent. The application of this method is as follows (for example with load effect c_M):

1. Look at a very long dataset and generate the ECDF of the T-extremes:

$$\hat{F}_T(X) = \hat{P}(c_M \leq X)_T \tag{8.9}$$

2. Also generate the ECDF of the t-extremes:

$$\hat{F}_t(X) = \hat{P}(c_M \leq X)_t \tag{8.10}$$

3. Shift the t-extremes ECDF to the T-extremes (univariate theorem):

$$\hat{F}_t(X) \longrightarrow \hat{F}_t(X)^N \tag{8.11}$$

A disadvantage of using this method is that a lot of data is needed to use it properly. In the case of this research it is therefore not suitable to use this method on the T-hourly extremes. Therefore, with the relatively small amount of data available, it is decided to compare the 10-minute extremes with the shifted 1-second, 10-second and 20-second extremes using the reversed univariate method.

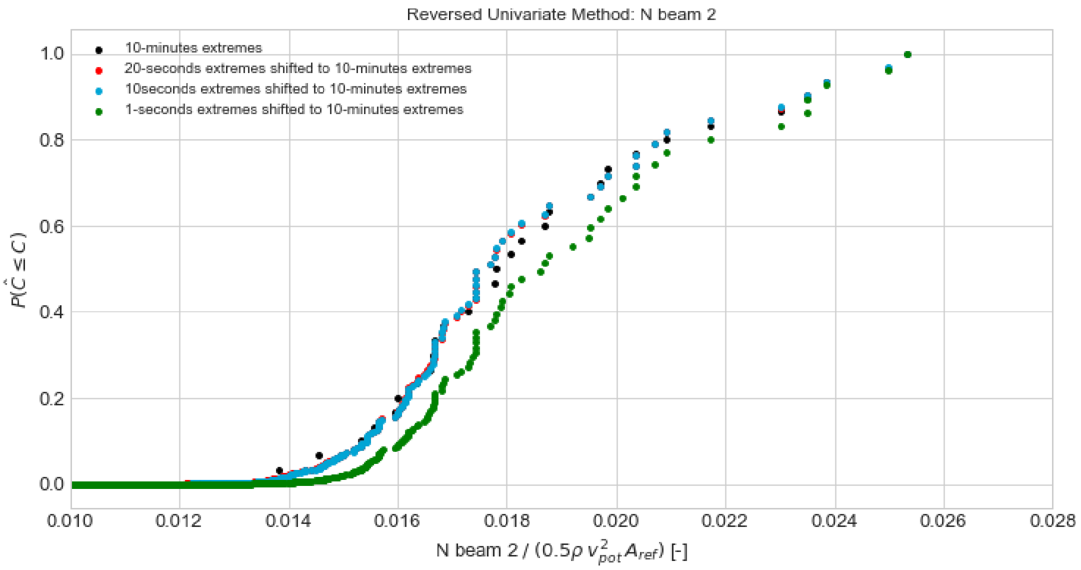

Figure 8.4: Reversed univariate method example for N beam 2; comparison between 10-minute extremes and the 1-second, 10-second and 20-second shifted extremes

In figures 8.4 and 8.5, the reversed univariate method is applied for N beam 2 as an example. The 10-minute extremes are plotted in black and the 1-second, 10-second and 20-second shifted extremes in green, blue and red, respectively. It can clearly be seen that the 1-second shifted extremes deviate from the actual 10-minute extremes. Applying a block duration of $t = 1s$ is therefore not suitable, as this results in dependent extremes. Both the 10-second and the 20-second shifted extremes show a better behaviour. However, the difference between the 10-second and 20-second shifted extremes is so small that there is no added value in making the block duration $t = 20\,s$. This results in fewer extreme values that can be used in fitting the extreme value distribution, i.e. an increase in sampling uncertainties. The best choice based on the reversed univariate method for this example would therefore be a block duration of $t = 10\ s$. However, it is necessary to determine the block duration for each load effect separately and it may therefore happen that some load effects need a different block duration, in order to get independent extremes.

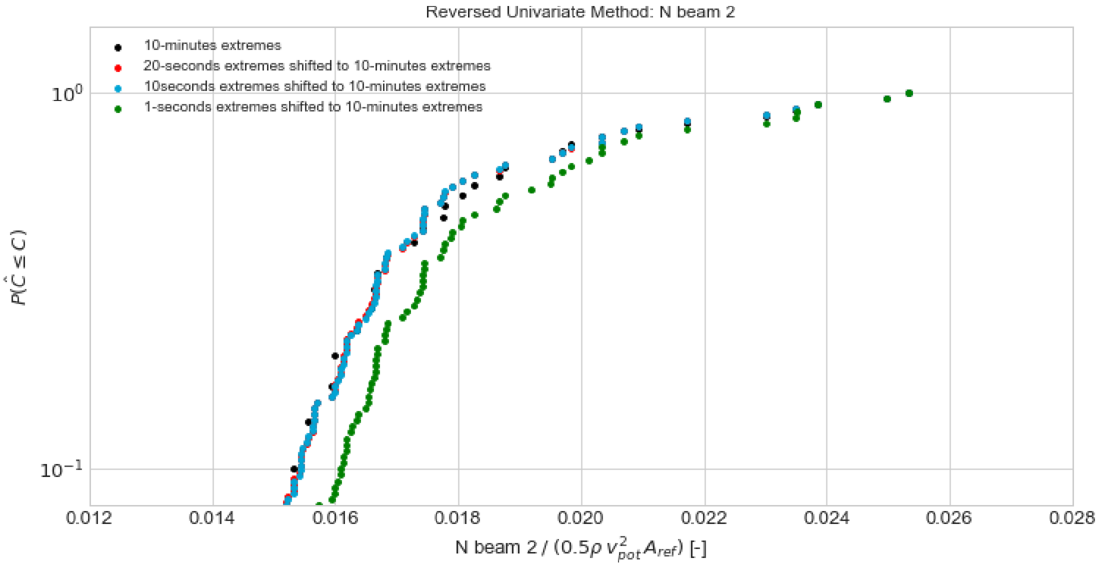

Figure 8.5: Tail behaviour reversed univariate method example for N beam 2; comparison between 10-minute extremes and the 1-second, 10-second and 20-second shifted extremes

8.3.2. Fit data to certain distribution

Now that a proper block duration is chosen, statistically independent extremes are taken to fit the generalized extreme value distribution. The maximum likelihood estimator (MLE) is used to determine the correct model parameters; the shape parameter ξ, location parameter μ and scale parameter σ. This method searches the values of the parameters such that the likelihood function is maximal.

Generalized extreme value distribution

To fit the normalised load effects to a given distribution function, there are several possibilities. One of the most commonly used options is the GEV distribution function. As mentioned in Chapter 4: Probabilistic Modelling of Extremes, there are different types of GEV. Based on the data, a general GEV can be fitted, where the three parameters are selected such that the fit is optimal through all data points. An example of such a GEV fit through the normalised load effects is shown in figure 8.6. It is important to note that the tail of the distribution, in particular, is not well-fitted by the GEV. In this specific case, the data and the fit deviate from about 3.7 and the tail of the fit shows a different behaviour. Also, the fit of the GEV in the tail shows lower probabilities than one would expect based on the data, which is not on the conservative side. It is precisely this tail that is very important in this study, which is why it is decided to use a different type of fit in this study, which attaches more value to the tail of the distribution and which also provides a better fit.

Gumbel (including threshold value)

Figure 8.6 shows that the tail of the distribution is quite straight. Therefore, it is decided to fit a Gumbel distribution function to this data, because in that case the shape parameter ξ is equal to 0 and corresponds to a straight line. If, however, a Gumbel distribution function is sought with all extreme value points (see figure 8.7), it deviates tremendously in the case of the higher values. The fit is so influenced by the lower extreme values that the fit in the tail is no longer accurate.

As a solution to this problem, it is decided to fit a Gumbel distribution function including the application of a certain threshold value. Some examples of this are shown in figures 8.8 and 8.9. All data points above this threshold value are taken into account to fit the Gumbel distribution function, but a correction is also made for all data points to the left of this threshold value and the probability that a data point lies in this area. In this way, all data points are still correctly included, but more value is given to the higher extreme values in the tail. And as mentioned before, the fitting of the tail of the distribution is the most important task.

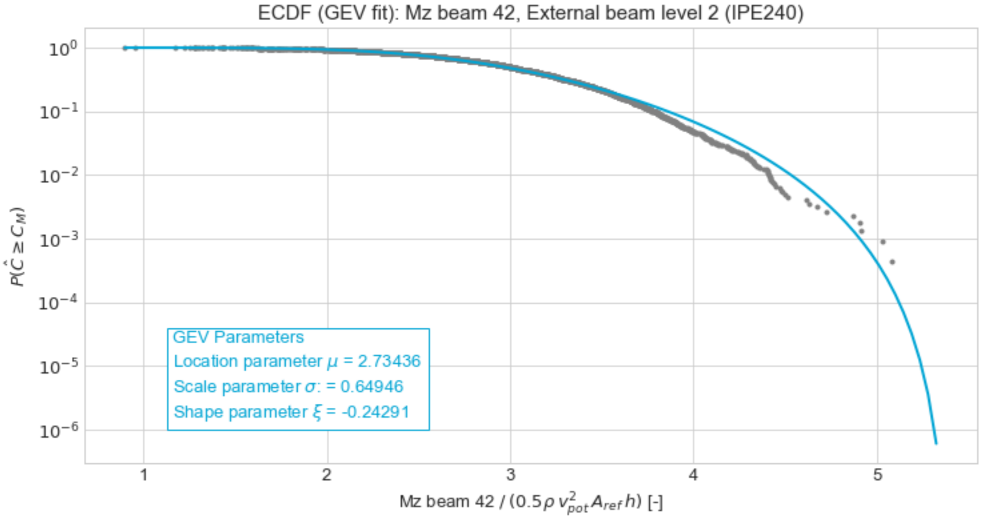

Figure 8.6: Generalized extreme value fit example

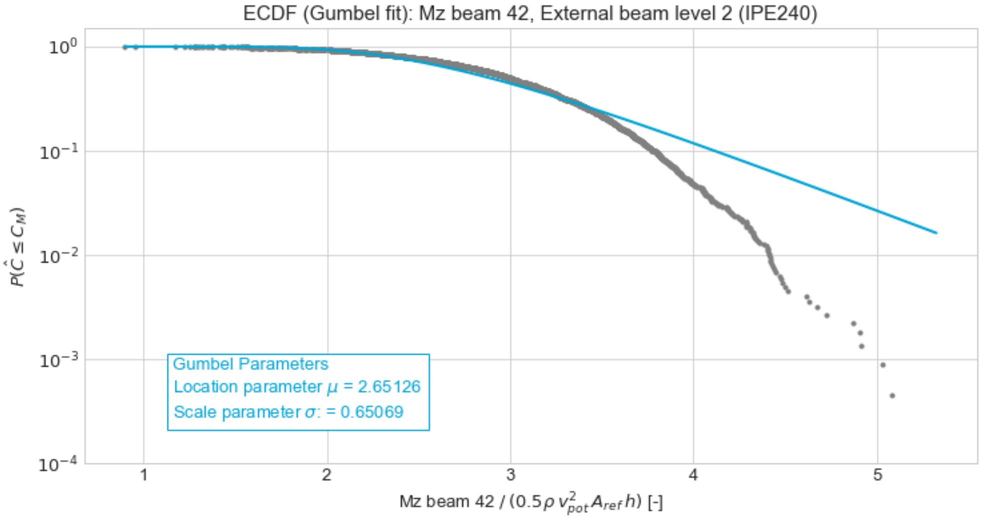

Figure 8.7: Gumbel fit example

Choice for threshold value

However, the parameters obtained for a specific Gumbel fit with this method, including a certain threshold value, are sensitive to the choice of this threshold value. At first glance - based on observations of the tail of the fit - a rough estimate can be given of what roughly speaking the best threshold value should be. It is also useful to know that if the fit lies to the right of the real data points, this fit is on the conservative side and the probability of certain values is higher. It should also be noted that the higher the threshold value, the greater the statistical uncertainties (see also next section Sampling uncertainties). The consideration of the threshold value is therefore very crucial.

Q-Q plot

In order to be able to say with a little more certainty whether a certain threshold value gives better results than another one, the quantiles of the data can be compared with the quantiles of the fit by means of the quantile-quantile plot (Q-Q plot). In the hypothetical case that the fit perfectly describes the data, a diagonal will appear in the Q-Q plot. The fit is on the conservative side if the Q-Q plot is above the diagonal. Figures 8.10a and 8.10b show two Q-Q plots as an example, for respectively a threshold value of 3.0 and 3.8. The plots are both zoomed in on the tail of the distribution, since this is the most important part.

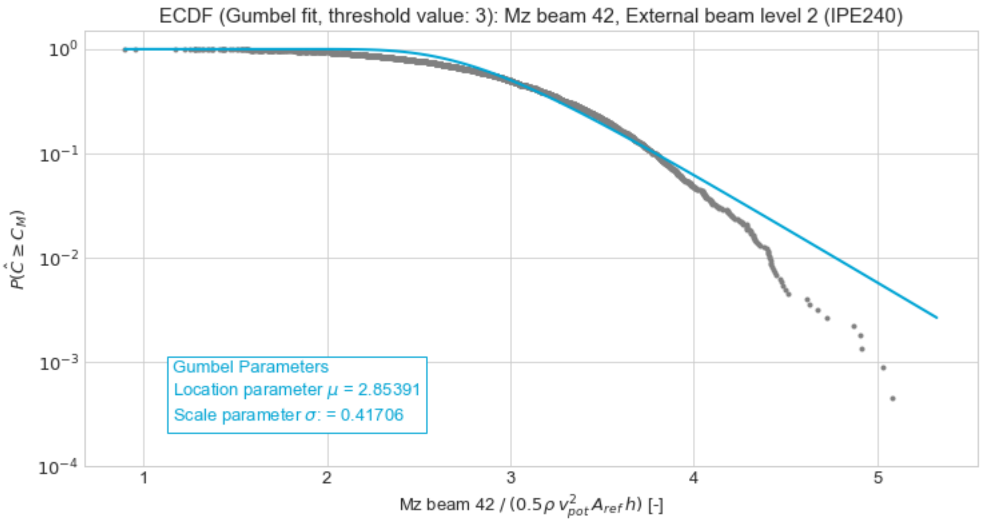

Figure 8.8: Gumbel including threshold value fit example, threshold 3.0

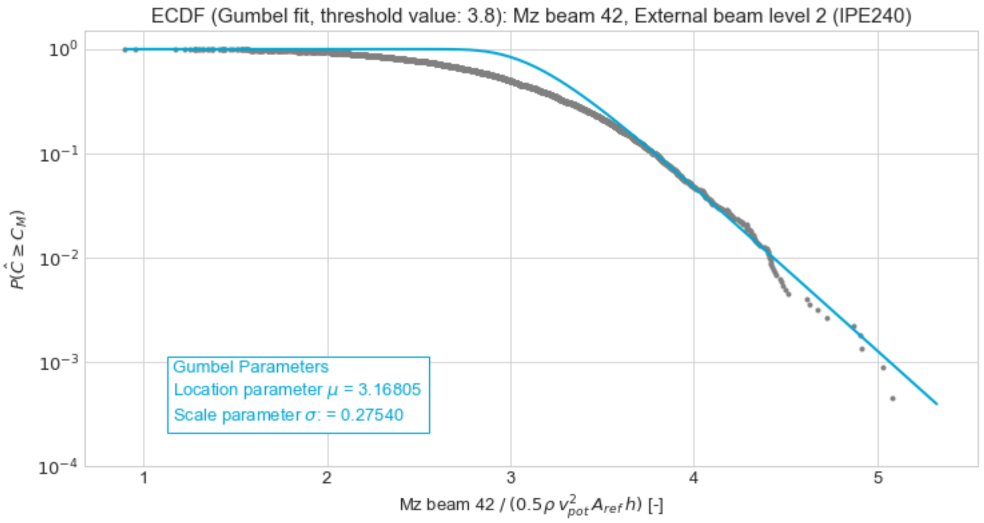

Figure 8.9: Gumbel including threshold value fit example, threshold 3.8

Figure 8.10a clearly shows that choosing the threshold value of 3.0 is a conservative choice (tail above the diagonal). However, the zone between 3 and 3.75 is on the less conservative side (the Q-Q plot is below the diagonal). This can also be seen in figure 8.8; here too, in the zone between 3 and 3.75, the fit is to the left of the data points and therefore corresponds to the observation in the Q-Q plot being not conservative.

Another example in figure 8.10b, with in this case a threshold value of 3.8, shows a different picture. Here, the entire tail is actually on the non-conservative side. In other words, the choice of this threshold value is on the high side. Based on these observations, a perfect threshold value can be chosen, which in this case is between 3.0 and 3.8, resulting in a conservative tail.

8.3.3. Sampling uncertainties

Modelling the extreme load effects is accompanied by the introduction of sampling uncertainties, as measurements are used to fit the extreme value distribution. If the measurements are only slightly different, the parameters used for fitting the distribution will be different. In other words, the fitting and

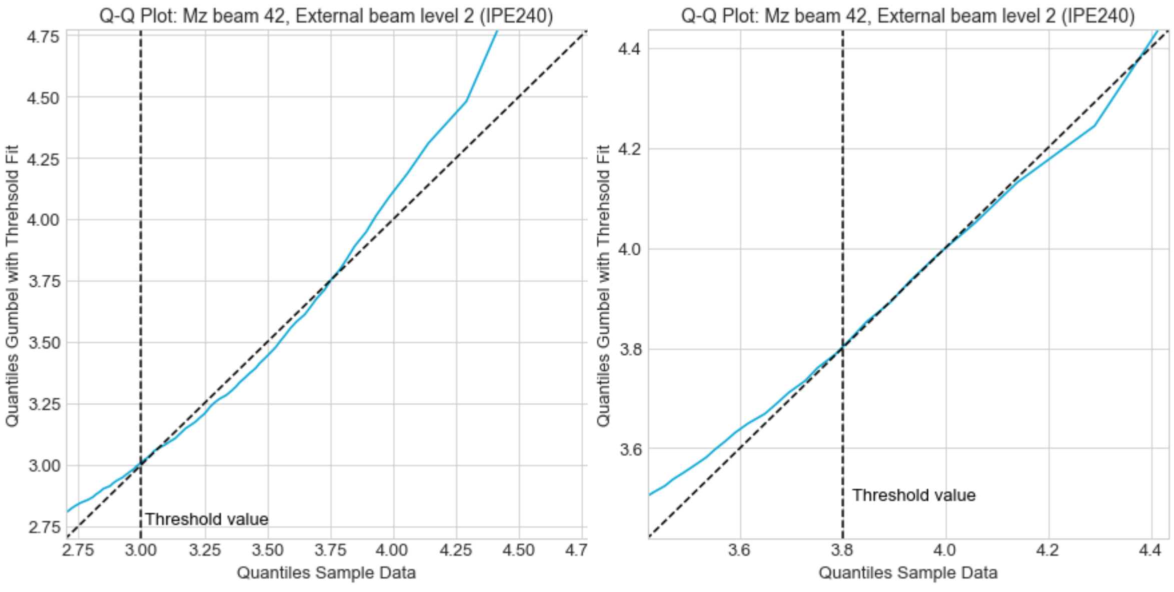

(a) Q-Q plot: Gumbel including threshold value fit example, threshold 3.0

(b) Q-Q plot: Gumbel including threshold value fit example, threshold 3.8

Figure 8.10: Q-Q plots; to illustrate the influence of the choice of the threshold value

determination of the parameters is very sensitive to the exact set of sample data present. As more data is present and thus more sample data for fitting the extreme value distribution is available, the sampling uncertainties will become smaller. In order to include this uncertainty in the further analyses, a factor $S_{\hat{C}_X}$ is defined with a certain distribution and corresponding parameters.

Bootstrap method

Various methods are available to get a grip on the size of these sampling uncertainties. In this study, however, the bootstrap method is used. The main reasons for this are; this method can be used without determining a certain distribution type - which makes the use of this method quite reliable - and it is fast and easy to apply.

This resampling method, generates new sample data based on the original sample data and for each new sample the parameters for fitting the distribution are determined. An example of the bootstrap method is shown in figure 8.11. The method can be explained as follows:

1. Use the original sample data consisting of N values to generate new samples.
2. Create a new sample from the original sample data; draw B times (sufficiently large) a value from the original sample with replacement.
3. For each of these new bootstrapped sample data; determine the model parameters (ξ, μ and σ) and fit the distribution to these data.
4. Plot the distributions for all generated bootstrapped sample data.

All these bootstrapped distributions can then be used to determine exactly how large the sampling uncertainties are. The Cook-Mayne fractile may be used to give a first approximation of the uncertainty (see also section Cook and Mayne method). After the reliability analysis results are available, this fractile value can be verified. This Cook-Mayne fractile is the 0.78 fractile and applies to the hourly T extreme coefficients. Since in this study not hourly extreme coefficients, but for instance the 10-seconds extreme coefficients are used, this fractile must first be converted:

$$P(\hat{X} \leq X)_t = \frac{1 - 0.78}{(3600/10)} = 6.111 \cdot 10^{-4} \tag{8.12}$$

Next, a horizontal line can be drawn on this value in the bootstrap plot. The values of variable X at a level of $P(\hat{X} \leq X) = 6.111 \cdot 10^{-4}$ can then be used to fit a normal distribution. The spread of the distribution subsequently says something about the COV that can be used for the sampling uncertainties.

Figures 8.11 and 8.13 show two examples (plotted all with 300 bootstraps) - respectively of a GEV and Gumbel including threshold fit - of bootstraps. Depending on the specific samples selected for each case, the fit is slightly different. The spread of all these different bootstrapped fits on the Cook-Mayne fractile indicates the degree of sampling uncertainties. This can then be summarised in a COV. Figures 8.12, 8.13 and 8.14 also show that as a larger threshold value is chosen, the sampling uncertainties increase. Therefore, the choice of this threshold value must be well-considered.

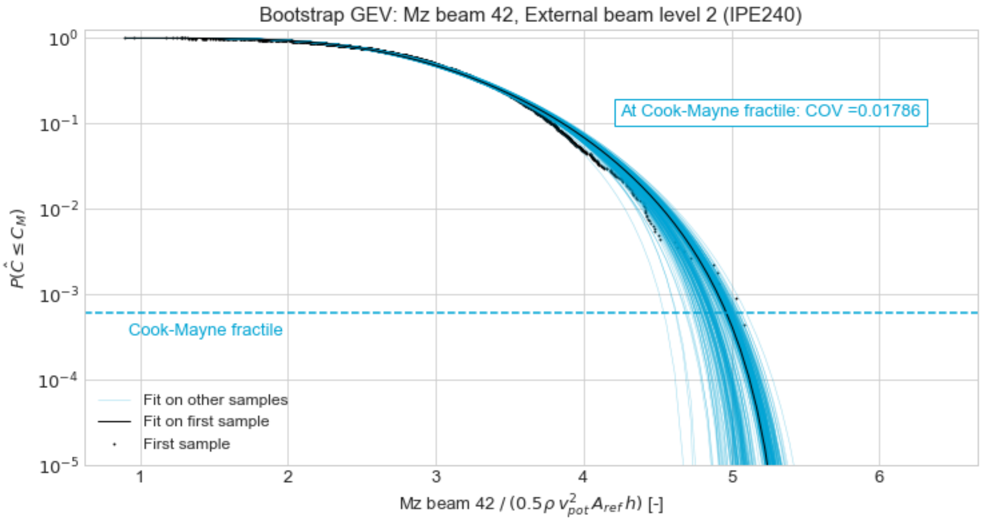

Figure 8.11: Bootstrap using GEV distribution example

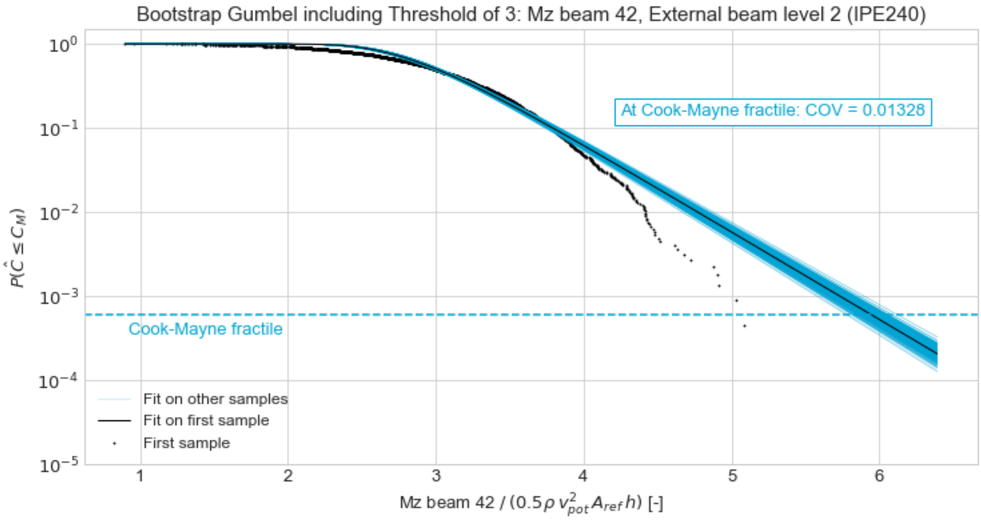

Figure 8.12: Bootstrap using Gumbel including threshold distribution example, threshold: 3.0

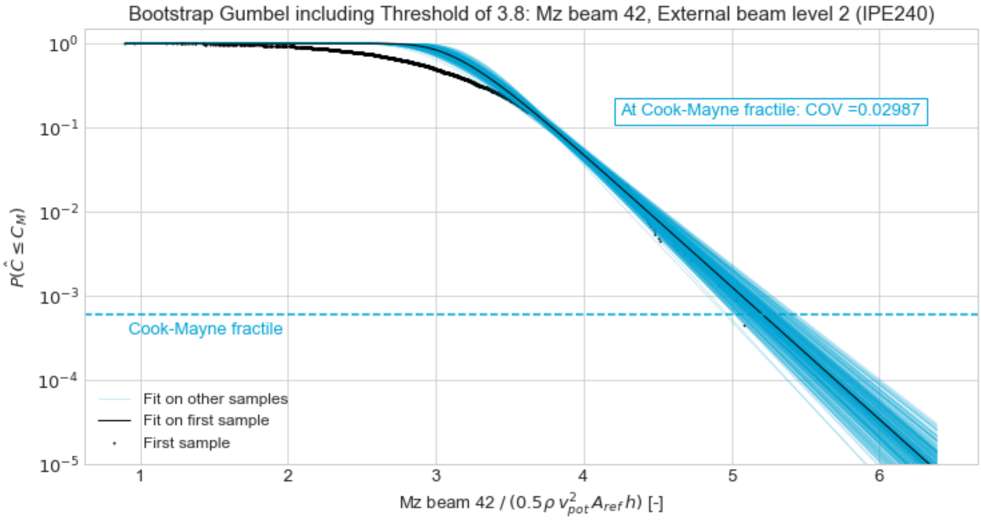

Figure 8.13: Bootstrap using Gumbel including threshold distribution example, threshold: 3.8

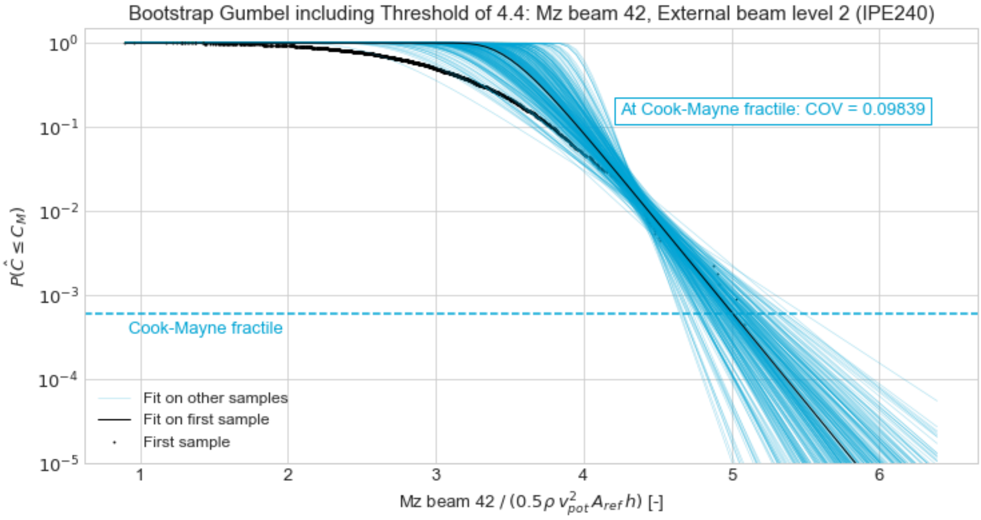

Figure 8.14: Bootstrap using Gumbel including threshold distribution example; threshold: 4.4

9

Reliability Assessment Procedure

This chapter deals with the assessment procedure for determining the structural reliability of various elements in a wind-loaded steel building. The full reliability assessment includes both probabilistic models for the resistance, load side and for the wind loading effect.

9.1. Generic assessment procedure

In order to determine the reliability - expressed in the reliability index β - and the corresponding probability of failure P_f, the theory described in Chapter 2: Structural Reliability is used. Firstly, a limit state function Z (see equation 9.1) is constructed, containing all relevant parameters. Next, the limit state function is examined by means of a level II (FORM) analysis.

$$Z = R_{Element} - E_{Load} - E_{Wind} \tag{9.1}$$

With:

$R_{Element}$ = Resistance of the element under consideration
E_{Load} = Permanent and variable load at element under consideration
E_{Wind} = Wind loading effect at element under consideration

This results in the failure probability which can be converted into the reliability index (see equation 9.2). The advantage of this method is that it is quite fast, in comparison to other methods, and it gives also insight in the influence of certain parameters in the final reliability index by means of the sensitivity factors α.

$$\beta = -\Phi^{-1}(P_f) \tag{9.2}$$

For the actual performance of the reliability assessment the *'Prob Toolbox'* developed by TNO is used. This software is used to do the following:

- Define distribution type and variables
- Define limit state function Z
- Execute FORM and/or Monte Carlo Simulation
- Obtain the failure probability and β-value
- In the case of FORM: obtain α-values and design points

9.2. Resistance

For the determination of the probabilistic model of the resistance, the governing failure mechanisms for all elements of interest are given below. These failure mechanisms in combination with all stochastic parameters will result in the probabilistic description of the resistance side of the reliability analysis.

The location in the building of the elements specified below for further examination are listed in Appendix Finite Element Model Case Study Building Figures - Designation of Various Elements. The deterministic design - based on the Eurocode - of all elements in this case study building can be found in Appendix Deterministic Design Case Study Building according to the Eurocode.

9.2.1. External beams level 1 and 2 (S18 & S42)

In the case study building, two different external beams can be distinguished:

- External beam level 1 (S18)
- External beam level 2 (S42)

However, the calculation method and the governing failure mechanisms are the same for each of these beams. Therefore, the reliability assessment procedure for these beams will be the same as well. The calculations based on the Eurocode show that the moment resistance for each of these beams is the design criterion. All beams are also classified as class 1, which means it can form a plastic hinge with the rotation capacity required from plastic analysis without reduction of the resistance.

For the beams, the plastic bending resistance is as follows:

$$M_{pl,y} = W_{pl,y} \cdot f_y \tag{9.3}$$

A plastic calculation is made to determine the governing failure mechanism used in the limit state function. Since the beams are simply supported on both sides, the formation of one plastic hinge in the middle is enough to form a mechanism. Figure 9.1 and equations 9.4a to 9.4c show the plastic calculation of a beam loaded by a general load p with a length l. Plastic failure of an element occurs when a mechanism forms (kinematically indeterminate $n = -1$), the limit state function is based on the principle of virtual work; moments x rotations, forces x displacements and work ($\delta A = 0$). In this factor p the weight of the structure or for instance the load on the floor can be taken into account. The load effects of wind on these beams are included in a separate factor E_{wind} in the limit state function (see equation 9.5). The detailed formulation of this factor E_{wind} can be found in section Wind loading effect model.

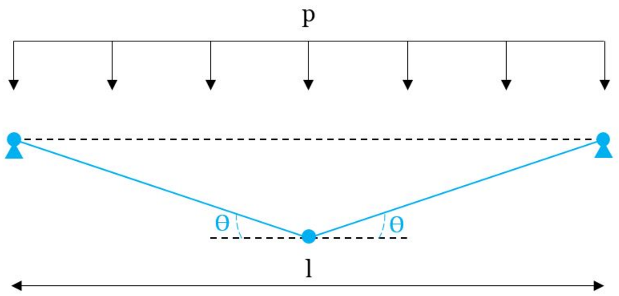

Figure 9.1: Plastic calculation of the beams

$$\delta A = 2 \cdot M_{pl,y} \cdot \theta - \frac{1}{4} \cdot p \cdot l^2 \cdot \theta = 0 \tag{9.4a}$$

$$\delta A = M_{pl,y} - \frac{1}{8} \cdot p \cdot l^2 = 0 \tag{9.4b}$$

$$\delta A = w_{pl,y} \cdot f_y - \frac{1}{8} \cdot p \cdot l^2 = 0 \tag{9.4c}$$

Limit State Function Z
The limit state function can then be formulated as follows:

$$Z = w_{pl,y} \cdot f_y \cdot m_{bending} - \frac{1}{8} \cdot p \cdot l^2 - E_{wind,M} \tag{9.5}$$

The factor $m_{bending}$ is the model uncertainty related to bending moment capacity (see table 5.6 in Chapter 5: Probabilistic Structural Resistance Model).

For p, also $Q \cdot m_i + G$ can be substituted to deal with both permanent and imposed loads. Keep in mind that the imposed load on the roof can't be combined with the wind loads.

9.2.2. Steel bracing (S65)

The horizontal forces on the building, i.e. the wind load, are absorbed by the bracing. In cooperation with the floor, which acts as a diaphragm, the forces are transferred to the foundation. For the design of the bracing it is assumed that it only absorbs tension forces. Since the bracing is always present as a pair, one of the bracings will be under tension force during wind from any direction. The governing failure mechanism for the bracing is therefore as follows:

$$\frac{N_{Ed}}{N_{t,Rd}} \leq 1.0 \tag{9.6}$$

Where $N_{t,Rd} = N_{pl,Rd}$

$$N_{pl,Rd} = A \cdot f_y \tag{9.7}$$

Limit State Function Z
The limit state function can then be formulated as follows:

$$Z = A \cdot f_y - E_{wind,N} \tag{9.8}$$

9.2.3. Internal column (S13)

The first type of column is the internal column. The load on this column is symmetrical, therefore it only results in an axial force in the column. The column is $8\ m$ tall, but it is simple connected in the middle at $4\ m$ height. The buckling length of the column for both axis is $4000\ mm$. In the deterministic design based on the Eurocode the column is classified as class 2 (HEA200), which means it can develop its plastic moment resistance, but have limited rotation capacity because of local buckling.

The governing failure mechanism for the internal column is the flexural buckling resistance. The basic requirement regarding flexural buckling resistance is:

$$\frac{N_{Ed}}{N_{b,Rd}} \leq 1.0$$

$N_{b,Rd}$ is the design buckling resistance and is calculated as follows (for class 1, 2 and 3 cross-sections):

$$N_{b,Rd} = \chi \cdot A \cdot f_y$$

χ is a reduction factor for the buckling resistance. In the case of profile HEA200: $\frac{h}{b} \leq 1.2$, $t_f \leq 100mm$, axis z-z, buckling curve c is used. The corresponding imperfection factor $\alpha = 0.49$.

The non-dimensional slenderness $\bar{\lambda}$ is (for class 1, 2 and 3 cross-sections):

$$\bar{\lambda} = \sqrt{\frac{Af_y}{N_{cr}}} = \frac{L_{cr}}{i}\frac{1}{\lambda_1}$$

Where L_{cr} is the buckling length and is modelled as a stochastic variable. Factor i is the radius of gyration about the relevant axis (z-z in this case) and is $i_y = \sqrt{\frac{I_y}{A}}$ which are both stochastic variables. And factor λ_1 is given by (for steel grade S355 $\longrightarrow \epsilon = 0.81$):

$$\lambda_1 = \pi\sqrt{\frac{E}{f_y}}$$

So $\bar{\lambda}$ is:

$$\bar{\lambda} = \frac{L_{cr}}{i_y}\frac{1}{\lambda_1}$$

$$\phi = 0.5\left(1 + \alpha\left(\bar{\lambda} - 0.2\right) + \bar{\lambda}^2\right)$$

$$\chi = \frac{1}{\phi + \sqrt{\phi^2 - \bar{\lambda}^2}} \qquad (\chi \leq 1.0)$$

Limit State Function Z

The limit state function can then be formulated as follows:

$$Z = \chi \cdot A \cdot f_y \cdot m_{buckling} - (Q \cdot m_i + G) \cdot B - E_{wind,N} \tag{9.9}$$

The factor m_i is the model uncertainty related to live or imposed load (see figure 5.7 in Chapter 5: Probabilistic Structural Resistance Model). The factor $m_{buckling}$ is the model uncertainty related to column buckling (see figure 5.7 in Chapter 5: Probabilistic Structural Resistance Model). Q and G are respectively related to the live load and the self-weight over an area B.

9.2.4. External column (S2)

The second type of column is the external column. The external columns are located on the periphery of the building, however, not in the corners (these are called 'corner' columns, see next section). The column is $8\,m$ tall, but it is simple connected in the middle at $4\,m$ height. The buckling length of the column for both axis is $4000\,mm$. Since the vertical loading is not completely symmetrical on the column, an additional moment at both the roof and floor level is present. Assume that the reaction force of the vertical loading acts at $100\,mm$ from the face of the column, then the moment arm is $\frac{h}{2} + 100\,mm$. In the deterministic design based on the Eurocode the column is classified as class 2 (HEA220), which means it can develop its plastic moment resistance, but have limited rotation capacity because of local buckling.

The governing failure mechanism for the external column is the combined bending moment and axial compression resistance:

$$\frac{N_{Ed}}{N_{b,Rd}} + \frac{M_{Ed}}{M_{b,Rd}} \leq 1.0$$

Flexural buckling resistance

$N_{b,Rd}$ is the design buckling resistance and is calculated as follows (for class 1, 2 and 3 cross-sections):

$$N_{b,Rd} = \chi A f_y$$

χ is a reduction factor for the buckling resistance. For profile HEA220, $\frac{h}{b} \leq 1.2$, $t_f \leq 100mm$, axis z-z, buckling curve c is used. The corresponding imperfection factor $\alpha = 0.49$.

The non-dimensional slenderness $\bar{\lambda}$ is (for class 1, 2 and 3 cross-sections):

$$\bar{\lambda} = \sqrt{\frac{Af_y}{N_{cr}}} = \frac{L_{cr}}{i}\frac{1}{\lambda_1}$$

Where L_{cr} is the buckling length and is modelled as a stochastic variable. Factor i is the radius of gyration about the relevant axis (z-z in this case) and is $i_y = \sqrt{\frac{I_y}{A}}$ which are both stochastic variables. And factor λ_1 is given by (for steel grade S355 $\longrightarrow \epsilon = 0.81$):

$$\lambda_1 = \pi\sqrt{\frac{E}{f_y}}$$

So $\overline{\lambda}$ is:

$$\overline{\lambda} = \frac{L_{cr}}{i_y}\frac{1}{\lambda_1}$$

$$\phi = 0.5\left(1 + \alpha\left(\overline{\lambda} - 0.2\right) + \overline{\lambda}^2\right)$$

$$\chi = \frac{1}{\phi + \sqrt{\phi^2 - \overline{\lambda}^2}} \quad (\chi \leq 1.0)$$

Lateral torsional buckling
The column is laterally unrestrained, so the member should also be verified against lateral torsional buckling. The basic design requirement is:

$$\frac{M_{Ed}}{M_{b,Rd}} \leq 1.0$$

Where $M_{b,Rd}$ is defined as follows (for class 2 sections use $W_y = W_{pl,y}$):

$$M_{b,Rd} = \chi_{LT} W_{pl,y} f_y$$

The non-dimensional slenderness related to lateral torsional buckling $\overline{\lambda_{LT}}$ is determined using the conservative formula:

$$\overline{\lambda_{LT}} = 0.9 \cdot \overline{\lambda}$$

For profile HEA220, rolled I-section, $\frac{h}{b} \leq 2$, buckling curve a is used. The corresponding imperfection factor $\alpha_{LT} = 0.21$. For rolled or equivalent welded sections, the values for $\overline{\lambda_{LT,0}}$ and β (not the reliability index!) in the formula for ϕ_{LT} are:

$$\overline{\lambda_{LT,0}} = 0.4$$

$$\beta = 0.75$$

$$\phi = 0.5\left(1 + \alpha_{LT}\left(\overline{\lambda} - \overline{\lambda_{LT,0}}\right) + \beta\overline{\lambda}^2\right)$$

$$\chi_{LT} = \frac{1}{\phi + \sqrt{\phi^2 - \overline{\lambda}^2}} \quad \left(\chi_{LT} \leq 1.0 \text{ and} \leq \frac{1}{\overline{\lambda}_{LT}^2}\right)$$

Combined bending moment and axial compression
The cross-section is verified using the combined bending moment and axial compression buckling unity check.

$$\frac{N_{Ed}}{N_{b,Rd}} + \frac{M_{Ed}}{M_{b,Rd}} \leq 1.0$$

Limit State Function Z
The limit state function can then be formulated as follows:

$$Z = 1 - \frac{(Q \cdot m_i + G) \cdot B + E_{wind,N}}{\chi \cdot A \cdot f_y \cdot m_{buckling}} - \frac{(Q \cdot m_i + G) \cdot B \cdot u + E_{wind,M}}{\chi_{LT} \cdot W_{pl,y} \cdot f_y \cdot m_{lat.buckling}} \tag{9.10}$$

The factor m_i is the model uncertainty related to live or imposed load (see figure 5.7 in Chapter 5: Probabilistic Structural Resistance Model). The factor $m_{buckling}$ is the model uncertainty related to column buckling (see figure 5.7 in Chapter 5: Probabilistic Structural Resistance Model). Factor $m_{lat.buckling}$ is related to lateral torsional buckling based on the model uncertainty classification 'Lateral torsional buckling of rolled class 1-3 beams' with $\alpha_{LT} = 0.21$ in Appendix Model uncertainties. Q and G are respectively related to the live load and the self-weight over an area B. u is the moment arm $h/2+100mm$, in which h is the height of the profile.

It should also be noted that there is a correlation between the magnitude of the internal forces such as the moment and the normal force. If a sample is drawn for a relatively high moment, this also means that the normal load is high. In the FORM analysis, it is therefore important to apply a correlation between the moment and normal load effects. It is assumed here that they are fully correlated.

9.2.5. Corner column (S1)

The corner columns are located on the corners of the building. The permanent and variable forces - using the governing combination - on both the roof and floor level lead to vertical forces. The area used for these loads is $5 \cdot 5\ m$. Also the horizontal wind load generates a bending moment in the column. The column is $8\ m$ tall, but it is simple connected in the middle at $4\ m$ height. The buckling length of the column for both axis is $4000\ mm$. Since the vertical loading is not completely symmetrical on the column, an additional moment at both the roof and floor level is present. Assume that the reaction force of the vertical loading acts at $100\,mm$ from the face of the column, then the moment arm is $\frac{h}{2} + 100\,mm$.

The cross-section is verified using the simplified combined bending moment and axial compression buckling unity check.

$$\frac{N_{Ed}}{N_{b,Rd}} + \frac{M_{Ed}}{M_{b,Rd}} + 1.5 \cdot \frac{M_{z,Ed}}{M_{z,Rd}} \leq 1.0$$

Flexural buckling resistance

$N_{b,Rd}$ is the design buckling resistance and is calculated as follows (for class 1, 2 and 3 cross-sections):

$$N_{b,Rd} = \chi A f_y$$

χ is a reduction factor for the buckling resistance. For profile HEA220, $\frac{h}{b} \leq 1.2$, $t_f \leq 100mm$, axis z-z, buckling curve c is used. The corresponding imperfection factor $\alpha = 0.49$.

The non-dimensional slenderness $\bar{\lambda}$ is (for class 1, 2 and 3 cross-sections):

$$\bar{\lambda} = \sqrt{\frac{A f_y}{N_{cr}}} = \frac{L_{cr}}{i}\frac{1}{\lambda_1}$$

Where L_{cr} is the buckling length and is modelled as a stochastic variable. Factor i is the radius of gyration about the relevant axis ($z-z$ in this case) and is $i_y = \sqrt{\frac{I_y}{A}}$ which are both stochastic variables. And factor λ_1 is given by (for steel grade S355 $\longrightarrow \epsilon = 0.81$):

$$\lambda_1 = \pi\sqrt{\frac{E}{f_y}}$$

So $\bar{\lambda}$ is:

$$\bar{\lambda} = \frac{L_{cr}}{i_y}\frac{1}{\lambda_1}$$

$$\phi = 0.5\left(1 + \alpha\left(\bar{\lambda} - 0.2\right) + \bar{\lambda}^2\right)$$

$$\chi = \frac{1}{\phi + \sqrt{\phi^2 - \bar{\lambda}^2}} \quad (\chi \leq 1.0)$$

Lateral torsional buckling
The column is laterally unrestrained, so the member should also be verified against lateral torsional buckling. The basic design requirement is:

$$\frac{M_{Ed}}{M_{b,Rd}} \leq 1.0$$

Where $M_{b,Rd}$ is defined as follows (for class 2 sections use $W_y = W_{pl,y}$):

$$M_{b,Rd} = \chi_{LT} W_{pl,y} f_y$$

The non-dimensional slenderness related to lateral torsional buckling $\overline{\lambda_{LT}}$ is determined using the conservative formula:

$$\overline{\lambda_{LT}} = 0.9 \cdot \bar{\lambda}$$

For profile HEA220, rolled I-section, $\frac{h}{b} \leq 2$, buckling curve a is used. The corresponding imperfection factor $\alpha_{LT} = 0.21$. For rolled or equivalent welded sections, the values for $\overline{\lambda_{LT,0}}$ and β in the formula for ϕ_{LT} are:

$$\overline{\lambda_{LT,0}} = 0.4$$

$$\beta = 0.75$$

$$\phi = 0.5\left(1 + \alpha_{LT}\left(\bar{\lambda} - \overline{\lambda_{LT,0}}\right) + \beta\bar{\lambda}^2\right)$$

$$\chi_{LT} = \frac{1}{\phi + \sqrt{\phi^2 - \bar{\lambda}^2}} \quad \left(\chi_{LT} \leq 1.0 \text{ and} \leq \frac{1}{\overline{\lambda_{LT}}^2}\right)$$

Bending moment resistance
For a class 2 section, the bending moment resistance (for the weak $z - z$ axis) is:

$$M_{z,Rd} = M_{pl,Rd} = W_{pl,z} \cdot f_y$$

Limit State Function Z
The limit state function can then be formulated as follows:

$$Z = 1 - \frac{1}{m_{interaction}} \cdot \left(\frac{(Q \cdot m_i + G) \cdot B + E_{wind,N}}{\chi \cdot A \cdot f_y} + \frac{(Q \cdot m_i + G) \cdot B \cdot u + E_{wind,My}}{\chi_{LT} \cdot W_{pl,y} \cdot f_y} + ..\right.$$
$$\left. ..1.5 \cdot \frac{(Q \cdot m_i + G) \cdot B \cdot u + E_{wind,Mz}}{W_{pl,z} \cdot f_y}\right) \tag{9.11}$$

The factor m_i is the model uncertainty related to live or imposed load (see figure 5.7 in Chapter 5: Probabilistic Structural Resistance Model). Factor $m_{interaction}$ is related to interaction of bending and compression based on the model uncertainty classification 'Interaction between biaxial bending and compression of class 1-3 beams' with $\alpha_{LT} = 0.21$ in Appendix Model uncertainties. Q and G are respectively related to the live load and the self-weight over an area B. u is the moment arm $h/2+100mm$, in which h is the height of the profile.

As in the previous case with the external column, the correlation between the moment and normal load effect must also be included in the FORM analysis. Please note that only the normal load and moment in the strong axis are fully correlated. The moment in the weak direction is not correlated with the other variables.

9.3. Wind loading effect model

In order to include the wind load in the reliability analysis, a wind loading effect model is developed. It is available for moment, normal force and shear force. The basis of this wind loading effect model is the Davenport's wind loading chain and also the model as used in the Eurocode. The wind loading chain presented here is in accordance with the recent investigations by Meinen [25] and la Gasse [23]. All aspects and associated uncertainties affecting wind loading are included.

$$\text{Moment} \longrightarrow E_{wind,M} = \frac{1}{2}\cdot\rho_{air}\cdot v_{pot}^2\cdot S_v^2\cdot c_r(h_{ref})^2\cdot\hat{c}_M\cdot S_{\hat{c}_M}\cdot A_{ref}\cdot h\cdot\chi_{model} \tag{9.12}$$

$$\text{Normal force} \longrightarrow E_{wind,N} = \frac{1}{2}\cdot\rho_{air}\cdot v_{pot}^2\cdot S_v^2\cdot c_r(h_{ref})^2\cdot\hat{c}_N\cdot S_{\hat{c}_N}\cdot A_{ref}\cdot\chi_{model} \tag{9.13}$$

$$\text{Shear force} \longrightarrow E_{wind,V} = \frac{1}{2}\cdot\rho_{air}\cdot v_{pot}^2\cdot S_v^2\cdot c_r(h_{ref})^2\cdot\hat{c}_V\cdot S_{\hat{c}_V}\cdot A_{ref}\cdot\chi_{model} \tag{9.14}$$

With:

ρ_{air} = Air density $[kg/m^3]$
v_{pot} = Basic wind velocity: t minute mean wind speeds at $z = 10$ m and for terrain roughness $z_{0,ref}$ m $[m/s]$
S_v = Sampling uncertainties of basic wind velocity model [-]
$c_r(h_{ref})$ = Terrain roughness factor at the reference height of the structure h_{ref} correcting for $z_{0,ref}$ m [-]
$\hat{c}_X$ = Peak load effect coefficient (1-hour extremes) [-]
$S_{\hat{c}_X}$ = Sampling uncertainties of load effect model [-]
A_{ref} = Area of the facade of the building $[m^2]$
h = Height of the building $[m]$
χ_{model} = Model uncertainty factor [-]

Air density ρ_{air}

In the reliability analysis, the air density is taken as a deterministic value of $1.225\ kg/m^3$. This value is the air density from the wind tunnel test. All irregularities and regional phenomena such as altitude, temperature and barometric pressure are not included in this analysis.

Wind velocity v_{pot}

For the modelling of the wind velocity, the research of la Gasse is used. In this study the same wind data is used and therefore these models can also be used in this study. Since the reference period of the construction is $T = 50$ years, the 50-yearly extreme wind speeds must also be modelled for v_{pot}. Using the maximum-likelihood estimation technique, both a type I and a type III generalized extreme value distribution are fitted. The uncertainties related to this wind velocity modelling are in factor S_v.

Roughness factor c_r

The roughness factor $c_r(z)$ refers to the change in mean wind speed over a height z and corrects directly for the terrain roughness z_0. This factor is subject to considerable variability, so it is wise to include it in the wind loading effect model. In the JCSS document on wind loading [27], a log-normal distribution with mean-to-specified value of 0.80 and $COV = 0.1 - 0.2$.

Based on the formula mentioned in the Eurocode, see also figure 3.6, the roughness factor can be determined. It is assumed that $z_0 = 0.8\,m$ and $z_{0,II} = 0.03\,m$. Based on the mean-to-specified value of 0.8, the following formulas for $c_r(Z_e)$ and the mean $\mu_{c_r^2}$ can be determined:

$$c_r(Z_e) = 0.19\cdot\left(\frac{z_0}{z_{0,II}}\right)^{0.07}\cdot ln\left(\frac{Z_e}{z_0}\right) \tag{9.15}$$

$$\mu_{c_r^2} = 0.8 \cdot c_r(Z_e)^2 \tag{9.16}$$

Based on these data and formulas, and also assuming that h_{ref} is at the top of the building at a height of $120\ m$, the distribution parameters of c_r become:

$$c_r(120) = 0.19 \cdot \left(\frac{0.8}{0.03}\right)^{0.07} \cdot ln\left(\frac{120}{0.8}\right) = 1.198 \tag{9.17}$$

$$\mu_{c_r^2} = 0.8 \cdot c_r(Z_e)^2 = 0.8 \cdot 1.198^2 = 1.15 \tag{9.18}$$

$$COV_{c_r^2} = 0.15 \tag{9.19}$$

Load effect coefficients $\hat{c}_M$, $\hat{c}_N$, $\hat{c}_V$

The exact and detailed explanation of the load effect coefficients can be found in Chapter 8: Technique for Obtaining Load Effects. In addition, there is the factor $S_{\hat{c}_X}$, which incorporates the sampling uncertainties of the load effect modelling.

Model uncertainty χ_{model}

All aspects that cannot be specifically quantified but still contribute to an uncertainty in the analysis are attributed to this general model uncertainty factor χ_{model}. This factor is modelled as a normal distribution with parameters: $\mu = 1.0$ and $COV_\chi = 0.1$.

III

Reliability Assessment of the Case Study Building

10

Case Study Description

To apply the method, it is decided to carry out a reliability assessment on a case study building. This chapter focuses on the description of the case study building and the wind tunnel data. First in section Case study building, a description of the case study building - which is of interest during the reliability analysis - is given. Then in section Wind tunnel data a description is given of the wind tunnel data which is used during this research.

10.1. Case study building

In order to assess the reliability of a steel structural system of a wind excited building, a case study building is designed. The design of this case study building is based on ultimate limit state design for consequence class 2 and a reference period of 50 years. In the reliability assessment it is assumed that global failure of the steel structural elements in the main bearing structure is of main focus.

In order to use the wind tunnel data in the best possible way - without any transformation - it is decided to relate the dimensions of the case study building to those of the wooden model in the wind tunnel. These wooden model dimensions are $h_{wt} = 0.48\,m$ and a square plan with sides of $b_{wt} = 0.12\,m$. The scale factor between the wind tunnel model and reality is $1 : 250$. So the case study building, for which the main steel supporting structure is designed, has dimensions of $30 \cdot 30 \cdot 120\,m$ (figure 10.1). It is assumed that the building is located at Schiphol Airport in Amsterdam. This location is chosen, because there is a huge amount of wind measurements available (KNMI measurements) and secondly, for the derivation of the fundamental basic wind velocity of Wind Area II (Dutch National Annex of EN1991-1-4), the same measurements are used.

The ’large’ case study building (which is based on a scale model from a wind tunnel test) has dimensions $30 \cdot 30 \cdot 120\ m$. In order to design the steel main bearing structure of this large building, first a relatively ’small’ case study building is designed to tackle all the design related problems and also to get familiarised with the reliability analysis of the structure. Therefore the top two levels (each $4m$ in height) of the case study building are designed (see building on the right in figure 10.1) and imagine these two top levels to be a building on itself.

In order to give accurate reliability analysis results, imagine the case study building to be subjected to wind speeds and pressures (as of in the Eurocode) that occur at a height of $112–120\,m$ above ground level, so then the wind pressures from the wind tunnel test can be used directly and don’t need any transformation.

A braced frame structure is chosen to provide stability to the structure. The horizontal forces caused by the wind are absorbed by two perpendicular bracing systems. The vertical bracing between the columns ensures that there is a load path for the horizontal forces towards the foundation, thus providing stability to the building. It is preferable to place the bracing on the outer layer of the building, both because of the torsion resulting from the wind load and because the functionalities of the building are

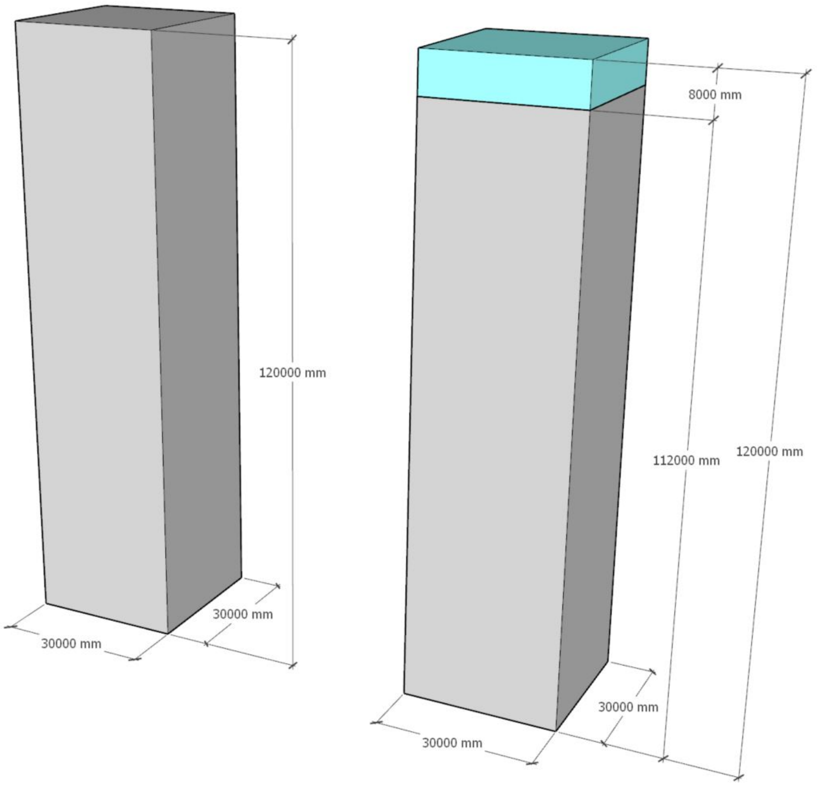

Figure 10.1: Case study building dimensions

not lost (no bracing in the middle of the building dividing the interior space). To make the design as efficient as possible, it is decided to place the bracing in the middle of the facade. For the horizontal bracing in the structure – which will carry the horizontal loads to the vertical bracing – the floor on each level will be able to act as horizontal diaphragm. The beams are simply connected to the columns and the columns are hinged to the ground level. Since the building is symmetric, the design of the several elements is made as efficient as possible.

Some remarks about the design of the case study building:

- Design is based on ultimate limit state design and a reference period of 50 years and consequence class 2
- Connections are not designed in great detail. It is only assumed that the connections are hinged or rigid, a detailed design of these connections is omitted. Global failure of the steel structural elements in the main bearing structure is of focus in this research
- It is assumed that the building is prone to wind forces, the imposed loads due to the function of the building (Class B, Office) and its own weight. Wind forces are considered the dominant loading
- Influence of surrounding buildings on the wind forces are not considered in this research
- Stability is provided through steel bracing
- Fire resistance and fatigue are not considered in the design
- The foundation of the building is not designed

The plan and side view of the building are in figure 10.2a and 10.2b. A 3d model of the case study building is in figure 10.3a and 10.3b.

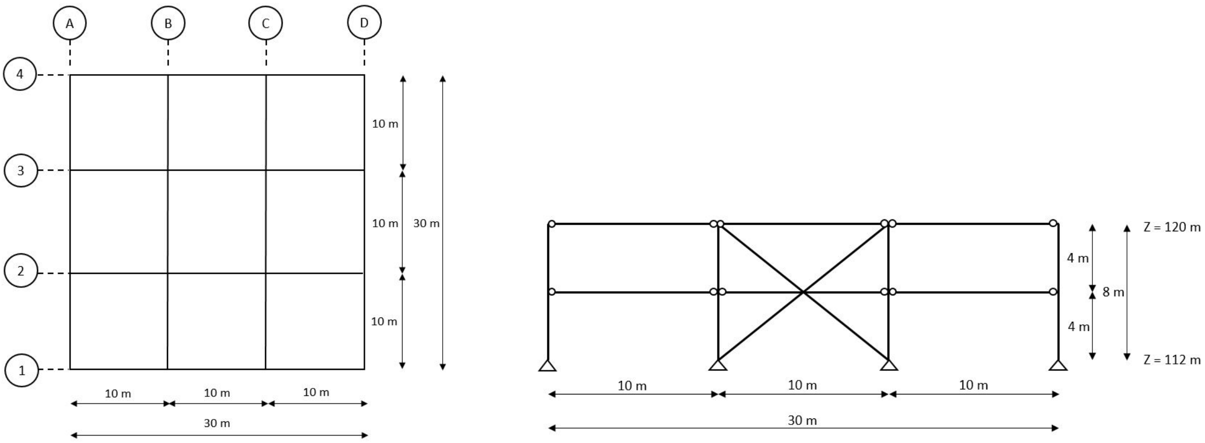

(a) Case study building plan view

(b) Case study building side view

Figure 10.2: Plan and side view of the case study building

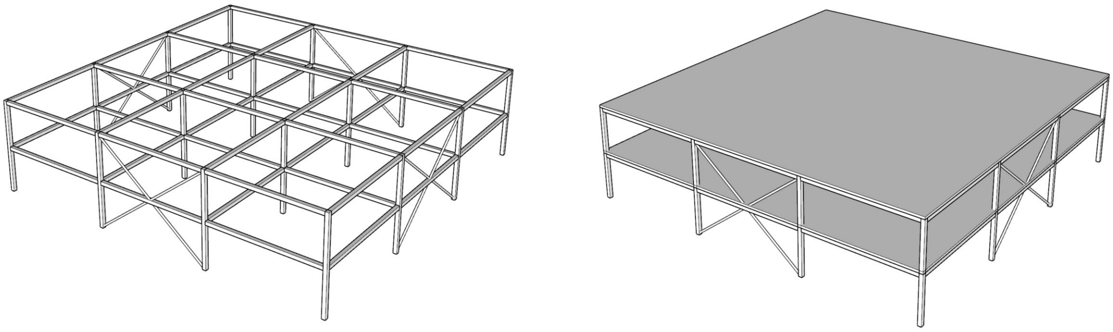

(a) Steel main bearing structure

(b) Steel main bearing structure (including the floor and roof)

Figure 10.3: 3d model of the case study building

The complete design - based on regulations in the *Eurocode* - of the steel main bearing structure of this case study building can be found in Annex Deterministic Design Case Study Building according to the Eurocode.

In addition, Annex Finite Element Model Case Study Building Figures - Designation of Various Elements contains figures of the structure as modelled in SCIA FEM, as well as an illustration of the elements in the model that are investigated further.

10.2. Wind tunnel data

This research uses the same wind tunnel data as in the research performed by Meinen [25] and la Gasse [23]. Several experiments - including 'long-run' (of interest in this research) and 'short-run' - are performed in the open-circuit atmospheric boundary layer wind tunnel at TNO [25], in order to derive the peak external pressure coefficients. In the 'long-run' experiment, the model is subjected to a frontal (angle of attack $0°$) incident wind flow for a considerably long duration of 176 hours in full-scale. A small scale wooden model is put to the test and pressure measurements are obtained. The terrain roughness in the wind tunnel corresponds to a value of $z_0 = 0.8\ m$ in full-scale.

86 pressure taps are placed at two opposite sides of the model. After the experiment is finished, the model is turned $90°$ and the two other sides are being put to the test. This results in measurements at 172 pressure taps on all sides of the model. In addition, 4 pressure taps measure the dynamic pressure at a reference height of $h_{ref,wt} = 0.48\ m$, which is the roof height. All the details regarding the wind tunnel test and data are in table 10.1.

Wind tunnel and incident flow	Dimensions	$13.5x3x2\ m$
	ρ_{air}	$1.225\ kg/m^3$
	$v_{ref,h}$	$14.7\ m/s$
Scaled model	Dimensions	$0.48x0.12\ m$
	Scale λ_g	$1:250$
	Taps	[1:7] Side A; [90:96] Side B; [39:45] Side C; [128:134] Side D; [77:86] (run 1) and [166:175] (run 2) Top; [87:88] (run 1) and [176:177] (run 2) Reference pressures
Test	Sampling duration	1.5701 hour
	Full-scale duration	176 hour
	Angle of attack	frontal, 0°
	Sampling frequency	400 Hz

Table 10.1: Wind tunnel data details [25]

11

Description Load Effects

This chapter is dedicated to obtaining the load effects. The exact procedure for obtaining these load effects can be found in Chapter 8: Technique for Obtaining Load Effects. For all elements that are investigated in the reliability analysis, several steps have to be taken to obtain a good fit of the load effects. Also the sampling uncertainties are identified by means of the bootstrap method including the variation on the Cook-Mayne fractile.

In total, 65,000 timesteps are calculated for both the timeseries and the probabilistic wind pressure model approach. This number is sufficiently large such that the sampling uncertainties are reasonably low, however, obtaining even more data would be preferable. Due to the large amount of computing power and time, this was not done in this study. The choice has been made to use the same number of timesteps for these two procedures in order to neglect further differences in the degree of uncertainties.

In Annex Extra Figures - Description Load Effects more figures can be found related to the description of these load effects. Since the procedure is the same for all elements, only one element is discussed in detail below. The figures related to the other elements can be found in the Annex. The final results that are used are shown in table 11.1 and 11.2. It is decided to determine only the load effects on the basis of the probabilistic wind pressure model for the steel bracing. A further explanation of why this choice is made can be found in section Comparison load effects time series vs probabilistic wind pressure model.

11.1. Example: Steel bracing (S65)

The structural element most affected by wind loads is the steel bracing in the building. This bracing mainly absorbs the horizontal wind forces that are present on the building.

11.1.1. $E_{wind,N}$

Load effects - Time series

To determine the correct block duration, the autocorrelation and reversed univariate method are plotted in figure 11.1. In the autocorrelation figure it can be clearly seen that the enveloping line intersects the threshold value at around $t = 20\ s$. The tail of the data in the reversed univariate method also shows great results for $t = 20\ s$. Based on both methods, a block duration of $t = 20\ s$ is chosen. This results in 902 extreme values remaining for fitting an extreme value distribution.

After varying the threshold value, a threshold of 0.4 is finally chosen (see figure 11.2a, including the parameters of the $20\ s$ extreme value fit). This means that the fit is still just on the conservative side. See also the Q-Q plot in the Annex. The bootstrap method at this threshold value is shown in figure 11.2b and the $COV = 0.02347$.

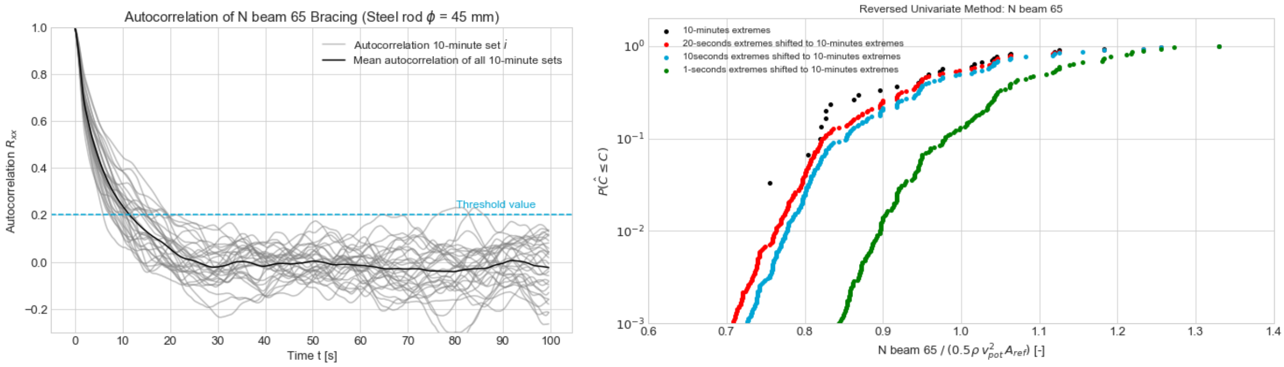

(a) Autocorrelation plot of N steel bracing (S65)

(b) Reversed univariate method plot of N steel bracing (S65)

Figure 11.1: Autocorrelation and Reversed univariate method plots of N steel bracing (S65), in order to obtain the correct block duration t

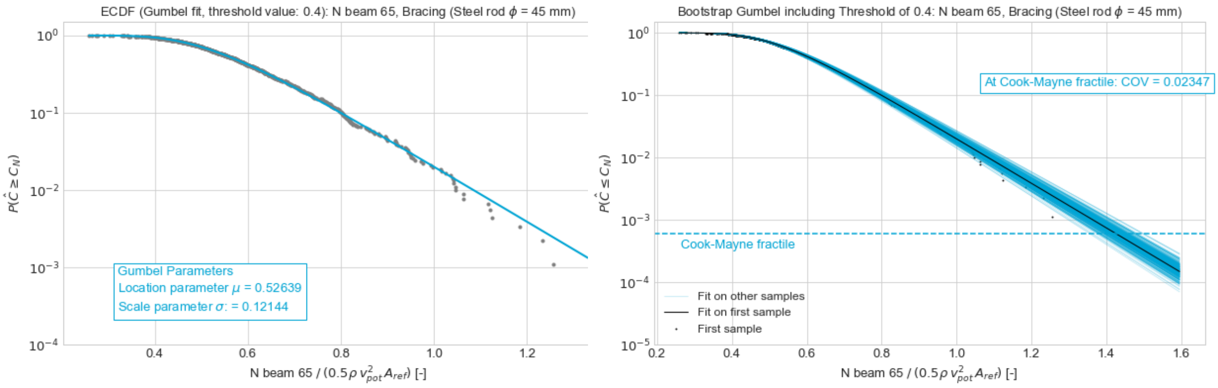

(a) Gumbel fit (threshold value: 0.4) of N steel bracing (S65)

(b) Bootstrap (threshold value: 0.4) of N steel bracing (S65) using 300 bootstrapped distributions

Figure 11.2: Gumbel fit and Bootstrap (threshold value: 0.4) of N steel bracing (S65) ($20s$-extremes)

Load effects - Probabilistic wind pressure model

In order to determine the load effects on the basis of the probabilistic wind pressure model, a choice for the block duration t must first be made. In order to make a good comparison between the different methods, it is decided to use the same block duration for both methods. As can also be seen in the appendix, the raw load effect data based on the probabilistic wind pressure model looks different than for the timeseries case. This is because all time steps are a random selection from the model and the time steps do not contain any correlation between each other. Therefore, it is not possible to choose a good block duration using the autocorrelation and reversed univariate method. In the timeseries case, zones are seen to be relatively high or low for a longer period, while in the probabilistic model case this is much more evenly distributed.

After varying the threshold value, a threshold of 0.8 is chosen (see figure 11.3a, including the parameters of the $20\ s$ extreme value fit). The fit is still just on the conservative side, however one outlier is visible. The bootstrap method at this threshold value is shown in figure 11.3b and the $COV = 0.02285$.

11.2. Load effects used in reliability assessment

In the reliability assessment it is necessary that the load effects distribution is related to the 1-hour extreme values. Since for the fitting of the various distributions not the 1 hour, but for example the 10- or 20-seconds extremes are used, the parameters of the Gumbel distribution need to be adjusted. The advantage of the Gumbel distribution is that the distribution keeps the same shape, but shifts over a certain distance. For this reason, the σ of the distribution remains unchanged. The μ associated with

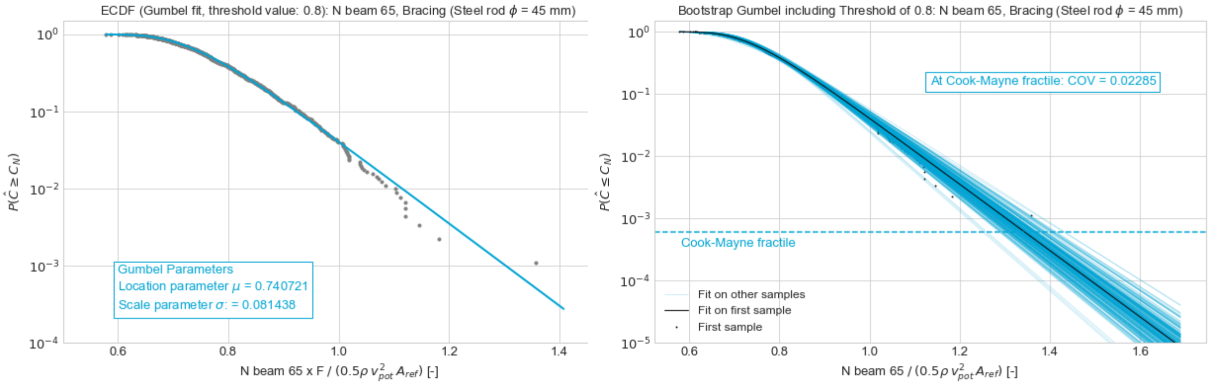

(a) Gumbel fit (threshold value: 0.8) of N steel bracing (S65) (probabilistic wind pressure model)

(b) Bootstrap (threshold value: 0.8) of N steel bracing (S65) using 300 bootstrapped distributions (probabilistic wind pressure model)

Figure 11.3: Gumbel fit and Bootstrap (threshold value: 0.8) of N steel bracing (S65) ($20s$-extremes) (probabilistic wind pressure model)

the 1-hour extreme values distribution can be calculated as follows (t is related to for example 10 or 20 seconds used for fitting the distribution):

$$\mu_{1-hour} = \mu_t + ln\left(\frac{3600}{t}\right) / \left(\frac{\pi}{\sigma \cdot \sqrt{6}}\right) \tag{11.1}$$

Element	**Load Effect**	**Block Duration t**	**Parameters t-extremes**	**Parameters 1-hour-extremes**	**Sampling Uncertainty COV** [1]
External beam level 2 (S42)	$E_{wind,M}$	$20\ s$	$\mu = 0.000499$, $\sigma = 0.000111$	$\mu = 0.000948$, $\sigma = 0.000111$	0.07234
External beam level 1 (S18)	$E_{wind,M}$	$20\ s$	$\mu = 0.002159$, $\sigma = 0.000498$	$\mu = 0.004175$, $\sigma = 0.000498$	0.03376
Steel bracing (S65)	$E_{wind,N}$	$20\ s$	$\mu = 0.52639$, $\sigma = 0.12144$	$\mu = 1.01810$, $\sigma = 0.12144$	0.02347
Internal column (S13)	$E_{wind,N}$	$20\ s$	$\mu = 0.02254$, $\sigma = 0.00564$	$\mu = 0.04538$, $\sigma = 0.00564$	0.12157
External column (S2)	$E_{wind,N}$	$10\ s$	$\mu = 0.17719$, $\sigma = 0.05107$	$\mu = 0.41157$, $\sigma = 0.05107$	0.02821
External column (S2)	$E_{wind,M}$	$20\ s$	$\mu = 0.004426$, $\sigma = 0.001027$	$\mu = 0.00858$, $\sigma = 0.001027$	0.03143
Corner column (S1)	$E_{wind,N}$	$20\ s$	$\mu = 0.12246$, $\sigma = 0.02796$	$\mu = 0.23567$, $\sigma = 0.02796$	0.07431
Corner column (S1)	$E_{wind,My}$	$10\ s$	$\mu = 0.004943$, $\sigma = 0.001221$	$\mu = 0.01055$, $\sigma = 0.001221$	0.03313
Corner column (S1)	$E_{wind,Mz}$	$20\ s$	$\mu = 0.002467$, $\sigma = 0.000673$	$\mu = 0.005192$, $\sigma = 0.000673$	0.09278

Table 11.1: Load effects results (based on time series of wind pressures), to be used in the reliability assessment

---

[1] Based on variation at Cook-Mayne fractile in bootstrap

Element	**Load Effect**	**Block Duration t**	**Parameters t-extremes**	**Parameters 1-hour-extremes**	**Sampling Uncertainty COV**
Steel bracing (S65)	$E_{wind,N}$	$20\ s$	$\mu = 0.740721$, $\sigma = 0.081438$	$\mu = 1.07046$, $\sigma = 0.081438$	0.02285

Table 11.2: Load effects results (based on probabilistic model of wind pressures), to be used in the reliability assessment

11.3. Comparison load effects time series vs probabilistic wind pressure model

The load effects based on the time series and the probabilistic wind pressure model show great similarities. However, there are also a few differences (see figure 11.4). On the basis of the raw load effect data for all the different elements for $n = 65,000$ timesteps, the following can be observed.

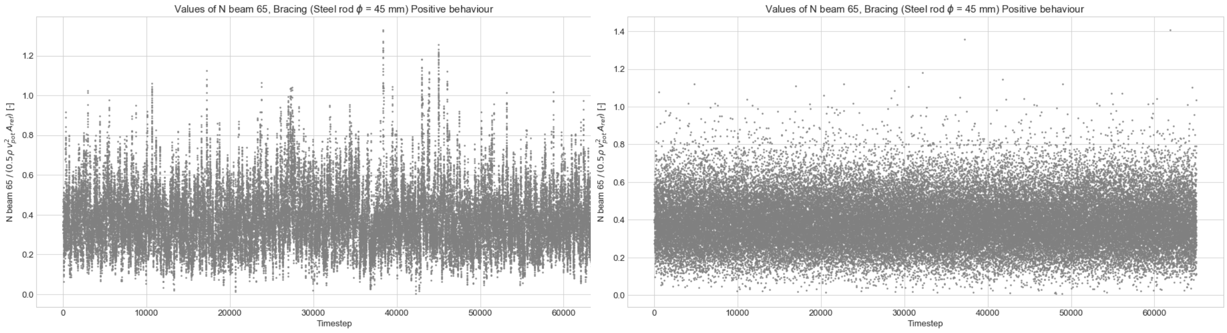

(a) Time series approach

(b) Probabilistic wind pressure model approach

Figure 11.4: All raw load effect data for $n = 65,000$ timesteps

The load effects based on a time series of wind pressures directly from the wind tunnel have a rather fluctuating character. This can be explained by the fact that the wind pressures here also have a certain correlation in time. It is therefore plausible that, for example, higher values occur over a longer period of time. This behaviour is not present in the probabilistic wind pressure model, where the correlation in time is not included. As a result, the load effects based on this probabilistic model have a much more uniform and random character.

This is clearly not the right outcome and affects the extremes load effect distribution. The parameters of the distribution will deviate as a result. Since the load effects based on the probabilistic wind pressure model have a much more uniform character in time, a relatively high value will occur in almost all blocks. This in comparison with the timeseries approach, in which many blocks also have relatively low extreme values, as the correlation in time ensures that there are peaks and dips in time. Because the load effects in this probabilistic model are now high in almost all blocks, the μ parameter of this distribution is also much higher. Another interesting fact is that due to the fact that the extreme value in most blocks is roughly the same, the σ parameter is a bit lower. All in all, the current probabilistic wind pressure model is not able to describe the complex wind behaviour in time very well. Differences can be observed between the load effects in time and this has major consequences for the fit of a distribution to these extremes.

What the probabilistic wind pressure model is capable of doing is taking into account the correlations between the different zones. Since the values that are adopted are approximately the same for both methods.

Another factor influencing the load effects is that for the time series case, only $n = 65,000$ timesteps (full scale duration: 5 hours) are used. Therefore, this is actually purely a snapshot of a much longer wind tunnel test. In total, over 2.3 million timesteps (full scale duration: 175 hours) are available from the wind tunnel, so only 3% of the total wind tunnel data is used. However, all data (2.3 million time steps) are used to generate the probabilistic wind pressure model. Therefore, this model is better able to include all intrinsic data and characteristics. This may explain some of the differences between the methods.

Since the two methods are not yet a perfect match, it is decided to determine only the load effects for both methods for the steel bracing. This element has the most impact of the wind forces and therefore the effects of the load effects are also the most visible. What this means for the reliability assessment is shown in the next chapter. For the other elements this comparison is not taken into account, because it gives little insight in the accuracy of the probabilistic wind pressure model. Moreover, the current probabilistic wind pressure model is not yet adequate enough to be really used for the analyses. As already indicated, the correlation in time must be added to the model in order to obtain better results.

12

Reliability Assessment

This chapter focuses on the actual reliability assessment. First an overview is given of all input parameters for the assessment. In combination with the limit state functions determined in Chapter 9: Reliability Assessment Procedure these can be used to determine the failure probability of the elements. As indicated earlier in this report, a FORM analysis is used. This gives, besides the reliability level β, also insights in the individual influences of the various variables on the final reliability in the form of sensitivity factors α^2.

12.1. General information

In order to include the influence of certain stochastic models in the reliability assessment of the elements, four different reliability analyses $RA_A - RA_D$ are performed (see table 12.1). For each type of analysis the v_{pot} model and the load effects model are varied. These v_{pot} models are based on the research of la Gasse and include both a Type I GEV and Type III GEV. Also the variation between the time-series load effects model and probabilistic wind pressure model is investigated. This probabilistic wind pressure model is further explained in Chapter 7: Probabilistic Wind Pressure Model.

All input variables, distribution types and corresponding parameters of the load and resistance side respectively can be found in tables 12.2 and 12.3. In addition, other input parameters can be found in Appendix Reliability Assessment - Additional Input Parameters.

For all investigated elements, both sensitivity factors α^2 and reliability index β are plotted. Based on these results, conclusions about the reliability of each specific element can be drawn. The deterministic design of the case study building based on the Eurocode, is designed based on a reference period of 50 years and consequence class 2. In other words, the recommended minimum reliability index β for this structure is 3.8. Next the obtained reliability index values can be compared with this β_{target}. If the reliability index value is above the β_{target} it is more reliable than necessary according to the Eurocode, in the opposite case when the value is below the target it is less reliable than recommended. Next, the reliability assessment can be used to further optimise the profile, such that the reliability is just above this β_{target}.

The loads acting on the structure vary in time. These loads are therefore also included as stochastic variables in the reliability analysis. However, for the combination of these different loads that vary in time, think of the imposed load and the wind load, it is good to note that the probability of these loads both reaching an extreme value at the same time is very unlikely. To take this into account, the Turkstra rule [33] can be used. The principle is that for one of the loads the extreme value is taken in combination with the instantaneous value of the other loads. The different combinations are then examined and the one with the highest probability of failure is considered governing.

In this study, however, it is assumed that both the wind load and the variable load can have extreme values at the same time. This is a conservative approach and will therefore result in higher failure probabilities. However, given that the effects of the wind in most elements are small, this will not differ much from the Turkstra method. And in the case of the steel bracing, which has to endure a lot of wind loads, this will not make any difference since there is no variable load acting on it.

The reliability analysis of the columns includes the buckling length. In order to simulate reality as good as possible, it is decided to make a stochastic model of this variable as well. Based on the tolerances of steel beams produced with regulations in the Eurocode (EN 10051), a stochastic model can be made. For steel beams with a length between 2000 and $8000\,mm$, the lower limit of the length tolerance is equal to 0 and the upper limit is equal to $+0.005\cdot$ length [2]. Or in this case with a l_{buck} of $4000\,mm$, the upper limit is equal to $20\,mm$. So the length is between 4000 and $4020\,mm$. The stochastic model for l_{buck} is created on this basis.

Indication Reliability Analysis (RA)	v_{pot} **model**	**Load effects model**
RA_A	Type I GEV (Gumbel)	Timeseries
RA_B	Type III GEV (Weibull)	Timeseries
RA_C	Type I GEV (Gumbel)	Probabilistic model
RA_D	Type III GEV (Weibull)	Probabilistic model

Table 12.1: Different types of reliability analyses, including indication for in the further analyses below in this chapter

12.2. Reliability assessment steel structural elements

A reliability assessment is carried out for the different elements of the main steel supporting structure of the case study building. The results are in the form of sensitivity factors α^2 and reliability index β. For most elements a distinction is also made between a type (1) and (2) calculation. This concerns the extent to which the uncertainties related to the strength side of the material / element are taken into account. These stochastic models related to the uncertainty of the strength of the material - think of $m_{bending}$, $m_{buckling}$, $m_{lat-buckling}$, $m_{interaction}$ - have a mean value higher than 1.0. In other words, on the basis of experiments that also form the basis of background documentation to *Eurocode 3*, the strength of the element often turns out to be higher than initially expected. The calculations in which this extra capacity is included with the higher mean values are type (1) calculations. This has subsequently also been compared with the type (2) calculations, whereby the mean value has been adjusted to 1.0. In other words, no extra reserve capacity of the element, as found in experiments, is included in the analysis. In this type (2) calculation, the COV is included in the same way as in type (1). The type (2) calculations are therefore on the conservative side.

It is good to realise that these experiments are carried out in the laboratory under practically perfect conditions. Therefore, the amount of extra capacity of the elements is quite high on the basis of these experiments. In reality, however, this will be more subtle, as there are different conditions on the building site in which the construction is realised. In theory, the geometry and positioning is all perfect, but this is of course not realistic in the real world. Therefore, small differences will always occur. To get a grip on these differences that can occur on the building site and to ensure that these discrepancies do not become too extreme, the allowed tolerances are described in standards such as NEN-EN 1090-2 [12] (*Execution of steel structures and aluminium structures - Part 2: Technical requirements for steel structures*). In this document requirements are set for the quality of construction products such as steel, for example strength, elongation, tolerances on dimensions and shape, chemical composition, etc. Various inspection documents serve to monitor the quality of the products. Since certain minimum requirements are often set, it appears that most products have properties that are considerably higher. Tests will show, for example, that the f_y of a steel profile is often much higher than how it is classified.

Variable	**Distribution type**	**Parameters**	**Remarks**
ρ_{air}	Deterministic	$\rho_{air} = 1.225\ kg/m^3$	-
v_{pot}	Type I GEV (Gumbel), Type III GEV (Weibull)	Type I: $u = 19.24$, $\alpha = 0.43$; Type III: $u = 19.42$, $\alpha = 0.41$, $\xi = -0.14$	Based on research la Gasse [23]
S_v	Normal	$\mu = 1.0$, $COV_{typeI} = 0.04$, $COV_{typeIII} = 0.09$	Based on research la Gasse [23]; Different COV for type I and type III GEV distribution of v_{pot}
c_r^2	Log-normal	$\mu_{c_r^2} = 1.15$, $COV_{c_r^2} = 0.15$	See Chapter 9: Reliability Assessment Procedure
$\hat{c}_M$, $\hat{c}_N$, $\hat{c}_V$	-	-	See Chapter 11: Description Load Effects
$S_{\hat{c}_M}$, $S_{\hat{c}_N}$, $S_{\hat{c}_V}$	-	-	See Chapter 11: Description Load Effects
χ_{model}	Normal	$\mu = 1.0$, $COV = 0.1$	-
A_{ref}	Deterministic	$8 \cdot 30\ m^2$	Area of the facade of the building
h	Deterministic	$8\ m$	Height of the building
z_0	Deterministic	$z_0 = 0.8$ m	-
$z_{0,II}$	Deterministic	$z_{0,II} = 0.03$ m	-
G	Normal	$\mu = G_k$, $COV = 0.05$	Based on 'Proqua' research, see table 5.6
Q	Gumbel	$\mu = 0.6Q_k$, $COV = 0.35$	Based on 'Proqua' research, see table 5.6

Table 12.2: Input variables, distribution types and associated parameters regarding load side of the reliability assessment of the case study building

Measurements in accordance with ISO 4463-1 must be taken before assembly of the structure on the building site. This is to ensure that the positioning of the steel element is correct. NEN-EN 1090-2 [12] also lists geometrical tolerances that influence both functional (e.g. fit and appearance) and constructive fundamental (e.g. influence on mechanical strength and stability of construction) criteria. A complete overview of these tolerances can be found in Annex Tolerances on construction building - NEN-EN 1090-2 [12].

As can be seen from the figures in the Annex, the deviations from the theoretical design can vary quite considerably. All these differences can result in a different play of forces in the entire structure. Therefore it is good to realise that the results obtained in this reliability assessment are valid in the theoretical case that the structure perfectly matches the drawings. This is often not completely the case and deviations within the allowed tolerances are therefore normal and have influence on the reliability of the various elements.

A further optimisation of the profiles based on the reliability assessment is performed for all elements. The input parameters of the relevant profile based on the deterministic Eurocode design are adjusted to other profile parameters. This gives a first indication what happens with the reliability of the elements if another profile is chosen. It should be noted that in principle, the change of a certain profile, affects the permanent loads of the other profiles that also carry this weight. However, for this first indication this

Variable	**Distribution type**	**Parameters**	**Remarks**
f_y	Log-normal	$\mu = f_{y,k} + 2 \cdot \sigma$, $COV = 0.08$	See table 5.1
$W_{pl,y}$	Normal	$\mu = 0.99X_{nom}$, $COV = 0.025$	See table 5.3
A	Normal	$\mu = 0.99X_{nom}$, $COV = 0.025$	See table 5.3
I	Normal	$\mu = 0.99X_{nom}$, $COV = 0.025$	See table 5.3
E	Log-normal	$\mu = E_k$, $COV = 0.03$	See table 5.1
l_{buck}	Normal	$\mu = l \cdot 1.0025$, $COV = 0.001$	See explanation in beginning of this chapter
$m_{bending}$	Normal	$\mu = 1.1$, $COV = 0.05$	See table 5.6
$m_{buckling}$	Normal	$\mu = 1.2$, $COV = \frac{0.1}{1.2} = 0.083$	See table 5.6
m_i	Normal	$\mu = 1.0$, $COV = \frac{0.05}{1.0} = 0.05$	See figure 5.7
$m_{lat.buckling}$	Normal	$\mu = 1.1755$, $COV = \frac{0.0954}{1.1755} = 0.081$	See Annex Model uncertainties
$m_{interaction}$	Normal	$\mu = 1.3$, $COV = \frac{0.122}{1.3} = 0.093$	See Annex Model uncertainties

Table 12.3: Input variables, distribution types and associated parameters regarding resistance side of the reliability assessment of the case study building

change of permanent weight is not included, also because the contribution of the weight of the profiles is relatively small compared to the permanent floor or roof load and the variable loads on the structure. This assumption is also conservative, since we now assume that the permanent load remains the same and does not decrease.

12.2.1. External beam level 2 (S42)

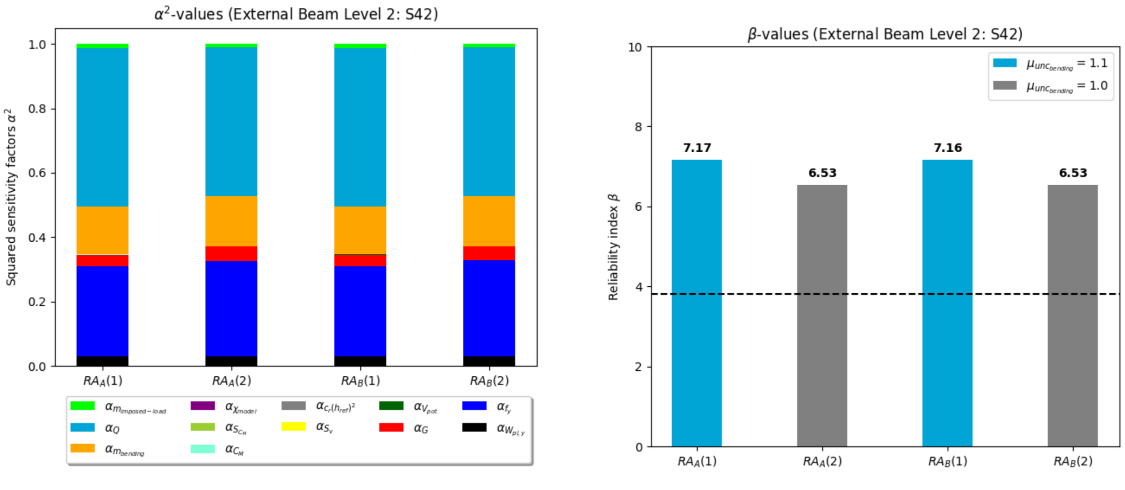

(a) Sensitivity factors α^2

(b) Reliability index values β

Figure 12.1: Sensitivity factors α^2 of the stochastic variables and β-values of the reliability assessment for external beam level 2 (S42) with IPE240 profile (deterministic Eurocode design). (A) v_{pot}: Type I GEV (Gumbel) and load effects based on timeseries, (B) v_{pot}: Type III GEV (Weibull) and load effects based on timeseries, (1) $\mu_{m_{bending}} = 1.1$, (2) $\mu_{m_{bending}} = 1.0$

Figure 12.1a and 12.1b show the sensitivity factors α^2 and the reliability index β for the various analyses, respectively. What is noticeable here is that the variable load Q has the largest contribution to the

	External Beam Level 2 (S42)				
u.c. = 0.91	Profile	$RA_A(1)$	$RA_A(2)$	$RA_B(1)$	$RA_B(2)$
Eurocode Design ⟶	IPE240	7.17	6.53	7.16	6.53
	IPE220	5.46	4.76	5.46	4.76
	IPE200	3.46	2.66	3.46	2.66

Table 12.4: Optimisation of profile for External beam level 2 (S42) based on reliability assessment including both probabilistic action and resistance models

reliability. This contribution of Q is smaller for the type (2) calculations, in those cases the influence of f_y is somewhat more influential. The stochastic variables related to the wind load side are almost not visible, i.e. the moments generated by the wind load are negligible relative to the permanent and variable load. The average bending moment that occurs due to G, Q and the wind respectively (assuming the average value of all factors) is roughly distributed as follows: 88%, 11%, 1%. In this case, G clearly creates the largest moment in this beam, but the spread of G is much smaller than Q. This explains why Q still has more influence in the reliability.

What is interesting is that the β-values based on the deterministic Eurocode design with profile IPE240 are relatively high. This while the u.c. based on the Eurocode standards is 0.91. This clearly shows that the partial factor in the Eurocode for the permanent load G is on the conservative side for this specific case. If the profile is further optimised in table 12.4, it can be seen that an IPE220 profile would be the best choice in this case. Further optimisation of the profile to an IPE200 results in a reliability below the β_{target} of 3.8 for all analyses. The further optimisation from IPE240 to IPE220 means a net decrease of 15% in material for this element.

12.2.2. External beam level 1 (S18)

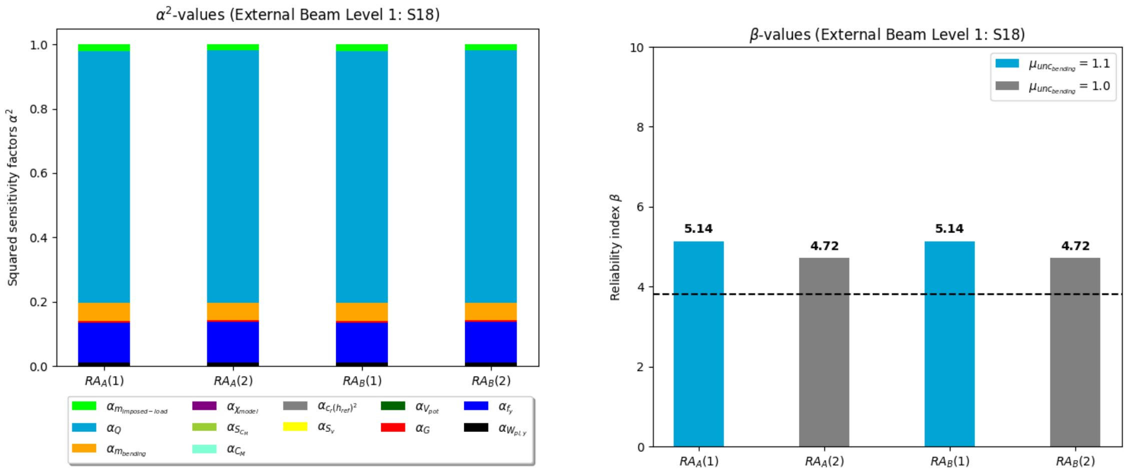

(a) Sensitivity factors α^2

(b) Reliability index values β

Figure 12.2: Sensitivity factors α^2 of the stochastic variables and β-values of the reliability assessment for external beam level 1 (S18) with IPE450 profile (deterministic Eurocode design). (A) v_{pot}: Type I GEV (Gumbel) and load effects based on timeseries, (B) v_{pot}: Type III GEV (Weibull) and load effects based on timeseries, (1) $\mu_{m_{bending}}$ = 1.1, (2) $\mu_{m_{bending}}$ = 1.0

Figure 12.2a and 12.2b show the sensitivity factors α^2 and the reliability index β for the various analyses, respectively. The reliability of this element is completely dominated by the variable load Q. The contributions of the different stochastic variables are also the same for the different methods. This also clearly shows that the wind related load effects hardly influence the reliability of this element. The

	External Beam Level 1 (S18)				
u.c. = 0.82	Profile	$RA_A(1)$	$RA_A(2)$	$RA_B(1)$	$RA_B(2)$
Eurocode Design ⟶	IPE450	5.14	4.72	5.14	4.72
	IPE400	3.98	3.55	3.98	3.55
	IPE360	2.82	2.34	2.82	2.34

Table 12.5: Optimisation of profile for External beam level 1 (S18) based on reliability assessment including both probabilistic action and resistance models

average bending moment that occurs due to G, Q and the wind respectively (assuming the average value of all factors) is roughly distributed as follows: 67%, 32%, 1%. In this case, the contribution of Q to the acting moment in the beam is considerably larger than in the previous case. Partly because the variable floor load on level 1 is greater than the variable roof load on level 2.

The β-values of this element are already relatively close to the target reliability of 3.8. The difference between including or excluding extra capacity in the strength (type (1) vs (2)) is roughly 0.4 - 0.5 β. If the profile is further optimised in table 12.5, it can be seen that an IPE400 profile would be the best choice in this case.

It should be noted that the type (2) analyses are on the conservative side and do not include additional strength capacity. Experiments and other test results, which also form the basis of the background documentation of Eurocode 3, show that the strength is often higher than purely based on theory. Based on those experiments and models that follow, it is very plausible that the reliability of the IPE400 profile should be above the beta target. However, it is very optimistic to assume the full additional capacity that follows from the laboratory experiments. After all, conditions on the building site are never perfect. However, the engineer always bears the final responsibility for this and will have to make a sound decision.

Further optimisation of the profile to an IPE360 results in a reliability below the β_{target} of 3.8 for all analyses. The further optimisation from IPE450 to IPE400 means a net decrease of 15% in material for this element.

12.2.3. Steel bracing (S65)

	Steel Bracing (S65)				
u.c. = 0.88	Profile	RA_A	RA_B	RA_C	RA_D
Eurocode Design ⟶	rod $\phi = 45\ mm$	4.77	5.48	4.83	5.80
	rod $\phi = 35\ mm$	3.82	4.21	3.85	4.38
	rod $\phi = 30\ mm$	3.22	3.45	3.24	3.53

Table 12.6: Optimisation of profile for Steel bracing (S65) based on reliability assessment including both probabilistic action and resistance models

Next, the element in which the wind load has a major influence. This provides insights into the specific variables that play a role in these wind loads. Figure 12.3a and 12.3b show the sensitivity factors α^2 and the reliability index β for the various analyses, respectively. This also shows the difference between the time series of wind pressures (A-B) and the probabilistic wind pressure model (C-D). The results show that the reliability is lower for a type I GEV v_{pot}. This is because of the fixed skewness is the type I GEV description, which results in a conservative distribution of the wind speeds. The contribution of v_{pot} on the reliability is also higher in the type I GEV cases (RA_A and RA_C) than for the type III GEV v_{pot}

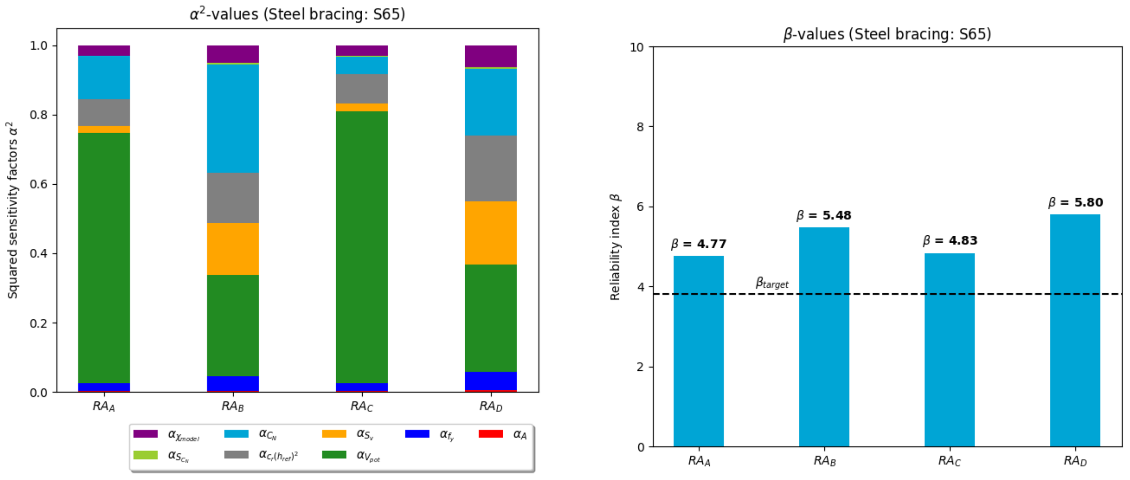

(a) Sensitivity factors α^2

(b) Reliability index values β

Figure 12.3: Sensitivity factors α^2 of the stochastic variables and β-values of the reliability assessment for steel bracing (S65) with steel rod $\phi = 45\ mm$ profile (deterministic Eurocode design). (A) v_{pot}: Type I GEV (Gumbel) and load effects based on timeseries, (B) v_{pot}: Type III GEV (Weibull) and load effects based on timeseries, (C) v_{pot}: Type I GEV (Gumbel) and load effects based on probabilistic wind pressure model, (D) v_{pot}: Type III GEV (Weibull) and load effects based on probabilistic wind pressure model

(RA_B and RA_D). Because of the larger sampling uncertainties for the type III GEV v_{pot}, the contribution of S_v to the reliability is also larger in those cases. What is also noticeable is that the contribution of C_N to the reliability is higher in the case of a type III GEV v_{pot}.

The reliability based on the deterministic design results in relatively high β-values. Further optimisations of the profile are shown in table 12.6. The diameter could be reduced such that it would result in a β just above the target. The β's based on the probabilistic wind pressure model are higher than in the time series case. This is mainly because the σ parameter in the Gumbel fit for the probabilistic wind pressure model case is smaller (0.081 vs 0.121). As a result, the tail in the C_N distribution is less present and will result in lower values, in other words, higher reliability.

Based on the reliability assessment, the design value of C_N can be determined and compared with the value of the Cook-Mayne fractile. If these values are similar, then the design value has been estimated correctly and the corresponding sampling uncertainties are also correctly estimated. Based on the $20s$-extremes, the design value based on RA_A is 1.375 and based on Cook-Mayne 1.42. In other words, the predetermined sampling uncertainties around the Cook-Mayne fractile are a good estimate. Since this is a Gumbel distribution, in which the tail lies on a straight line, the values do not differ much from each other.

	RA_A	RA_B	Eurocode
A	1565.71	1560.64	1590.43
f_y	398.56	384.87	355
v_d	32.67	32.84	33.1[1]
$c_r(h_{ref})^2$	1.38	1.51	1.79
χ_{model}	1.08	1.12	1.00

Table 12.7: Design values (steel bracing) based on reliability assessments in comparison with design values based on deterministic Eurocode design

In order to get a better understanding of the individual stochastic variables, an overview of the design values based on the reliability assessments is given in table 12.7. Only the design values based on the timeseries approach (RA_A and RA_B) are considered. In table 12.7 it can be seen that most of the variables are in line with the Eurocode value. The yield strength f_y of the steel in the Eurocode is lower than what is shown in the reliability assessment. Therefore the material can handle more than what we expect. The wind speed also corresponds well to the Eurocode design value. The main difference is the roughness factor $c_r(h_{ref})^2$, which implies that the wind load on the building according to the design values of the reliability assessment is lower than according to the Eurocode. Also in the reliability assessment a model uncertainty factor χ_{model} is introduced. This factor is not present in the Eurocode design and is therefore set to 1.0. As can be seen the factor causes a small increase in the design wind load.

12.2.4. Internal column (S13)

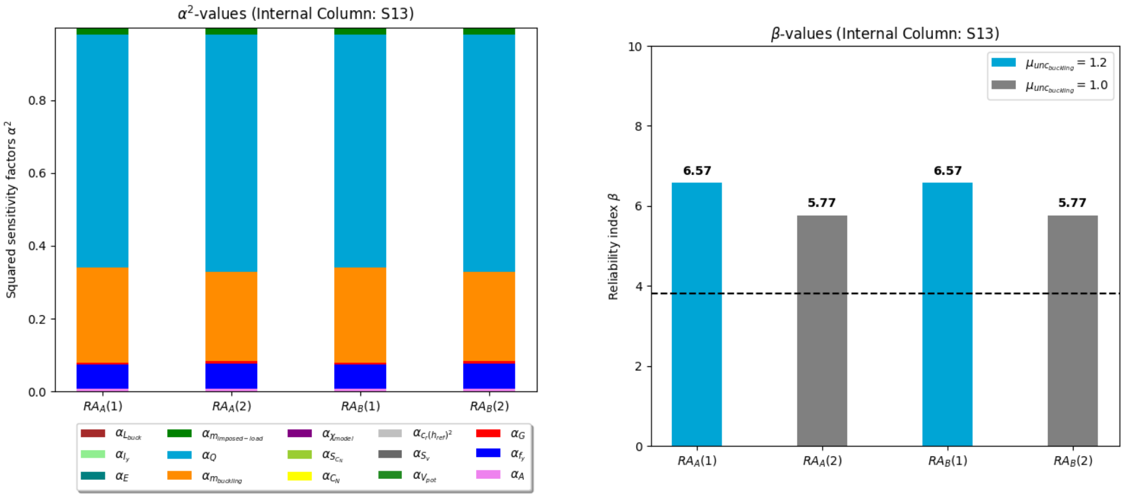

(a) Sensitivity factors α^2

(b) Reliability index values β

Figure 12.4: Sensitivity factors α^2 of the stochastic variables and β-values of the reliability assessment for internal column (S13) with HEA200 profile (deterministic Eurocode design). (A) v_{pot}: Type I GEV (Gumbel) and load effects based on timeseries, (B) v_{pot}: Type III GEV (Weibull) and load effects based on timeseries, (1) $\mu_{m_{buckling}} = 1.2$, (2) $\mu_{m_{buckling}} = 1.0$

	Internal Column (S13)				
u.c. = 0.89	Profile	$RA_A(1)$	$RA_A(2)$	$RA_B(1)$	$RA_B(2)$
Eurocode Design ⟶	HEA200	6.57	5.77	6.57	5.77
	HEA180	5.53	4.69	5.53	4.69
	HEA160	4.39	3.50	4.39	3.50
	HEA140	2.66	1.57	2.66	1.57

Table 12.8: Optimisation of profile for Internal column (S13) based on reliability assessment including both probabilistic action and resistance models

Figure 12.4a and 12.4b show the sensitivity factors α^2 and the reliability index β for the various analyses, respectively. Also for this element, the variable load Q has the most influence on the reliability. However, a small difference can be seen between type (1) and (2); the contribution of $m_{buckling}$ is just slightly smaller for the type (2) analyses than for type (1). The difference in contribution of $m_{buckling}$ is

---

[1] $v_d = \sqrt{1.5}v_b$

then compensated by the variable load Q. Otherwise, all stochastic variables are almost the same for the different analyses.

The β-values are relatively high based on the deterministic Eurocode design with HEA200. If the profile is further optimised in the reliability assessment, a HEA160 profile would also suffice. The difference between including or excluding the extra capacity of the element is quite large. The further optimisation from HEA200 to HEA160 means a net decrease of 28% in material for this element.

12.2.5. External column (S2)

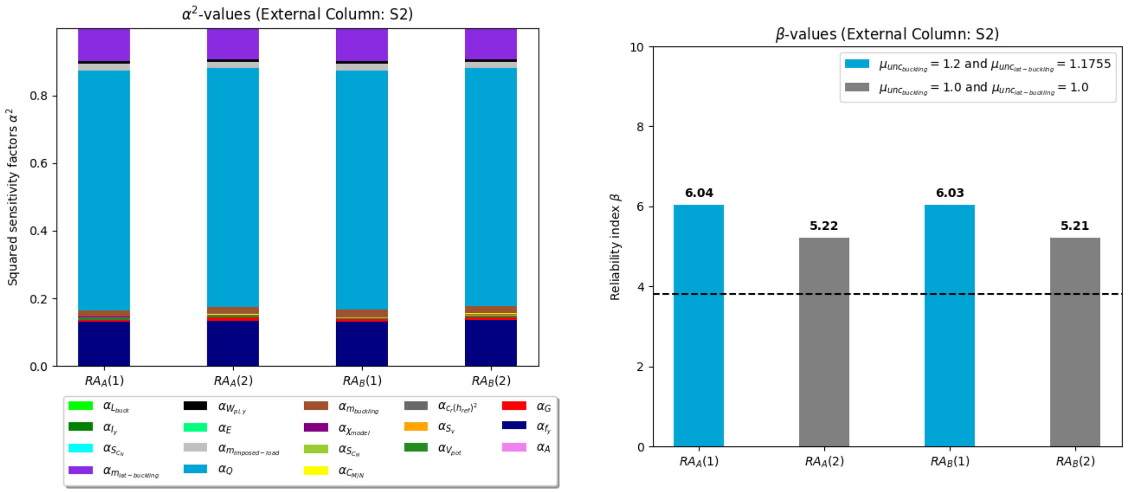

(a) Sensitivity factors α^2

(b) Reliability index values β

Figure 12.5: Sensitivity factors α^2 of the stochastic variables and β-values of the reliability assessment for external column (S2) with HEA220 profile (deterministic Eurocode design). (A) v_{pot}: Type I GEV (Gumbel) and load effects based on timeseries, (B) v_{pot}: Type III GEV (Weibull) and load effects based on timeseries, (1) $\mu_{m_{buckling}} = 1.2$ and $\mu_{m_{lat-buckling}} = 1.1755$, (2) $\mu_{m_{buckling}} = 1.0$ and $\mu_{m_{lat-buckling}} = 1.0$

	External Column (S2)				
u.c. = 0.68	Profile	$RA_A(1)$	$RA_A(2)$	$RA_B(1)$	$RA_B(2)$
Eurocode Design ⟶	HEA220	6.04	5.22	6.03	5.21
	HEA200	4.76	3.89	4.75	3.88
	HEA180	3.37	2.39	3.36	2.38

Table 12.9: Optimisation of profile for External column (S2) based on reliability assessment including both probabilistic action and resistance models

Figure 12.5a and 12.5b show the sensitivity factors α^2 and the reliability index β for the various analyses, respectively. Also in this element, especially the variable load Q and the f_y of the material are important factors in the reliability. Furthermore, here also little difference can be seen in the influence of the various stochastic variables on the reliability in the different analyses. However, the reliability in the type (2) cases is significantly lower than for type (1). The average normal force that occurs due to G, Q and the wind respectively (assuming the average value of all factors) is roughly distributed as follows: 68%, 24%, 8%. And these distributions in the case of the bending moment are as follows for G, Q and wind: 69%, 24%, 7%. In this element, the contributions of the wind to the internal forces are present to a reasonable extent. However, the permanent load G clearly dominates. The large influence of Q on the reliability can be explained by the large variation that occurs with this factor.

What is remarkable is that the β-values based on the deterministic Eurocode design with profile HEA220 are relatively high. If the profile is further optimised in table 12.4, it can be seen that an HEA200 profile would be the best choice in this case. Further optimisation of the profile to an HEA180 results in a reliability below the β_{target} of 3.8 for all analyses. The further optimisation from HEA220 to HEA200 means a net decrease of 16% in material for this element.

12.2.6. Corner column (S1)

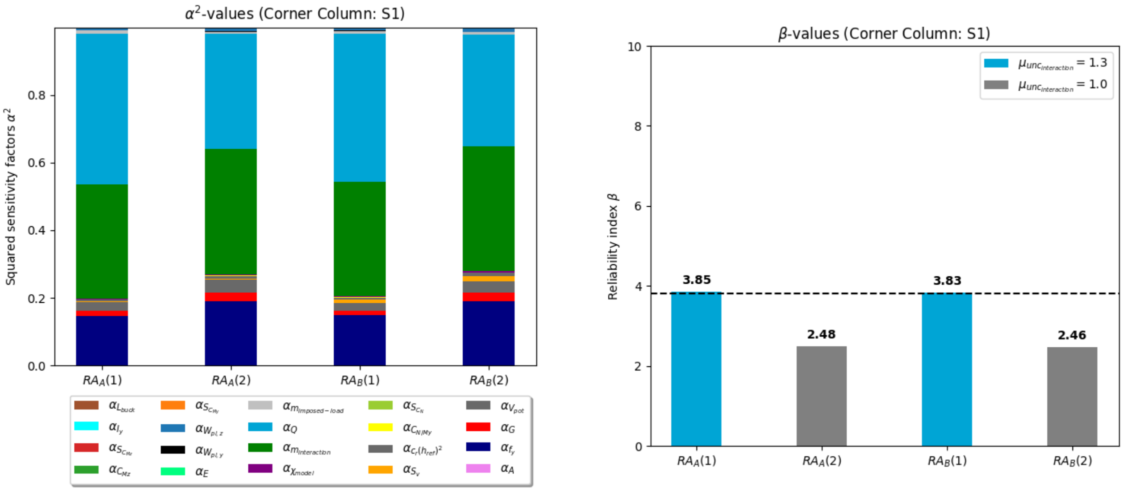

(a) Sensitivity factors α^2

(b) Reliability index values β

Figure 12.6: Sensitivity factors α^2 of the stochastic variables and β-values of the reliability assessment for corner column (S1) with HEA220 profile (deterministic Eurocode design). (A) v_{pot}: Type I GEV (Gumbel) and load effects based on timeseries, (B) v_{pot}: Type III GEV (Weibull) and load effects based on timeseries, (1) $\mu_{m_{interaction}}$ = 1.3, (2) $\mu_{m_{interaction}}$ = 1.0

	Corner Column (S1)				
u.c. = 0.66	Profile	$RA_A(1)$	$RA_A(2)$	$RA_B(1)$	$RA_B(2)$
	HEA240	5.06	3.83	5.05	3.81
Eurocode Design ⟶	HEA220	3.85	2.48	3.83	2.46
	HEA200	2.40	0.84	2.38	0.82

Table 12.10: Optimisation of profile for Corner column (S1) based on reliability assessment including both probabilistic action and resistance models

Figure 12.6a and 12.6b show the sensitivity factors α^2 and the reliability index β for the various analyses, respectively. For the type (1) analyses, the reliability is dominated mainly by the variable load Q. This contribution of Q is smaller in the type (2) analyses. In addition, the factor $m_{interaction}$ has a relatively large contribution to the reliability. Also, the influence of f_y is larger in the type (2) cases than for type (1). The average normal force that occurs due to G, Q and the wind respectively (assuming the average value of all factors) is roughly distributed as follows: 67%, 23%, 10%. And these distributions in the case of the bending moment M_y are as follows for G, Q and wind: 63%, 22%, 15% and in the case of bending moment M_z: 68%, 24%, 8%. The wind has comparatively the most influence in the bending moment M_y.

The deterministic design based on the Eurocode, resulted in profile HEA220. The reliability results with this profile also show well that this was indeed the optimal profile for this element. The additional capacity of the element in the type (1) analyses demonstrates this. However, if one wants even more certainty, one could always go for a heavier profile (in this case a HEA240). Then the element also satisfies for the conservative case (2).

	$RA_A(1)$	$RA_A(2)$	$RA_B(1)$	$RA_B(2)$	Eurocode
A	6363.00	6364.78	6363.02	6364.82	6434
E	209911.95	209933.44	209911.93	209933.82	210000
f_y	372.70	386.05	372.80	386.32	355
I_y	$5.35 \cdot 10^7$	$5.35 \cdot 10^7$	$5.35 \cdot 10^7$	$5.35 \cdot 10^7$	$5.41 \cdot 10^7$
$W_{pl,Y}$	560827.28	561219.70	560825.34	561224.07	568000
$W_{pl,Z}$	266164.00	266739.21	266170.68	266752.71	271000
l_{buck}	4010	4010	4010	4010	4000
v_d	22.42	22.00	23.45	22.98	33.1[2]
$c_r(h_{ref})^2$	1.20	1.19	1.20	1.19	1.79
χ_{model}	1.02	1.02	1.02	1.02	1.00
Q	71.26	56.49	70.78	56.08	93.75
G	110.62	110.25	110.61	110.23	145.94

Table 12.11: Design values (corner column) based on reliability assessments in comparison with design values based on deterministic Eurocode design

Table 12.11 shows the design values based on the reliability assessments and the Eurocode. What is noticeable here is that the variables related to the profile - i.e. A, I_y, $W_{pl,Y}$, $W_{pl,Z}$ - based on the reliability assessments are quite a bit lower than those based on the Eurocode. However, the yield strength f_y of the material is a higher value than assumed in the Eurocode. The buckling length is in all cases slightly higher than the deterministic design, therefore the element is slightly more buckling sensitive. The derived design value of the wind speed is significantly lower than based on the Eurocode, therefore the wind load on the building is also lower. The guidelines in the Eurocode are formulated in such a way that in a general sense it results in safe structures, therefore it can happen that the design value of a certain variable is on the conservative side in specific cases. This is clearly visible in the case of the wind speed. Also the roughness factor $c_r(h_{ref})^2$ is on the conservative side in the Eurocode design. Finally, it can be seen that the permanent and variable load, respectively G and Q, in the Eurocode are on the high end and therefore conservative. Based on this it can be concluded that the partial factors $\gamma_G = 1.35$ and $\gamma_Q = 1.5$ are on the high side in the Eurocode design for this specific case. This reliability assessment shows that the design value of both the permanent and variable load may be a little lower.

12.3. Conclusions

Based on the results of this reliability assessment on this case study building, the following conclusions can be made:

- The results of the reliability assessment on this particular case study building show that in most cases; the deterministic design based on Eurocode standards result in too safe elements which could have been optimised further. Applying an (extensive) reliability assessment for this case study building, has certainly added value with respect to the optimisation of the profiles and thus realising an economical design. The disadvantage is that this probabilistic design requires more knowledge and time of the engineer.
- These reliability assessment results show for this specific building that the reliability is often on the high side, but this does not mean that this is true for all structures based on these Eurocode guidelines. This reliability assessment is only one case which has been examined in detail. Drawing

---

[2] $v_d = \sqrt{1.5}v_b$

conclusions about the reliability of other buildings - with a different form factor, height, typology, etc. - based on these results is therefore not advisable.

- The reliability assessment of the steel bracing shows the most insights into the different wind-related aspects. Since the wind forces are mainly absorbed by this bracing.
  - What stands out here is that the wind speed variable v_{pot} has the most influence on the reliability. If a type I GEV (Gumbel) distribution is used for the stochastic variable v_{pot}, the contribution of v_{pot} to the reliability is greater than for a type III GEV (Weibull) v_{pot} distribution. In the case of a type III GEV (Weibull) v_{pot}, however, the associated sampling uncertainties S_v are larger and also have a larger influence on the reliability. Also the contribution of C_N to the reliability is larger in the case of a type III GEV v_{pot}. The total reliability of the bracing is lower in the case of a type I GEV. This can be explained by the fact that the type I description of v_{pot} has a fixed skewness and therefore generates very conservative wind speeds.
  - For the stochastic model of v_{pot} both a type I and type III generalized extreme value (GEV) distribution are used, based on research by la Gasse. The major difference is mainly that type I GEV has a fixed skewness value and type III GEV does not, i.e. for type I GEV only 2 parameters are needed (shape parameter $\xi = 0$) and for type III GEV 3 are needed. Since more parameters need to be estimated for the type III GEV, this type is more sensitive to sampling uncertainties. The advantage of type III GEV, however, is that due to the skewness parameter not being fixed, the wind speed data can be better fitted. Whereas type I GEV has a fixed skewness parameter, resulting in more conservative values.
  - The deterministic design based on the Eurocode results in an overly safe design for the steel bracing. The occurring wind forces on the building based on the Eurocode standards are higher than the transformed full-scale wind loads as measured in the wind tunnel. Partly because the design value of roughness factor $c_r(h_{ref})^2$ in the Eurocode is considerably higher than that based on the reliability assessment. For tall buildings in particular, conducting a wind tunnel test is very useful to properly account for the effects of wind on the structure. This wind tunnel data is also useful to perform other type of calculations, like dynamic analysis.
- In elements dominated by permanent and variable load, G and Q respectively, it appears that the design value of those variables based on the Eurocode is higher than that based on the reliability assessment for this specific case study building. The partial factors $\gamma_G = 1.35$ and $\gamma_Q = 1.5$ are in that case too high.
- From the reliability assessment of most of the elements in this case study building, it is evident that the variable load Q has by far the greatest influence on the final reliability. This is mainly explained by the large uncertainty associated with this variable ($COV = 0.35$). Being able to better predict and identify what this variable load will do, could go a long way in improving reliability and optimising the design.
- The reliability assessment results show that further optimisation is certainly worthwhile. What is noticeable is that the difference in β-value between successive profiles (e.g. HEA200 - HEA180) is quite present. The difference in β-value between the different profiles is often in the range of $1.0 - 2.0\,\beta$.

13

Discussion

In this chapter a discussion follows on the reliability assessment carried out in this research. Certain assumptions and also their influence on the final result are discussed. Firstly, the newly developed method in this study is discussed, in which wind tunnel data, wind speed models and a finite element model are coupled. Then, by means of a reliability assessment on a case study building, the use of the method is demonstrated. The assumptions that influence the determination of the load effects and finally the reliability assessment itself are also discussed.

13.1. Developed method

- In this research, a method is developed in which wind tunnel data, wind speed models and a finite element model are coupled. This was not possible until now and this research offers a lot of exciting prospects for the future. The great advantage of linking the different models is that the reliability based design gives more accurate results, since the behaviour of the structure in a FEM is included. Furthermore it is a lot easier to perform the reliability based design because the models and data are often already available but now they can be directly linked in the analysis. The big advantage of a reliability based design is that the design can often be further optimised compared to a deterministic design based on the Eurocode. Normally a full reliability based design is not feasible because of the longer time and more knowledge required (also in the field of statistics) of an engineer compared to a relatively fast deterministic Eurocode design. However, with the newly developed method a first step has been made to make a reliability based design more efficient and therefore more interesting to use. Some examples of how this method can be used and what the possibilities for the future are are as follows:

    - Imagine that somewhere a (wind excited) building has to be designed and built. With the new method, the process will look like this. First of all, it is possible to use representative wind speed measurements (such as from KNMI) and create stochastic wind speed models from these. Next, a wind tunnel study can be carried out, in which the shape of the building is matched with the design and surrounding buildings are included. This will then result in a series of pressure measurements on the building over a certain period of time (just like in this research). Finally, a FEM is made, in which the structure is modelled (elements not yet optimised) or possibly only the boundary conditions are modelled in combination with the parametric design methodology. Then it is possible with the new method to link all models and data and a reliability based design is created. With one push on the button all elements are optimised and the design of the building emerges from the analysis based on certain minimum reliability requirements.
    - This study focuses mainly on linking wind tunnel data, but the possibilities are much more diverse. Some examples of other data / measurements that can be directly linked are as follows: traffic measurements, temperature measurements, earthquake measurements, etc.

- This research revealed that the bottleneck of the new method is in particular the required computing power and time. In the case of a linear calculation to obtain the load effects it took about

$9\ s$ per calculation in this study. If another type of calculation such as a non-linear calculation is performed, the required time will be even longer. It is therefore advisable to increase the computational power. Think for example of computing in the cloud methods, where many calculations are performed parallel to each other.

13.2. Determination load effects

- It is assumed that the wind only comes from one direction (resulting in wind pressures on all sides and top of the building), perpendicular to side A of the building. However, previous studies such as that by Meinen [25] show that the orientation of the wind in respect to the building does influence the reliability. It is therefore recommended that this orientation of the wind on the building should be included in the analysis to determine the governing wind direction and resulting load effects. It is possible that wind from a different direction will result in lower reliability in the various elements.

- Something that is worth noting and affects the determination of the load effects and also the reliability assessment results, which is also described in section Remark on fully uncorrelated zones in Chapter 7: Probabilistic Wind Pressure Model, is the fact that the pressure measurements obtained from the wind tunnel research contain uncorrelated zones. This is due to the way the pressure measurements are obtained in the wind tunnel; 86 measuring points on 2 sides and top of the building. After the first experiment and obtaining the pressure measurements on these two sides (side A and C) and top (run 1), the model is rotated and the measurements for the other two sides (side B and D) and top (run 2) are obtained in experiment two. Later, all data is combined and therefore does not include the correlation between, for example, pressure measurements on the front of the building (side A) and the sides of the building (side B and D). Because of this, the wind tunnel research does not contain a crucial part and this has influence on the obtained reliability assessment results, both in the case of timeseries approach and probabilistic wind pressure model approach. Since it is very logical that when a relatively high wind pressure occurs at the front of the building (side A), the pressures on the sides of the building (side B and D) will also be relatively high. As a result, the total wind loads on the building will be higher than what is currently assumed in the case of uncorrelation between side A and B-D for example. The wind load on the building is probably underestimated, which makes it very likely that the reliability of the various elements will be on the higher side. It is therefore recommended that wind tunnel studies are conducted in such a way that measurements are obtained on all sides at the same time, so that the correlations between all zones are fully accounted for.

13.3. Reliability assessment

- What is good to point out here is that there are differences between theory and reality. All these deviations ultimately affect the reliability of the elements. In this research, factors such as - $m_{bending}$, $m_{buckling}$, $m_{lat-buckling}$ and $m_{interaction}$ - are used, whereby on the basis of experiments in a laboratory, extra capacity of elements under certain load configurations is demonstrated. However, the full inclusion of this extra capacity would be very optimistic, as structures built in the real world are subject to deviations such as initial imperfections. As explained in the beginning of Chapter 12: Reliability Assessment, for the construction there are certain guidelines concerning geometry tolerances. If these initial imperfections, which occur during construction, are taken into account in the reliability assessment, the reliability of the various elements will be reduced. It is therefore good to consider the results of the reliability assessment in this perspective and not to draw any firm conclusions based on these results. Incorporating these initial imperfections as stochastic models directly into the FEM will be very interesting and will result in even more accurate results.

- In this reliability assessment it is assumed that both the wind load and the other loads can reach an extreme value at the same time. This is a conservative approach, as the probability of both loads reaching an extreme value at the same moment is very unlikely. Because of the relatively small wind effects in most elements and the fact that the bracing only takes wind load, this conservative approach is justified. However, applying the Turkstra rule [33] would be an improvement. Here different combinations of loads are considered, where for one load an extreme value is taken and for the other loads the instantaneous load. The combination that results in the highest failure probability is considered governing.

- In this study also a further optimisation of the profiles is performed based on the reliability assessment. The fact that changing a certain profile also influences the permanent load of another profile is not included in the analysis. This assumption is on the conservative side, since it assumes that the permanent load remains the same and does not decrease (which would happen if a profile is further optimised). The influence of this assumption on the reliability values of the further optimised profiles will be minimal, since the difference in weight of the profiles with respect to the permanent floor or roof load and the variable loads is small. However, this assumption should be kept in mind.
- In this reliability assessment, the stochastic models related to A, W and I are assumed to be uncorrelated with each other. However, it would be better to include a correlation between these factors. After all, if for example a higher value for A is found, also W and I are higher.
- In the case of buckling or lateral torsional buckling in the limit state function, one specific value of respectively α or α_{LT} is assumed. This value corresponds to the profile as it is derived from the deterministic Eurocode design. In further optimisations this imperfection factor is not reconsidered. Therefore it is possible that in further optimisations with smaller profiles, the imperfection factor should have been adjusted. This has consequences for the reduction factor χ and ultimately also for the reliability results. It is worthwhile to investigate if and how the imperfection factor can be implemented in a better way in the reliability assessment.
- In this study, probabilistic models for both the load and resistance side are used, based on an extensive literature study. The exact choice of these input variables, distribution types and associated parameters will ultimately influence the results of the reliability assessment. For example, for f_y the most conservative option is used (see table 5.1 in Chapter 5: Probabilistic Structural Resistance Model, version 2, $k_s = 2$). If for example version 1 for f_y is used, the β's are approximately $0.5 - 2.0\beta$ higher for the various elements. It is clearly visible that the analysis is sensitive to the input parameters. In this reliability assessment the COV for A, W and I variables is set to 0.025 (the average as indicated in literature). Another choice for this COV would also have led to slightly different results.

111

IV

Conclusions and Recommendations

Conclusions

In this research, all relevant previous researches, probabilistic models and uncertainties are taken into account, also the load side as well as the resistance side of the reliability analysis are investigated. Where previous researches used simplistic models for the strength or modelled buildings as one element or did not include the construction interaction for the reliability analysis of certain elements, this research focuses on these aspects. The behaviour of the structure is included by means of a FEM - consisting of all the elements of a steel main bearing structure - and subsequent load effects. This is achieved by using a newly developed method in this research, in which various models and data, such as wind tunnel data, can be linked to a finite element model. This method is also very flexible and can be used for other research purposes as well.

In this way a more complete reliability analysis is developed taking into account more aspects. In doing so, the deterministic design based on the Eurocode (see Appendix Deterministic Design Case Study Building according to the Eurocode) is compared with the results of the reliability analysis of the various elements. This gives an insight in the level of reliability and also which elements in this case study building are the most reliable or unreliable. This study is only a small part of the larger quest for the most optimal design of buildings; designing buildings in such an efficient and economic way (minimizing resources) while still complying with the current reliability standards.

At the beginning of this report in the introduction, the main question is described, to which an answer is sought in this report. The main question is as follows:

> *"How can the reliability of the steel structural system of wind excited buildings be assessed, based on probabilistic models accounting for uncertainties in wind forces and resistance, resulting in failure probabilities on element level?"*

This research firstly provides a method to carry out a reliability assessment and then applies it to a case study building. In order to decompose this main research question in a thorough and structured manner, a number of sub-questions are formulated. Each of these sub-questions relates to a particular part of this research. Answers to these sub-questions are provided below.

- *How can a probabilistic model of the resistance part be made to account for all the uncertainties in the material and the structural behaviour?*
  On the basis of an extensive literature study, the probabilistic models known on the resistance side of the reliability assessment were identified. With this, an attempt has been made to include the material properties and uncertainties in the best possible way. Also different models are used that serve as basis for the background documentation of the Eurocode, where certain load configurations are investigated in the laboratory. This shows that the material often has more reserve capacity than would be apparent at first sight according to purely theoretical considerations.
- *How can a wind load effect model be incorporated into the reliability assessment procedure?*
  In order to be able to quantify the forces - caused by the wind load - occurring in the structure, a wind load effect model is created in this research. There are different types of effect models; related to moment, normal force or shear force. These models have several deterministic (ρ_{air}, A_{ref}, h) and stochastic parameters as input; think of basic wind velocity v_{pot} and associated sampling uncertainties S_v, terrain roughness factor $c_r(h_{ref})$, model uncertainty χ_{model} and finally the peak load effects $\hat{C}_X$ and associated sampling uncertainties $S_{\hat{C}_X}$. For the determination of these peak load effects and the associated sampling uncertainties, a FEM of the case study building is used on which the transformed full-scale wind pressures from the wind tunnel data are applied. For each element considered in the reliability assessment, the governing wind load effects are

determined in a linear calculation. Next, extreme value analyses is applied, resulting in distribution functions for the peak load effects due to the wind load. Next, the sampling uncertainties are quantified using the bootstrap method. This results in a wind load effect model that can be used in combination with the other probabilistic models in the reliability assessment.

- *How can the reliability assessment procedure be linked with a finite element model?*
  In this study SCIA Engineer FEM is used in combination with SCIA OpenAPI and a Python module. The big advantage of this approach is that a lot of data, like loads or geometry of the structure, can be adjusted and updated in the FEM by means of a Python script. This python script can then control the FEM for a large number of time steps and adjust data. It is therefore also suitable for the application of a reliability assessment. This relatively new method certainly offers plenty of new opportunities and could be very interesting for other studies. Further explanation of the developed method in this study can be found in Annex Explanation on Coupling SCIA FEM with Python using SCIA OpenAPI.

- *Which reliability method (such as Monte Carlo, FORM, etc.) is best suited for the analysis?*
  The Monte Carlo method executes a large number of simulations and if failure occurs this is reported. Eventually, the failure probability can be determined in this way. The major disadvantage of this method is that it is pretty computationally heavy and has to run for quite a long time to get results. A second disadvantage is that the specific influence of certain factors cannot be determined in most cases. However, with certain software and methods, this could be determined. The great advantage of FORM is that, based on the sensitivity factors, it can be determined how large the contribution of specific factors is. This provides a lot of insight into the reliability at a detailed level. The FORM method also converges quite quickly, which makes it computationally more efficient than Monte Carlo. Therefore, the FORM method is used in this study.

- *How do the reliability values compare to the target reliability of $\beta = 3.8$ according to the Eurocode for this type of structure?*

  - The reliability assessment of this specific case study building shows that the Eurocode standards in most cases result in elements with a higher reliability than necessary. Most profiles could have been further optimised. Performing a probabilistic analysis for the design of a structure, certainly has its added value. However, compared to a deterministic design based on the Eurocode, it requires more knowledge and time of the engineer. Keep in mind that this reliability assessment examined only one case study building in detail. Reaching conclusions about the reliability of other buildings - with a different form factor, height, typology, etc. - based on these results is therefore not advisable.
  - The wind pressures on the building according to the Eurocode calculation are higher than those based on the wind tunnel data. For tall buildings in particular, it is therefore advisable to carry out a wind tunnel study in order to accurately determine the wind load on the building. After all, this can be used to further optimise the design.
  - In almost all cases, the variable load Q is the biggest factor in reliability. This is because of the large uncertainty associated with it. The ability to properly map this uncertainty will benefit the reliability and will enable further optimisation of the design.
  - Experiments in the laboratory show that elements can often cope with more than we initially think on the basis of theory alone. It is therefore very useful to identify these discrepancies between theory and reality. As the reliability assessment results also show, the inclusion or exclusion of this extra capacity has a significant impact on the reliability results. However, it must be kept in mind that these results obtained under perfect conditions in the laboratory differ from the actual conditions on the building site.

To return to the main question posed in this study, the following conclusions are presented.

In this study, wind speed models from the study by la Gasse [23], boundary layer wind tunnel pressure measurements and a FEM of the case study building are used and coupled using a newly developed method. This in combination with probabilistic models that take into account the strength of the material, the extra capacity regarding certain failure modes based on experiments in the laboratory, but also other load related aspects. A full reliability assessment procedure is developed which is able to determine the reliability and associated failure probability of elements in a (case study) building, taking into account uncertainties in wind forces, other loads and resistance. All in all, this research shows that the possibilities with the new method, where the link can be made between the various data and FEM, are very optimistic for the future. The application of a reliability based design will become more efficient and therefore more interesting in the future, where the design is further optimised taking into account the minimum reliability requirements.

Recommendations

As a result of this study, there are certainly a number of aspects that can be further investigated. These are discussed further below.

Recommendations for future research

- This research made use of the relatively new *SCIA Engineer OpenAPI*, which supports various programming languages and can be linked to a *SCIA Engineer* finite element model. This technique offers many new possibilities for research purposes. Possible further aspects for research related to this are as follows:
    - The current calculation method requires quite a lot of computing power and time, even in the case of linear calculations as in this study. It is therefore advisable to be able to scale up the required calculation power, for example by applying computing in the cloud, which also reduces the required calculation time. Then more data can be collected in the same time and the sampling uncertainties will further decrease. This is certainly worthwhile in the case of non-linear calculations, where the calculation time per time step is already considerably larger.
    - Instead of a linear calculation, performing a non-linear calculation will also give interesting results. This will then be particularly relevant for higher case study buildings, where significant displacements can occur that generate additional eccentricity and thus additional forces in the main bearing structure elements.
    - Initial imperfections of the elements could be added to the model as stochastic variables. Whereby the FEM is updated based on these stochastic models. In this way, these imperfections are included directly in the model and not as a separate model uncertainty.
    - As buildings become taller and more slender in the future, while the design is further optimized and the structure becomes lighter, aspects related to dynamic response will become more important. Performing dynamic calculations related to wind loaded buildings within the framework of structural reliability will therefore also be interesting, think also about the different types of response; alongwind, across-wind and torsional.
- The advantages and potential of a probabilistic wind pressure model are certainly present. However, for the correct application of such a model, an extra aspect needs to be added to the model made in this report. In this report the model takes into account all characteristics and correlations over the different zones. However, for the best result the correlation of the pressures over time should also be taken into account. This should result in a more accurate description of the wind pressures and should better correspond to the wind pressures as they occur in the wind tunnel.
- In this research only one case study building is investigated, it is recommended to investigate more different case study buildings with different characteristics and typologies. Also the inclusion of surrounding buildings and their influence on the reliability of the building can be investigated.
- Finally, in addition to the reliability assessment on element level, the reliability of the entire building - on system level - could also be examined. The failure of one element does not necessarily mean that the whole building has failed. The associated robustness of the structure and aspects like; redundancy, continuity, ductility and energy absorption of the structure, may be incorporated. Some questions that can be asked here are; how can the dependency between the different elements be included in the analysis? How many elements need to fail before the complete collapse of the structure?

Bibliography

[1] Mir M Ali and Kheir Al-Kodmany. Tall buildings and urban habitat of the 21st century: a global perspective. *Buildings*, 2(4):384–423, 2012.

[2] ArcelorMittal. Tolerance conversion tables.

[3] August A Balkema and Laurens De Haan. Residual life time at great age. *The Annals of probability*, pages 792–804, 1974.

[4] ME Brettle and DG Brown. Steel building design: worked examples for students. *The Steel Construction Institute*, 2009.

[5] LG Cajot, M Haller, Y Conan, G Sedlacek, O Kraus, J Rondla, F Cerfontaine, O Lagerqvist, and B Johansson. Probabilistic quantification of safety of a steel structure highlighting the potential of steel versus other materials. *EUR*, (21695):1–242, 2005.

[6] CEN Comité Européen de Normalisation. Eurocode 1: Actions on structures-part 1-4: General actions-wind actions. Technical report, EN1991-1-4, 2005.

[7] Nicholas John Cook. *Static Structures*. BRE Building Research Establishment, Department of the Environment, 1990.

[8] NJ Cook and JR Mayne. A novel working approach to the assessment of wind loads for equivalent static design. *Journal of Wind Engineering and Industrial Aerodynamics*, 4(2):149–164, 1979.

[9] AG Davenport. On the assessment of the reliability of wind loading on low buildings. *Journal of Wind Engineering and Industrial Aerodynamics*, 11(1-3):21–37, 1983.

[10] Alan Garnett Davenport. The application of statistical concepts to the wind loading of structures. *Proceedings of the Institution of Civil Engineers*, 19(4):449–472, 1961.

[11] I Elishakoff, GQ Cai, and JH Starnes Jr. Non-linear buckling of a column with initial imperfection via stochastic and non-stochastic convex models. *International Journal of Non-Linear Mechanics*, 29(1):71–82, 1994.

[12] CEN Eurocode. Nen-en 1090-2 execution of steel structures and aluminium structures - part 2: Technical requirements for steel structures.

[13] CEN Eurocode. En 1991-1-1. *Actions on Structures, Part*, pages 1–1, 1.

[14] Ronald Aylmer Fisher and Leonard Henry Caleb Tippett. Limiting forms of the frequency distribution of the largest or smallest member of a sample. In *Mathematical proceedings of the Cambridge philosophical society*, volume 24, pages 180–190. Cambridge University Press, 1928.

[15] European Committee for Standardization. Nen-en 1990. eurocode: basis of structural design, 2011.

[16] ISABELLA IASMINA GAETANI DELL'AQUILA D'ARAGONA. Energy saving potential of night natural ventilation in the urban environment: the effect of wind shielding and solar shading. 2013.

[17] Boris Gnedenko. Sur la distribution limite du terme maximum d'une serie aleatoire. *Annals of mathematics*, pages 423–453, 1943.

[18] Abraham M Hasofer. An exact and invarient first order reliability format. *J. Eng. Mech. Div., Proc. ASCE*, 100(1):111–121, 1974.

[19] SN Jonkman, RDJM Steenbergen, O Morales-Nápoles, ACWM Vrouwenvelder, and JK Vrijling. Probabilistic design: risk and reliability analysis in civil engineering. *Collegedictaat CIE4130*, 2015.

[20] Zdeněk Kala. Sensitivity analysis of steel plane frames with initial imperfections. *Engineering Structures*, 33(8):2342–2349, 2011.

[21] M Kasperski. A consistent model for the codification of wind loads. *Journal of wind engineering and industrial aerodynamics*, 95(9-11):1114–1124, 2007.

[22] K Suresh Kumar and T Stathopoulos. Wind loads on low building roofs: a stochastic perspective. *Journal of structural engineering*, 126(8):944–956, 2000.

[23] LC la Gasse. Structural reliability assessment of buildings subjected to wind loading: An assessment of the main bearing structure at foundation level of dynamically sensitive buildings designed within the eurocode framework. 2017.

[24] Jiann-Jong Lou and Jon A Peterka. *Extreme value analysis of peak wind pressures on buildings*. PhD thesis, Colorado State University. Libraries, 1981.

[25] NE Meinen. *A reliability based assessment of the partial factor for wind loads in the Eurocode framework*. PhD thesis, Master thesis, Delft University of Technology, 2015.

[26] Bouwen met staal. Duurzame stalen vloersystemen, 2013.

[27] JCSS (Joint Committee on Structural Safety). Probabilistic model code—part 2: Loads, wind, 2001.

[28] JCSS (Joint Committee on Structural Safety). Probabilistic model code—part 3: Material properties, 2001.

[29] International Standards Organization. Iso 2394: General principles on reliability for structures, 2014.

[30] James Pickands III et al. Statistical inference using extreme order statistics. *Annals of statistics*, 3(1):119–131, 1975.

[31] Fahim Sadek and Emil Simiu. Peak non-gaussian wind effects for database-assisted low-rise building design. *Journal of Engineering Mechanics*, 128(5):530–539, 2002.

[32] Y Sun, ZG Cao, and Y Wu. Characteristics of wind pressure pulse on large-span flat roof. *Journal of Harbin Institute of Technology*, 16(1):75–80, 2009.

[33] Carl J Turkstra and Henrik O Madsen. Load combinations in codified structural design. *Journal of the Structural Division*, 106(12):2527–2543, 1980.

[34] Isaac Van der Hoven. Power spectrum of horizontal wind speed in the frequency range from 0.0007 to 900 cycles per hour. *Journal of Atmospheric Sciences*, 14(2):160–164, 1957.

[35] J Wacker. Wind tunnel tests and climate condition measurements for determining the main carrying structures and the diaphragm roof of the foshan century lotus stadium under quasi-static and dynamic wind loads. *Wacker of Engineers, Foshan*, 2004.

A

Deterministic Design Case Study Building according to the Eurocode

In order to determine the reliability of specific elements of a steel main bearing structure, first a representative case study building need to be designed according to the *Eurocode*. The design of the case study building is not fully optimised, since the main focus of this study is to perform a reliability analysis and not on designing the building.

A.1. Actions on the building

The structure need to withstand the loads - also called the actions - which might occur on the building. There are several types of actions; permanent actions are loads which are always present, like the self-weight of the structure and variable actions only occur in certain situations and are therefore not always present. The Eurocode formulated certain critical combinations of actions for certain elements in the structure, the most governing load case is used to design the specific element.

A.1.1. Permanent actions

The permanent actions consist of the total self-weight of the (non-)structural elements. The structure consists of certain elements and they all have a specific self-weight (formulated in kg/m or kN/m). For the roof construction a typical value of $0.9\ kN/m^2$ is used based on literature [4] and for the floor construction a value of $3\ kN/m^2$ is used [26].

A.1.2. Imposed loads

The imposed loads are due to the specific function of the building. There are several categories mentioned in table 6.1 of En 1991-1-1 [13]. The case study building is assumed to be an office building (category B). The associated characteristics values - as stated in the Dutch National Annex - on the floors, balconies and stairs in the building are $q_k = 2.5\ kN/m^2$ and $Q_k = 3kN$. The q_k value is used for general effects and the Q_k value for local effects.

The imposed loads on the roof of the building, depend on the use and accessibility of this roof. For the case study building it is assumed that the roof is not accessible except for maintenance and repair (category H). The imposed loads are therefore (for a roof inclination of $\alpha = 0$) $q_k = 1.0kN/m^2$ (on a surface area of $10m^2$) and $Q_k = 1.5kN$ (on a surface area of $0.1\ m \cdot 0.1\ m$). An additional statement in paragraph 3.3.2 of EN 1991-1-1 [13] is that for roofs, the imposed loads and wind loads should not be applied together simultaneously.

A.1.3. Wind loads

The dominant loading on the case study building is due to the wind loads. Since the building is symmetric, only one wind direction is assumed: $\theta = 0$. The wind load is determined using the EN 1991-1-4 [6] regulations. Also the Dutch National Annex is used, since the case study building is located at Schiphol

(Amsterdam) in The Netherlands. The wind forces are calculated based on the original building shape $30 \cdot 30 \cdot 120m$, which is also the subject in the wind tunnel test.

Wind forces

The wind forces on the building are determined using both the external $F_{w,e}$ and the internal $F_{w,i}$ forces. These forces are determined using equations A.1 and A.2. The $c_s c_d$ factor is a structural factor, which is set to 1.0 in this case (the facade and roof elements are not subjected to dynamic effects, since they have a natural frequency greater than 5 Hz). Factor A_{ref} is the reference area of the structure or the structural element.

$$F_{w,e} = c_s c_d \cdot \sum_{surfaces} w_e \cdot A_{ref} \tag{A.1}$$

$$F_{w,i} = \sum_{surfaces} w_i \cdot A_{ref} \tag{A.2}$$

The external and internal pressures w_e and w_i respectively are calculated in equation A.3 and A.4. Where $q_p(z)$ is the peak velocity pressure and the pressure coefficients for external and internal are c_{pe} and c_{pi}, respectively.

$$w_e = q_p(z_e) \cdot c_{pe} \tag{A.3}$$

$$w_i = q_p(z_i) \cdot c_{pi} \tag{A.4}$$

Reference height and velocity pressure distribution

The reference heights z_e depend on the aspect ratio h/b. The case study building has dimensions: $30m \cdot 30m \cdot 120m$, so $h > 2b$ and figure A.1 hold [6]. For the case study building, the shaded mid-section in figure A.1 is $60m$. An appropriate length for $h_{strip} = 12m$, so in total there are 5 strips in the velocity pressure profile in the mid-section of the building. All these strips have a different $q_p(z)$ value and this increases with height. Since the velocity of the wind increases with height.

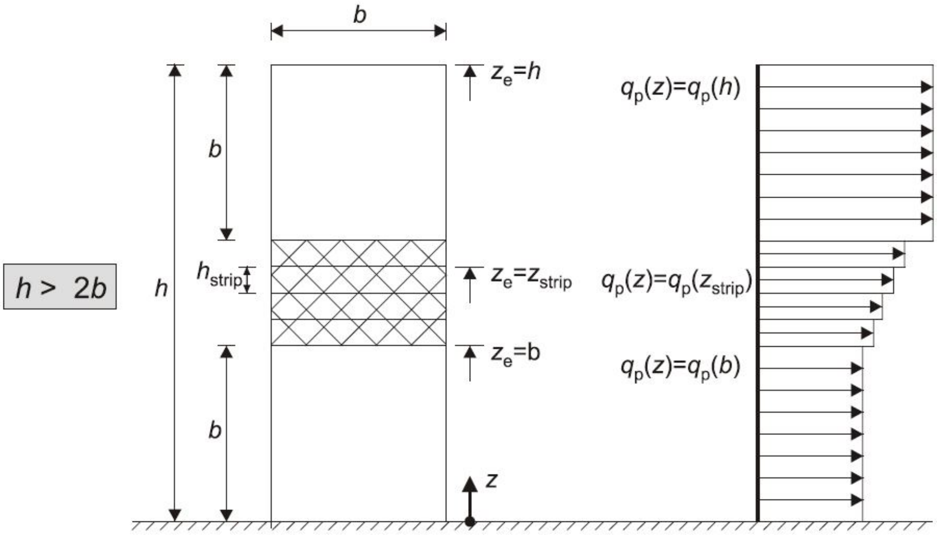

Figure A.1: Reference height z_e, depending on h and b, and corresponding velocity pressure profile [6]

External and internal pressure coefficients

The external and internal pressure coefficients are determined according to 7.2 of EN 1991-1-4. For the external pressure coefficients c_{pe}, two different cases are considered in the Eurocode; loaded areas A of $1m^2$ and $10m^2$ resulting in $c_{pe,1}$ and $c_{pe,10}$, respectively. For the design of the overall load bearing

Zone	A	B	D	E	F	G	H	I
$c_{pe,10}$	-1.2	-0.8	0.8 (0.68)	-0.65 (-0.55)	-1.8	-1.2	-0.7	+0.2 and -0.2

Table A.1: External pressure coefficients for the facade and roof zones

structure - which is relevant for this design of this case study building - value $c_{pe,10}$ may be used. It is assumed that the external and internal pressures act at the same time.

The facade and also the roof is divided in several pressure zones (labelled A up to I). The dimensions of these pressure zones depend on factor e, which is the minimum of b or $2h$:

$$e = min(30; 240) = 30\ m \geq d = 30\ m$$

The pressure zones on the facade are in figure A.2 and A.3. The pressures on the flat roof are in figure A.4.The external pressure coefficients $c_{pe,10}$ can be determined using table NB.6-7.1 in the Dutch National Annex. These values also depend on the $h/d = 120/30 = 4$ ratio. Linear interpolation between the $h/d = 5$ and the $h/d \leq 1$ is performed. The external pressure coefficients for the different zones on the facade and on the roof are in table A.1.

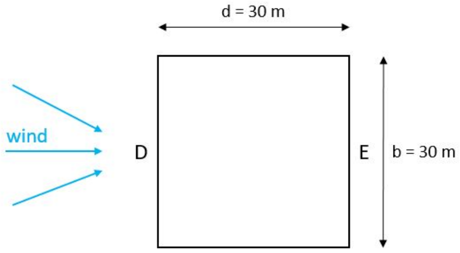

Figure A.2: Wind pressure zones top view

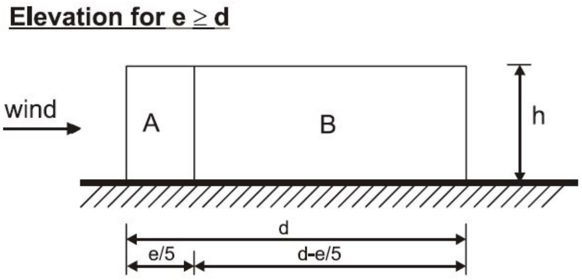

Figure A.3: Wind pressure zones side view for $e \geq d$ [6]

The internal pressure coefficient c_{pi} depend on the size and distribution of the openings in the building envelope. For the case study building, this is not possible, so the internal pressure coefficient c_{pi} should be taken as the most unfavourable of $+0.2$ or -0.3.

Finally, paragraph 7.2.2(3) of EN 1991-1-1 [13], states that the lack of correlation between the wind pressures on the windward and leeward zone (D and E) may be taken into account by a factor of 0.85 (Dutch National Annex). The corrected external pressure coefficients for zone D and E are between brackets in table A.1.

Peak velocity pressure $q_p(z)$

In the Eurocode a mean and fluctuating part of the wind velocity and the velocity pressure are considered. Therefore first some basic variables need to be calculated (see section 4.2 of [6]). The fun-

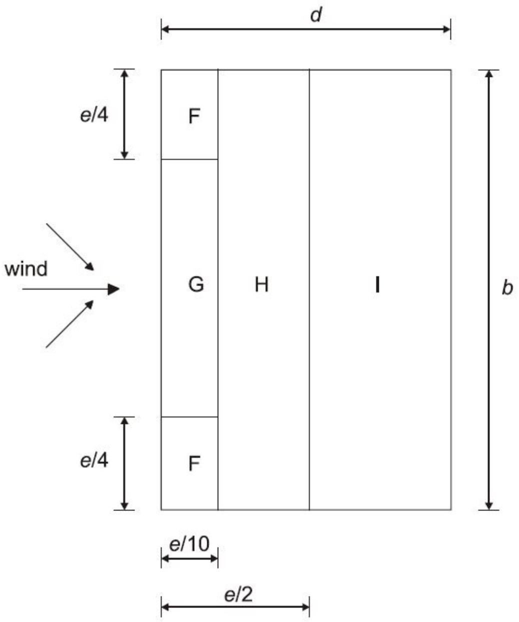

Figure A.4: Wind pressure zones for flat roofs [6]

damental value of the basic wind velocity $v_{b,0}$ [1], depends on the location in The Netherlands (figure A.5) and is formulated in the Dutch National Annex. For the location of the case study building, which is Schiphol, wind zone II is of interest and result in a value of; $v_{b,0} = 27.0\ m/s$. The peak velocity pressure $q_p(z)$ is determined using equation A.5. Where $I_v(z)$ is the turbulence intensity, ρ is the air density ($1.25\ kg/m^3$) and $v_m(z)$ is the mean wind velocity.

$$q_p(z) = (1 + 7 \cdot I_v(z)) \cdot 0.5 \cdot \rho \cdot v_m^2(z) \tag{A.5}$$

Mean wind velocity v_m

The mean wind velocity $v_m(z)$ at a height z above the ground is determined using equation A.6. Where $c_r(z)$ is the terrain roughness factor, $c_o(z)$ is the orography factor and v_b is the basic wind velocity, which is calculated in equation A.7. The c_{dir} and c_{season} factors deal with the direction of the wind and the seasonal variations respectively. The recommended values for both factors are 1.0 in the Dutch National Annex.

$$v_m(z) = c_r(z) \cdot c_o(z) \cdot v_b \tag{A.6}$$

$$v_b = c_{dir} \cdot c_{season} \cdot v_{b,0} = 1.0 \cdot 1.0 \cdot 27.0 = 27.0 m/s \tag{A.7}$$

In order to calculate the terrain roughness factor $c_r(z)$ a certain terrain category (as stated in the Dutch National Annex in table NB.3-4.1) is determined. For this case study building, terrain category II (area with low vegetation and few obstacles) is assumed. For this category the values for the roughness length z_0, minimum height z_{min} and maximum height z_{max} are respectively $0.2m$, $4.0m$ and $200.0m$. Since $z_{min} \leq z \leq z_{max}$, the procedure to determine the $c_r(z)$ value is in equation A.8. The value for the terrain orography $c_o(z)$ is set to 1.0. The terrain factor depending on the roughness length z_0 is k_r and is calculated using equation A.9.

$$c_r(z) = k_r \cdot ln\left(\frac{z}{z_0}\right) \tag{A.8}$$

---

[1] "The characteristic 10 minutes mean wind velocity, irrespective of wind direction and time of year, at 10 m above ground level in open country terrain with low vegetation such as grass and isolated obstacles with separations of at least 20 obstacle heights" [6]

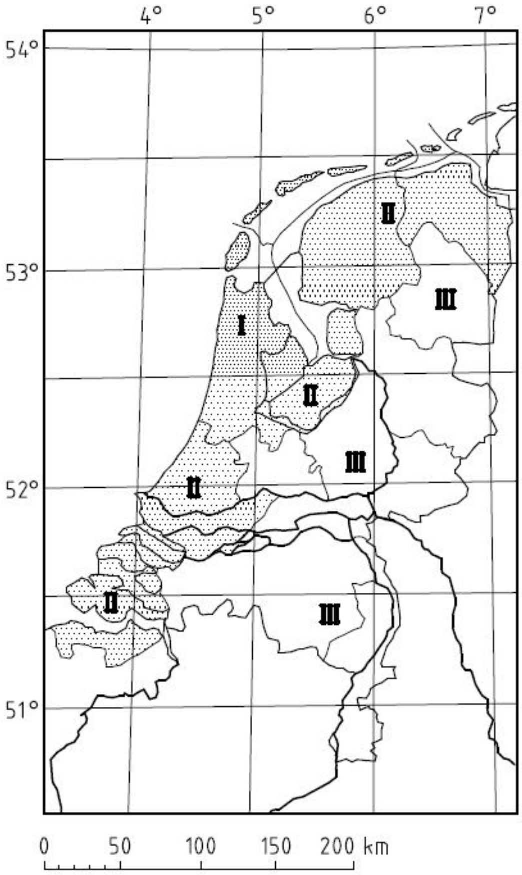

Figure A.5: Wind zones in The Netherlands (Dutch National Annex [6])

$$k_r = 0.19 \cdot \left(\frac{z_0}{0.05}\right)^{0.07} = 0.2094 \quad (z_0 = 0.2m) \tag{A.9}$$

Turbulence intensity I_v

The turbulence intensity I_v is given in equation A.10 (in the case of $z_{min} \leq z \leq z_{max}$), where σ_v is the standard deviation of the turbulence and is given in equation A.11. With the terrain factor $k_r = 0.2094$, $v_b = 27m/s$ and turbulence factor $k_l = 1.0$.

$$I_v(z) = \frac{\sigma_v}{v_m(z)} \tag{A.10}$$

$$\sigma_v = k_r \cdot v_b \cdot k_l = 0.2094 \cdot 27 \cdot 1.0 = 5.6538 \tag{A.11}$$

Finally, the peak velocity pressure $q_p(z)$ for the different heights z are determined, using equations A.6 up to A.11. The results are in table A.2.

External and internal pressures

The $q_p(z)$ values from table A.2 can be used in combination with the pressure coefficients from figures A.6 and A.7. For all the different heights and zones, the wind pressures (kN/m^2) on the facades and roof are in table A.3.

A.1.4. Load combinations

In order to design the structural elements, the governing loads on these elements need to be calculated. These governing loads depend on specific load combinations for the ultimate limit state design.

z	$c_r(z)$	$v_m(z)$	$I_v(z)$	$q_p(p)[kN/m^2]$
30 m	1.0492	28.3284	0.1996	1.2023
42 m	1.1197	30.2319	0.1870	1.3190
54 m	1.1723	31.6521	0.1786	1.4090
66 m	1.2143	32.7861	0.1724	1.4826
78 m	1.2493	33.7311	0.1676	1.5454
90 m	1.2793	34.5411	0.1637	1.6002
120 m	1.3395	36.1665	0.1563	1.7120

Table A.2: Calculation of the peak velocity pressure $q_p(z)$ for all relevant heights z

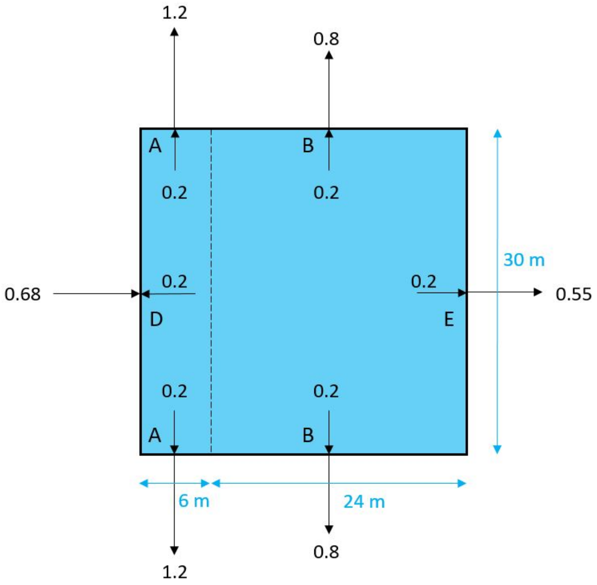
1.2
0.8
A
B
0.2
0.2
30 m
0.68
0.2
0.2
0.55
D
E
0.2
0.2
A
B
6 m
24 m
0.8
1.2

Figure A.6: Pressure coefficients on walls, wind coming from D

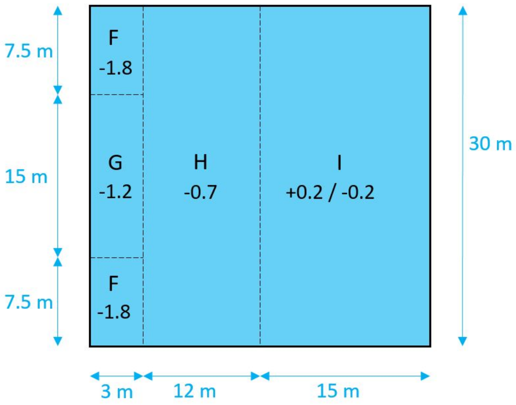
7.5 m
F
-1.8
15 m
G
-1.2
H
-0.7
I
+0.2 / -0.2
30 m
7.5 m
F
-1.8
3 m
12 m
15 m

Figure A.7: Pressure coefficients on roof, wind coming from the left

Equation A.12 is used to determine the load combination based on the Eurocode.

$$\sum_{j\geq 1} \gamma_{G,j} G_{k,j} + \gamma_{Q,1} Q_{k,1} + \sum_{i>1} \gamma_{Q,i} \psi_{0,i} Q_{k,i} \tag{A.12}$$

Height z	A	B	D	E	F	G	H	I
0 - 30 m	-1.6832	-1.2023	0.5771	-0.9017				
30 - 42 m	-1.8466	-1.3190	0.6331	-0.9893				
42 - 54 m	-1.9726	-1.4090	0.6763	-1.0568				
54 - 66 m	-2.0756	-1.4826	0.7116	-1.1120				
66 - 78 m	-2.1636	-1.5454	0.7418	-1.1591				
78 - 90 m	-2.2403	-1.6002	0.7681	-1.2002				
90 - 120 m	-2.3968	-1.7120	0.8218	-1.2840				
120 m					-3.0816	-2.0544	-1.1984	±0.3424

Table A.3: Wind pressures kN/m^2 over height on facade (A - E) and roof (F - I) zones

The reduction factors ψ for the combination of actions is formulated in the Dutch National Annex. The relevant values are in table A.4. The γ_G value (permanent load factor) is 1.35 and γ_Q (variable load factor) is 1.5.

Type of action	ψ_0	ψ_1	ψ_2
Imposed load office (category B)	0.5	0.5	0.3
Imposed load roof	0	0	0
Wind load	0	0.2	0

Table A.4: Reduction factors ψ

The different types of loads and the corresponding values are in table A.5. The abbreviations are used in the formulation of the load combinations.

	Description	Type	Value
Ac_1	Self-weight structural elements	Permanent	Varies per profile
Ac_2	Imposed load office (category B)	Variable	$q_k = 2.5kN/m^2$
Ac_3	Imposed load roof	Variable	$q_k = 1.0kN/m^2$ [2]
Ac_4	Wind load	Variable	Varies per zone

Table A.5: Description, type and value of the loads

It is assumed that the wind load is the dominant loading. The load combinations which are of interest and are further investigated are as follows:

$$Ed_1 = 1.35 \cdot Ac_1 + 1.5 \cdot Ac_2$$

$$Ed_2 = 1.35 \cdot Ac_1 + 1.5 \cdot Ac_3$$

$$Ed_3 = 1.35 \cdot Ac_1 + 1.5 \cdot Ac_4 + 1.5 \cdot 0.5 \cdot Ac_2$$

$$Ed_4 = 1.0 \cdot Ac_1 + 1.5 \cdot Ac_4$$

---

[2] On a surface area of $10m^2$, not in combination with wind loads

A.2. Design of the structural elements

The calculations in this report only show the highlights. The analysis of all the different load cases is not in this report, only the most governing load case and the associated bending moments, axial and shear forces are formulated. And also the design of certain elements took several iterations to perform, however, in this report only the final iteration is shown.

Since the building is symmetrical, only the significant elements are designed. Then the other elements which are related, by means of symmetry, can be designed in the same way.

A.2.1. External beam level 2

Beam A-B on grid 1, level 2

Let's consider beam A-B on grid 1. The beam is simply supported and spans $10\ m$. The bay width is $5m$ (figure A.8). Based on all the different wind pressure zones and the different load combinations, the most governing load case is analysed. After checking all the possible load cases, the maximum design moment is $M_{Y,Ed} = 118.16kNm$ (occurs in wind pressure zone I for load case Ed_3) and the maximum shear force is $V_Ed = 55.46kN$ (occurs in wind pressure zone $F-H$ for load case Ed_4). It is assumed that the compression (top flange) is fully restrained due to the roof construction.

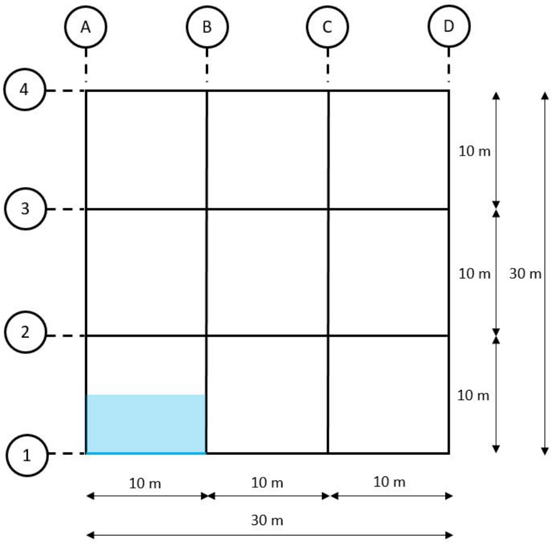

Figure A.8: Beam A-B on grid 1, level 2

$M_{Y,Ed} = 118.16\ kNm$ (occurs at mid-span), $V_Ed = 55.46\ kN$ (occurs at the end supports)

$\gamma_{M0} = 1.00$, $f_y = 355\ N/mm^2$ and $E = 210000\ N/mm^2$

Using the $M_{Y,Ed}$ value, a possible profile could be estimated. The profile needs to have a plastic modulus $W_{pl,y}$ bigger than:

$$\sigma = \frac{M}{W} \longrightarrow W_{pl,y} = \frac{M_{Y,Ed} \cdot \gamma_{M0}}{f_y} = 332563.38\ mm^3$$

Possible profile: IPE240 ($W_{pl,y} = 366000\ mm^3$)

Classification cross-section

First the cross-section needs to be classified. Since steel grade S355 is used, $\epsilon = 0.81$. The internal compression parts are subjected to bending and the outstand flanges to compression.

Internal web bending:

$$\frac{c}{t} = \frac{190.4}{6.2} = 30.71 \leq 72\epsilon = 58.32 \longrightarrow Class\ 1$$

Outstand flange pure compression:

$$\frac{c}{t} = \frac{(120 - 6.2 - 2 \cdot 15)/2}{9.8} = 4.28 \leq 9\epsilon = 7.29 \longrightarrow Class\ 1$$

So the section is class 1, which means it can form a plastic hinge with the rotation capacity required from plastic analysis without reduction of the resistance.

Shear resistance
The basic design requirement is:

$$\frac{V_{Ed}}{V_{C,Rd}} \leq 1.0$$

For class 1 sections:

$$V_{C,Rd} = V_{pl,Rd} = \frac{A_v \cdot (f_y/\sqrt{3})}{\gamma_{M0}}$$

For rolled I and H sections, load parallel to the web, A_v may be taken as follows (η may be taken as 1.0 to be conservative):

$$A_v = A - 2bt_f + (t_w + 2r)t_f \geq \eta h_w t_w \longrightarrow A_v = 1912.76\,mm^2 \geq 1366.48\,mm^2$$

$$V_{C,Rd} = V_{pl,Rd} = \frac{1912.76 \cdot (355/\sqrt{3})}{1.0} \cdot 10^{-3} = 392.04\,kN$$

$$\frac{V_{Ed}}{V_{C,Rd}} = \frac{55.46}{392.04} = 0.141 \leq 1.0$$

So profile IPE240 fulfils the requirement regarding shear resistance.

Shear buckling
The shear buckling resistance need to be considered if:

$$\frac{h_w}{t_w} > 72\frac{\epsilon}{\eta} \longrightarrow 35.55 > 58.32$$

This is not the case, so shear buckling is not considered.

Moment resistance
The basic design requirement is:

$$\frac{M_{Ed}}{M_{c,Rd}} \leq 1.0$$

For class 1 sections:

$$M_{c,Rd} = M_{pl,Rd} = \frac{W_{pl} \cdot f_y}{\gamma_{M0}} = \frac{366000 \cdot 355}{1.0} \cdot 10^{-6} = 129.93\,kNm$$

$$\frac{M_{Ed}}{M_{c,Rd}} = \frac{118.16}{129.93} = 0.91 \leq 1.0$$

Therefore the design bending resistance is good enough. Thus **IPE240** is a suitable profile.

Beam B-C on grid 1, level 2

Another possible external beam, is beam B-C on grid 1 (figure A.9). The wind loads - and thus the calculation - differ slightly from beam A-B. The beam is simply supported and spans $10m$. The bay width is $5m$. After checking all the possible load cases, the maximum design moment is $M_{Y,Ed} = 114.79kNm$ (occurs in wind pressure zone I for load case Ed_3) and the maximum shear force is $V_Ed = 45.91kN$ (occurs in wind pressure zone I for load case Ed_3). It is assumed that the compression (top flange) is fully restrained due to the roof construction.

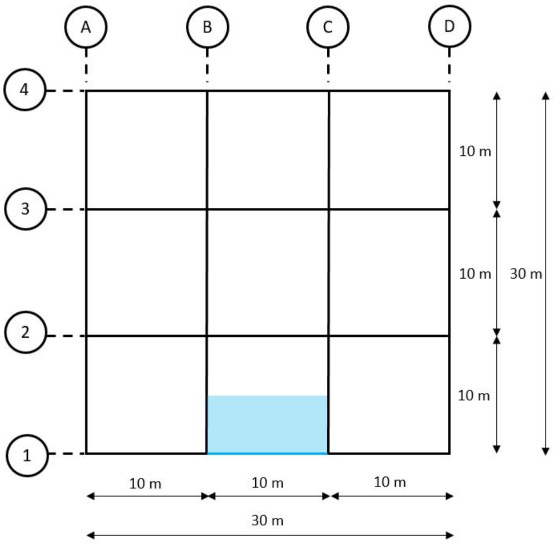

Figure A.9: Beam B-C on grid 1, level 2

$M_{Y,Ed} = 114.79\ kNm$ (occurs at mid-span), $V_Ed = 45.91\ kN$ (occurs at the end supports)

$\gamma_{M0} = 1.00$, $f_y = 355\ N/mm^2$ and $E = 210000\ N/mm^2$

Using the $M_{Y,Ed}$ value, a possible profile could be estimated. The profile needs to have a plastic modulus $W_{pl,y}$ bigger than:

$$\sigma = \frac{M}{W} \longrightarrow W_{pl,y} = \frac{M_{Y,Ed \cdot \gamma_{M0}}}{f_y} = 323352.11\ mm^3$$

Possible profile: IPE240 ($W_{pl,y} = 366000\ mm^3$)

Classification cross-section
This is the same cross-section as for beam A-B on grid 1, so this is also a class 1 section.

Shear resistance
Since the same cross-section is used as for beam A-B on grid 1, the shear resistance is already known:

$$V_{C,Rd} = V_{pl,Rd} = 392.04\ kN$$

$$\frac{V_{Ed}}{V_{C,Rd}} = \frac{45.91}{392.04} = 0.12 \leq 1.0$$

So profile IPE240 fulfils the requirement regarding shear resistance.

Shear buckling
The shear buckling resistance need to be considered if:

$$\frac{h_w}{t_w} > 72\frac{\epsilon}{\eta} \longrightarrow 35.55 > 58.32$$

This is not the case, so shear buckling is not considered.

Moment resistance
Since the same cross-section is used as for beam A-B on grid 1, the moment resistance is already known:

$$M_{c,Rd} = M_{pl,Rd} = 129.93\ kNm$$

$$\frac{M_{Ed}}{M_{c,Rd}} = \frac{114.79}{129.93} = 0.88 \leq 1.0$$

Therefore the design bending resistance is good enough. Thus **IPE240** is a suitable profile.

A.2.2. Internal beam level 2

Beam B-C on grid 2, level 2

Let's consider beam B-C on grid 2. The beam is simply supported and spans $10\ m$. The bay width is $10\ m$ (figure A.10). Based on all the different wind pressure zones and the different load combinations, the most governing load case is analysed. After checking all the possible load cases, the maximum design moment is $M_{Y,Ed} = 222.83\ kNm$ (occurs in wind pressure zone I for load case Ed_3) and the maximum shear force is $V_Ed = 89.13\ kN$ (occurs in wind pressure zone I for load case Ed_3). It is assumed that the compression (top flange) is fully restrained due to the roof construction.

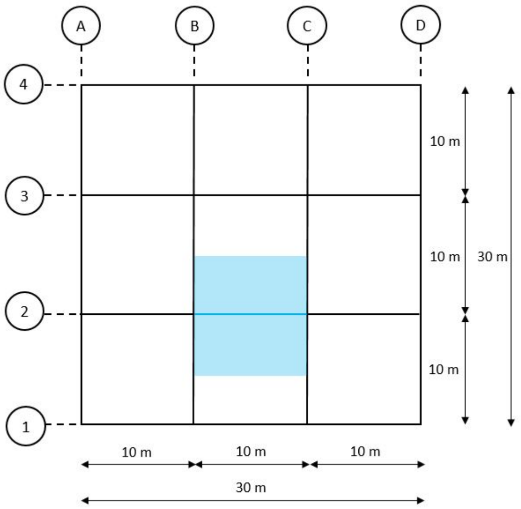

Figure A.10: Beam B-C on grid 2, level 2

$M_{Y,Ed} = 222.83\ kNm$ (occurs at mid-span), $V_Ed = 89.13\ kN$ (occurs at the end supports)

$\gamma_{M0} = 1.00$, $f_y = 355\ N/mm^2$ and $E = 210000\ N/mm^2$

Using the $M_{Y,Ed}$ value, a possible profile could be estimated. The profile needs to have a plastic modulus $W_{pl,y}$ bigger than:

$$\sigma = \frac{M}{W} \longrightarrow W_{pl,y} = \frac{M_{Y,Ed} \cdot \gamma_{M0}}{f_y} = 627690.14\ mm^3$$

Possible profile: IPE300 ($W_{pl,y} = 628000\ mm^3$)

Classification cross-section

First the cross-section needs to be classified. Since steel grade S355 is used, $\epsilon = 0.81$. The internal compression parts are subjected to bending and the outstand flanges to compression.

Internal web bending:

$$\frac{c}{t} = \frac{248.6}{7.1} = 35.01 \leq 72\epsilon = 58.32 \longrightarrow Class\ 1$$

Outstand flange pure compression:

$$\frac{c}{t} = \frac{(150 - 7.1 - 2 \cdot 15)/2}{10.7} = 5.28 \leq 9\epsilon = 7.29 \longrightarrow Class\ 1$$

So the section is class 1, which means it can form a plastic hinge with the rotation capacity required from plastic analysis without reduction of the resistance.

Shear resistance The basic design requirement is:

$$\frac{V_{Ed}}{V_{C,Rd}} \leq 1.0$$

For class 1 sections:

$$V_{C,Rd} = V_{pl,Rd} = \frac{A_v \cdot (f_y/\sqrt{3})}{\gamma_{M0}}$$

For rolled I and H sections, load parallel to the web, A_v may be taken as follows (η may be taken as 1.0 to be conservative):

$$A_v = A - 2bt_f + (t_w + 2r)t_f \geq \eta h_w t_w \longrightarrow A_v = 2566.97\,mm^2 \geq 1978.06\,mm^2$$

$$V_{C,Rd} = V_{pl,Rd} = \frac{2566.97 \cdot (355/\sqrt{3})}{\gamma_{M0}} \cdot 10^{-3} = 526.12\,kN$$

$$\frac{V_{Ed}}{V_{C,Rd}} = \frac{89.13}{526.12} = 0.17 \leq 1.0$$

So profile IPE300 fulfils the requirement regarding shear resistance.

Shear buckling
The shear buckling resistance need to be considered if:

$$\frac{h_w}{t_w} > 72\frac{\epsilon}{\eta} \longrightarrow 39.24 > 58.32$$

This is not the case, so shear buckling is not considered.

Moment resistance
The basic design requirement is:

$$\frac{M_{Ed}}{M_{c,Rd}} \leq 1.0$$

For class 1 sections:

$$M_{c,Rd} = M_{pl,Rd} = \frac{W_{pl} \cdot f_y}{\gamma_{M0}} = \frac{628000 \cdot 355}{1.0} \cdot 10^{-6} = 222.94\,kNm$$

$$\frac{M_{Ed}}{M_{c,Rd}} = \frac{222.83}{222.94} = 0.99 \leq 1.0$$

Therefore the design bending resistance is good enough. Thus **IPE300** is a suitable profile.

Beam A-B on grid 2, level 2

Another possible external beam, is beam A-B on grid 2 (figure A.11). The wind loads - and thus the calculation - differ slightly from beam B-C. The beam is simply supported and spans $10\,m$. The bay width is $10\,m$. After checking all the possible load cases, the maximum design moment is $M_{Y,Ed} = 148.05\,kNm$ (occurs in wind pressure zone $F - G - H$ for load case Ed_4) and the maximum shear force is $V_Ed = 85.44\,kN$ (occurs in wind pressure zone $F - G - H$ for load case Ed_4). Since these forces are lower than in the previous case of the beam B-C on grid 2, profile **IPE300** also fulfils the requirements in this case and is thus a good profile to use.

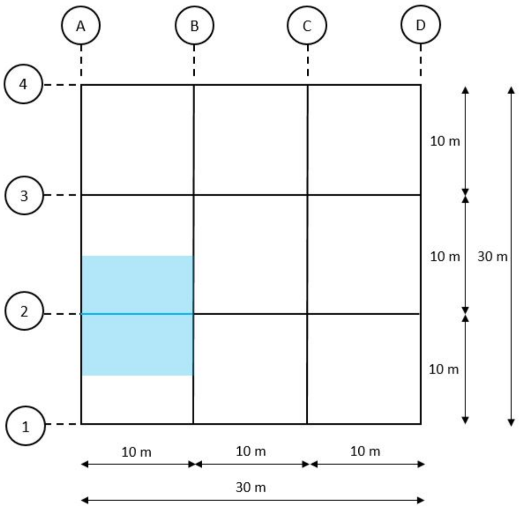

Figure A.11: Beam A-B on grid 2, level 2

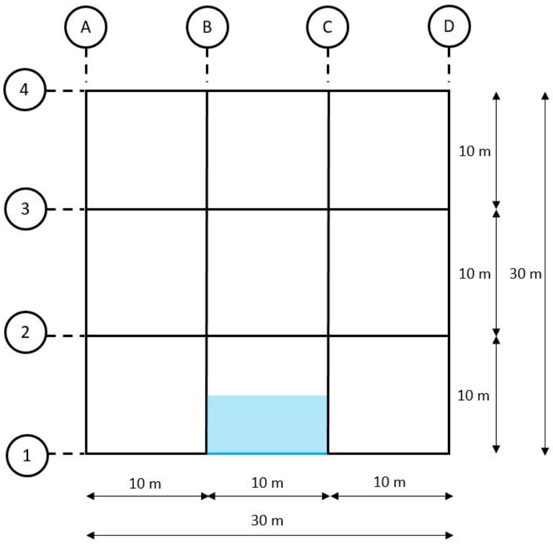

Figure A.12: External beams level 1

A.2.3. External beam level 1

For the external beams on level 1, the self-weight of the floor is $3\ kN/m^2$ and the variable imposed load for offices (category B) is $2.5\ kN/m^2$. The beam is simply supported and spans $10\ m$. The bay width is $5\ m$ (figure A.12). The design moment is $M_{Y,Ed} = 497.63\ kNm$ and the design shear force is $V_E d = 199.05\ kN$. It is assumed that the compression (top flange) is fully restrained due to the floor construction.

$M_{Y,Ed} = 497.63\ kNm$ (occurs at mid-span), $V_E d = 199.05\ kN$ (occurs at the end supports)

$\gamma_{M0} = 1.00$, $f_y = 355\ N/mm^2$ and $E = 210000\ N/mm^2$

Using the $M_{Y,Ed}$ value, a possible profile could be estimated. The profile needs to have a plastic modulus $W_{pl,y}$ bigger than:

$$\sigma = \frac{M}{W} \longrightarrow W_{pl,y} = \frac{M_{Y,Ed} \cdot \gamma_{M0}}{f_y} = 1401760.56\ mm^3$$

There are two possible profiles: HEA320 ($W_{pl,y} = 1630000\ mm^3$, $G = 97.6\ kg/m$) and IPE450

($W_{pl,y} = 1700000\,mm^3$, $G = 77.6\,kg/m$). Since the IPE450 profile uses less steel and is thus lighter, this profile is used. The additional height due to the higher profile is not a problem, since the story height is big enough.

Classification cross-section

First the cross-section needs to be classified. Since steel grade S355 is used, $\epsilon = 0.81$. The internal compression parts are subjected to bending and the outstand flanges to compression.

Internal web bending:

$$\frac{c}{t} = \frac{378.8}{9.4} = 40.30 \leq 72\epsilon = 58.32 \longrightarrow Class\ 1$$

Outstand flange pure compression:

$$\frac{c}{t} = \frac{(190 - 9.4 - 2 \cdot 21)/2}{14.6} = 4.75 \leq 9\epsilon = 7.29 \longrightarrow Class\ 1$$

So the section is class 1, which means it can form a plastic hinge with the rotation capacity required from plastic analysis without reduction of the resistance.

Shear resistance

The basic design requirement is:

$$\frac{V_{Ed}}{V_{C,Rd}} \leq 1.0$$

For class 1 sections:

$$V_{C,Rd} = V_{pl,Rd} = \frac{A_v \cdot (f_y/\sqrt{3})}{\gamma_{M0}}$$

For rolled I and H sections, load parallel to the web, A_v may be taken as follows (η may be taken as 1.0 to be conservative):

$$A_v = A - 2bt_f + (t_w + 2r)t_f \geq \eta h_w t_w \longrightarrow A_v = 5082.44\,mm^2 \geq 3955.52\,mm^2$$

$$V_{C,Rd} = V_{pl,Rd} = \frac{5082.44 \cdot (355/\sqrt{3})}{\gamma_{M0}} \cdot 10^{-3} = 1041.69\,kN$$

$$\frac{V_{Ed}}{V_{C,Rd}} = \frac{199.05}{1041.69} = 0.191 \leq 1.0$$

So profile IPE450 fulfils the requirement regarding shear resistance.

Shear buckling

The shear buckling resistance need to be considered if:

$$\frac{h_w}{t_w} > 72\frac{\epsilon}{\eta} \longrightarrow 44.77 > 58.32$$

This is not the case, so shear buckling is not considered.

Moment resistance The basic design requirement is:

$$\frac{M_{Ed}}{M_{c,Rd}} \leq 1.0$$

For class 1 sections:

$$M_{c,Rd} = M_{pl,Rd} = \frac{W_{pl} \cdot f_y}{\gamma_{M0}} = \frac{1700000 \cdot 355}{1.0} \cdot 10^{-6} = 603.5\,kNm$$

$$\frac{M_{Ed}}{M_{c,Rd}} = \frac{497.63}{603.5} = 0.82 \leq 1.0$$

Therefore the design bending resistance is good enough. Thus **IPE450** is a suitable profile.

A.2.4. Internal beam level 1

For the internal beams on level 1, the self-weight of the floor is $3\ kN/m^2$ and the variable imposed load for offices (category B) is $2.5\ kN/m^2$. The beam is simply supported and spans $10\ m$. The bay width is $10\ m$ (figure A.13). The design moment is $M_{Y,Ed} = 990.19\ kNm$ and the design shear force is $V_E d = 396.08\ kN$. It is assumed that the compression (top flange) is fully restrained due to the floor construction.

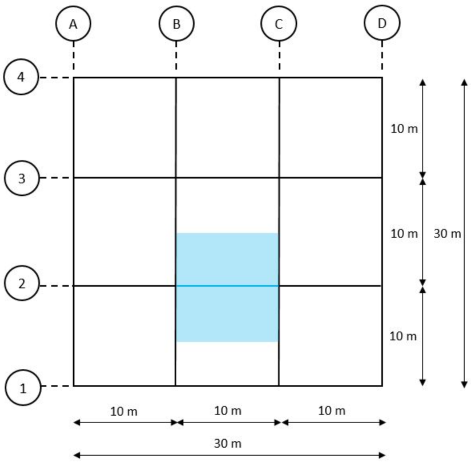

Figure A.13: Internal beams level 1

$M_{Y,Ed} = 990.19\ kNm$ (occurs at mid-span), $V_E d = 396.08\ kN$ (occurs at the end supports)

$\gamma_{M0} = 1.00$, $f_y = 355\ N/mm^2$ and $E = 210000\ N/mm^2$

Using the $M_{Y,Ed}$ value, a possible profile could be estimated. The profile needs to have a plastic modulus $W_{pl,y}$ bigger than:

$$\sigma = \frac{M}{W} \longrightarrow W_{pl,y} = \frac{M_{Y,Ed} \cdot \gamma_{M0}}{f_y} = 2789260.56\ mm^3$$

There are two possible profiles: IPE600 ($W_{pl,y} = 3512000\ mm^3$, $G = 122\ kg/m$) and HEA450 ($W_{pl,y} = 3216000\ mm^3$, $G = 140\ kg/m$). Since the IPE600 profile uses less steel and is thus lighter, this profile is used. The additional height due to the higher profile is not a problem, since the story height is big enough.

Classification cross-section

First the cross-section needs to be classified. Since steel grade S355 is used, $\epsilon = 0.81$. The internal compression parts are subjected to bending and the outstand flanges to compression.

Internal web bending:

$$\frac{c}{t} = \frac{514}{12} = 42.83 \leq 72\epsilon = 58.32 \longrightarrow Class\ 1$$

Outstand flange pure compression:

$$\frac{c}{t} = \frac{(220 - 12 - 2 \cdot 24)/2}{19} = 4.21 \leq 9\epsilon = 7.29 \longrightarrow Class\ 1$$

So the section is class 1, which means it can form a plastic hinge with the rotation capacity required from plastic analysis without reduction of the resistance.

Shear resistance

The basic design requirement is:

$$\frac{V_{Ed}}{V_{C,Rd}} \leq 1.0$$

For class 1 sections:

$$V_{C,Rd} = V_{pl,Rd} = \frac{A_v \cdot (f_y/\sqrt{3})}{\gamma_{M0}}$$

For rolled I and H sections, load parallel to the web, A_v may be taken as follows (η may be taken as 1.0 to be conservative):

$$A_v = A - 2bt_f + (t_w + 2r)t_f \geq \eta h_w t_w \longrightarrow A_v = 8380\, mm^2 \geq 6744\, mm^2$$

$$V_{C,Rd} = V_{pl,Rd} = \frac{8380 \cdot (355/\sqrt{3})}{\gamma_{M0}} \cdot 10^{-3} = 1717.56\, kN$$

$$\frac{V_{Ed}}{V_{C,Rd}} = \frac{396.08}{1717.56} = 0.23 \leq 1.0$$

So profile IPE600 fulfils the requirement regarding shear resistance.

Shear buckling

The shear buckling resistance need to be considered if:

$$\frac{h_w}{t_w} > 72\frac{\epsilon}{\eta} \longrightarrow 46 > 58.32$$

This is not the case, so shear buckling is not considered.

Moment resistance

The basic design requirement is:

$$\frac{M_{Ed}}{M_{c,Rd}} \leq 1.0$$

For class 1 sections:

$$M_{c,Rd} = M_{pl,Rd} = \frac{W_{pl} \cdot f_y}{\gamma_{M0}} = \frac{3512000 \cdot 355}{1.0} \cdot 10^{-6} = 1246.76\, kNm$$

$$\frac{M_{Ed}}{M_{c,Rd}} = \frac{990.19}{1246.76} = 0.79 \leq 1.0$$

Therefore the design bending resistance is good enough. Thus **IPE600** is a suitable profile.

A.2.5. Steel bracing

The wind loads on the building are taken by the two bracing systems on both side of the building. The floors will transfer the forces and acts as diaphragms. Also the equivalent horizontal forces, due to the vertical loads on respectively the roof and the floor are taken by the bracing system. Since the building is symmetric, only consider the most severe load case.

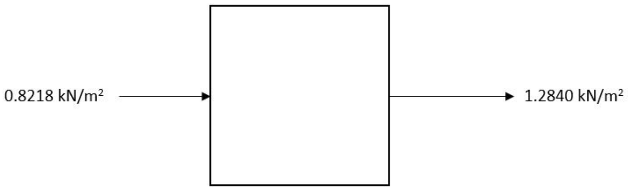

Figure A.14: Most severe wind pressures on building

The most severe wind force on the building is (figure A.14):

$$F_w = (0.8218 + 1.2840) \cdot 30 \cdot 8 = 505.392\, kN$$

So for each braced bay:

$$F_w = \frac{505.392}{2} = 252.7\ kN$$

In addition to the horizontal wind loads, also the equivalent loads on the two levels are of interest for the design of the bracing. The vertical loads based on the permanent and (most severe wind) variable loads and the governing combination, result in a total roof load of $330.80\,kN$ and floor load of $5332.5\,kN$.

The equivalent horizontal forces are calculated using the initial sway imperfections:

$$\phi = \phi_0 \alpha_h \alpha_m$$

Where:

$$\phi_0 = \frac{1}{200}$$

$$\alpha_h = \frac{2}{\sqrt{h}} = \frac{2}{\sqrt{8}} = 0.707 \ \left(\frac{2}{3} \leq \alpha_h \leq 1.0\right)$$

$$\alpha_m = \sqrt{0.5 + \left(1 + \frac{1}{m}\right)} = \sqrt{0.5 + \left(1 + \frac{1}{4}\right)} = 0.791$$

So:

$$\phi = \phi_0 \alpha_h \alpha_m = \frac{1}{200} \cdot 0.707 \cdot 0.791 = 0.0027962$$

Thus the equivalent horizontal force for each bracing system:

Roof level: $330.80 \cdot 0.0027962 \cdot 0.5 = 0.462\ kN$

Floor level: $5332.5 \cdot 0.0027962 \cdot 0.5 = 7.456\ kN$

The total horizontal load per bracing system:

$$F_h = 1.5 \cdot 252.7 + 0.462 + 7.456 = 386.97\ kN$$

Using the geometry, spacing between the columns and the story height, the axial force in the bracing can be computed (figure A.15).

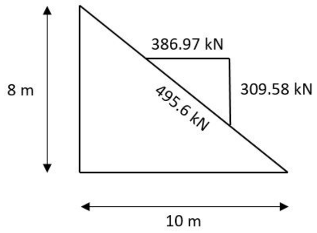

Figure A.15: Axial force in bracing

$N_{Ed} = 495.6\ kN$

$\gamma_{M0} = 1.00$, $f_y = 355\ N/mm^2$ and $E = 210000\ N/mm^2$

It is assumed that the bracing only takes tension forces. The bracing act as a system, so the horizontal loads on the building from each direction will be taken by one of the bracing diagonals (under tension). For a steel bracing, a steel rod is very convenient. Based on the tension force $N_{Ed} = 495.6\ kN$, a suitable profile is determined.

$$\frac{N_{Ed}}{N_{t,Rd}} \leq 1.0$$

Where $N_{t,Rd} = N_{pl,Rd}$

$$N_{pl,Rd} = \frac{Af_y}{\gamma_{M0}}$$

So a suitable profile has a minimal surface A_{min} of:

$$A_{min} = \frac{N_{pl,Rd\gamma_{M0}}}{f_y} = \frac{495.6 \cdot 10^3 \cdot 1.0}{355} = 1396.06\, mm^2$$

So a steel rod with a round diameter of $45mm$ and surface of $A = 1590.43\, mm^2$ is sufficient. The associated unity check is:

$$\frac{N_{Ed}}{N_{t,Rd}} = \frac{495.6 \cdot 10^3}{\left(\frac{1590.43 \cdot 355}{1.0}\right)} = 0.88 \leq 1.0$$

A.2.6. Internal column

There are three types of columns in this building. This section is about the internal column. There are 4 internal columns on 2-B, 2-C, 3-B and 3-C. The calculation is performed for the column on 2-B (figure A.16), however, this design also holds for the other internal columns. The permanent and variable forces - using the governing combination - on both the roof and floor level lead to vertical forces (figure A.17). The area used for these loads is $10 \cdot 10m$. The column is $8\, m$ tall, but it is simple connected in the middle at $4\, m$ height. The buckling length of the column for both axis is $4000\, mm$.

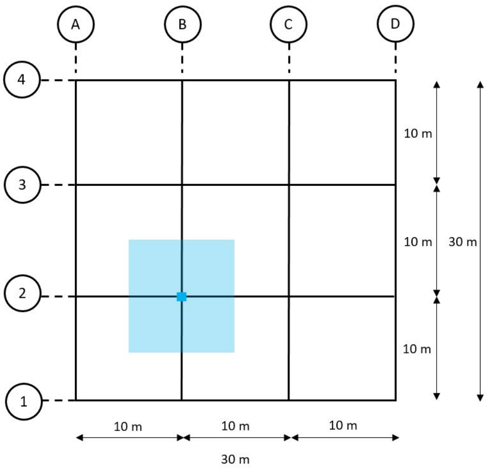

Figure A.16: Internal column

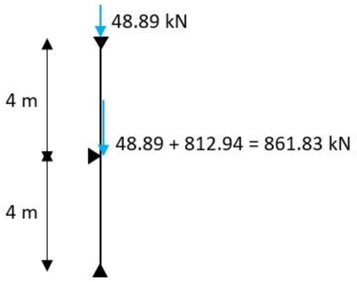

Figure A.17: Internal column forces

$N_{Ed} = 861.83\, kN$

$\gamma_{M0} = 1.00$, $f_y = 355\ N/mm^2$ and $E = 210000\ N/mm^2$

After several iterations, profile HEA200 (S355) is used in the calculation.

Classification cross-section
First the cross-section needs to be classified. Since steel grade S355 is used, $\epsilon = 0.81$. Both the internal and external parts are subjected by pure compression.

Internal web pure compression:

$$\frac{c}{t} = \frac{134}{6.5} = 20.62 \leq 33\epsilon = 26.73 \longrightarrow Class\ 1$$

Outstand flange pure compression:

$$\frac{c}{t} = \frac{(200 - 6.5 - 2 \cdot 18)/2}{10} = 7.875 \leq 10\epsilon = 8.1 \longrightarrow Class\ 2$$

So the section is class 2, which means it can develop their plastic moment resistance, but have limited rotation capacity because of local buckling.

Compression resistance
The axial compression basic requirement is:

$$\frac{N_{Ed}}{N_{c,Rd}} \leq 1.0$$

For class 2 sections:

$$N_{c,Rd} = \frac{A \cdot f_y}{\gamma_{M0}} = \frac{5383 \cdot 335}{1.0} \cdot 10^{-3} = 1910.97\ kN$$

$$\frac{N_{Ed}}{N_{C,Rd}} = \frac{861.83}{1910.97} = 0.45 \leq 1.0$$

So profile HEA200 fulfils the requirement regarding axial compression resistance.

Flexural buckling resistance
The basic requirement regarding flexural buckling resistance is:

$$\frac{N_{Ed}}{N_{b,Rd}} \leq 1.0$$

$N_{b,Rd}$ is the design buckling resistance and is calculated as follows (for class 1, 2 and 3 cross-sections):

$$N_{b,Rd} = \frac{\chi A f_y}{\gamma_{M1}}$$

χ is a reduction factor for the buckling resistance. For profile HEA200, $\frac{h}{b} \leq 1.2$, $t_f \leq 100mm$, axis z-z, buckling curve c is used. The corresponding imperfection factor $\alpha = 0.49$.

The non-dimensional slenderness $\bar{\lambda}$ is (for class 1, 2 and 3 cross-sections):

$$\bar{\lambda} = \sqrt{\frac{A f_y}{N_{cr}}} = \frac{L_{cr}}{i}\frac{1}{\lambda_1}$$

Where L_{cr} is the buckling length:

$$L_{cr} = 4000\ mm$$

Factor i is the radius of gyration about the relevant axis (z-z in this case), and for profile HEA200 this is $49.8\ mm$. And factor λ_1 is given by (for steel grade S355 ⟶ $\epsilon = 0.81$):

$$\lambda_1 = \pi\sqrt{\frac{E}{f_y}} = 93.9\epsilon = 93.9 \cdot 0.81 = 76.06$$

So $\bar{\lambda}$ is:

$$\bar{\lambda} = \frac{4000}{49.8}\frac{1}{76.06} = 1.056$$

$$\phi = 0.5\left(1 + \alpha\left(\bar{\lambda} - 0.2\right) + \bar{\lambda}^2\right) = 1.267$$

$$\chi = \frac{1}{\phi + \sqrt{\phi^2 - \bar{\lambda}^2}} = 0.508 \quad (\chi \leq 1.0)$$

So the design buckling resistance $N_{b,Rd}$ is:

$$N_{b,Rd} = \frac{\chi A f_y}{\gamma_{M1}} = \frac{0.508 \cdot 5383 \cdot 355}{1.0} \cdot 10^{-3} = 971.46\ kN$$

$$\frac{N_{Ed}}{N_{b,Rd}} = \frac{861.83}{971.46} = 0.89 \leq 1.0$$

Therefore the design flexural buckling resistance is good enough. Thus **HEA200** is a suitable profile.

A.2.7. External column

The external columns are located on the periphery of the building, however, not in the corners (these are called 'corner' columns, see next section). The calculation is performed for the column on 1-B (figure A.18), however, this design also holds for the other external columns. The permanent and variable forces - using the governing combination - on both the roof and floor level lead to vertical forces (figure A.20). The area used for these loads is $10 \cdot 5\ m$. Also the horizontal wind load q generates a bending moment in the column. The most governing wind load case is examined. The column is $8\ m$ tall, but it is simple connected in the middle at $4m$ height. The buckling length of the column for both axis is $4000mm$. Since the vertical loading is not completely symmetrical on the column, an additional moment at both the roof and floor level is present. Assume that the reaction force of the vertical loading acts at $100\ mm$ from the face of the column, then the moment arm is $\frac{h}{2} + 100\ mm$ (figure A.19).
The wind loading q is varied for wind zone A, B, C and D. The bending moments in the column are examined and the most governing forces (normal and bending moments) are in table A.6. The bottom part is $0 - 4m$ height and top part $4 - 8m$.

	N_{Ed}	M_{Ed}
Top part	25.74 kN	111.79 kNm
Bottom part	434.45 kN	55.85 kNm

Table A.6: Forces in external column for bottom and top part

After two iterations, profile HEA220 (S355) is used in the analysis.

Classification cross-section

First the cross-section needs to be classified. Since steel grade S355 is used, $\epsilon = 0.81$. The internal part is subjected to bending and compression and the external parts to compression. Considering both the top and bottom part of the column, the cross-section is classified as a class 2 section.

Cross-section resistance: bending and axial force

Since both an axial force and moment are present, the effect of the axial force on the plastic moment

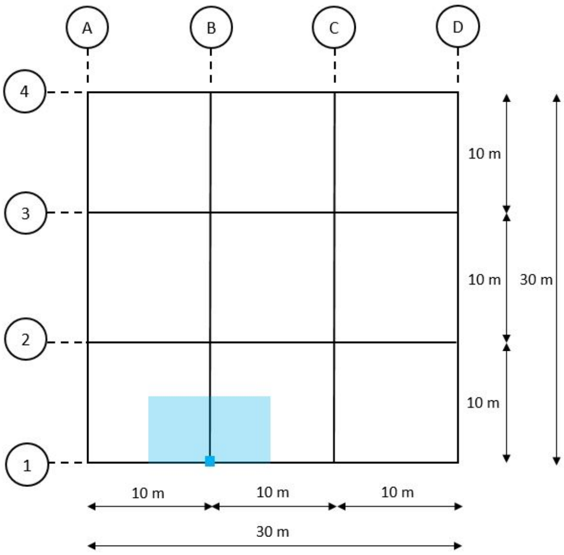
A
B
C
D
4
3
2
1
10 m
10 m
10 m
30 m
10 m
10 m
10 m
30 m

Figure A.18: External column

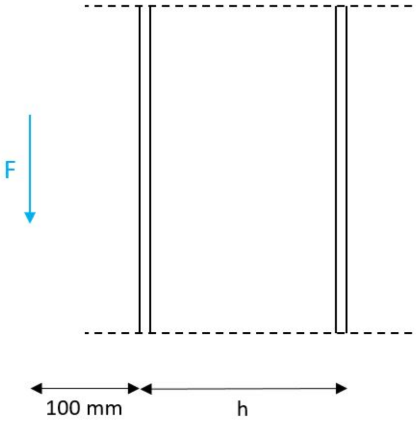

Figure A.19: External column vertical force generates bending moment due to eccentric loading (moment arm)

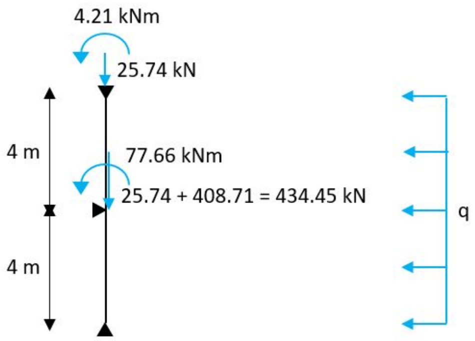
4.21 kNm
25.74 kN
77.66 kNm
25.74 + 408.71 = 434.45 kN
4 m
4 m
q

Figure A.20: External column forces

resistance need to be investigated. For class 1 and 2 cross-sections the following criterion hold, where $M_{N,Rd}$ is the reduced plastic moment resistance due to axial force N_{Ed}:

$$M_{Ed} \leq M_{N,Rd}$$

This reduction on the plastic moment resistance about the y-y axis need only be considered, if one of these criteria below is not true:

$$N_{Ed} \leq 0.25 \cdot N_{pl,Rd} \longrightarrow 434.45 \leq 571.0$$

$$N_{Ed} \leq \frac{0.5 \cdot h_w \cdot tw \cdot fy}{\gamma_{M0}} \longrightarrow 434.45 \leq 188.9$$

Since the second criterion is not true, a reduction on the plastic moment resistance is accounted for. Two parameters n and a are introduced to calculate the exact reduction:

$$n = \frac{N_{Ed}}{N_{pl,Rd}} \longrightarrow \frac{434.45}{2284.1} = 0.19$$

$$a = \frac{(A - 2 \cdot b \cdot t_f)}{A} \leq 0.5 \longrightarrow 0.25 \leq 0.5$$

The reduced plastic bending moment resistance about the y-y axis therefore becomes:

$$M_{N,y,Rd} = M_{pl,y,Rd} \cdot \frac{1-n}{1-0.5 \cdot a} \leq M_{pl,y,Rd} \longrightarrow 201.64 \cdot 0.93 = 187.5\ kNm$$

The cross-section resistance check of the combination of bending and axial force becomes:

$$\frac{N_{Ed}}{N_{Rd}} + \frac{M_{Ed}}{M_{N,y,Rd}} \leq 1.0 \longrightarrow 0.79$$

Flexural buckling resistance

The basic requirement regarding flexural buckling resistance is:

$$\frac{N_{Ed}}{N_{b,Rd}} \leq 1.0$$

$N_{b,Rd}$ is the design buckling resistance and is calculated as follows (for class 1, 2 and 3 cross-sections):

$$N_{b,Rd} = \frac{\chi A f_y}{\gamma_{M1}}$$

χ is a reduction factor for the buckling resistance. For profile HEA220, $\frac{h}{b} \leq 1.2$, $t_f \leq 100mm$, axis z-z, buckling curve c is used. The corresponding imperfection factor $\alpha = 0.49$.

The non-dimensional slenderness $\bar{\lambda}$ is (for class 1, 2 and 3 cross-sections):

$$\bar{\lambda} = \sqrt{\frac{A f_y}{N_{cr}}} = \frac{L_{cr}}{i} \frac{1}{\lambda_1}$$

Where L_{cr} is the buckling length:

$$L_{cr} = 4000\ mm$$

Factor i is the radius of gyration about the relevant axis (z-z in this case), and for profile HEA220 this is $55.1\ mm$. And factor λ_1 is given by (for steel grade S355 $\longrightarrow \epsilon = 0.81$):

$$\lambda_1 = \pi \sqrt{\frac{E}{f_y}} = 93.9\epsilon = 93.9 \cdot 0.81 = 76.06$$

So $\bar{\lambda}$ is:

$$\bar{\lambda} = \frac{4000}{55.1} \frac{1}{76.06} = 0.954$$

$$\phi = 0.5\left(1 + \alpha\left(\overline{\lambda} - 0.2\right) + \overline{\lambda}^2\right) = 1.1398$$

$$\chi = \frac{1}{\phi + \sqrt{\phi^2 - \overline{\lambda}^2}} = 0.567 \quad (\chi \leq 1.0)$$

So the design buckling resistance $N_{b,Rd}$ is:

$$N_{b,Rd} = \frac{\chi A f_y}{\gamma_{M1}} = \frac{0.567 \cdot 6434 \cdot 355}{1.0} \cdot 10^{-3} = 1295.18\, kN$$

Lateral torsional buckling

The column is laterally unrestrained, so the member should also be verified against lateral torsional buckling. The basic design requirement is:

$$\frac{M_{Ed}}{M_{b,Rd}} \leq 1.0$$

Where $M_{b,Rd}$ is defined as follows (for class 2 sections use $W_y = W_{pl,y}$):

$$M_{b,Rd} = \chi_{LT} W_{pl,y} \frac{f_y}{\gamma_{M1}}$$

The non-dimensional slenderness related to lateral torsional buckling $\overline{\lambda_{LT}}$ is determined using the conservative formula:

$$\overline{\lambda_{LT}} = 0.9 \cdot \overline{\lambda} = 0.9 \cdot 0.954 = 0.859$$

For profile HEA220, rolled I-section, $\frac{h}{b} \leq 2$, buckling curve a is used. The corresponding imperfection factor $\alpha_{LT} = 0.21$. For rolled or equivalent welded sections, the values for $\overline{\lambda_{LT,0}}$ and β in the formula for ϕ_{LT} are:

$$\overline{\lambda_{LT,0}} = 0.4$$

$$\beta = 0.75$$

$$\phi = 0.5\left(1 + \alpha_{LT}\left(\overline{\lambda} - \overline{\lambda_{LT,0}}\right) + \beta\overline{\lambda}^2\right) = 0.825$$

$$\chi = \frac{1}{\phi + \sqrt{\phi^2 - \overline{\lambda}^2}} = 0.846 \left(\chi_{LT} \leq 1.0 \text{ and} \leq \frac{1}{\overline{\lambda_{LT}}^2} = 1.35\right)$$

$$M_{b,Rd} = \chi_{LT} W_{pl,y} \frac{f_y}{\gamma_{M1}} = \frac{0.846 \cdot 5.68 \cdot 10^5 \cdot 355}{1.0} = 170.59\, kNm$$

Combined bending moment and axial compression

The cross-section is verified using the simplified combined bending moment and axial compression buckling unity check.

$$\frac{N_{Ed}}{N_{b,Rd}} + \frac{M_{Ed}}{M_{b,Rd}} \leq 1.0$$

For both the top and bottom part the unity check is performed:

$$\text{Top part: } \frac{25.74}{1295.18} + \frac{111.79}{170.59} = 0.68 \leq 1.0$$

$$\text{Bottom part: } \frac{434.45}{1295.18} + \frac{55.85}{170.59} = 0.66 \leq 1.0$$

Thus **HEA220** is a suitable profile.

A.2.8. Corner column

The corner columns are located on the corners of the building. The calculation is performed for the column on 1-A (figure A.21), however, this design also holds for the other corner columns. The permanent and variable forces - using the governing combination - on both the roof and floor level lead to vertical forces (figure A.23). The area used for these loads is $5 \cdot 5\,m$. Also the horizontal wind load q generates a bending moment in the column. The most governing wind load case is examined. The column is $8\,m$ tall, but it is simple connected in the middle at $4\ m$ height. The buckling length of the column for both axis is $4000\,mm$. Since the vertical loading is not completely symmetrical on the column, an additional moment at both the roof and floor level is present. Assume that the reaction force of the vertical loading acts at $100\,mm$ from the face of the column, then the moment arm is $\frac{h}{2} + 100\,mm$ (figure A.22).

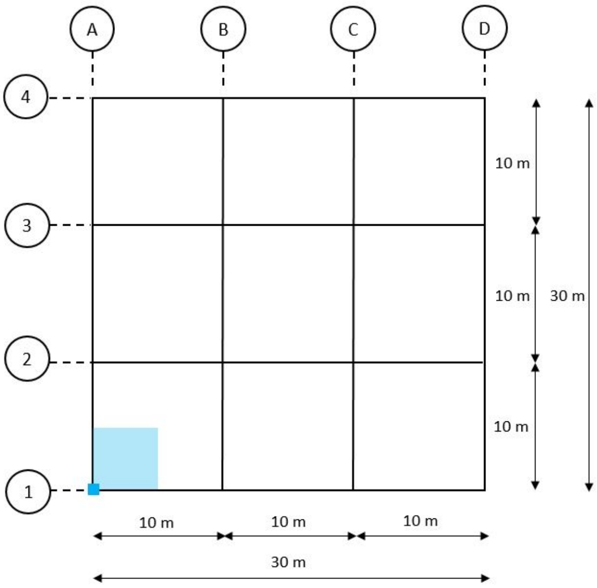

Figure A.21: Corner column

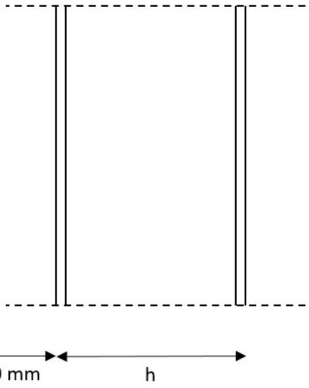

Figure A.22: Corner column vertical force generates bending moment due to eccentric loading (moment arm)

The wind loading q is different for wind zone A and D. The bending moments in the column are examined and the most governing forces (normal and bending moments) are in table A.7. The bottom part is $0 - 4\ m$ height and top part $4 - 8\ m$.

For the analysis use the same profile as for the external columns, HEA220 (S355), which is a class 2 section. The $N_{b,Rd}$ value is $1295.18\ kN$ and $M_{b,Rd}$ is $170.59\ kNm$.

Bending moment resistance

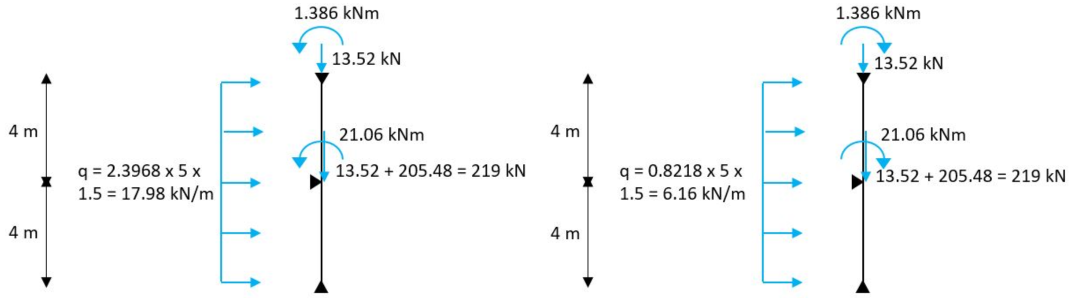

Figure A.23: Corner column forces

	N_{Ed}	$M_{y,Ed}$	$M_{z,Ed}$
Top part	13.52 kN	46.84 kNm	10.91 kNm
Bottom part	219 kN	24.23 kNm	22.5 kNm

Table A.7: Forces in corner column for bottom and top part

For a class 2 section, the bending moment resistance (for the weak z-z axis) is:

$$M_{z,Rd} = M_{pl,Rd} = \frac{W_{pl,z} f_y}{\gamma_{M0}} = \frac{2.71 \cdot 10^5 \cdot 355}{1.0} \cdot 10^{-6} = 96.205\ kNm$$

Cross-section resistance: bending and axial force

Since both an axial force and moment are present, the effect of the axial force on the plastic moment resistance need to be investigated. For class 1 and 2 cross-sections the following criterion hold, where $M_{N,Rd}$ is the reduced plastic moment resistance due to axial force N_{Ed}:

$$M_{Ed} \leq M_{N,Rd}$$

This reduction on the plastic moment resistance about the y-y axis need only be considered, if one of these criteria below is not true:

$$N_{Ed} \leq 0.25 \cdot N_{pl,Rd} \longrightarrow 219 \leq 571.0$$

$$N_{Ed} \leq \frac{0.5 \cdot h_w \cdot tw \cdot fy}{\gamma_{M0}} \longrightarrow 219 \leq 188.9$$

Since the second criterion is not true, a reduction on the plastic moment resistance for axis y-y is accounted for.

This reduction on the plastic moment resistance about the z-z axis need only be considered, if this criteria below is not true:

$$N_{Ed} \leq \frac{h_w \cdot tw \cdot fy}{\gamma_{M0}} \longrightarrow 219 \leq 377.8$$

So a reduction for the plastic moment resistance about the z-z axis is not needed. Two parameters n and a are introduced to calculate the exact reduction:

$$n = \frac{N_{Ed}}{N_{pl,Rd}} \longrightarrow \frac{219}{2284.1} = 0.10$$

$$a = \frac{(A - 2 \cdot b \cdot t_f)}{A} \leq 0.5 \longrightarrow 0.25 \leq 0.5$$

The reduced plastic bending moment resistance about the y-y axis therefore becomes:

$$M_{N,y,Rd} = M_{pl,y,Rd} \cdot \frac{1-n}{1-0.5 \cdot a} \leq M_{pl,y,Rd} \longrightarrow 201.64 \cdot 1.02 = 201.64\ kNm$$

The cross-section resistance check of the combination of bending and axial force becomes:

$$\frac{N_{Ed}}{N_{Rd}} + \frac{M_{y,Ed}}{M_{N,y,Rd}} + 1.5 \cdot \frac{M_{z,Ed}}{M_{z,Rd}} \leq 1.0 \longrightarrow 0.56$$

Combined bending moment and axial compression

The cross-section is verified using the simplified combined bending moment and axial compression buckling unity check.

$$\frac{N_{Ed}}{N_{b,Rd}} + \frac{M_{Ed}}{M_{b,Rd}} + 1.5 \cdot \frac{M_{z,Ed}}{M_{z,Rd}} \leq 1.0$$

For both the top and bottom part the unity check is performed:

$$\text{Top part: } \frac{13.52}{1295.18} + \frac{46.84}{170.59} + 1.5 \cdot \frac{10.91}{96.205} = 0.46 \leq 1.0$$

$$\text{Bottom part: } \frac{219}{1295.18} + \frac{24.23}{170.59} + 1.5 \cdot \frac{22.5}{96.205} = 0.66 \leq 1.0$$

Thus **HEA220** is a suitable profile.

A.2.9. Frame stability

The building is verified for frame stability to check whether the building is susceptible for sway instability or in other words second-order effects. The Eurocode provides an approximate formula for factor α_{cr}, which can be used for portal frames with shallow roof slopes and beam-and-column type plane frames. Where H_{Ed} is the design value of the horizontal reaction force, V_{Ed} is the total design vertical load, h is the storey height and $\delta_{H,Ed}$ is the horizontal displacement due to horizontal wind loads and equivalent loads due to the vertical loads. Second-order effects may be ignored if $\alpha_{cr} \geq 10$.

$$\alpha_{cr} = \left(\frac{H_{Ed}}{V_{Ed}}\right)\left(\frac{h}{\delta_{H,Ed}}\right)$$

Wind loads

The leading action on the building is the wind load. The total wind load is:

$$F_w = 505.39\ kN \longrightarrow F_w \cdot \gamma_Q = 505.39 \cdot 1.5 = 758.09\ kn$$

So the wind load per braced bay is:

$$F_{w,bracing} = \frac{758.09}{2} = 379.04\ kN$$

This wind load is distributed over the roof and floor level as follows:

$$\text{Roof level: } \frac{379.04}{4} = 94.76\ kN$$

$$\text{Floor level: } \frac{379.04}{2} = 189.52\ kN$$

Equivalent horizontal loads due to vertical loads

Roof loading (the value of -0.56 is the average wind load on the roof due the different pressures and zones):

$$15 \cdot 30 \cdot (1.35 \cdot 0.9 + 1.5 \cdot -0.56) = 168.75\ kN$$

The equivalent horizontal load is determined as follows ($\alpha_h = \frac{2}{\sqrt{8}}$ and $\alpha_m = \sqrt{0.5 + \left(1 + \frac{1}{4}\right)}$):

$$168.75 \cdot \frac{1}{200} \cdot \alpha_h \cdot \alpha_m = 0.47\ kN$$

Floor loading:

$$15 \cdot 30 \cdot (1.35 \cdot 3 + 1.5 \cdot 0.5 \cdot 2.5) = 2666.25\ kN$$

The equivalent horizontal load is determined as follows ($\alpha_h = \frac{2}{\sqrt{8}}$ and $\alpha_m = \sqrt{0.5 + \left(1 + \frac{1}{4}\right)}$):

$$2666.25 \cdot \frac{1}{200} \cdot \alpha_h \cdot \alpha_m = 7.44\ kN$$

The total horizontal forces, summation of the wind and equivalent loads, are in figure A.24. In order to determine the horizontal displacements $\delta_{H,Ed}$ due to the horizontal loads, the building is modelled in the finite element program *Matrixframe*. The displacements and the corresponding $\delta_{H,Ed}$ are in figure A.25.

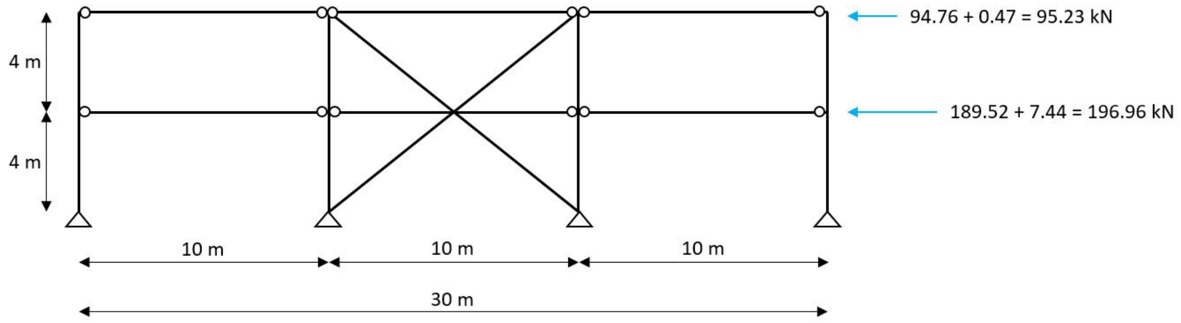

Figure A.24: Total horizontal forces for the frame stability verification

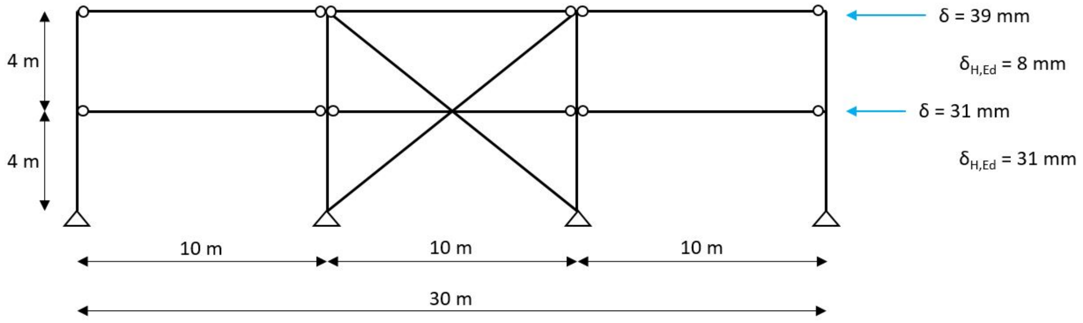

Figure A.25: Displacements due to the total horizontal loads

Finally, for both levels, it is calculated if it is sway sensitive. This is not the case if $\alpha_{cr} \geq 10$ and then the second-order effects may be ignored.

Top level: $\alpha_{cr} = \left(\frac{H_{Ed}}{V_{Ed}}\right)\left(\frac{h}{\delta_{H,Ed}}\right) = \left(\frac{95.23}{168.75}\right) \cdot \left(\frac{4000}{8}\right) = 282.2 > 10 \longrightarrow$ not sway sensitive

Bottom level: $\alpha_{cr} = \left(\frac{H_{Ed}}{V_{Ed}}\right)\left(\frac{h}{\delta_{H,Ed}}\right) = \left(\frac{95.23 + 196.96}{168.75 + 2666.25}\right) \cdot \left(\frac{4000}{31}\right) = 13.3 > 10 \longrightarrow$ not sway sensitive

A.3. Overview chosen structural elements

In table A.8 an overview is provided of all the chosen structural elements and the associated governing unity check for that element. It can be seen that most of the elements could have been optimised further, however, for this study regarding the reliability analysis, this design is good enough.

Element	Level	Profile	Grade	Governing unity check	Unity check value
Internal beam	2	IPE300	S355	Bending moment	0.99
External beam	2	IPE240	S355	Bending moment	0.91
Internal beam	1	IPE600	S355	Bending moment	0.79
External beam	1	IPE450	S355	Bending moment	0.82
Internal column	-	HEA200	S355	Flexural buckling	0.89
External column	-	HEA220	S355	Combined bending and compression	0.68
Corner column	-	HEA220	S355	Combined bending and compression	0.66
Bracing	-	Steel rod diameter 45 mm	S355	Tension	0.88

Table A.8: Overview chosen structural elements and related unity checks

B

Explanation on Coupling SCIA FEM with Python using SCIA OpenAPI

In this research, a new technique is applied that makes it possible to adapt and control a finite element model via another software, in this research via Python, using the SCIA Engineer OpenAPI. This offers many new research possibilities and the use of this method is very convenient. However, a basic knowledge of programming is required to use this method correctly. Since the SCIA OpenAPI has not been out for long, there are not many examples to see how this method works. Therefore, below some tips and tricks are given to use the method in the best and most efficient way.

Below is a step by step description of how to use the SCIA OpenAPI [1]. The focus here is on the use of Python, since that is what was used in this research. However, other programming languages, such as C#, VB.Net, Python, VBA, PowerShell etc., are also possible.

Please check the following websites for additional explanation and documentation on the use of SCIA OpenAPI (make sure to use the correct version):
`https://github.com/scia-garage`
`https://help.scia.net/api/19.1.0031/index.html`

(1) Prepare the environment

- install Scia Engineer (32 / 64 bit)
  - .NET Framework is included in setup
  - start Scia Engineer to test it (set protection, open new project, etc.)
- install python 3.7
  - choose correct platform (32 / 64 bit) based on the Scia Engineer platform
  - install using setup `https://www.python.org/downloads/release/python-370/` (check the ”add Python to path” checkbox)
  - copy the ./res/python.exe.config and pythonw.exe.config to the directory where the python.exe and pythonw.exe are (e.g. run cmd ”where python.exe”), download at `https://github.com/scia-garage`
  - setup should also install the PIP package manager for Python
  - test python by running cmd ”python”
  - test pip by running cmd ”pip”

---

[1] The method described below is applied at the beginning of 2021. Therefore, always check for the latest version of the software. New features, such as calculation methodologies, may be available via software updates.

    - upgrade PIP by running ”python -m pip install –upgrade pip”
    - install the WHEEL package by running ”pip install wheel”

- install python.net `https://github.com/pythonnet/pythonnet/wiki/Installation`
    - via PIP from local .whl file
    - get .whl file
        - from `https://github.com/scia-garage/SciaOpenAPI_example_parabolic/tree/master/res`
    - cmd ”pip install .<path.to.whl.file>.whl”

(2) Build the finite element model
There are two ways to perform this step. The first and most obvious option is to model your building, as usual, directly in the normal graphical SCIA Engineer interface. This works very efficiently and you can see exactly if the model that you make is correct. Check the SCIA Engineer manual to see how to make this model and to see how to put all geometry, elements, connections, etc. in the model correctly.

The second possibility is by modelling the building - so also the geometry, elements, connections, etc. - through the OpenAPI language. This is less intuitive than the first method, but it does offer more freedom to modify the model as desired via a python script, for example. This makes it possible to design parametrically, whereby on the basis of, for example, a set of data or boundary conditions, the required profiles and positioning can then be fully determined. An example of how to create such a model entirely in the OpenAPI environment can be found here: `https://github.com/scia-garage/SciaOpenAPI_example_Python_simple_structure/blob/master/OpenAPIExamplePython/OpenAPIExamplePython.py`

In this study, the first method is applied, where an existing model is linked via the OpenAPI. Since the documentation for this method is rather limited, a more detailed explanation on how to achieve this result is given below.

(3) Export all necessary data from the SCIA Engineer FEM into a XML data-file
In order to ensure that the python script can refer to certain aspects in the model, such as construction elements, load panels, loads, etc., the necessary aspects that need to be referred to later must first be exported via a XML data file. This is necessary because otherwise the program does not understand what you want to do with certain elements, for example. Each element such as a beam or load gets a unique id in the program, which allows for communication and manipulation by means of SCIA OpenAPI.

Example from this study
In this investigation the building is fully modelled in SCIA Engineer via the normal graphical interface. All structural elements, supports, connections and also for example extra requirements like only tensile forces in the bracing elements, are added in this model. Since in this research the wind loads have to be placed on the building in the model in a similar way as in the wind tunnel research, the correct tributary areas and corresponding dimensions of the various wind zones are placed on the model as load panels. In this research, a total of 48 different wind zones are used, spread over the 4 side façades and the top of the building. All these load panels get in the SCIA Engineer program a unique name (e.g. ”LP1”) and ID. Subsequently on all these 48 load panels, surface loads are put with an arbitrary value of $1\ kN/m^2$. Pay attention to the coordinate system and in which direction positive is in the program. All these 48 surface loads also get a certain name (for example ”SF1”) and ID.

In this study, it is necessary to adjust, for each time step, the value of the 48 surface loads present on the building to the values that occur in the wind tunnel. To avoid confusion, an overview is made of the location of ”SF1” to ”SF48” and how this corresponds to which pressure point from the wind tunnel research. Furthermore, several pre-process steps are performed on the wind tunnel data in order to be able to use it on a full-scale building. Since in this research only these surface loads need to be modified via python, the XML export also only needs to contain data related to these surface loads.

In the general case: export all data via an XML file which you want to be able to control via a Python script, for example.

The creation of an XML document is as follows:
Tools > XML IO Document > New > Select elements you want to be able to control (e.g. in this study: ”Surface load”) > click right mouse button > Export > Select path and set type as XML-file

Below is an example of the exported XML file, which contains only all aspects related to the surface loads. For clarification, only surface load 1 and 2 (”SF1” and ”SF2”) are shown below. In reality, this XML file contains all 48 surface loads. This XML file is built up as a kind of table, in which data is specified further and further. Under the engine of SCIA Engineer all this information is noted for the surface loads, like on which load panel (”LPx”) it is applied, which load case, direction, coordinate system, and also the value of the surface load. This value, here visible in the lines <ns0 : p6 v=”1000.0” />, we want to adjust to the correct wind tunnel data. Notice that $1\ kN/m^2$ in XML is specified as 1000.

```
<ns0:project xmlns:ns0=”http://www.scia.cz”>

    <ns0:def uri=”Case_Study_Building_Wind_Tunnel_Areas.xml.def” />

    <ns0:container id=”{BC16B3CA−F464−11D4−94D3−000000000000}” t=”DataAddLoad.EP_SurfaceForceSurface.1”>
        <ns0:table id=”0EF1839D−EB17−4D4D−950D−40DEA876DC10” name=”Forces on surface”
        t=”DataAddLoad.EP_SurfaceForceSurface.1”>
            <ns0:h>
                <ns0:h0 t=”Reference Table” />
                <ns0:h1 t=”Load case” />
                <ns0:h2 t=”Name” />
                <ns0:h3 t=”UniqueID” />
                <ns0:h4 t=”Direction” />
                <ns0:h5 t=”Type” />
                <ns0:h6 t=”Value” />
                <ns0:h7 t=”System” />
                <ns0:h8 t=”Location” /></ns0:h>
            <ns0:obj id=”14” nm=”SF1”>
                <ns0:p0 t=””>
                <ns0:h>
                <ns0:h0 t=”Member Type” />
                <ns0:h1 t=”Member Type Name” />
                <ns0:h2 t=”Member Id” />
                <ns0:h3 t=”Member Name” />
                </ns0:h>
                <ns0:row id=”0”>
                <ns0:p0 v=”{7B422CC0−6394−403B−8386−1584D5E5E4FD}” />
                <ns0:p1 v=”EP_DSG_Elements.8.00.EP_LoadPanel.1” />
                <ns0:p2 v=”12” />
                <ns0:p3 v=”LP1” />
                </ns0:row>
                </ns0:p0>
                <ns0:p1 i=”7” n=”BG2” />
                <ns0:p2 v=”SF1” />
                <ns0:p3 v=”{C6F78488−277A−4E07−B3D8−AA51C45FB9AC}” />
                <ns0:p4 t=”X” v=”0” />
                <ns0:p5 t=”Force” v=”0” />
                <ns0:p6 v=”1000.0” />
                <ns0:p7 t=”GCS” v=”0” />
                <ns0:p8 t=”Length” v=”0” /></ns0:obj>

            <ns0:obj id=”15” nm=”SF2”>
                <ns0:p0 t=””>
                <ns0:h>
                <ns0:h0 t=”Member Type” />
                <ns0:h1 t=”Member Type Name” />
                <ns0:h2 t=”Member Id” />
                <ns0:h3 t=”Member Name” />
                </ns0:h>
                <ns0:row id=”0”>
            <ns0:p0 v=”{7B422CC0−6394−403B−8386−1584D5E5E4FD}” />
            <ns0:p1 v=”EP_DSG_Elements.8.00.EP_LoadPanel.1” />
            <ns0:p2 v=”13” />
            <ns0:p3 v=”LP2” />
             </ns0:row>
             </ns0:p0>
            <ns0:p1 i=”7” n=”BG2” />
            <ns0:p2 v=”SF2” />
            <ns0:p3 v=”{525911CF−1E8B−4DE9−9CCC−CCFA81A2F39F}” />
            <ns0:p4 t=”X” v=”0” />
            <ns0:p5 t=”Force” v=”0” />
            <ns0:p6 v=”1000.0” />
            <ns0:p7 t=”GCS” v=”0” />
            <ns0:p8 t=”Length” v=”0” /></ns0:obj>
      </ns0:table>
   </ns0:container>
</ns0:project>
```

(4) Write Python script which is able to modify the SCIA Engineer FEM

Below is a python script used in this research. Certain parts are shown in a more condensed form ([...]), as this python script only serves as an illustration, and in particular concerns the link between python and the SCIA finite element model. There are also extra explanations in the script itself behind #.

One important aspect that can cause problems is the amount of free memory available. In this study it was found that it works best if you reload (proj = env.OpenProject(proj-path)) the SCIA environment every 50 time steps (iter-per-block variable) and remove recent variables in the SCIA environment from memory (env.Dispose()). Otherwise, Python will have problems and the script will often stop (sometimes even without an error message). This means in most cases that the memory allocation does not go well and is due to the fact that there is too little free memory available.

```
# Import necessary programs and packages
import numpy as np
import pandas as pd
import scipy
from scipy import stats
import time
import random
import uuid
import sys
import clr
import os
from pathlib import Path

# Select the correct paths of the OpenAPI_dll files
sys.path.append(r”C:\Program Files\SCIA\Engineer19.1\OpenAPI_dll”)
clr.AddReference(r”C:\Program Files\SCIA\Engineer19.1\OpenAPI_dll\SCIA.OpenAPI.dll”)

from SCIA.OpenAPI import *
from SCIA.OpenAPI.StructureModelDefinition import *
from SCIA.OpenAPI.Results import *
from Results64Enums import *
from SCIA.OpenAPI.OpenAPIEnums import *
from SCIA.OpenAPI.Utils import *
from System import Guid
import xml.etree.ElementTree as ET

# Pre−processing steps raw wind tunnel data to full-scale wind loads
    [ ... ]
# Results in below distributed loads for side A − D and Top (run 1 and 2):

# Converting the pressure coefficient data into distributed load data
Load_SideA = 0.5 * rho * v_fs**2 * CP_SideA_Smooth
Load_SideB = 0.5 * rho * v_fs**2 * CP_SideB_Smooth
Load_SideC = 0.5 * rho * v_fs**2 * CP_SideC_Smooth
Load_SideD = 0.5 * rho * v_fs**2 * CP_SideD_Smooth
Load_Top1 = 0.5 * rho * v_fs**2 * CP_Top1_Smooth
Load_Top2 = 0.5 * rho * v_fs**2 * CP_Top2_Smooth
```

```
# Clear some memory: remove data related to variables no longer needed
# (from pre-processing wind load step)
    [ ... ]

# Make empty data arrays which will be filled during the calculations
    [ ... ]

# Define functions which store the results for the elements in the data arrays
def get_results(Entity_Name, Load_Case, N, Vy, Vz, Mx, My, Mz):
    IntFor1D = Result()
    keyIntFor1D = ResultKey()
    keyIntFor1D.CaseType = eDsElementType.eDsElementType_LoadCase
    keyIntFor1D.CaseId = Load_Case
    keyIntFor1D.EntityType = eDsElementType.eDsElementType_Beam
    keyIntFor1D.EntityName = Entity_Name
    keyIntFor1D.Dimension = eDimension.eDim_1D
    keyIntFor1D.ResultType = eResultType.eFemBeamInnerForces
    keyIntFor1D.CoordSystem = eCoordSystem.eCoordSys_Local
    IntFor1D = rapi.LoadResult(keyIntFor1D)
    N_max = 0.0
    pivot_N = N_max
    Vy_max = 0.0
    pivot_Vy = Vy_max
    Vz_max = 0.0
    pivot_Vz = Vz_max
    Mx_max = 0.0
    pivot_Mx = Mx_max
    My_max = 0.0
    pivot_My = My_max
    Mz_max = 0.0
    pivot_Mz = Mz_max
    elemcount = IntFor1D.GetMeshElementCount()
    for k in range(elemcount):
        pivot_N = IntFor1D.GetValue(0, k)
        pivot_Vy = IntFor1D.GetValue(1, k)
        pivot_Vz = IntFor1D.GetValue(2, k)
        pivot_Mx = IntFor1D.GetValue(3, k)
        pivot_My = IntFor1D.GetValue(4, k)
        pivot_Mz = IntFor1D.GetValue(5, k)
        if (abs(pivot_N) > abs(N_max)):
            N_max = pivot_N
        if (abs(pivot_Vy) > abs(Vy_max)):
            Vy_max = pivot_Vy
        if (abs(pivot_Vz) > abs(Vz_max)):
            Vz_max = pivot_Vz
        if (abs(pivot_Mx) > abs(Mx_max)):
            Mx_max = pivot_Mx
        if (abs(pivot_My) > abs(My_max)):
            My_max = pivot_My
        if (abs(pivot_Mz) > abs(Mz_max)):
            Mz_max = pivot_Mz
    # Store the results and normalize them
    N.append(N_max/(0.5 * rho * v_pot**2))
    Vy.append(Vy_max/(0.5 * rho * v_pot**2))
    Vz.append(Vz_max/(0.5 * rho * v_pot**2))
    Mx.append(Mx_max/(0.5 * rho * v_pot**2))
    My.append(My_max/(0.5 * rho * v_pot**2))
    Mz.append(Mz_max/(0.5 * rho * v_pot**2))
# Also a specific function related to columns
    [ ... ]

# Divide the total amount of timesteps needed to performed (n_iter) by amount of timesteps per block
# (iter_per_block = 50 in this study)
for k in range(int(n_iter/iter_per_block)):
    # Make the SCIA Engineer project, insert here the correct paths
    env = Environment(r”C:\Program Files\SCIA\Engineer19.1”, r”C:\Temp\OpenAPITemp”,”1.0.0.0”)
    EnumGuiMode = Environment.GuiMode.ShowWindowHide
    env.RunSCIAEngineer(Environment.GuiMode.ShowWindowHide)

    # Proj_path contains the path to 3D model of the building
    proj_path = r”C:<project_path_3d_FEM>.esad”
```

```
# XML_path contains the XML file in which the surface loads are changed and the
# project is updated with this XML
xml_path = r”C:<XML_path>.xml”

# Open the FEM
proj = env.OpenProject(proj_path)

for i in range(iter_per_block):
    # Change the surface loads based on the wind tunnel data, update the XML file
    xmlTree = ET.parse(xml_path)
    root = xmlTree.getroot()

    namespaceTranslation = {'ns0': 'http://www.scia.cz',}

    for container in root.findall(”ns0:container”, namespaceTranslation):
        if container.get(”t”) == ”DataAddLoad.EP_SurfaceForceSurface.1”:
            table =  container.find(”ns0:table”, namespaceTranslation)
            if table:
                for obj in table.findall(”ns0:obj”, namespaceTranslation):
                    if obj.get(”nm”) == ”SF1”:
                        p6Object = obj.find(”ns0:p6”, namespaceTranslation)
                        p6Object.set(”v”, str(Load_SideA[0][(k*iter_per_block)+i]))
                    if obj.get(”nm”) == ”SF2”:
                        p6Object = obj.find(”ns0:p6”, namespaceTranslation)
                        p6Object.set(”v”, str(Load_SideA[1][(k*iter_per_block)+i]))
                    if obj.get(”nm”) == ”SF3”:
                        p6Object = obj.find(”ns0:p6”, namespaceTranslation)
                        p6Object.set(”v”, str(Load_SideA[2][(k*iter_per_block)+i]))
                    if obj.get(”nm”) == ”SF4”:
                        p6Object = obj.find(”ns0:p6”, namespaceTranslation)
                        p6Object.set(”v”, str(Load_SideA[3][(k*iter_per_block)+i]))
                    if obj.get(”nm”) == ”SF5”:
                        p6Object = obj.find(”ns0:p6”, namespaceTranslation)
                        p6Object.set(”v”, str(Load_SideA[4][(k*iter_per_block)+i]))
                    if obj.get(”nm”) == ”SF6”:
                        p6Object = obj.find(”ns0:p6”, namespaceTranslation)
                        p6Object.set(”v”, str(Load_SideA[5][(k*iter_per_block)+i]))
                    if obj.get(”nm”) == ”SF7”:
                        p6Object = obj.find(”ns0:p6”, namespaceTranslation)
                        p6Object.set(”v”, str(Load_SideA[6][(k*iter_per_block)+i]))

                    # Also for all the other surface loads up to SF48
                        [ ... ]

    xmlTree.write(xml_path)

    # Update the SCIA Project with the updated XML file (with surface loads for timestep i)
    env.UpdateProject(Environment.TypeOfExtProject.TypeXML, xml_path, proj.ProjectID)

    # Perform calculation in SCIA Engineer
    proj.RunCalculation()

    # Setup for storing the results
    rapi = proj.Model.InitializeResultsAPI()

    # Get the correct APiGuid for the load_case you are interested in, using XML
    # in SCIA Engineer > load_cases
    BG2 = ApiGuid(”{9C5EC6D3-EC26-4487-9772-5E8AB71ABED9}”)
    if rapi !=  None :

        # Also get results for other elements
            [ ... ]

        # NR8: Element S65: Bracing
        get_results(Entity_Name=”S65”, Load_Case=BG2, N=N8, Vy=Vy8, Vz=Vz8, Mx=Mx8, My=My8, Mz=Mz8)

    # Clear memory for the results for timestep i
    rapi.Dispose()

# After all iterations are performed, project is closed and environment memory is cleared
```

```
    proj.CloseProject(SaveMode.SaveChangesNo)
    env.Dispose()

# Store all results in a dataframe and export to excel file when finished in result map
    [ ... ]
```

C

Finite Element Model Case Study Building Figures - Designation of Various Elements

The green plane on the left side of the building indicates the direction of incidence of the wind.

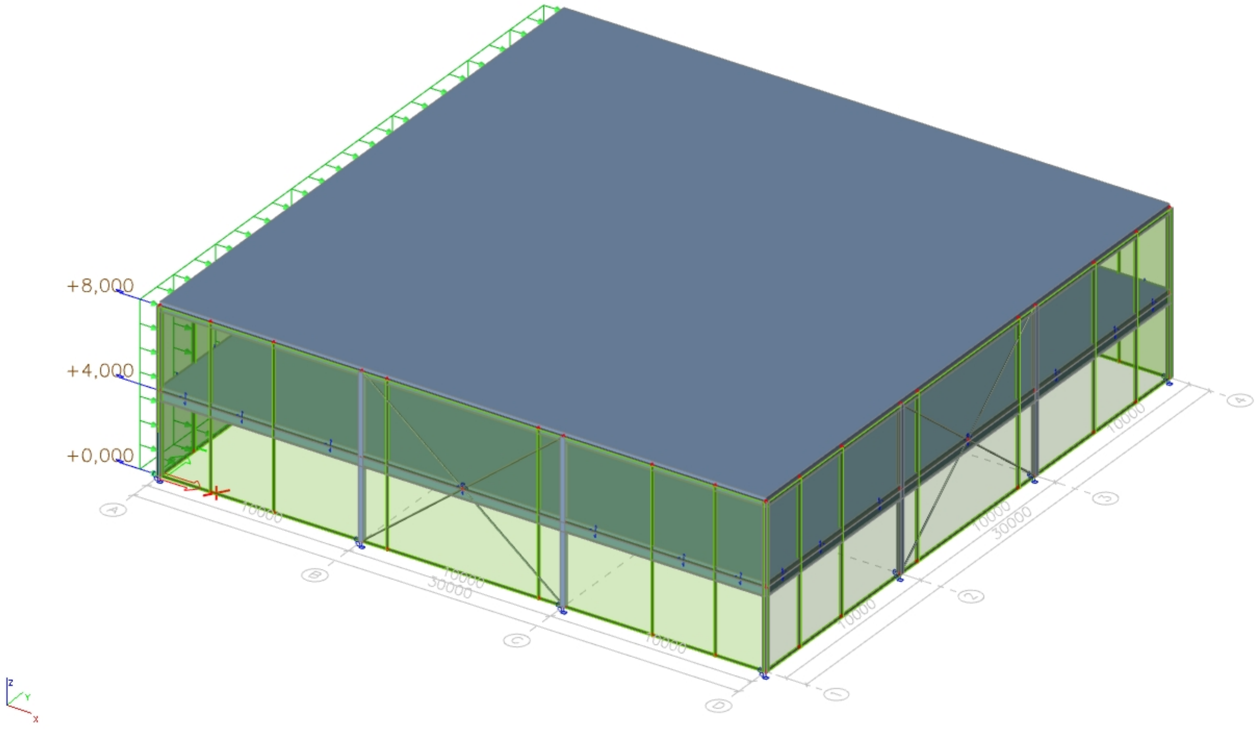
+8,000
+4,000
+0,000
A
B
C
D
1
2
3
4
10000
10000
30000
10000
10000
10000
30000
10000
10000
Z
Y
X

Figure C.1: Render of the Case Study Building in the SCIA FEM

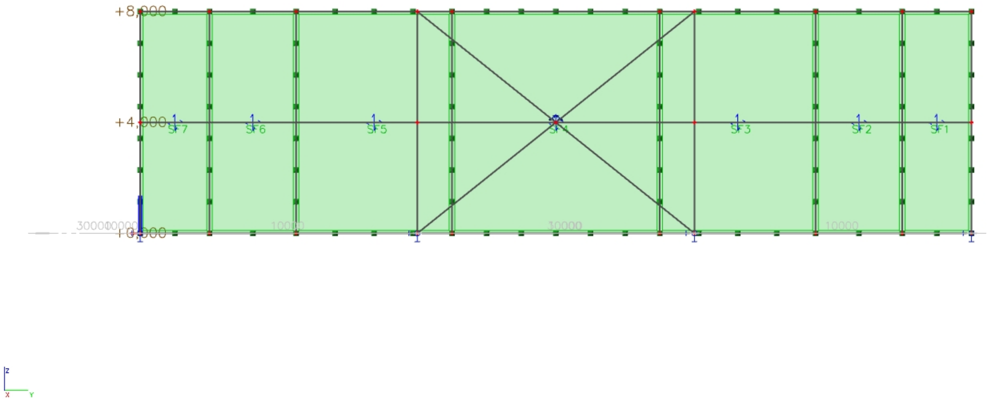
+8,000
+4,000
+0,000
SF7
SF6
SF5
SF4
SF3
SF2
SF1
10000
30000
10000
Z
X
Y

Figure C.2: Side view of the Case Study Building in the SCIA FEM, the green areas are the load panels on the building facade

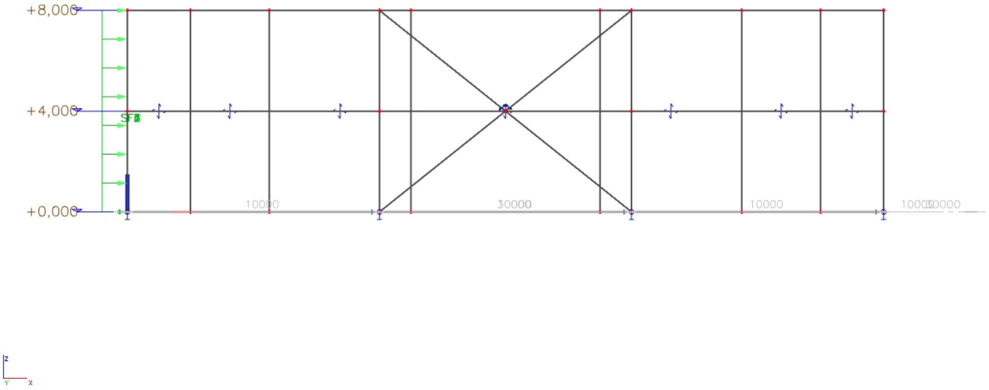
+8,000
+4,000
+0,000
SF8
10000
30000
10000
Z
Y
X

Figure C.3: Side view 2 of the Case Study Building in the SCIA FEM, wind load is shown on the left of the building

Name in SCIA FEM model	Element	Level	Profile	Grade
S42	External Beam	2	IPE240	S355
S18	External Beam	1	IPE450	S355
S13	Internal Column	-	HEA200	S355
S2	External Column	-	HEA220	S355
S1	Corner Column	-	HEA220	S355
S65	Bracing	-	Steel Rod ϕ = 45 mm	S355

Table C.1: Designation of various elements - used in the further analysis - in the FEM

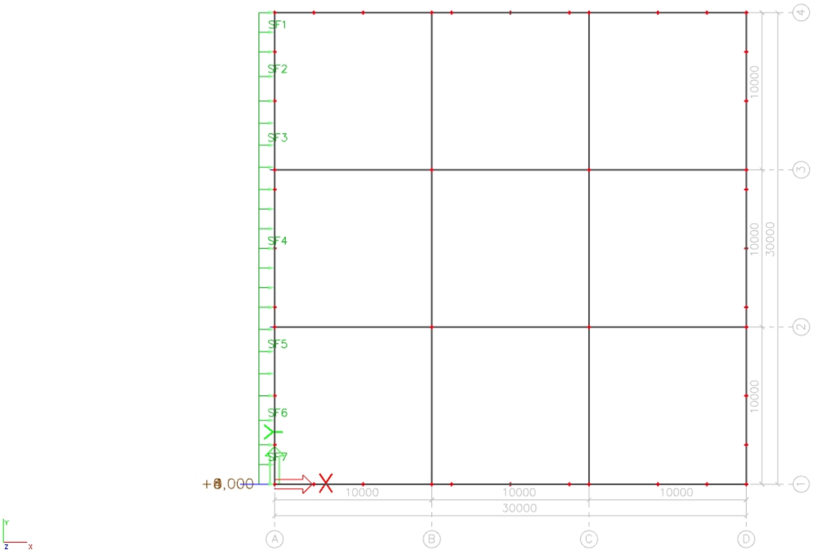
SF1
SF2
SF3
SF4
SF5
SF6
SF7
+8,000
10000
10000
10000
30000
10000
10000
10000
30000
A
B
C
D
1
2
3
4

Figure C.4: Top view of the Case Study Building in the SCIA FEM

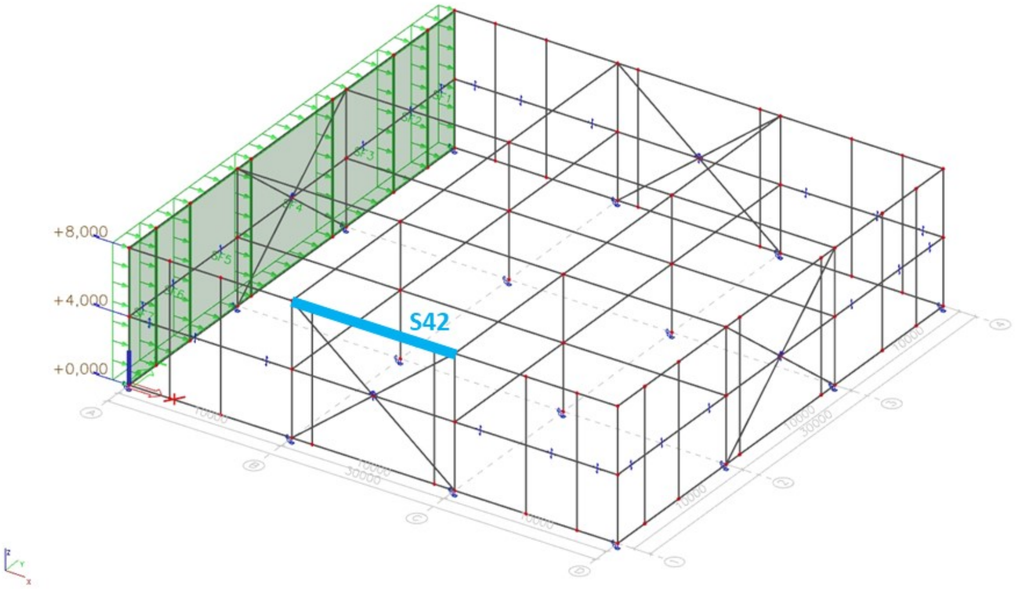
+8,000
+4,000
+0,000
S42
10000
30000
10000
10000
30000
10000
10000

Figure C.5: Element: S42, External Beam Level 2

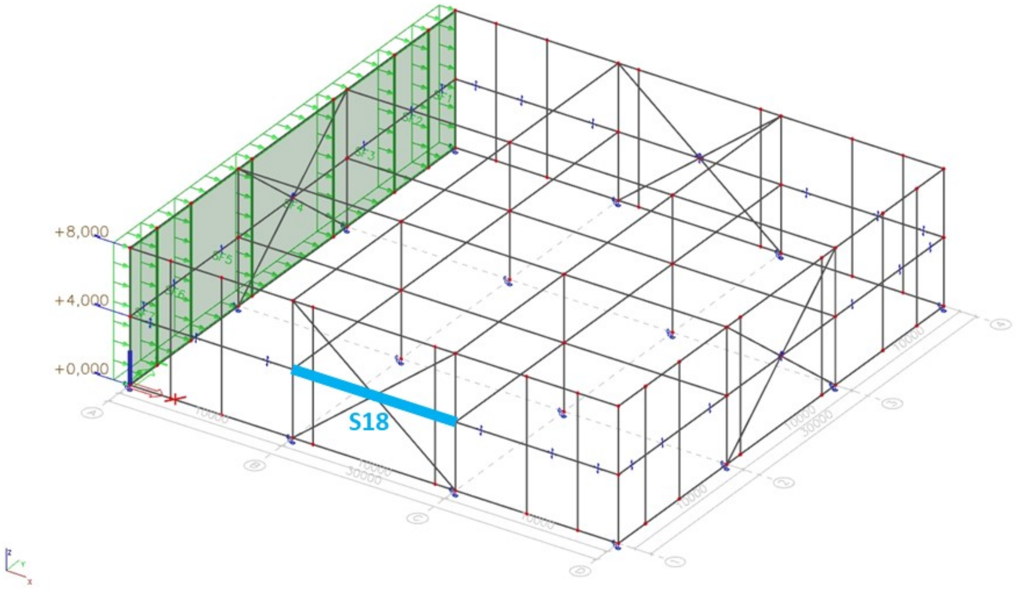
+8,000
+4,000
+0,000
S18
10000
30000
SF1
SF2
SF3
SF4
SF5
SF6

Figure C.6: Element: S18, External Beam Level 1

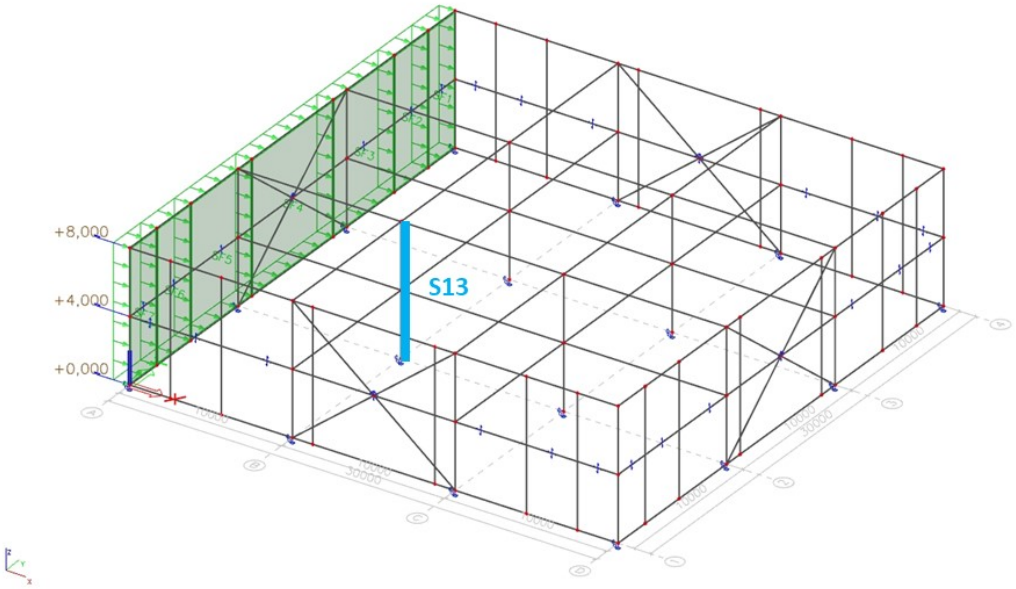
+8,000
+4,000
+0,000
S13
10000
30000
SF2
SF3
SF4
SF5
SF6

Figure C.7: Element: S13, Internal Column

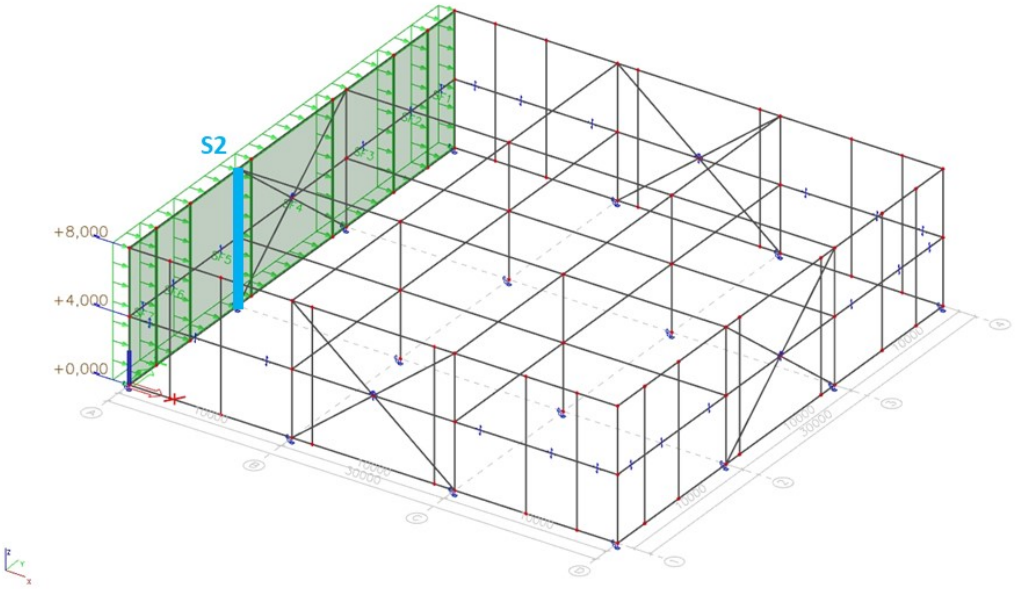
S2
+8,000
+4,000
+0,000
10000
30000

Figure C.8: Element: S2, External Column

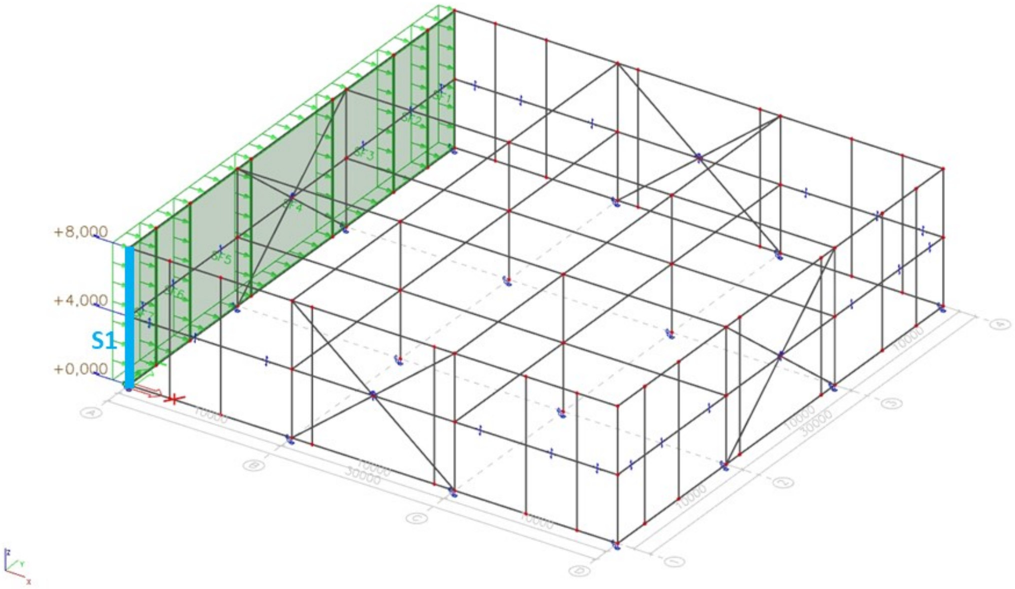
S1
+8,000
+4,000
+0,000
10000
30000

Figure C.9: Element: S1, Corner Column

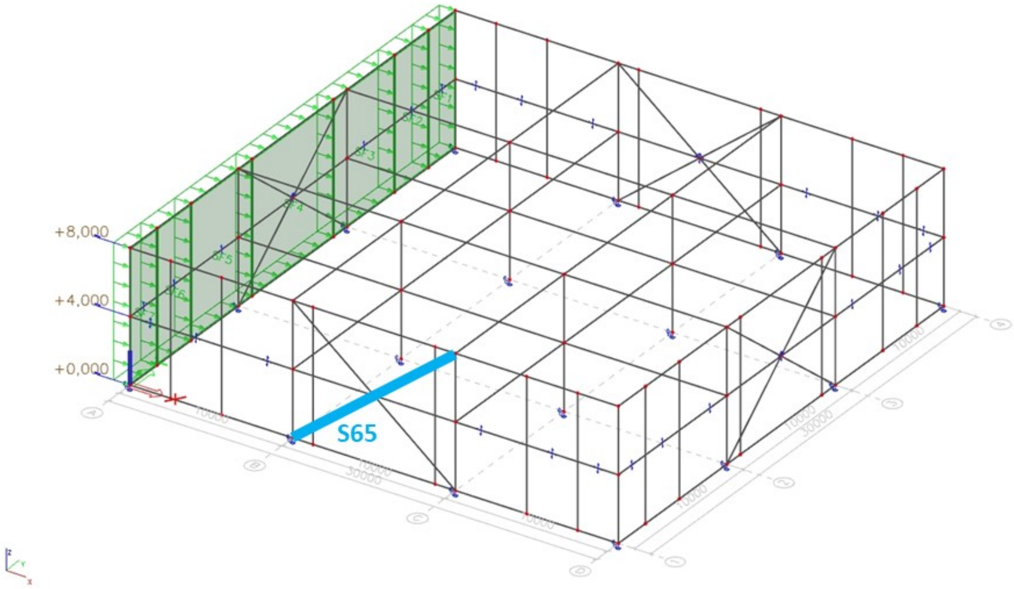
+8,000
+4,000
+0,000
S65
10000
30000

Figure C.10: Element: S65, Bracing

D

Resistance Model Uncertainties

Based on tables from the *'Probabilistic quantification of safety of a steel structure highlighting the potential of steel versus other materials'* [5] document. The tables provide statistical parameters such as the mean value $\overline{b}$ and standard deviation s_δ.

"Basis for these values are the background documentation to Eurocode 3 where test results are described and evaluated. In case of some tests results of different test evaluations are presented, once using the entire sample, and additionally differentiating in dependence on the steel grade of the specimen." [5]

document		5.01	5.01	5.01
		According to EC 3	**According to EC 3**	**According to EC 3**
		- members -	**- members -**	**- members -**
		Resistance moment of rolled class-1-beams (strong axis)	**Resistance moment of rolled class-1-beams (weak axis)**	**Axial resistance of rolled class-1-beams (weak axis)**
		Fe 360 and Fe 510	Fe 360 and Fe 510	Fe 360 and Fe 510
		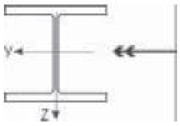 	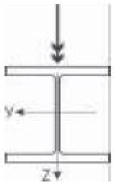 	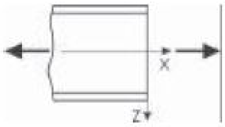
		$M_{pl,y} = W_{pl,y} \cdot f_y$	$M_{pl,z} = W_{pl,z} \cdot f_y$	$N_{pl} = A \cdot f_y$
all tests	$\bar{b}$	1,11 - 1,15 ***	1,14 - 1,17 (1,31*) ***	1,105 - 1,13 ***
	S_δ	0,045 - 0,059	0,06 - 0,08	0,05 - 0,054
subtests	variations	thickness and steel strength	thickness and steel strength	steel strength
	$\bar{b}$	1,07 - 1,21	1,09 - 1,2	1,08 - 1,2
	S_δ	0,033 - 0,076	0,059 - 0,08	0,041 - 0,054
comment			* Fe 510	
		*** (test Fe510 - test Fe360)	*** (test Fe510 - test Fe360)	*** (test Fe510 - test Fe360)

document		6.02	6.02/D.02	6.02
		According to EC 3	**According to EC 3**	**According to EC 3**
		- connections -	**- connections -**	**- connections -**
		Tensile failure in the thread of bolts	**Shear failure in the shank of bolts**	**Shear failure in the thread of bolts**
		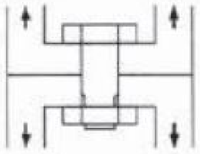	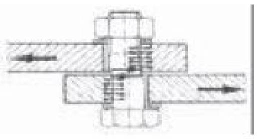	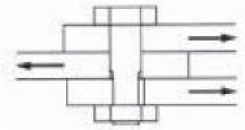
		$F_{ts} = 0,9 \cdot f_{ub} \cdot A_s$	$F_{vs} = 0,6 \cdot f_{ub} \cdot A$	$4.6,\ 5.6,\ 8.8: F_{vs} = 0,6 \cdot f_{ub} \cdot A_s$ $10.9: F_{vs} = 0,5\ f_{ub} \cdot A_s$
all tests	$\bar{b}$	1.098	1,107 - 1,116 ***	1.198
	S_δ	0.1	0,083 - 0,1 ***	0.124
subtests	variations	grades	grades, connection	grades
	$\bar{b}$	1,008 - 1,052 (1,176*)	0,982 - 1,16	1,126 - 1,242
	S_δ	0,042 - 0,06 (0,103*)	0,039 - 0,088	(0,012*) 0,076 - 0,137
comment		* grade 4.6		* grad 5.6
			***(test 6.02 - test D.02)	

document		6.02	6.02/D.02	6.02
		According to EC 3	**According to EC 3**	**According to EC 3**
		- connections -	**- connections -**	**- connections -**
		Combined shear and tensile failure of bolts	**Hole bearing failure at bolts (plates)**	**Hole bearing failure at bolts (angles)**
		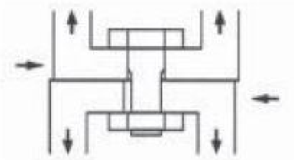	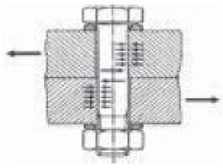	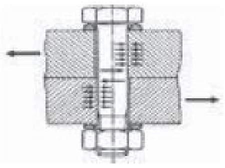
		$\frac{F_t}{1,4F_{ts}}+\frac{F_v}{F_{vs}}\le 1$	$F_{bs}=2,5\cdot\alpha\cdot f_u\cdot d\cdot t$	$F_{bs}=2,5\cdot\alpha\cdot f_u\cdot d\cdot t$
all tests	$\bar{b}$	1,296 - 1,33 ***	1,279 - 1,524 ***	1.18
	S_δ	0,118 - 0,123 ***	0,056 - 0,195 ***	0.128
subtests	variations	grades, angles, thread/shank	materials, connection	materials and number of bolts
	$\bar{b}$	1,141 - 1,455	1,295 - 1,561	1,051 - 1,341
	S_δ	0,009 - 0,148	0,016 - 0,201	0,06 - 0,135
comment				
		*** (test thread - test shank)	***(test 6.02 - test D.02)	

document		6.02/D.02	6.02	6.02
		According to EC 3	**According to EC 3**	**According to EC 3**
		- connections -	**- connections -**	**- connections -**
		Net section failure of bolted connections	**Net section failure of angles connected at one side with one bolt**	**Net section failure of angles connected at one side with two bolts**
		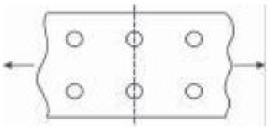	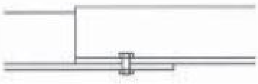	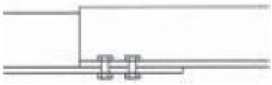
		$F_{ns}=0,9\cdot A_n\cdot f_u$	$F_{as}=2,0\cdot(e_2-0,5\cdot d)\cdot t\cdot f_u$	$F_{as}=\beta_2\cdot A_n\cdot f_u$
all tests	$\bar{b}$	1,105 - 1,232 ***	1.148	1.206
	S_δ	0,07 - 0,135 ***	0.095	0.147
subtests	variations	materials, connection, thickness	materials	materials
	$\bar{b}$	1,084 - 1,242	1,148 - 1,149	1,129 - 1,214
	S_δ	0,022 - 0,139	0,095 - 0,097	0,107 - 0,149
comment				
		***(test 6.02 - test D.02)		

document		6.02	D.03	D.03
		According to EC 3	**According to EC 3**	**According to EC 3**
		- connections -	**- connections -**	**- connections -**
		Net section failure of angles connected at one side with 3 or more bolts	**Resistance of welded connections**	**Resistance of welded connections**
			Stress component method	Mean stress method
		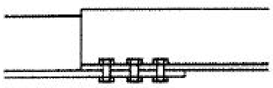	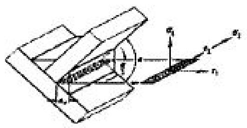	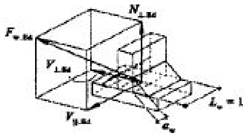 $F_{w,Rd}$ $N_{\perp,Rd}$ $V_{\perp,Rd}$ $V_{\parallel,Rd}$ $L_w = 1$ σ_w
		$F_{as} = \beta_3 \cdot A_n \cdot f_u$	$\sqrt{\sigma_{\parallel}^2 + 3\cdot\left(\tau_{\parallel}^2 + \tau_{\perp}^2\right)} \leq \frac{f_u}{\beta}$ $Fe235/355/460 : \beta = 0,8/0,9/1,0$	$\sigma_w \leq \frac{f_u}{\sqrt{3}\cdot\beta}$ $Fe235/355/460 : \beta = 0,8/0,9/1,0$
all tests	$\bar{b}$	1.343	(1,294*) 1,43 - 1,473	(1,427*) 1,544 - 1,56
	S_δ	0.136	(0,165*) 0,198 - 0,238	(0,195*) 0,252 - 0,286
subtests	variations	materials	strength, materials and welds	strength, materials and welds
	$\bar{b}$	1,327 - 1,352	(0,943 - 1,597)*	(1,048 - 1,956)*
	S_δ	0,118 - 0,145	(0,042 - 0,203)*	(0,047 - 0,203)*
comment			* for Fe460	* for Fe460

document		5.03 /5.03p	5.03 /5.03p	5.03
		According to EC 3	**According to EC 3**	**According to EC 3**
		- members -	**- members -**	**- members -**
		Lateral torsional buckling of rolled class- 1 3 -beams	**Lateral torsional buckling of welded class- 1-3 -beams**	**Interaction between monoaxial bending and compression of class- 1-3 -beams**
		$\alpha_{LT} = 0,21$	$\alpha_{LT} = 0,49$	
		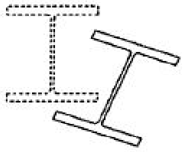	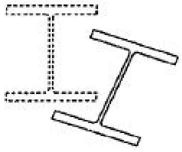	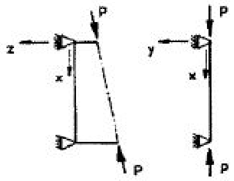
		$\chi_{LT} = \frac{1}{\phi_{LT} + \sqrt{\phi_{LT}^2 - \bar{\lambda}_{LT}^2}} \leq 1$ $\bar{\lambda}_{LT} = \sqrt{M_u / M_{cr,LT}}$ $M_{b,Rd} = \chi_{LT} \cdot M_u$	$\chi_{LT} = \frac{1}{\phi_{LT} + \sqrt{\phi_{LT}^2 - \bar{\lambda}_{LT}^2}} \leq 1$ $\bar{\lambda}_{LT} = \sqrt{M_u / M_{cr,LT}}$ $M_{b,Rd} = \chi_{LT} \cdot M_u$	$\frac{N}{\chi_z \cdot N_p} + \frac{M_y}{\chi_{LT} \cdot M_{p,y}} \cdot k_{LT} \leq 1$
all tests	$\bar{b}$	1,173 - 1,178	1,2108 - 1,22	1,3194 - 1,5159
	S_δ	0,0853 - 0,1055	0,1517 - 0,1612	0,1092 - 0,1482
subtests	variations	loading, λ_{LT}	λ_{LT}, k_d	different reports, profiles, β_m
	$\bar{b}$	1,036 - 1,257	1,055 - 1,399	1,4949 - 1,6102
	S_δ	0,0742 - 0,117	0,0653 - 0,1342	0,0808 - 0,1468
comment				

document		5.03	5.07	5.07
		According to EC 3	**According to EC 3**	**According to EC 3**
		- members -	**- connections -**	**- connections -**
		Interaction between biaxial bending and compression of class- 1-3 -beams	**Axial resistance of welded T- and Y- joints (class 1) between circular hollow sections**	**Axial resistance of welded X- joints between circular hollow sections**
			Within the validity range	Within the validity range
		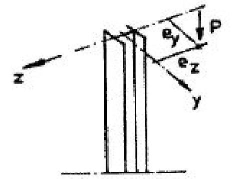	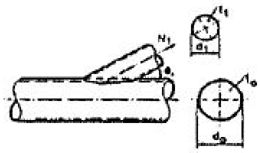	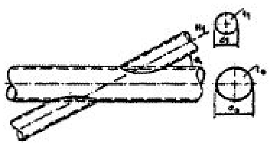
		$\frac{N}{\chi_z \cdot N_p}+\frac{M_y \cdot k_{LT}}{\chi_{LT} \cdot M_{p,y}}+\frac{M_z \cdot k_z}{M_{p,z}} \leq 1$	$N_{k1}=\frac{\gamma^{0,2} \cdot k_p \cdot f_{y0} \cdot t_0{}^2}{\sin \Theta_1} \cdot\left(2,8+14,2 \cdot \beta^2\right)$	$N_{k1}=\frac{k_p \cdot f_{y0} \cdot t_0{}^2}{\sin \Theta_1} \cdot \frac{5,2}{1-0,81 \cdot \beta}$
all tests	$\bar{b}$	1,2824 - 1,3163 (1,5833*)	1.02	1.018
	s_δ	0,1184 - 0,1246 (0,1648*)	0.052	0.078
subtests	variations	different reports, profiles		
	$\bar{b}$	1,1774 - 1,4484		
	s_δ	0,0718 - 0,1246		
comment		* tests of Matthey		

document		5.07	5.07	5.07
		According to EC 3	**According to EC 3**	**According to EC 3**
		- connections -	**- connections -**	**- connections -**
		Axial resistance of welded K- and N- joints (gap) between circular hollow sections	**Axial resistance of welded K- and N- joints (overlap) between circular hollow sections**	**Axial resistance of welded T-, Y-, X- joints between square hollow section brace and chord; evaluation according to Gauss-paper**
		Within the validity range	Within the validity range	Within the validity range
		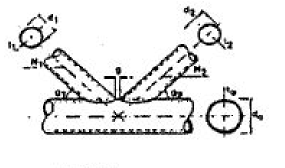 d 1 t 1 d 2 t 2 N 1 N 2 g θ 1 θ 2 t o d o	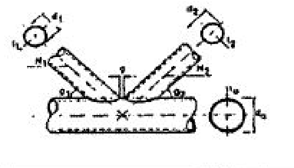 d 1 t 1 d 2 t 2 N 1 N 2 g θ 1 θ 2 t o d o	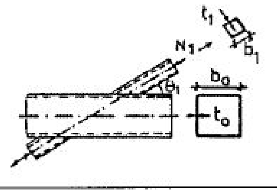
		$N_{k1}=\frac{k_g \cdot k_p \cdot f_{y0} \cdot t_0{}^2}{\sin \Theta_1} \cdot\left(1,8+10,2 \cdot \frac{d_1}{d_0}\right)$	$N_{k1}=\frac{k_g \cdot k_p \cdot f_{y0} \cdot t_0{}^2}{\sin \Theta_1} \cdot\left(1,8+10,2 \cdot \frac{d_1}{d_0}\right)$	$N_k=\frac{k_n \cdot f_{y0} \cdot t_0{}^2}{(1-\beta) \cdot \sin \Theta_1} \cdot\left(\frac{2 \beta}{\sin \Theta_1}+4 \cdot(1-\beta)^{0,5}\right)$
all tests	$\bar{b}$	1.091	1.169	1.225
	s_δ	0.103	0.114	0.04
subtests	variations			
	$\bar{b}$			
	s_δ			
comment				

document		5.07	5.07	5.07
		According to EC 3	**According to EC 3**	**According to EC 3**
		- connections -	**- connections -**	**- connections -**
		Axial resistance of welded K- and N- joints (gap) between square hollow section brace and chord; evaluation according to Gauss-paper	**Axial resistance of welded K- and N- joints (gap) between SHS brace and chord; evaluation according to Gauss-paper; β = 0,35-0,45 and 0,55-0,65**	**Axial resistance of welded K- and N- joints (gap) between square hollow section brace and chord; β = 0,85 - 1,0**
		Within the validity range	Within the validity range	Within the validity range
		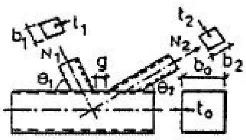	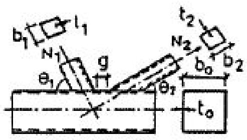	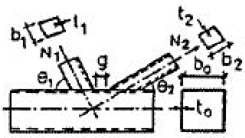
		$N_k = \frac{8{,}9 \cdot \gamma^{0,5} \cdot k_n \cdot f_{y0} \cdot t_0^2}{\sin \Theta_1} \cdot \left(\frac{b_1 + b_0}{2b_0}\right)$	$N_k = \frac{8{,}9 \cdot \gamma^{0,5} \cdot k_n \cdot f_{y0} \cdot t_0^2}{\sin \Theta_1} \cdot \left(\frac{b_1 + b_0}{2b_0}\right)$	$N_k = \frac{8{,}9 \cdot \gamma^{0,5} \cdot k_n \cdot f_{y0} \cdot t_0^2}{\sin \Theta_1} \cdot \left(\frac{b_1 + b_0}{2b_0}\right)$
all tests	$\bar{b}$	0.9	0.955	1.003
	S_δ	0.025	0.043	0.072
subtests	variations			
	$\bar{b}$			
	S_δ			
comment				

document		5.07	5.07	5.07
		According to EC 3	**According to EC 3**	**According to EC 3**
		- connections -	**- connections -**	**- connections -**
		Axial resistance of welded K- and N- joints (overlap < 50%) between square hollow section brace and chord; evaluation according to Gauss-paper	**Resistance of welded T-, Y- and X- joints between RHS brace member and I-section chord; evaluation according to Gauss-paper**	**Resistance of welded K- and N- joints (gap) between RHS brace member and I-section chord; evaluation according to Gauss-paper**
		Within the validity range	Chord web yielding	Chord shear failure
		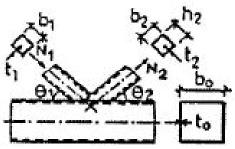	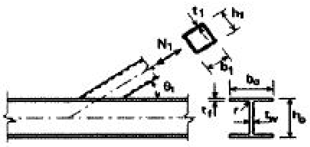	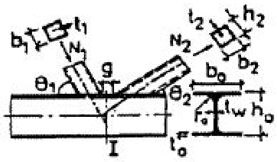
		$N_k = f_{yk} \cdot t_i \cdot \left(\frac{\lambda_{ov}}{50} \cdot (2h_i - 4t_i) + b_e + b_{e(ov)}\right)$	$N_k = \frac{f_y \cdot t_w \cdot b_w}{\sin \Theta}$	$N_k = \frac{f_y \cdot A_V}{\sqrt{3} \cdot \sin \Theta}$
all tests	$\bar{b}$	1.1	0.989	1.175
	S_δ	0.032	0.032	0.075
subtests	variations			
	$\bar{b}$			
	S_δ			
comment				

document		5.07	5.07	5.07
		According to EC 3	According to EC 3	According to EC 3
		- connections -	- connections -	- connections -
		Resistance moment of welded T-, X- and Y-joints between circular hollow section chords	**Resistance moment of welded T-, X- and Y-joints between circular hollow section chords**	**Axial resistance of welded X- joints connecting gusset plate to circular hollow section member**
		Bending in-plane	Bending out-of-plane	
		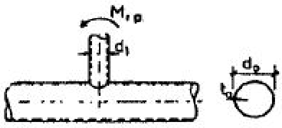	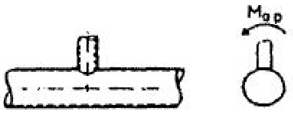	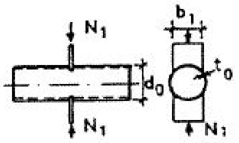
		$M_{ip} = 4,85 \frac{f_{yo} \cdot t_0^2 \cdot d_1}{\sin\theta_1} \sqrt{\gamma} \cdot \beta \cdot k_p$	$M_{op} = \frac{f_{yo} \cdot t_0^2 \cdot d_1}{\sin\theta_1} \cdot \frac{2,7 \cdot k_p}{1-0,81\beta}$	$N_i = \frac{5k_p \cdot f_{y0} \cdot t_0^2}{1-0,81\beta}$
all tests	$\bar{b}$	1,025 -1,05 (1,325*)	1,141 - 1,225	1.118
	s_δ	0,02 - 0,143	0,059 - 0,09	0.043
subtests	variations	reports	reports	
	$\bar{b}$			
	s_δ			
comment		* report from Gibstein		

document		5.07	5.07	5.07
		According to EC 3	According to EC 3	According to EC 3
		- connections -	- connections -	- connections -
		Axial resistance of welded X- joints connecting gusset plate to circular hollow section member	**Axial resistance of welded X- joints connecting gusset plate to circular hollow section member**	**Axial resistance of welded X- joints connecting gusset plate to circular hollow section member**
		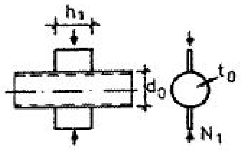	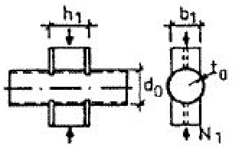	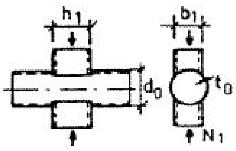
		$N_i = 5k_p \cdot f_{y0} \cdot t_0^2 (1+0,25\eta)$	$N_i = \frac{5k_p \cdot f_{y0} \cdot t_0^2}{1-0,81\beta} (1+0,25\eta)$	$N_i = \frac{5k_p \cdot f_{y0} \cdot t_0^2}{1-0,81\beta} (1+0,25\eta)$
all tests	$\bar{b}$	1.295	1.146	1.125
	s_δ	0.087	0.056	0.033
subtests	variations			
	$\bar{b}$			
	s_δ			
comment				

document		5.07	5.07	5.07
		According to EC 3	**According to EC 3**	**According to EC 3**
		- connections -	**- connections -**	**- connections -**
		Axial resistance of welded T- joints connecting gusset plate to circular hollow section member	**Axial resistance of welded T- joints connecting gusset plate to circular hollow section member**	**Resistance moment of welded T- and X- joints between rectangular hollow section brace member and chord**
				In-plane bending; β ≤ 0,8
		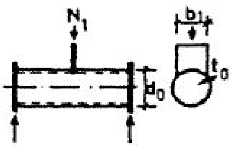	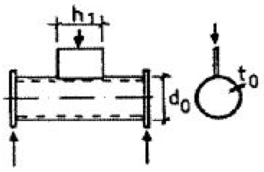	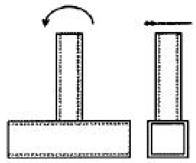
		$N_i = k_p \cdot f_{y0} \cdot t_0^2 \left(4+20\beta^2\right)$	$N_i = 5k_p \cdot f_{y0} \cdot t_0^2 \left(1+0,25\eta\right)$	$M_{ip} = k_n \cdot f_{y0} \cdot t_0^2 \cdot h_1 \cdot \left(\frac{1}{2\eta}+\frac{2}{\sqrt{1-\beta}}+\frac{\eta}{1-\beta}\right)$
all tests	$\bar{b}$	1.11	1.12	1,11 - 1,15 ***
	S_δ	0.048	0.033	0.025
subtests	variations			*** RHS - SHS
	$\bar{b}$			
	S_δ			
comment				

document		5.07	5.04	5.04
		According to EC 3	**According to EC 3**	**According to EC 3**
		- connections -	**- members -**	**- members -**
		Resistance moment of welded T- and X- joints between rectangular hollow section brace member and chord	**Centrally compressed class-4- C-members**	**Centrally compressed class-4- C-members**
		In-plane bending; β ≥ 0,8	Fe 235	Fe 355
		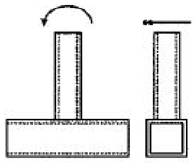	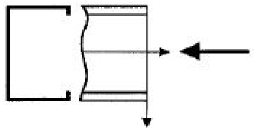	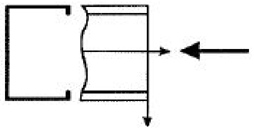
		$M_{ip} = 0,5 f_{y0} \cdot t_0 \left(h_1+5t_0\right)^2$	$N_c = \chi \cdot A_{eff} \cdot f_{yb}$	$N_c = \chi \cdot A_{eff} \cdot f_{yb}$
all tests	$\bar{b}$	1,11 - 1,2 ***	1.313	1,138 - 1,166 (1,411*)
	S_δ	0,015 - 0,025	0.075	0,0722 - 0,1522 (0,767**)
subtests	variations	*** RHS - SHS		λ
	$\bar{b}$			* Fe355, 0,9<λ<1, 2
	S_δ			** Fe355, 0,6<λ<0 9
comment				

document		5.04	5.04	5.04
		According to EC 3	**According to EC 3**	**According to EC 3**
		- members -	**- members -**	**- members -**
		Centrally compressed class-4-hollow-members	**Interaktion between major axis bending and compression of class-4-C-profiles; all Q-values**	**Interaktion between major axis bending and compression of class-4-C-profiles; all Q-values**
		Fe 355		With lateral torsional buckling
		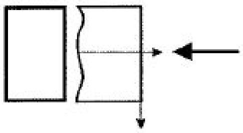	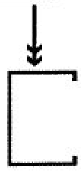	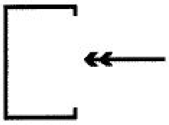
		$N_c = \chi \cdot A_{eff} \cdot f_{yb}$	$\frac{N}{\chi_z \cdot N_d} + \frac{M_z}{M_{d,z}} \cdot k_z \le 1$	$\frac{N}{\chi_z \cdot N_d} + \frac{M_y}{\chi_D \cdot M_{d,y}} \cdot k_{yD} \le 1$
all tests	$\bar{b}$	1,2121 - 1,4274	1.252	1.308
	s_δ	0,1126 - 0,1559	0.1386	0.1076
subtests	variations	λ		
	$\bar{b}$			
	s_δ			
comment				

document		5.04	5.04	A.01
		According to EC 3	**According to EC 3**	**According to EC 3**
		- members -	**- members -**	**- connections -**
		Interaktion between major axis bending and compression of class-4-C-profiles; all Q-values	**Interaktion between biaxial bending and compression of class-4-C-profiles; all Q-values**	**Bearing resistance of screwed connections in thin-walled sheetings and members**
		Without lateral torsional buckling		Inclination failure
		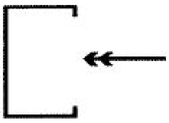	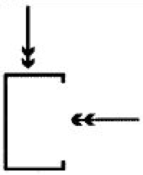	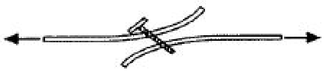
		$\frac{N}{\chi_z \cdot N_d} + \frac{M_y}{M_{d,y}} \cdot k_y \le 1$	$\frac{N}{\chi_z \cdot N_c} + \frac{M_y}{\chi_D \cdot M_c} \cdot k_{yD} + \frac{M_z}{M_{d,z}} \cdot k_z \le 1$	$F_b = \alpha \cdot f_u \cdot d_n \cdot t$
all tests	$\bar{b}$	1.255	1.428	(1,074*) 1,309 - 1,705
	s_δ	0.0932	0.1376	0,118 - 0,247
subtests	variations			different reports
	$\bar{b}$			
	s_δ			
comment				* report Hannover 4

document		A.01	A.01	A.01
		According to EC 3	According to EC 3	According to EC 3
		- connections -	- connections -	- connections -
		Bearing resistance of screwed connections in thin-walled sheetings and members	**Net-section resistance of screwed connections in thin-walled sheetings and members**	**Pull-through resistance of screwed connections in thin-walled sheetings and members**
		Hole Bearing failure		
		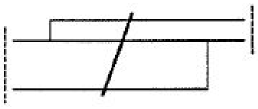	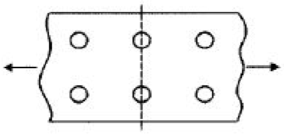	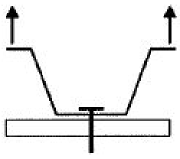
		$F_b = \alpha \cdot f_u \cdot d_n \cdot t$	$F_n = f_u \cdot A_{netto}$	$F_p = f_u \cdot t \cdot d_w$
all tests	$\bar{b}$	1,309 - 1,877	1.031	0,998 - 1,924
	s_δ	0,074 - 0,244	0.046	0,032 - 0,207
subtests	variations	different reports	different reports	different reports
	$\bar{b}$			
	s_δ			
comment				

document		A.01	A.01	A.01
		According to EC 3	According to EC 3	According to EC 3
		- connections -	- connections -	- connections -
		Pull-out resistance of screwed connections in thin-walled sheetings and members	**Bearing resistance of rivet-connections in thin-walled sheetings and members**	**Pull-through resistance of connections with cartridge fired pins in thin-walled sheetings and members**
		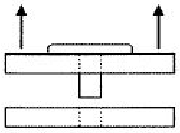	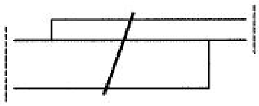	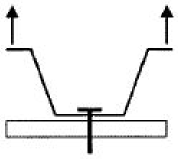
		$F_p = 0,65 \cdot f_u \cdot t_1 \cdot d_n$	$F_b = \alpha \cdot f_u \cdot t \cdot d_n$	$F_p = d_w \cdot t \cdot f_u$
all tests	$\bar{b}$	0,982 - 2,62	1,08 - 1,487	1,139 - 1,528
	s_δ	0,009 - 0,235	0,061 - 0,157	0,121 - 0,196
subtests	variations	different reports	different reports	different reports
	$\bar{b}$			
	s_δ			
comment				

document		A.01	A.01	A.01
		According to EC 3	**According to EC 3**	**According to EC 3**
		- connections -	**- connections -**	**- connections -**
		Pull-out resistance of connections with cartridge fired pins in thin-walled sheetings and members	**Pull-out resistance of connections with cartridge fired pins in thin-walled sheetings and members**	**Bearing resistance of bolted connections in thin-walled sheetings and members**
		t1 < tp	t1 > tp	
		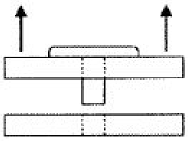	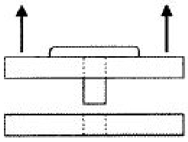	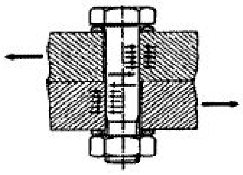
		$F_o = 0{,}65 \cdot d_n \cdot t' \cdot f_u$	$F_o = 0{,}65 \cdot d_n \cdot t' \cdot f_u$	$F_b = 2{,}5 \cdot \alpha \cdot t \cdot d_n \cdot f_u$
all tests	$\bar{b}$	1,108 - 1,996	1,206 - 2,138	1,182 - 1,577
	S_δ	0,103 - 0,179	0,101 - 0,184	0,116 - 0,195
subtests	variations	different reports	different reports	different reports
	$\bar{b}$			
	S_δ			
comment				

document		A.01	5.05	
		According to EC 3	**According to EC 3**	
		- connections -	**- members -**	
		Net-section resistance of bolted connections in thin-walled sheetings and members	**Thin-walled plate girders; local buckling of the compression flange; bending capacities M_u**	
		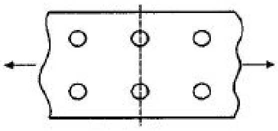	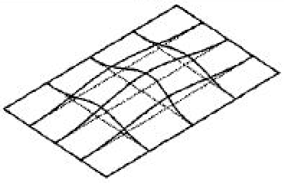	
		$F_n = A_n \cdot f_n$ $f_n = \left(1 - 0{,}9r + 3r \cdot \frac{d}{u}\right) \cdot f_u$	$\rho = 1 \;\; for \;\; \bar{\lambda}_p \leq 0{,}673$ $\rho = \frac{1 - \frac{0{,}22}{\bar{\lambda}_p}}{\bar{\lambda}_p} \;\; for \;\; \bar{\lambda}_p > 0{,}673$	
all tests	$\bar{b}$	1.168	1.106	
	S_δ	0.203	0.062	
subtests	variations	different reports		
	$\bar{b}$	1,065 - 1,14 (1,604*)		
	S_δ	0,063 - 0,148 (0,35*)		
comment		* report Braunschweig 23		

E

Tolerances on construction building - NEN-EN 1090-2 [12]

B.3 Erection tolerances

Table B.15 — Erection tolerances - Buildings

No	Criterion	Parameter	Functional tolerances [a] Permitted deviation Δ	
			Class 1	**Class 2**
1	Height: 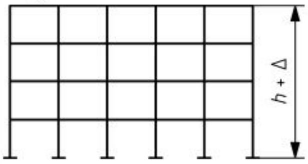	Overall height, relative to the base level: $h \leq 20$ m 20 m < h < 100 m $h \geq 100$ m	 Δ = ± 20 mm Δ = ± 0,5 (h+20) mm Δ = ± 0,2 (h+200) mm [h in metres]	 Δ = ± 10 mm Δ = ± 0,25(h+20) mm Δ = ± 0,1 (h+200) mm [h in metres]
2	Storey height: 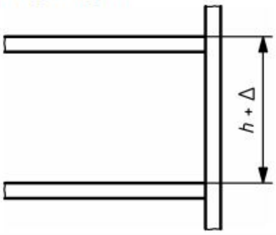	Height relative to the adjacent levels:	Δ = ± 10 mm	Δ = ± 5 mm

No	Criterion	Parameter	Functional tolerances [a] Permitted deviation Δ	
			Class 1	**Class 2**
3	Slope: 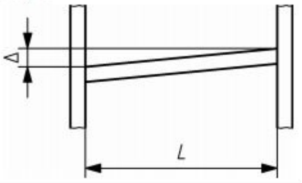	Height relative to the other end of a beam:	$\Delta = \pm L/500$ but $\lvert\Delta\rvert \le 10$ mm	$\Delta = \pm L/1000$ but $\lvert\Delta\rvert \le 5$ mm
4	Column slice 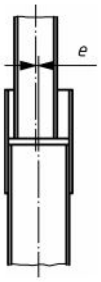	Non-intended eccentricity *e* about either axis:	5 mm	3 mm
5	Column base: 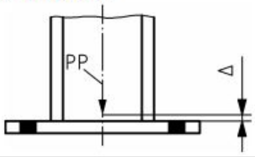	Level of bottom of column shaft, relative to specified level of its position point (PP):	$\Delta = \pm 5$ mm	$\Delta = \pm 5$ mm
6	Relative levels: 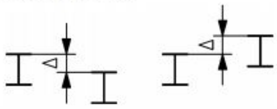	Levels of adjacent beams, measured at corresponding ends:	$\Delta = \pm 10$ mm	$\Delta = \pm 5$ mm
7	Connection levels: 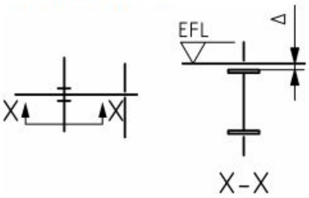	Level of the beam at a beam-to-column connection, measured relative to the established floor level (EFL):	$\Delta = \pm 10$ mm	$\Delta = \pm 5$ mm

[a] No essential tolerance specified

Table B.16 — Erection tolerances - Beams in buildings

No	Criterion	Parameter	Functional tolerances [a] Permitted deviation Δ	
			Class 1	**Class 2**
1	Spacing between beam centrelines: 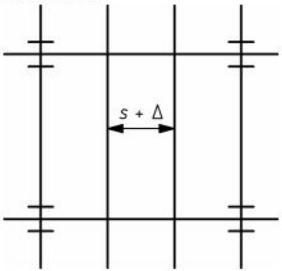	Deviation Δ from intended distance (s) between adjacent erected beams, measured at each end:	Δ = ± 10 mm	Δ = ± 5 mm
2	Location at columns: 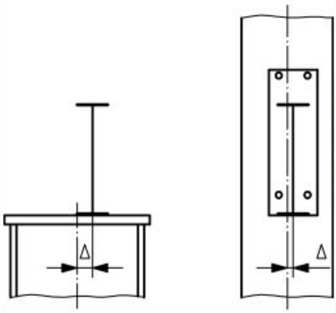	Deviation Δ from intended location of a beam-to-column connection, measured relative to the column:	Δ = ± 5 mm	Δ = ± 3 mm
3	Straightness in plan: 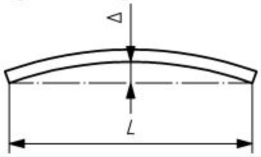	Deviation Δ from straightness of an erected beam or cantilever of length L:	Δ = ± L /500	Δ = ± L /1000
4	Camber: 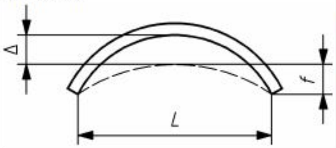	Deviation Δ at mid span from intended camber f of an erected beam or lattice component of length L:	Δ = ± L /300	Δ = ± L /500
5	Pre-set of cantilever: 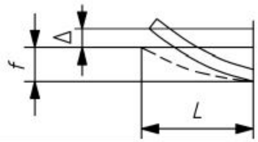	Deviation Δ from intended pre-set at end of an erected cantilever of length L:	Δ = ± L /200	Δ = ± L /300

[a] No essential tolerance specified

Table B.17 — Erection tolerances - Columns of single storey buildings

No	Criterion	Parameter	Essential tolerances Permitted deviation Δ	Functional tolerances Permitted deviation Δ	
			Class 1 and 2	Class 1	Class 2
1	Inclination of columns of single-storey buildings: 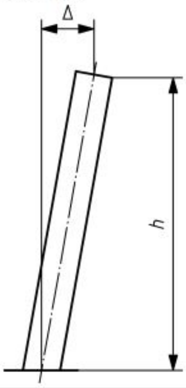	Overall inclination in storey height h:	$\Delta = \pm h/300$	$\Delta = \pm h/300$	$\Delta = \pm h/500$
2	Inclination of individual columns in single storey portal frame buildings: 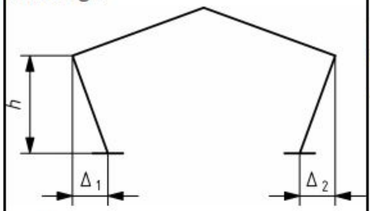	Inclination Δ of each column: $\Delta = \Delta_1$ or Δ_2	No requirement	$\Delta = \pm h/150$	$\Delta = \pm h/300$
3	Inclination of single storey portal frame buildings: 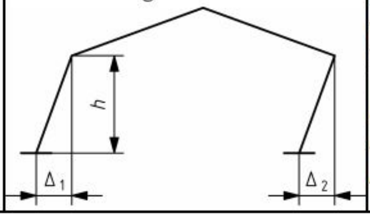	Average inclination of all the columns in the same frame: [For two columns the average is: $\Delta = (\Delta_1 + \Delta_2)/2$]	$\Delta = \pm h/500$	$\Delta = \pm h/500$	$\Delta = \pm h/500$

No	Criterion	Parameter	Essential tolerances Permitted deviation Δ	Functional tolerances Permitted deviation Δ	
			Class 1 and 2	Class 1	Class 2
4	Inclination of any column that supports a crane gantry: 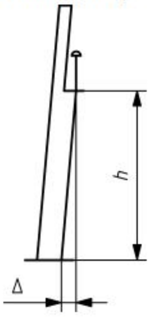	Inclination from floor level to bearing of crane beam:	$\Delta = \pm h/1000$	$\Delta = \pm 25$ mm	$\Delta = \pm 15$ mm
5	Straightness of a single storey column: 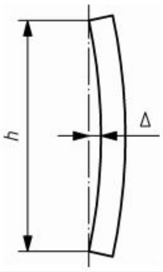	Location of the column in plan, relative to a straight line between position points at top and bottom:	$\Delta = \pm h/1000$	No requirement	No requirement

Table B.18 — Erection tolerances - Multi-storey buildings

No	Criterion	Parameter	Essential tolerances Permitted deviation Δ	Functional tolerances Permitted deviation Δ	
			Class 1 and 2	Class 1	Class 2
1	Location at the storey level n levels above the base, relative to that at the base: 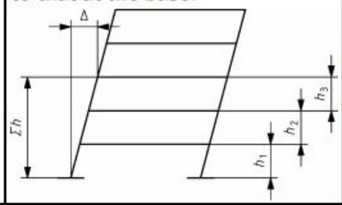	Location of the column in plan, relative to a vertical line through its centre at base level:	$\Delta = \pm \Sigma h/(300\sqrt{n})$	$\Delta = \pm \Sigma h/(300\sqrt{n})$	$\Delta = \pm \Sigma h/(500\sqrt{n})$
2	Inclination of a column, between adjacent storey levels: 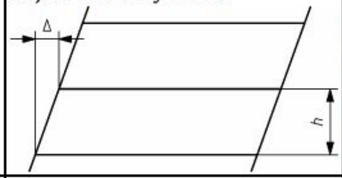	Location of the column in plan, relative to a vertical line through its centre at the next lower level:	$\Delta = \pm h/300$	$\Delta = \pm h/300$	$\Delta = \pm h/500$
3	Straightness of a continuous column between adjacent storey levels: 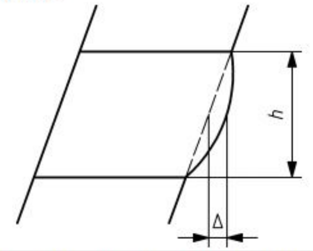	Location of the column in plan, relative to a straight line between position points at adjacent storey levels:	$\Delta = \pm h/1000$	$\Delta = \pm h/1000$	$\Delta = \pm h/1000$
4	Straightness of a spliced column, between adjacent storey levels: 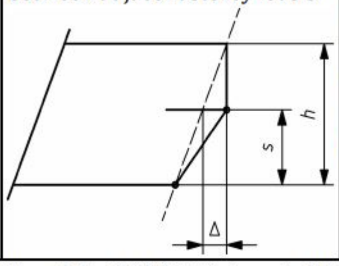	Location of the column in plan at the splice, relative to a straight line between position points at adjacent storey levels:	$\Delta = \pm s/1000$ with $s \leq h/2$	$\Delta = \pm s/1000$ with $s \leq h/2$	$\Delta = \pm s/1000$ with $s \leq h/2$

NOTE Table B.18 "Multi-storey buildings" applies to columns that are continuous over more than one storey. Table B.17 applies to storey-height columns in multi-storey buildings.

Table B.19 — Erection tolerances - Full contact end bearing

No	Criterion	Parameter	Essential tolerances Permitted deviation Δ	Functional tolerances Permitted deviation Δ
			Class 1 and 2	**Class 1 and 2**
1	Local angular misalignment Δθ occurring at the same time as gap Δ at point "X": 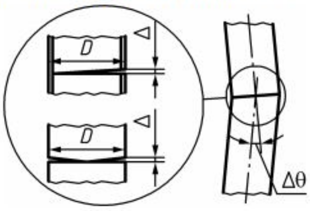 		$\Delta\theta = \pm 1/500$ and Δ = 0,5 mm over at least two thirds of the area, and Δ = 1,0 mm maximum locally	No requirement

Table B.20 — Erection tolerances - Positions of columns

No	Criterion	Parameter	Functional tolerances [a] Permitted deviation Δ	
			Class 1	Class 2
1	Location: 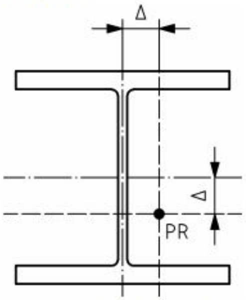	Location in plan of the centre of the column at the level of its base, relative to the position point of reference (PR):	Δ = ± 10 mm	Δ = ± 5 mm
2	Overall length of a building: 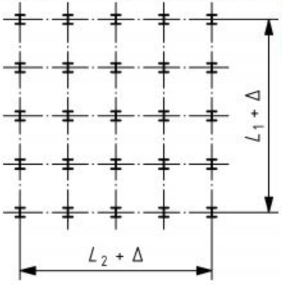	Distance between end columns in each line, at base level: $L \leq 30$ m 30 m < L < 250 m $L \geq 250$ m	Δ = ± 20 mm Δ = ± 0,25 (L+50) mm Δ = ± 0,1 (L+500) mm [L in metres]	Δ = ± 16 mm Δ = ± 0,2 (L+50) mm Δ = ± 0,1 (L+350) mm [L in metres]
3	Column spacing: 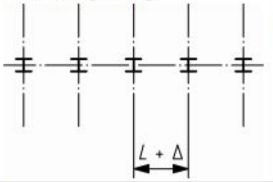	Distance between centres of adjacent columns at base level: $L \leq 5$ m $L > 5$ m	Δ = ± 10 mm Δ = ± 0,2 (L+45) mm [L in metres]	Δ = ± 7 mm Δ = ± 0,2 (L+30) mm [L in metres]
4	Column alignment generally: 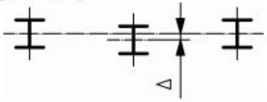	Location of the centre of the column at base level, relative to the established column line (ECL):	Δ = ± 10 mm	Δ = ± 7 mm
5	Perimeter column alignment: 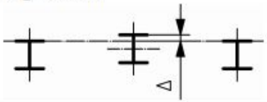	Location of the outer face of a perimeter column at base level, relative to the line joining the faces of the adjacent columns:	Δ = ± 10 mm	Δ = ± 7 mm

[a] No essential tolerance specified

F

Assessment Procedure: la Gasse and Meinen

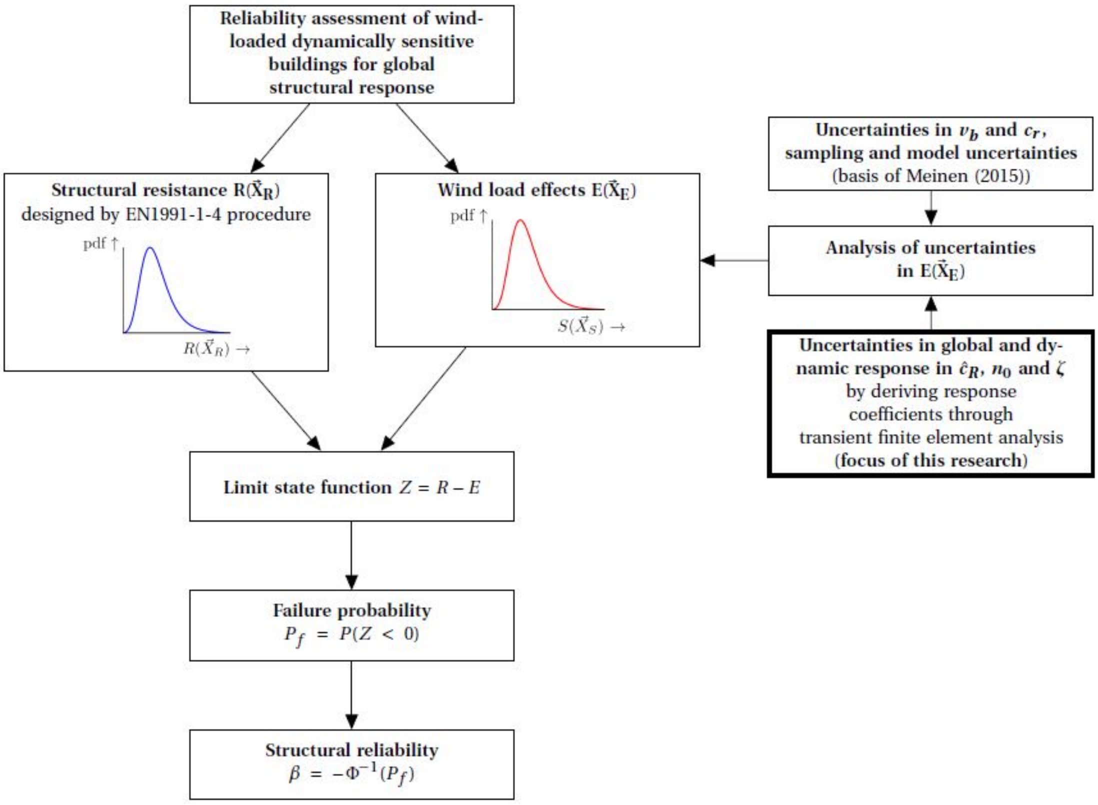
Reliability assessment of wind-loaded dynamically sensitive buildings for global structural response
Structural resistance R($\vec{X}_R$) designed by EN1991-1-4 procedure
pdf ↑
$R(\vec{X}_R)$ →
Wind load effects E($\vec{X}_E$)
pdf ↑
$S(\vec{X}_S)$ →
Uncertainties in v_b and c_r, sampling and model uncertainties (basis of Meinen (2015))
Analysis of uncertainties in E($\vec{X}_E$)
Uncertainties in global and dynamic response in $\hat{c}_R$, n_0 and ζ by deriving response coefficients through transient finite element analysis (focus of this research)
Limit state function $Z = R - E$
Failure probability $P_f = P(Z < 0)$
Structural reliability $\beta = -\Phi^{-1}(P_f)$

Figure F.1: Assessment procedure by la Gasse [23]

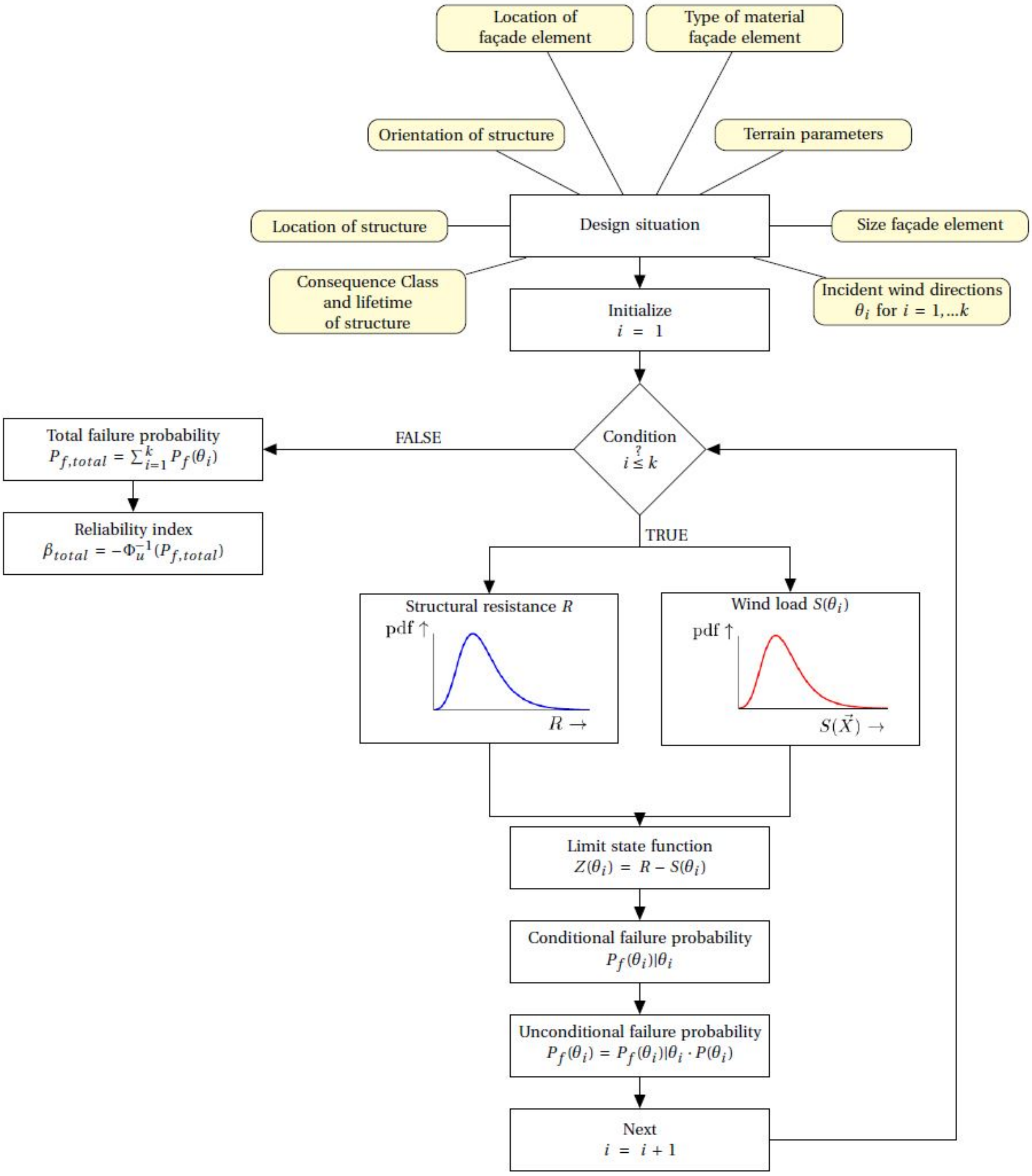
Location of façade element
Type of material façade element
Orientation of structure
Terrain parameters
Location of structure
Design situation
Size façade element
Consequence Class and lifetime of structure
Initialize $i = 1$
Incident wind directions θ_i for $i = 1,...k$
Total failure probability $P_{f,total} = \sum_{i=1}^{k} P_f(\theta_i)$
FALSE
Condition $i \overset{?}{\leq} k$
Reliability index $\beta_{total} = -\Phi_u^{-1}(P_{f,total})$
TRUE
Structural resistance R
pdf ↑
$R \rightarrow$
Wind load $S(\theta_i)$
pdf ↑
$S(\vec{X}) \rightarrow$
Limit state function $Z(\theta_i) = R - S(\theta_i)$
Conditional failure probability $P_f(\theta_i)|\theta_i$
Unconditional failure probability $P_f(\theta_i) = P_f(\theta_i)|\theta_i \cdot P(\theta_i)$
Next $i = i + 1$

Figure F.2: Assessment procedure by Meinen [25]

G

Extra Figures - Description Load Effects

G.1. External beam level 2 (S42)

G.1.1. $E_{wind,M}$

Load effects - Time series

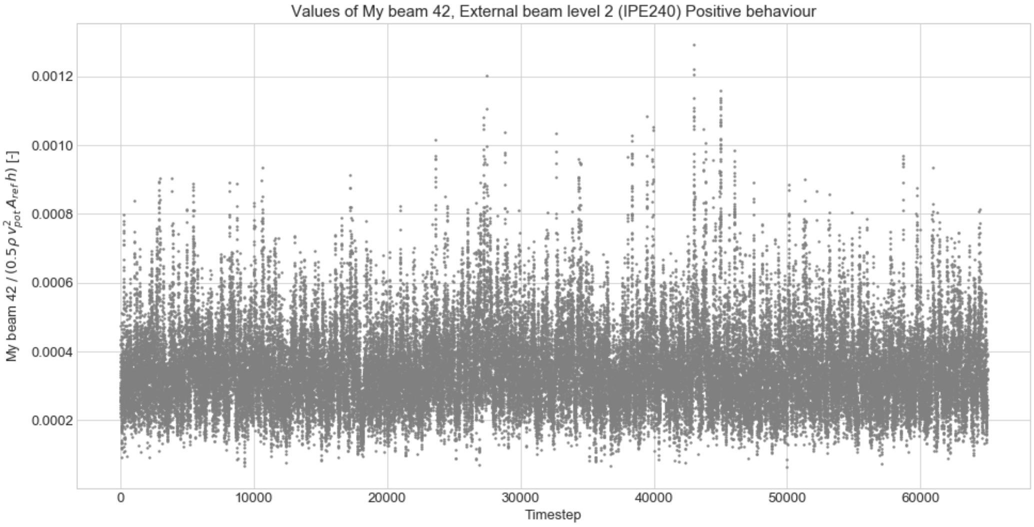

Figure G.1: All the load effect data used for external beam level 2 (S42): M_y

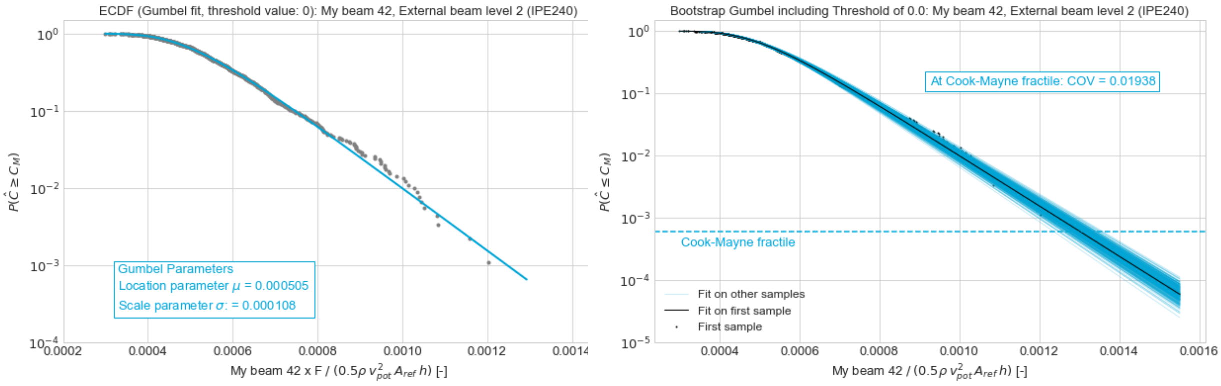

(a) Gumbel fit (threshold value: 0.0) of M_y internal column (S13)

(b) Bootstrap (threshold value: 0.0) of M_y internal column (S13) using 300 bootstrapped distributions

Figure G.2: Gumbel fit and Bootstrap (threshold value: 0.0) of M_y external beam level 2 (S42)

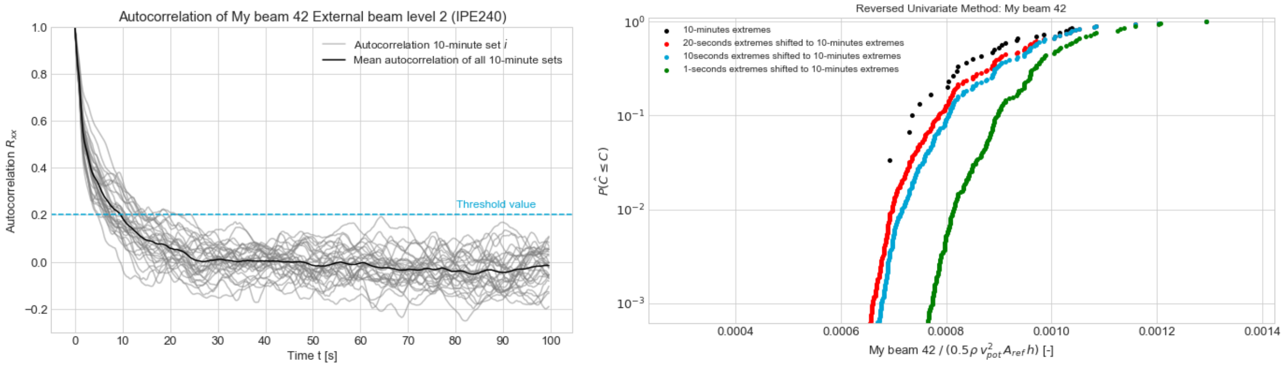

(a) Autocorrelation plot of M_y external beam level 2 (S42)

(b) Reversed univariate method plot of M_y external beam level 2 (S42)

Figure G.3: Autocorrelation and Reversed univariate method plots of M_y external beam level 2 (S42), in order to obtain the correct block duration t

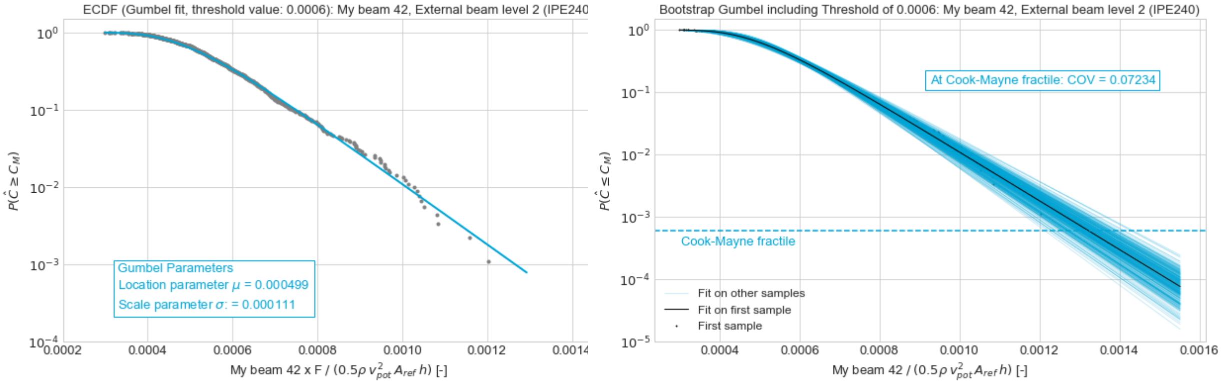

(a) Gumbel fit (threshold value: 0.0006) of M_y external beam level 2 (S42)

(b) Bootstrap (threshold value: 0.0006) of M_y external beam level 2 (S42) using 300 bootstrapped distributions

Figure G.4: Gumbel fit and Bootstrap (threshold value: 0.0006) of M_y external beam level 2 (S42) ($20s$-extremes)

Load effects - Probabilistic wind pressure model

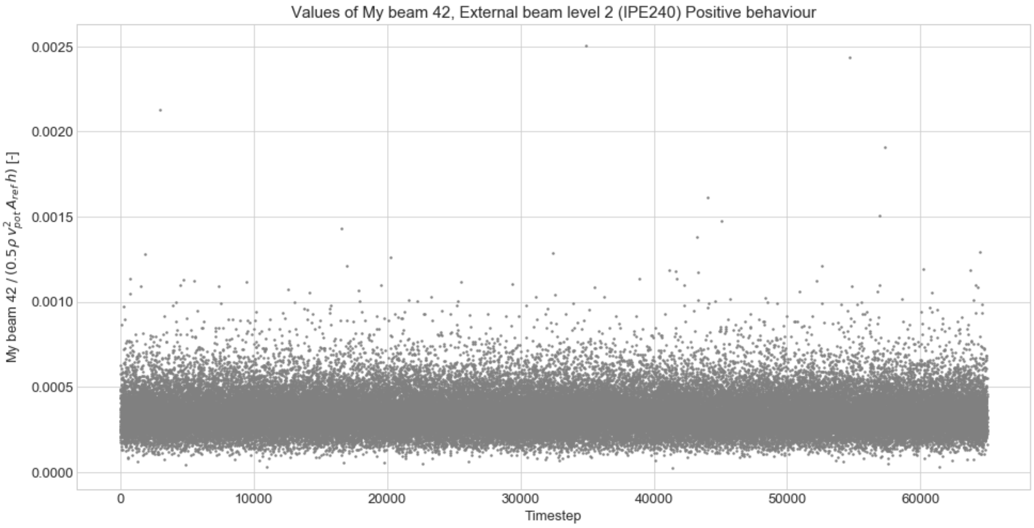

Figure G.5: All the load effect data used for external beam level 2 (S42): M_y (probabilistic wind pressure model)

G.2. External beam level 1 (S18)

G.2.1. $E_{wind,M}$

Load effects - Time series

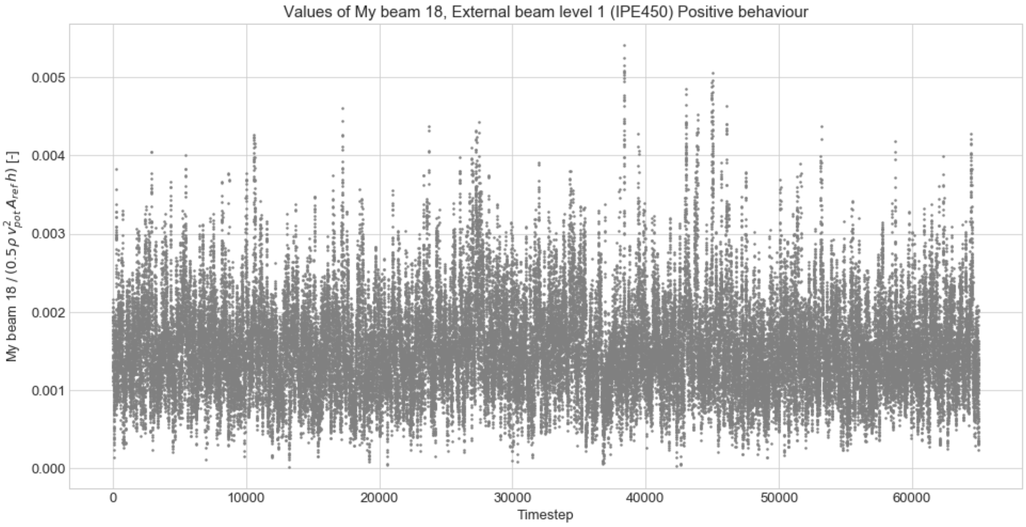

Figure G.6: All the load effect data used for external beam level 1 (S18): M_y

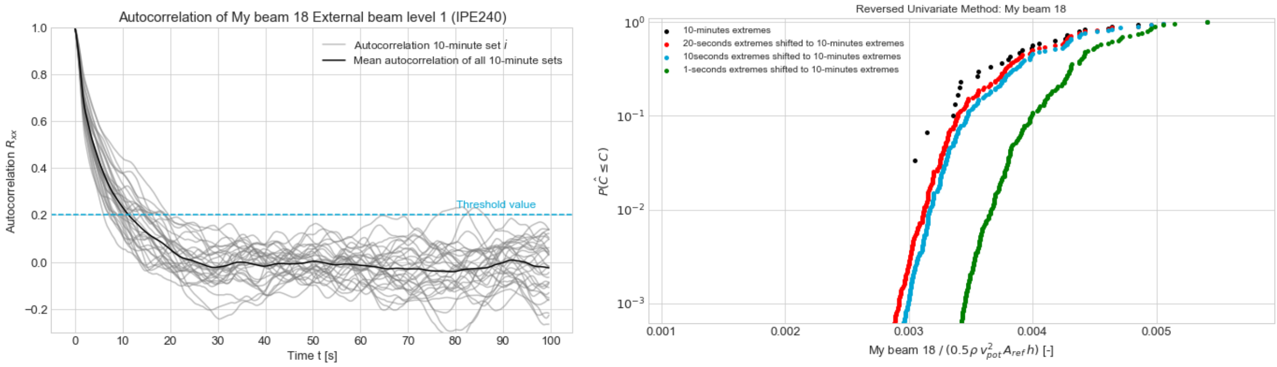

(a) Autocorrelation plot of M_y external beam level 1 (S18)

(b) Reversed univariate method plot of M_y external beam level 1 (S18)

Figure G.7: Autocorrelation and Reversed univariate method plots of M_y external beam level 1 (S18), in order to obtain the correct block duration t

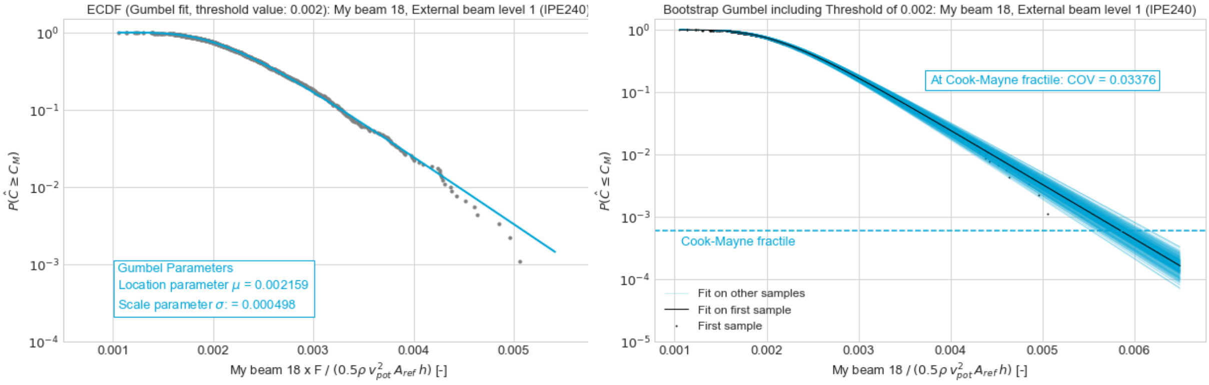

(a) Gumbel fit (threshold value: 0.002) of M_y external beam level 1 (S18)

(b) Bootstrap (threshold value: 0.002) of M_y external beam level 1 (S18) using 300 bootstrapped distributions

Figure G.8: Gumbel fit and Bootstrap (threshold value: 0.002) of M_y external beam level 1 (S18) ($20s$-extremes)

Load effects - Probabilistic wind pressure model

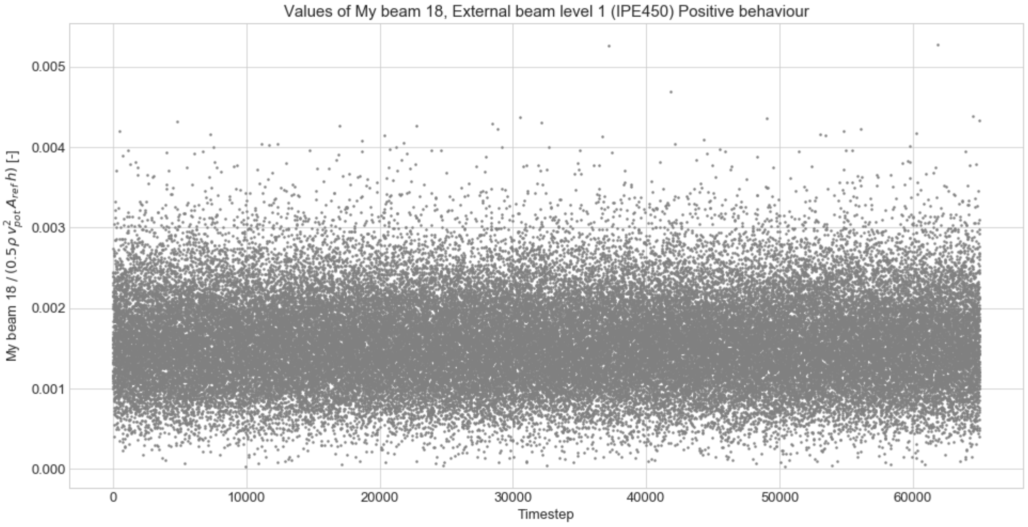

Figure G.9: All the load effect data used for external beam level 1 (S18): M_y (probabilistic wind pressure model)

G.3. Steel bracing (S65)

G.3.1. $E_{wind,N}$

Load effects - Time series

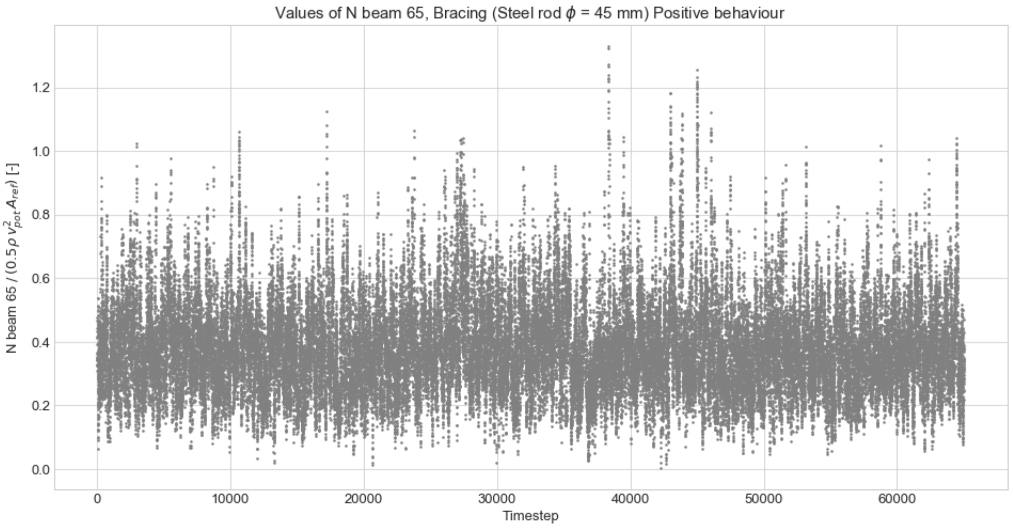

Figure G.10: All the load effect data used for steel bracing (S65): N

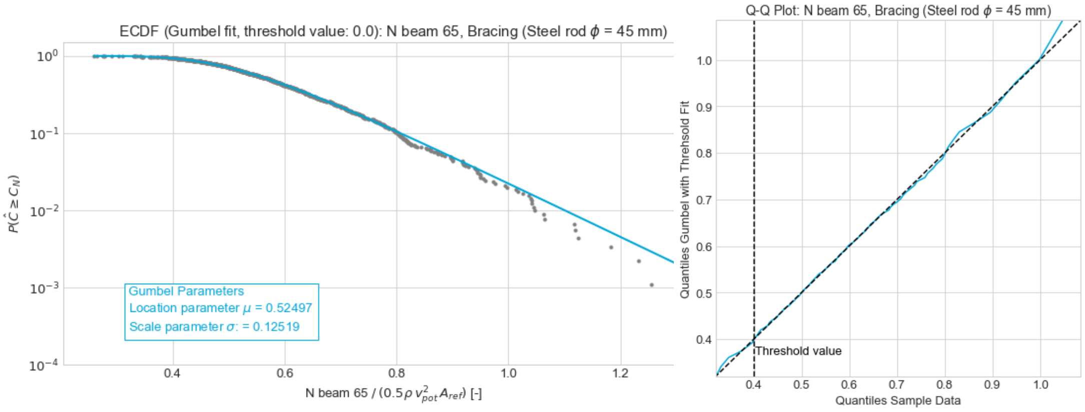

(a) Gumbel fit (threshold value: 0.0) of N steel bracing (S65)

(b) Q-Q Plot (threshold value: 0.4) of N steel bracing (S65)

Figure G.11: Gumbel fit (threshold 0.0) and Q-Q plot (threshold value: 0.4) of N steel bracing (S65), in order to obtain the correct block duration t

Load effects - Probabilistic wind pressure model

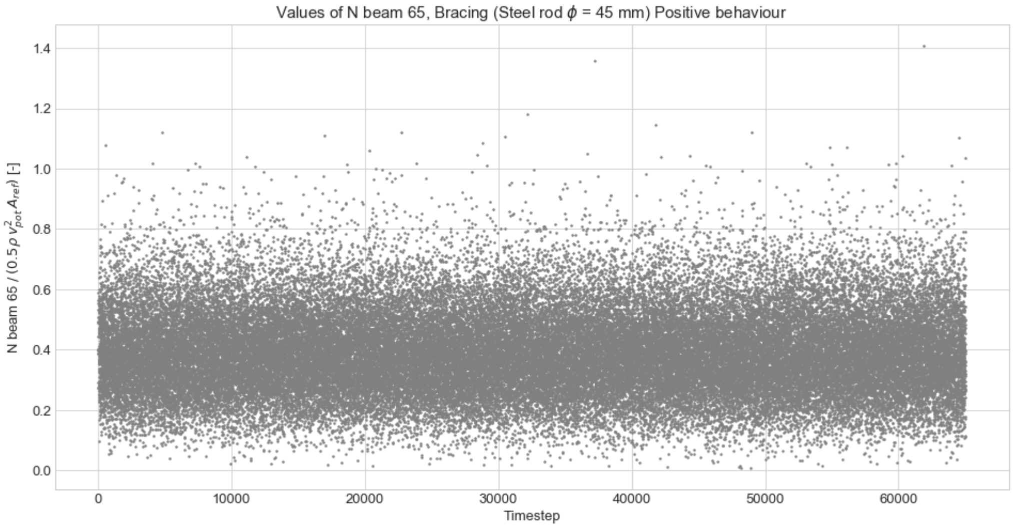

Figure G.12: All the load effect data used for steel bracing (S65): N (probabilistic wind pressure model)

G.4. Internal column (S13)

G.4.1. $E_{wind,N}$

Load effects - Time series

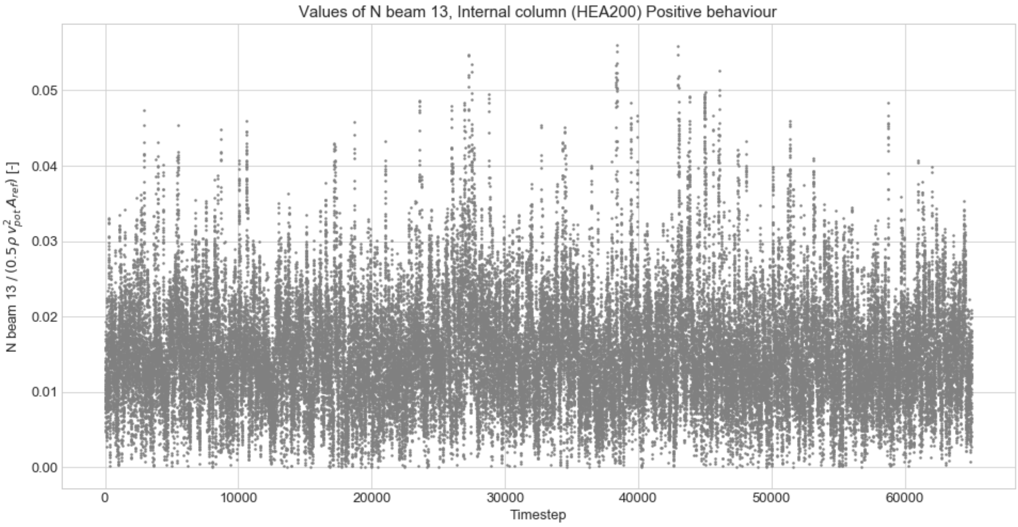

Figure G.13: All the load effect data used for internal column (S13): N

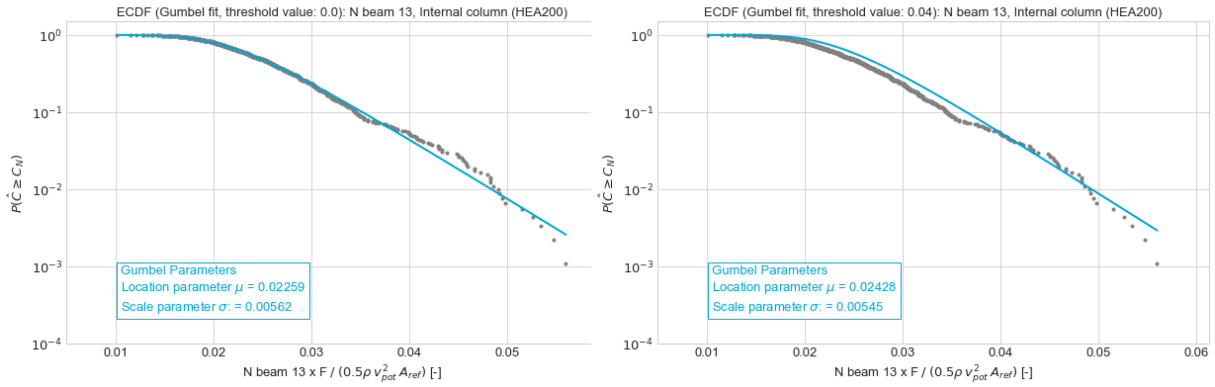

(a) Gumbel fit (threshold value: 0.0) of N internal column (S13)

(b) Gumbel fit (threshold value: 0.04) of N internal column (S13)

Figure G.14: Gumbel fit (threshold 0.0 and 0.04) of N internal column (S13), in order to obtain the correct block duration t

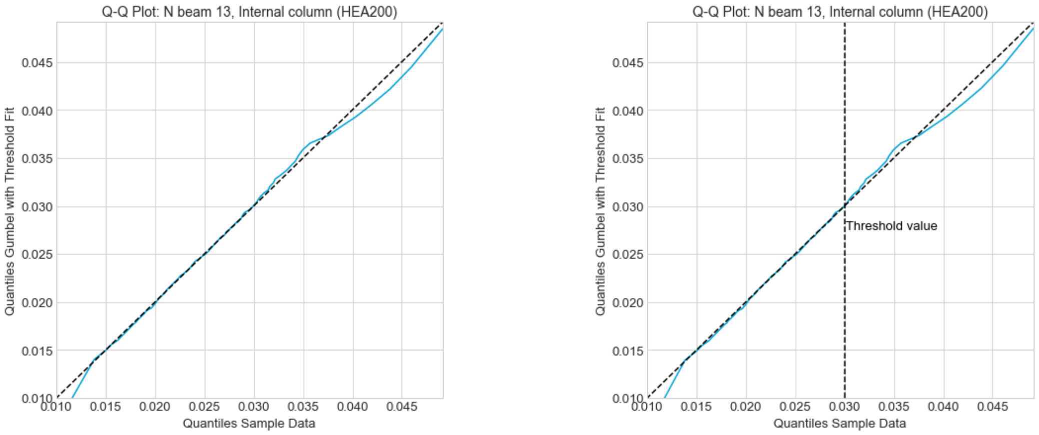

(a) Q-Q Plot (threshold value: 0.0) of N internal column (S13)

(b) Q-Q Plot (threshold value: 0.03) of N internal column (S13)

Figure G.15: Q-Q plot (threshold 0.0 and 0.03) of N internal column (S13)

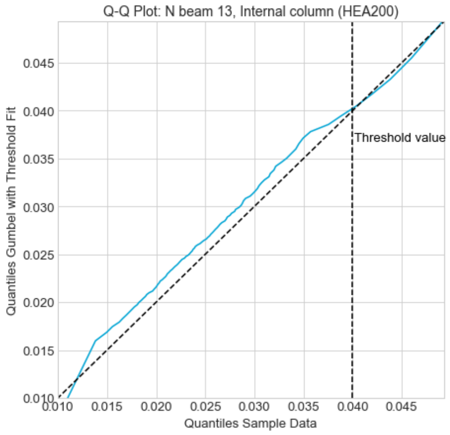

Figure G.16: Q-Q Plot (threshold value: 0.04) of N internal column (S13)

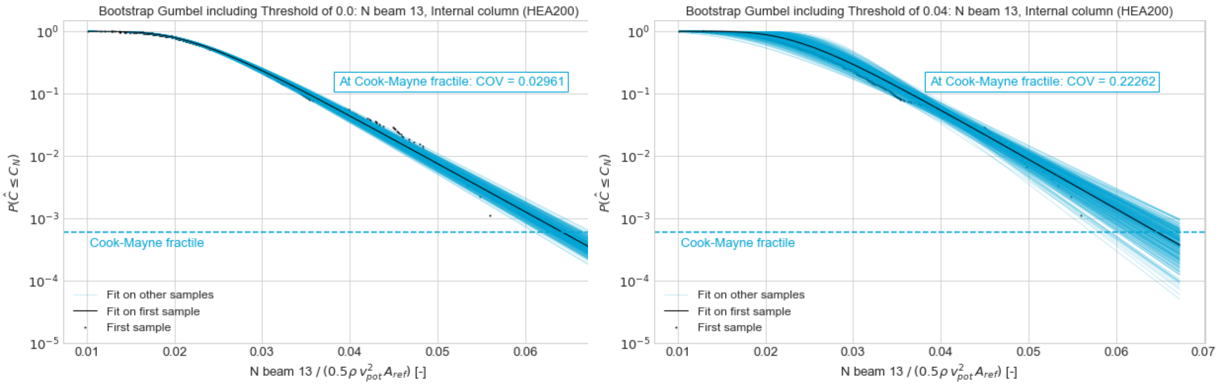

(a) Bootstrap (threshold value: 0.0) of N internal column (S13) using 300 bootstrapped distributions

(b) Bootstrap (threshold value: 0.04) of N internal column (S13) using 300 bootstrapped distributions

Figure G.17: Bootstrap (threshold value: 0.0 and 0.04) of N internal column (S13)

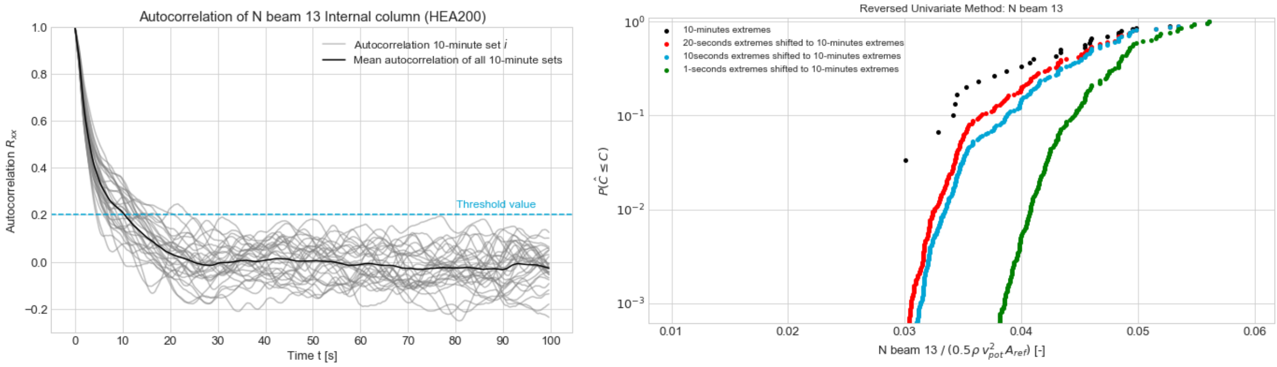

(a) Autocorrelation plot of N internal column (S13)

(b) Reversed univariate method plot of N internal column (S13)

Figure G.18: Autocorrelation and Reversed univariate method plots of N internal column (S13), in order to obtain the correct block duration t

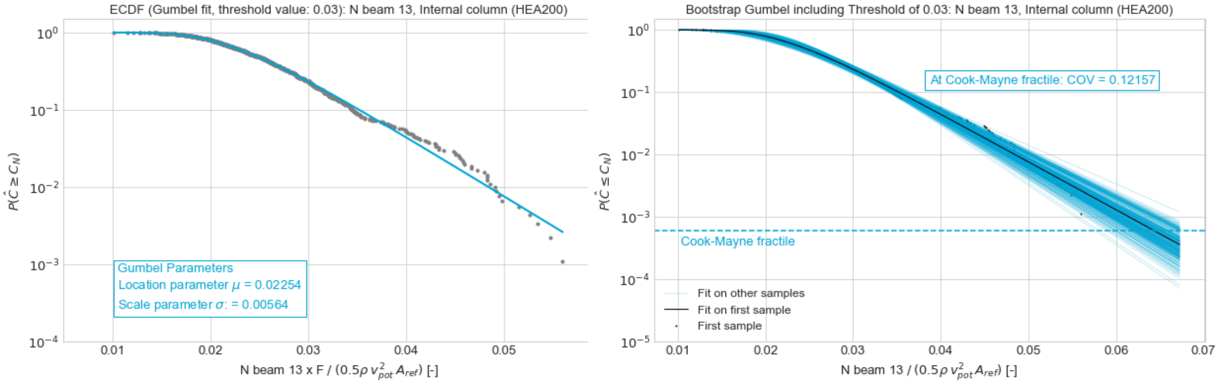

(a) Gumbel fit (threshold value: 0.03) of N internal column (S13)

(b) Bootstrap (threshold value: 0.03) of N internal column (S13) using 300 bootstrapped distributions

Figure G.19: Gumbel fit and Bootstrap (threshold value: 0.03) of N internal column (S13) ($20s$-extremes)

Load effects - Probabilistic wind pressure model

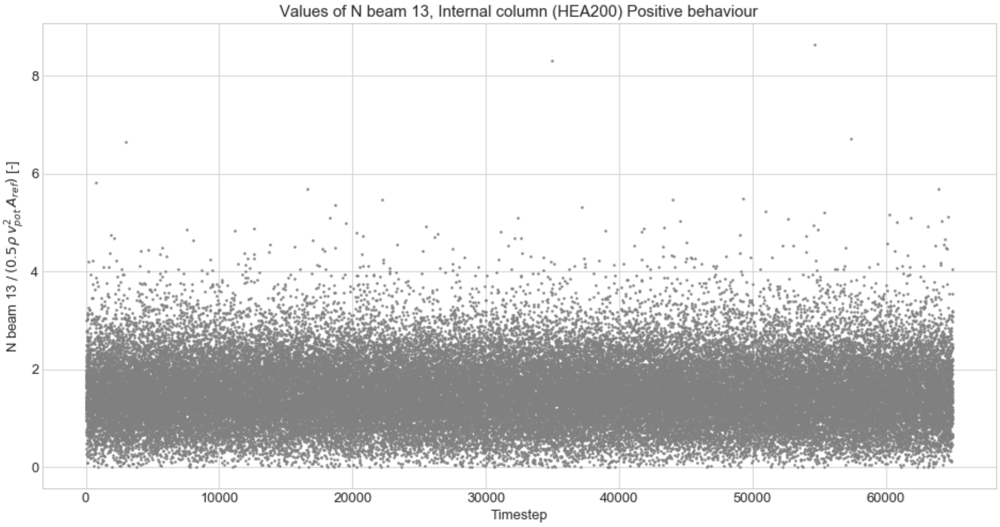

Figure G.20: All the load effect data used for internal column (S13): N $(F = 100)$ (probabilistic wind pressure model)

G.5. External column (S2)

G.5.1. $E_{wind,N}$

Load effects - Time series

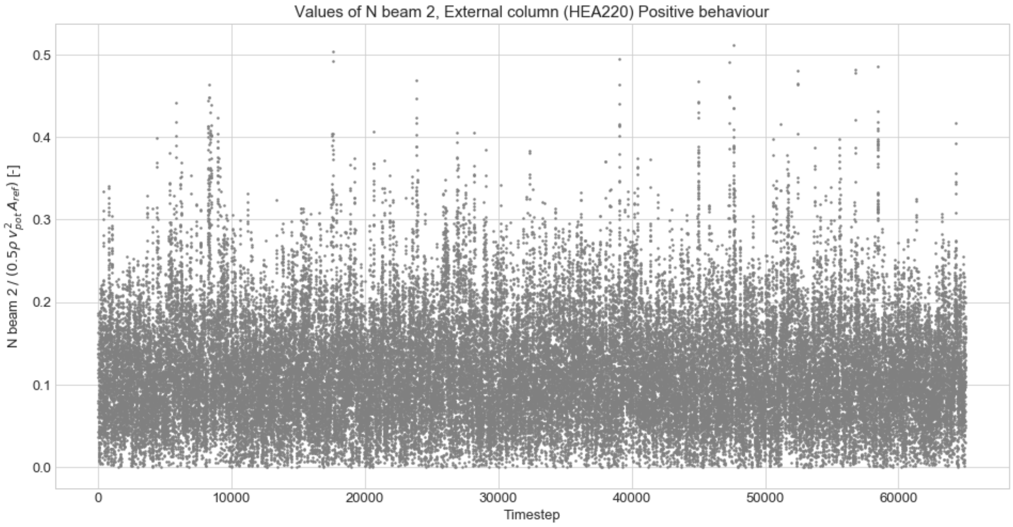

Figure G.21: All the load effect data used for external column (S2): N

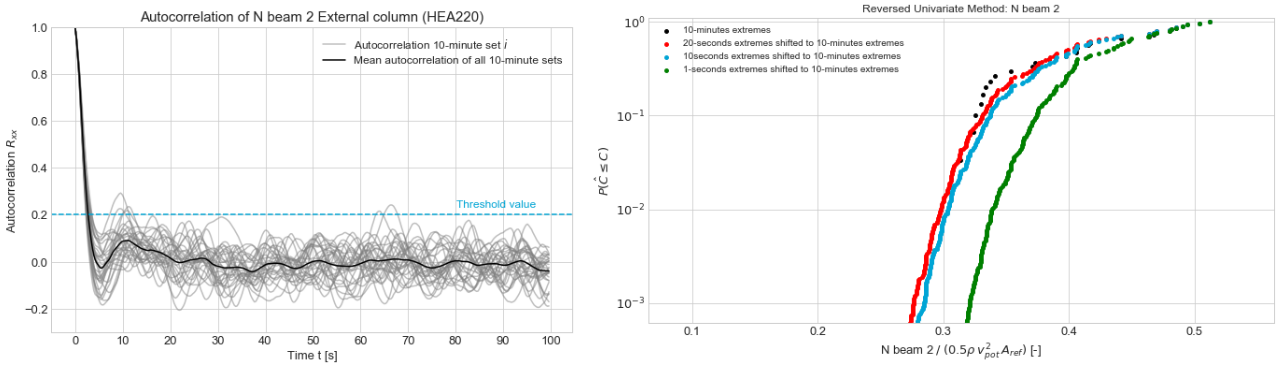

(a) Autocorrelation plot of N external column (S2)

(b) Reversed univariate method plot of N external column (S2)

Figure G.22: Autocorrelation and Reversed univariate method plots of N external column (S2), in order to obtain the correct block duration t

Load effects - Probabilistic wind pressure model

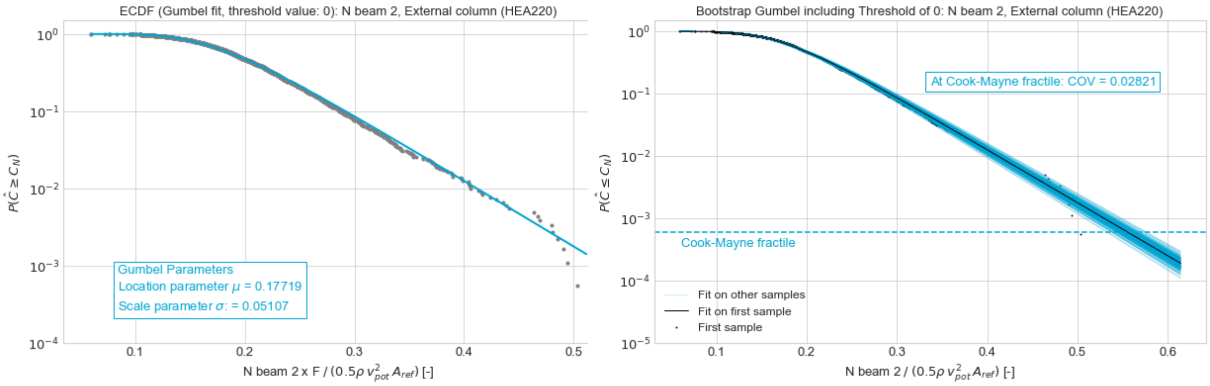

(a) Gumbel fit (threshold value: 0.0) of N external column (S2)

(b) Bootstrap (threshold value: 0.0) of N external column (S2) using 300 bootstrapped distributions

Figure G.23: Gumbel fit and Bootstrap (threshold value: 0.0) of N external column (S2) ($10s$-extremes)

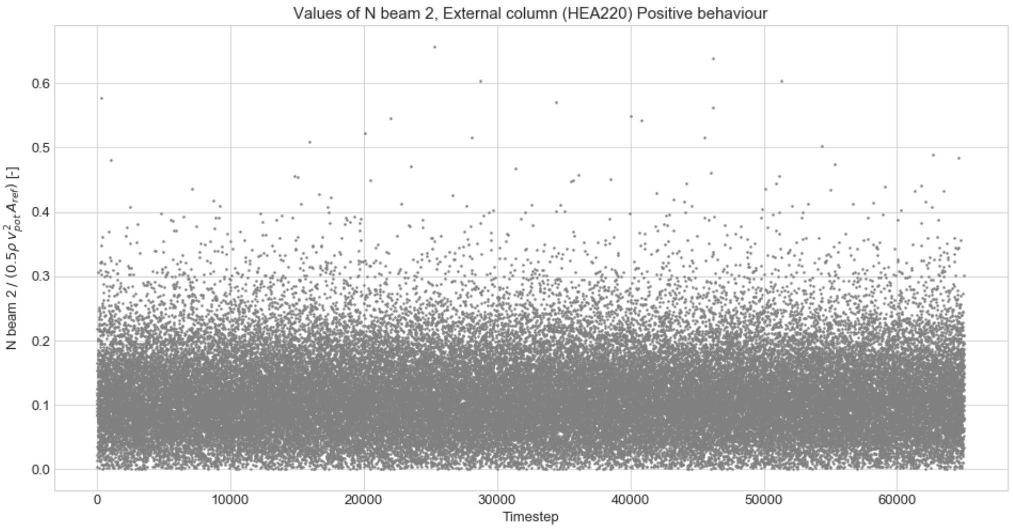

Figure G.24: All the load effect data used for external column (S2): N (probabilistic wind pressure model)

G.5.2. $E_{wind,M}$

Load effects - Time series

Load effects - Probabilistic wind pressure model

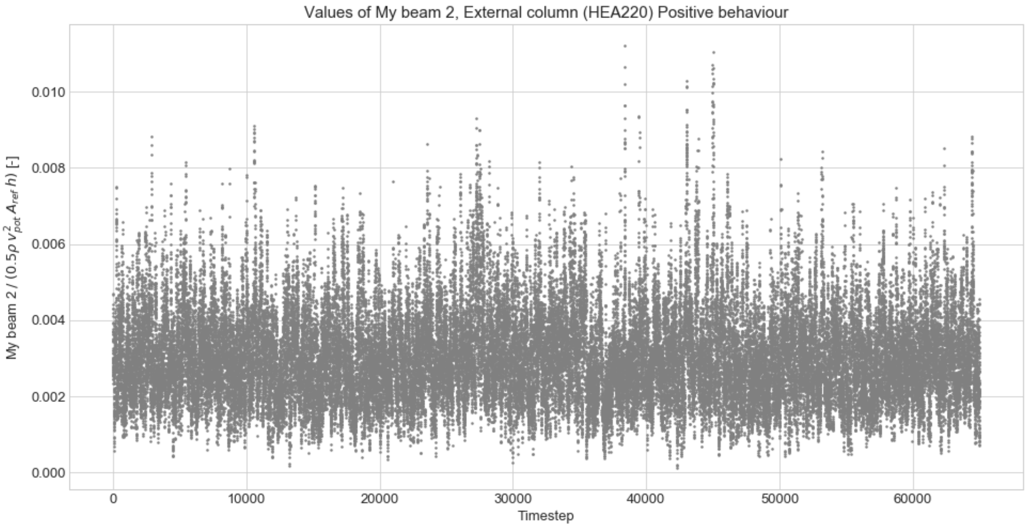

Figure G.25: All the load effect data used for external column (S2): M_y

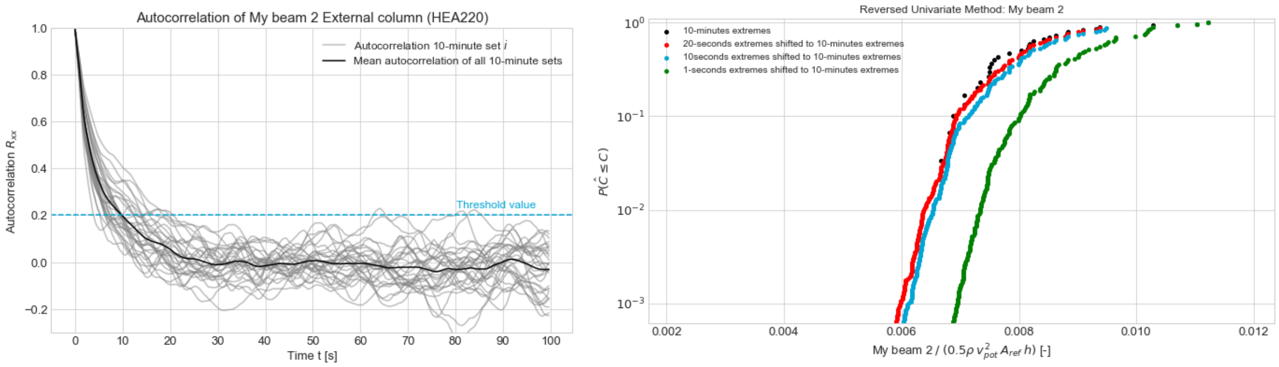

(a) Autocorrelation plot of M_y external column (S2)

(b) Reversed univariate method plot of M_y external column (S2)

Figure G.26: Autocorrelation and Reversed univariate method plots of M_y external column (S2), in order to obtain the correct block duration t

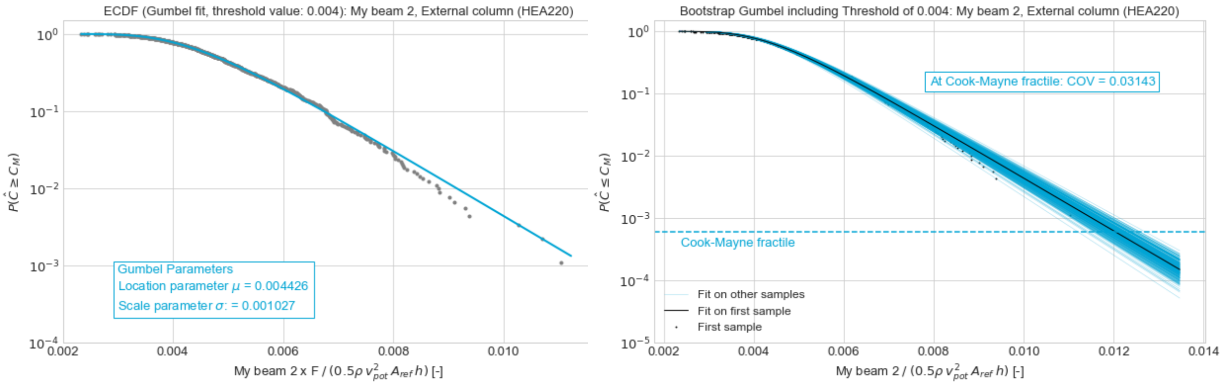

(a) Gumbel fit (threshold value: 0.004) of M_y external column (S2)

(b) Bootstrap (threshold value: 0.004) of M_y external column (S2) using 300 bootstrapped distributions

Figure G.27: Gumbel fit and Bootstrap (threshold value: 0.004) of M_y external column (S2) ($20s$-extremes)

G.6. Corner column (S1)

G.6.1. $E_{wind,N}$

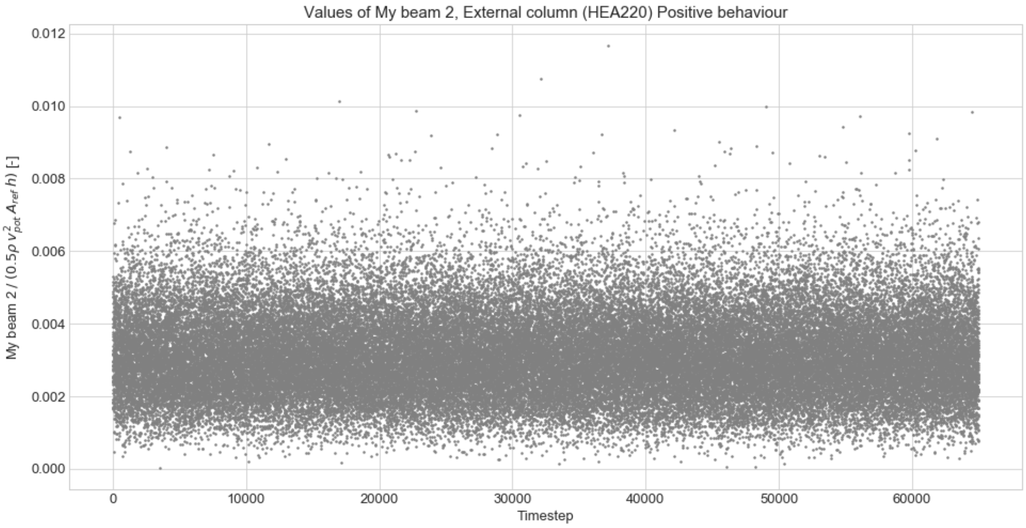

Figure G.28: All the load effect data used for external column (S2): M_y (probabilistic wind pressure model)

Load effects - Time series

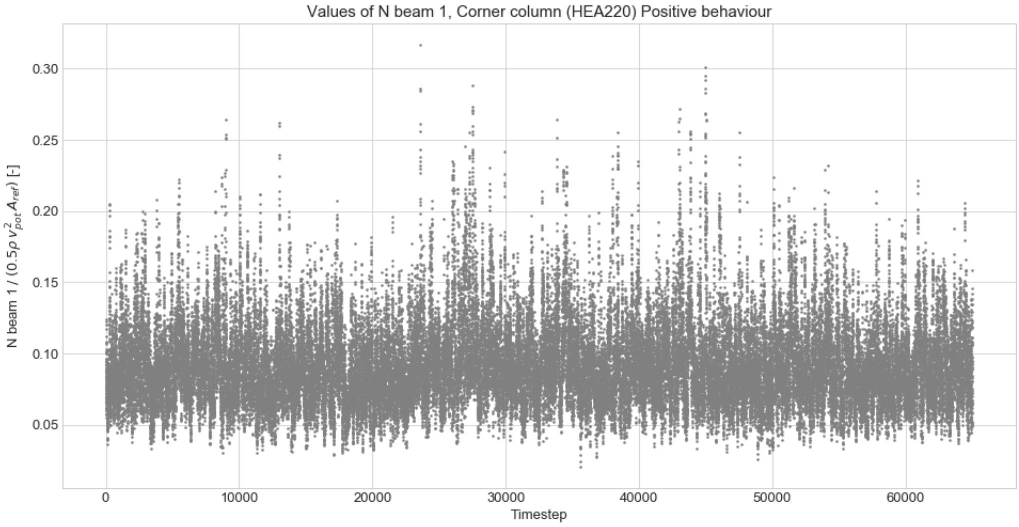

Figure G.29: All the load effect data used for corner column (S1): N

Load effects - Probabilistic wind pressure model

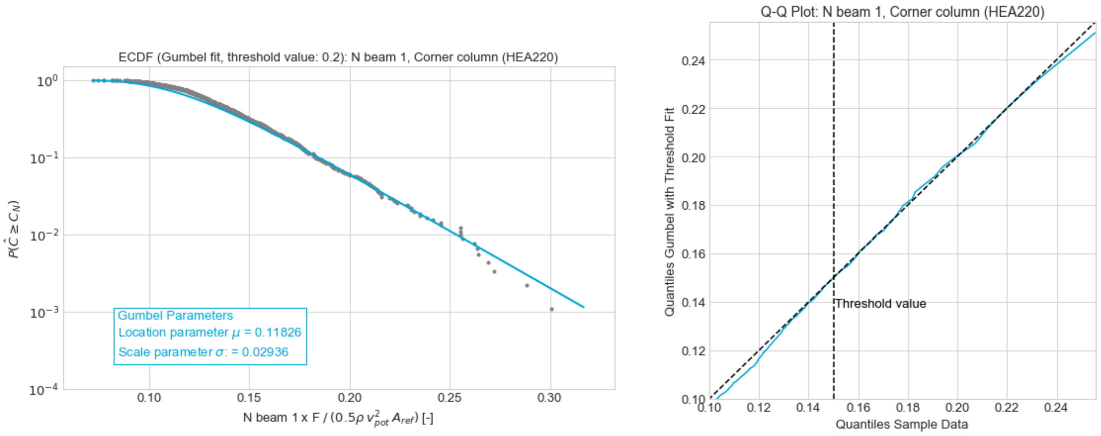

(a) Gumbel fit (threshold value: 0.2) of N corner column (S1)

(b) Q-Q Plot (threshold value: 0.15) of N corner column (S1)

Figure G.30: Gumbel fit (threshold value: 0.2) and Q-Q plot (threshold value: 0.15) of N corner column (S1)

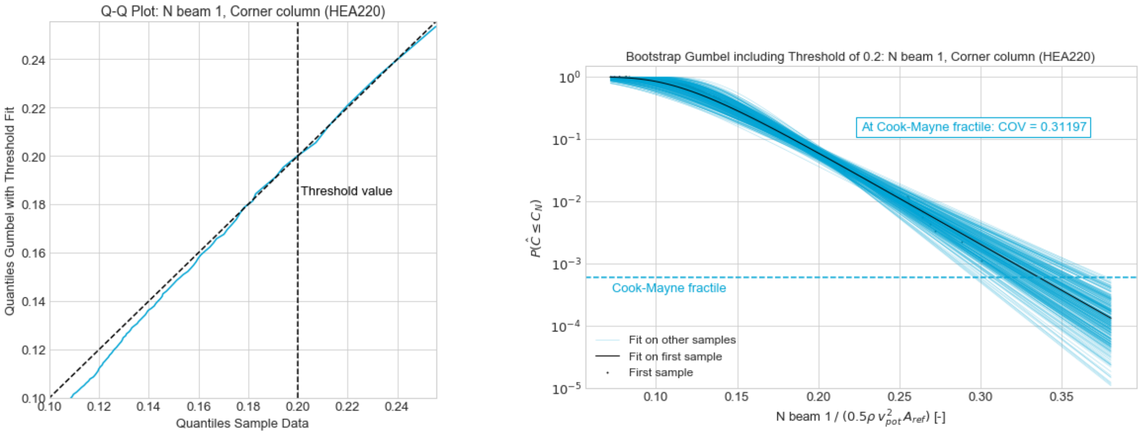

(a) Q-Q Plot (threshold value: 0.2) of N corner column (S1)

(b) Bootstrap (threshold value: 0.2) of N corner column (S1) using 300 bootstrapped distributions

Figure G.31: Q-Q plot and Bootstrap (threshold value: 0.2) of N corner column (S1)

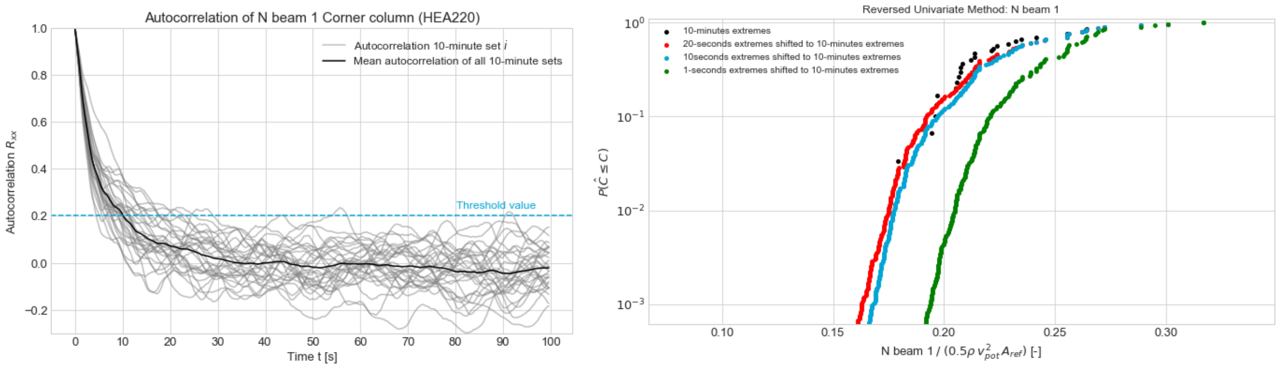

(a) Autocorrelation plot of N corner column (S1)

(b) Reversed univariate method plot of N corner column (S1)

Figure G.32: Autocorrelation and Reversed univariate method plots of N corner column (S1), in order to obtain the correct block duration t

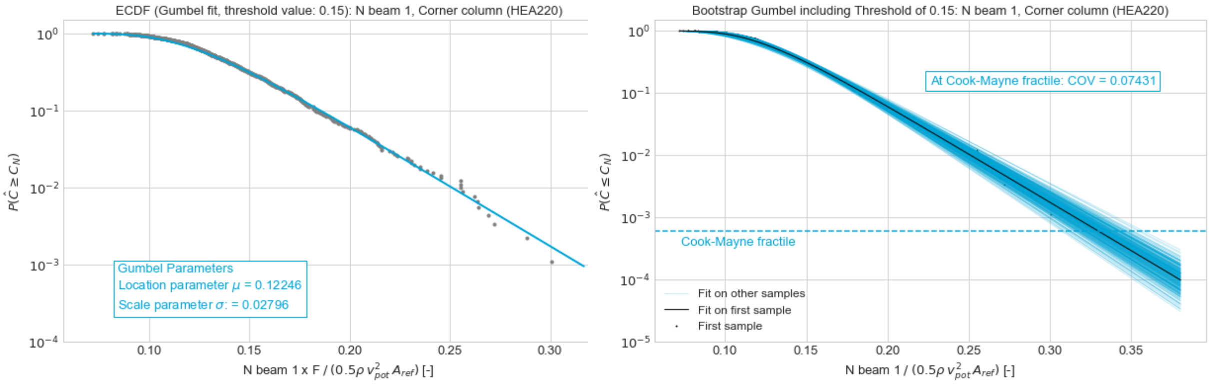

(a) Gumbel fit (threshold value: 0.15) of N corner column (S1)

(b) Bootstrap (threshold value: 0.15) of N corner column (S1) using 300 bootstrapped distributions

Figure G.33: Gumbel fit and Bootstrap (threshold value: 0.15) of N corner column (S1) ($20s$-extremes)

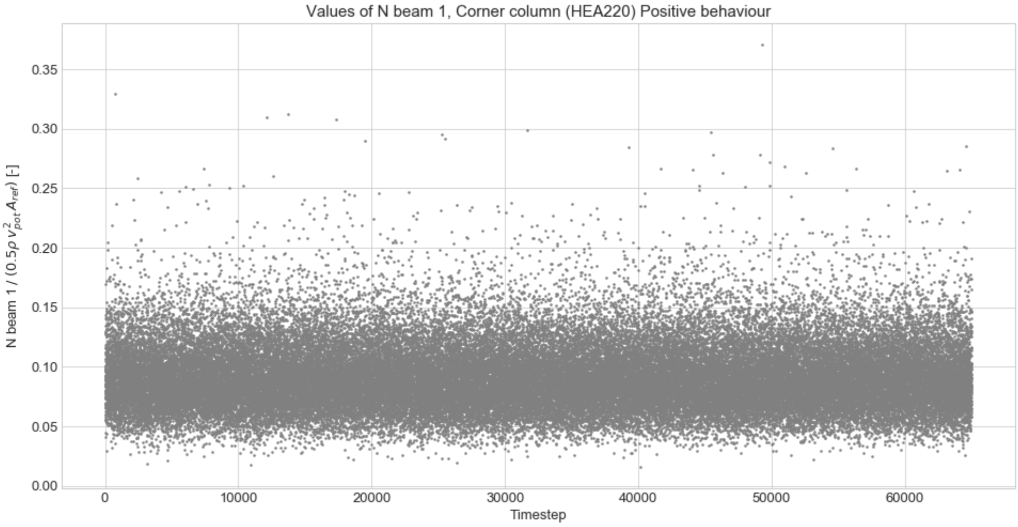

Figure G.34: All the load effect data used for corner column (S1): N (probabilistic wind pressure model)

G.6.2. $E_{wind,My}$

Load effects - Time series

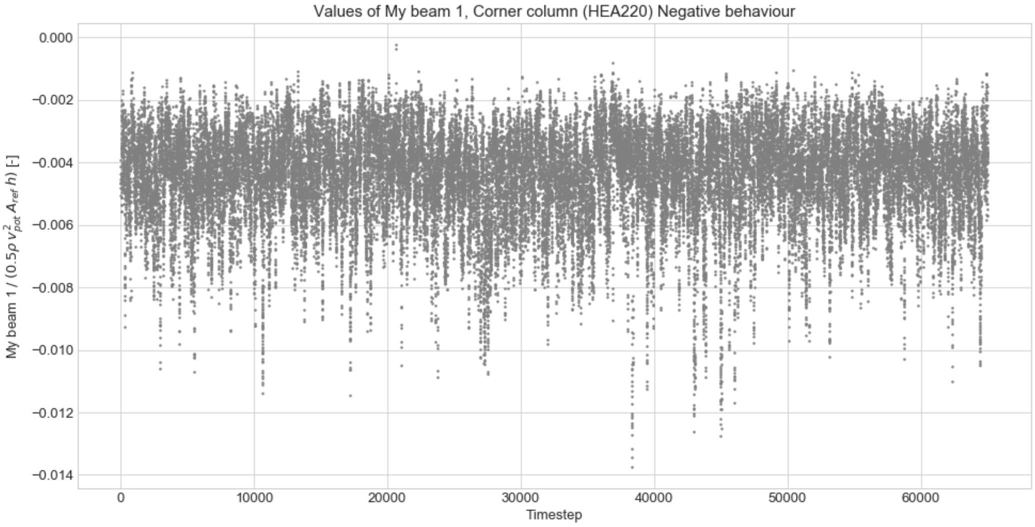

Figure G.35: All the load effect data used for corner column (S1): M_y

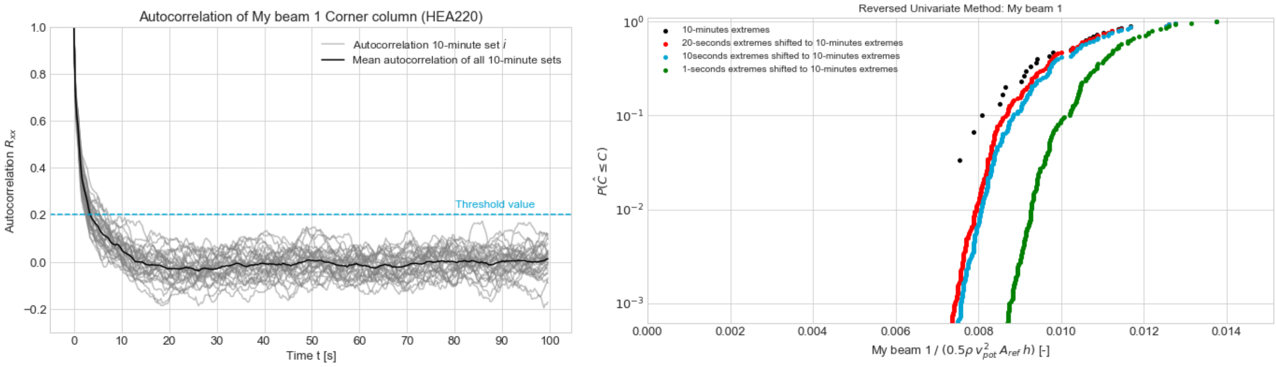

(a) Autocorrelation plot of M_y corner column (S1)

(b) Reversed univariate method plot of M_y corner column (S1)

Figure G.36: Autocorrelation and Reversed univariate method plots of M_y corner column (S1), in order to obtain the correct block duration t

Load effects - Probabilistic wind pressure model

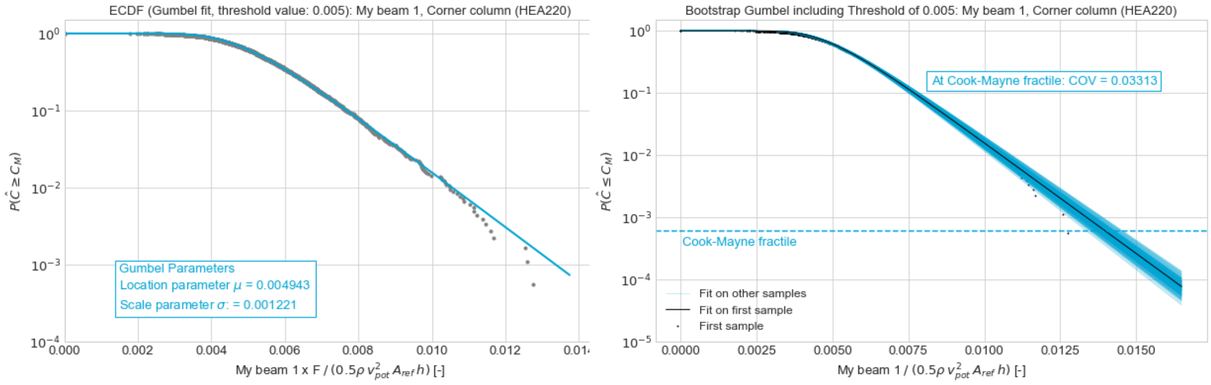

(a) Gumbel fit (threshold value: 0.005) of M_y corner column (S1)

(b) Bootstrap (threshold value: 0.005) of M_y corner column (S1) using 300 bootstrapped distributions

Figure G.37: Gumbel fit and Bootstrap (threshold value: 0.005) of M_y corner column (S1) ($10s$-extremes)

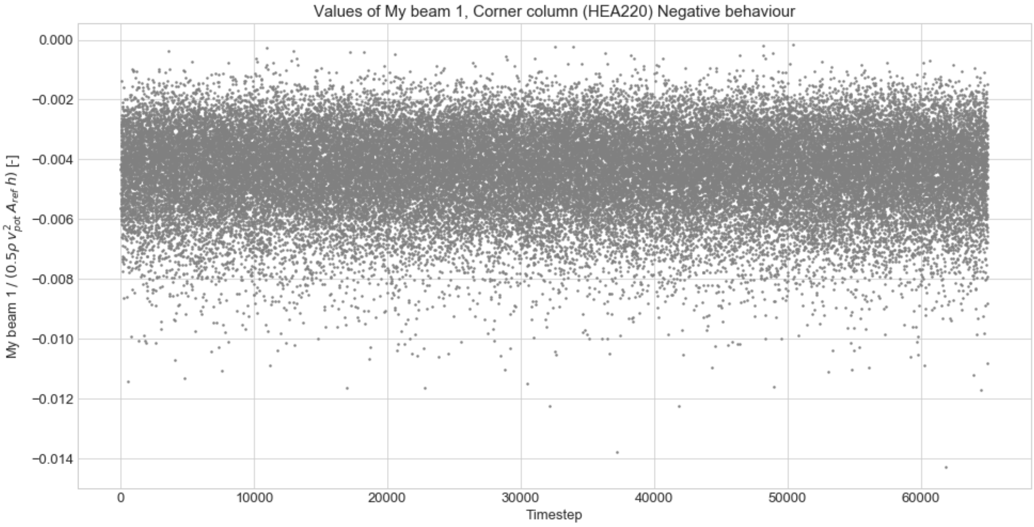

Figure G.38: All the load effect data used for corner column (S1): M_y (probabilistic wind pressure model)

G.6.3. $E_{wind,Mz}$

Load effects - Time series

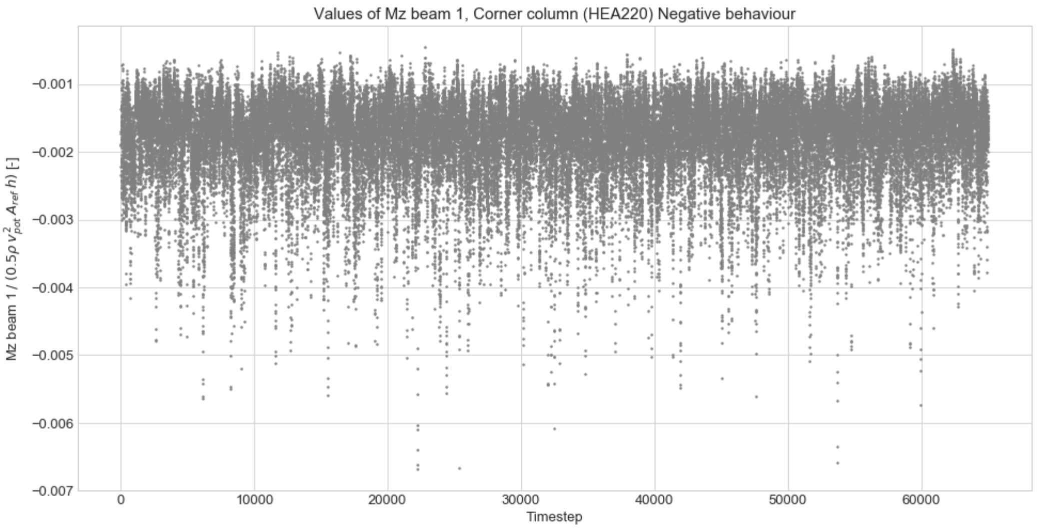

Figure G.39: All the load effect data used for corner column (S1): M_z

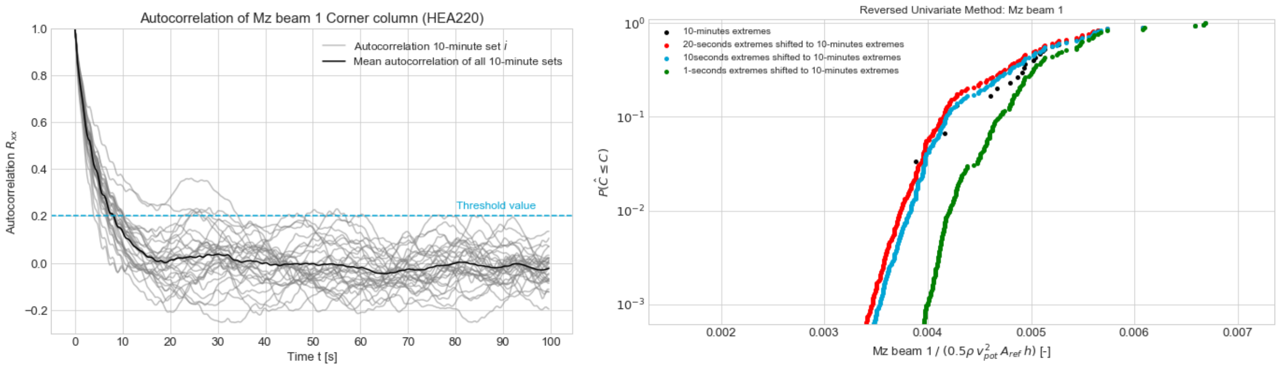

(a) Autocorrelation plot of M_z corner column (S1)

(b) Reversed univariate method plot of M_z corner column (S1)

Figure G.40: Autocorrelation and Reversed univariate method plots of M_z corner column (S1), in order to obtain the correct block duration t

Load effects - Probabilistic wind pressure model

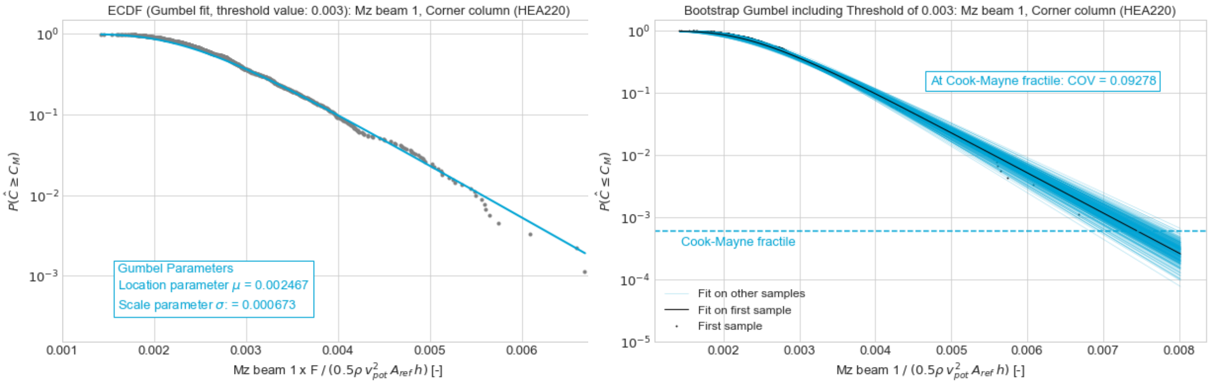

(a) Gumbel fit (threshold value: 0.003) of M_z corner column (S1)

(b) Bootstrap (threshold value: 0.003) of M_z corner column (S1) using 300 bootstrapped distributions

Figure G.41: Gumbel fit and Bootstrap (threshold value: 0.003) of M_z corner column (S1) ($20s$-extremes)

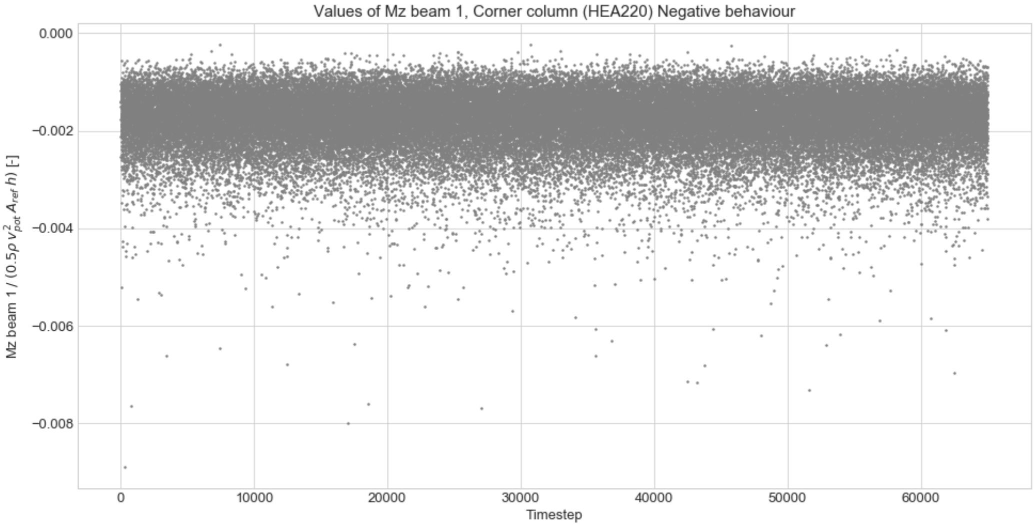

Figure G.42: All the load effect data used for corner column (S1): M_z (probabilistic wind pressure model)

H

Analysis Wind Pressures from Wind Tunnel Test - For Making Probabilistic Wind Pressure Model

A distribution may be considered normal if the absolute value of the skewness is less than 0.5 and the absolute value of the kurtosis is less than 3.5 [22].

Zone	Mean μ	Standard deviation σ	Skewness	Kurtosis	Distribution Type
Zone 1	0.31	0.20	0.53	1.23	Log-Normal
Zone 2	0.46	0.22	0.68	1.50	Log-Normal
Zone 3	0.47	0.22	0.67	1.41	Log-Normal
Zone 4	0.46	0.22	0.65	1.36	Log-Normal
Zone 5	0.46	0.22	0.60	1.23	Log-Normal
Zone 6	0.44	0.22	0.54	1.07	Log-Normal
Zone 7	0.29	0.19	0.35	0.73	Normal
Zone 90	-0.76	0.29	-1.37	3.92	Log-Normal
Zone 91	-0.76	0.30	-1.26	3.11	Log-Normal
Zone 92	-0.80	0.31	-1.19	2.75	Log-Normal
Zone 93	-0.77	0.32	-1.03	2.61	Log-Normal
Zone 94	-0.59	0.31	-0.96	2.43	Log-Normal
Zone 95	-0.49	0.29	-1.04	2.78	Log-Normal
Zone 96	-0.45	0.26	-1.06	2.69	Log-Normal
Zone 39	-0.40	0.20	-1.08	2.90	Log-Normal
Zone 40	-0.39	0.19	-1.09	2.97	Log-Normal
Zone 41	-0.38	0.18	-1.10	3.19	Log-Normal
Zone 42	-0.39	0.18	-1.10	3.00	Log-Normal
Zone 43	-0.37	0.18	-1.10	3.26	Log-Normal
Zone 44	-0.39	0.19	-1.08	3.04	Log-Normal
Zone 45	-0.40	0.20	-1.04	2.75	Log-Normal
Zone 128	-0.42	0.25	-0.95	2.10	Log-Normal
Zone 129	-0.47	0.27	-0.97	2.40	Log-Normal
Zone 130	-0.56	0.29	-0.92	2.12	Log-Normal
Zone 131	-0.76	0.32	-1.02	2.52	Log-Normal
Zone 132	-0.80	0.32	-1.30	3.36	Log-Normal
Zone 133	-0.79	0.32	-1.42	3.95	Log-Normal
Zone 134	-0.76	0.31	-1.48	4.53	Log-Normal
Zone 77	-0.42	0.23	-0.88	2.08	Log-Normal
Zone 78	-0.43	0.24	-0.93	2.23	Log-Normal
Zone 79	-0.49	0.25	-0.88	2.29	Log-Normal
Zone 80	-0.60	0.25	-0.83	2.06	Log-Normal
Zone 81	-0.78	0.31	-1.03	2.54	Log-Normal
Zone 82	-0.80	0.31	-1.20	2.59	Log-Normal
Zone 83	-0.84	0.30	-1.26	2.99	Log-Normal
Zone 84	-0.86	0.32	-1.26	3.26	Log-Normal
Zone 85	-0.84	0.33	-1.80	7.24	Log-Normal
Zone 86	-0.85	0.32	-1.38	3.83	Log-Normal
Zone 166	-0.86	0.34	-1.44	4.04	Log-Normal
Zone 167	-0.88	0.33	-1.30	3.38	Log-Normal
Zone 168	-0.86	0.35	-1.98	8.51	Log-Normal
Zone 169	-0.89	0.31	-1.25	3.09	Log-Normal
Zone 170	-0.78	0.27	-1.16	2.79	Log-Normal
Zone 171	-0.45	0.23	-1.04	2.54	Log-Normal
Zone 172	-0.56	0.25	-0.80	1.92	Log-Normal
Zone 173	-0.44	0.24	-1.01	2.66	Log-Normal
Zone 174	-0.49	0.26	-0.87	2.13	Log-Normal
Zone 175	-0.44	0.25	-0.93	2.33	Log-Normal

Table H.1: Analysis of wind pressures and associated distribution type, based on values of skewness and kurtosis

Reliability Assessment - Additional Input Parameters

Profile	IPE240
$W_{pl,y}$	$366000\ mm^3$
f_y	$355\ N/mm^2$
Weight profile	$30.7\ kg/m$
Permanent roof load	$0.9 kN/m^2$
Bay width	$5m$
G	$(30.7 \cdot 9.81)^{-3} + 0.9 \cdot 5 = 4.8\ kN/m$
Q	$1\ kN/m$

Table I.1: Input for the reliability analyses of External beam level 2 (S42)

Profile	IPE450
$W_{pl,y}$	$1700000\ mm^3$
f_y	$355\ N/mm^2$
Weight profile	$77.6\ kg/m$
Permanent floor load	$3kN/m^2$
Imposed load office (category B)	$2.5kN/m^2$
Bay width	$5m$
G	$(77.6 \cdot 9.81)^{-3} + 3 \cdot 5 = 15.8\ kN/m$
Q	$2.5 \cdot 5 = 12.5\ kN/m$

Table I.2: Input for the reliability analyses of External beam level 1 (S18)

Profile	Steel rod $\phi = 45\ mm$
A	$1590.43\ mm^2$
f_y	$355\ N/mm^2$

Table I.3: Input for the reliability analyses of Steel bracing (S65)

Profile	HEA200
I_y	$3.69 \cdot 10^7\ mm^4$
A	$5383\ mm^2$
f_y	$355\ N/mm^2$
Permanent roof load	$0.9kN/m^2$
Permanent floor load	$3kN/m^2$
Imposed load office (category B)	$2.5kN/m^2$
Bay width	$10 \cdot 10\ m^2$
G_{level_2}	$0.9 \cdot 10^2 + (2 \cdot 10 \cdot 42.2 \cdot 9.81)^{-3} = 98.3\ kN$
G_{level_1}	$3 \cdot 10^2 + (2 \cdot 10 \cdot 122 \cdot 9.81)^{-3} = 323.9\ kN$
G	$98.3 + 323.9 = 422.2\ kN$
Q	$2.5 \cdot 10^2 = 250\ kN$

Table I.4: Input for the reliability analyses of Internal column (S13)

Profile	HEA220
I_y	$5.41 \cdot 10^7\ mm^4$
$W_{pl,y}$	$568000\ mm^3$
A	$6434\ mm^2$
f_y	$355\ N/mm^2$
$u_{moment_{arm}}$	$210/2 + 100 = 205\ mm$
Permanent roof load	$0.9kN/m^2$
Permanent floor load	$3kN/m^2$
Imposed load office (category B)	$2.5kN/m^2$
Bay width	$5 \cdot 10\ m^2$
G_{level_2}	$0.9 \cdot 5 \cdot 10 + (5 \cdot 42.2 \cdot 9.81 + 10 \cdot 30.7 \cdot 9.81)^{-3} = 50.1\ kN$
G_{level_1}	$3 \cdot 5 \cdot 10 + (5 \cdot 122 \cdot 9.81 + 10 \cdot 77.6 \cdot 9.81)^{-3} = 163.6\ kN$
G	$50.1 + 163.6 = 213.7\ kN$
Q	$2.5 \cdot 5 \cdot 10 = 125\ kN$

Table I.5: Input for the reliability analyses of External column (S2)

Profile	HEA220
I_y	$5.41 \cdot 10^7\ mm^4$
$W_{pl,y}$	$568000\ mm^3$
$W_{pl,z}$	$271000\ mm^3$
A	$6434\ mm^2$
f_y	$355\ N/mm^2$
$u_{moment_{arm-yy}}$	$210/2 + 100 = 205\ mm$
$u_{moment_{arm-zz}}$	$220/2 + 100 = 210\ mm$
Permanent roof load	$0.9kN/m^2$
Permanent floor load	$3kN/m^2$
Imposed load office (category B)	$2.5kN/m^2$
Bay width	$5 \cdot 5\ m^2$
G_{level_2}	$0.9 \cdot 5 \cdot 5 + (2 \cdot 5 \cdot 30.7 \cdot 9.81)^{-3} = 25.5\ kN$
G_{level_1}	$3 \cdot 5 \cdot 5 + (2 \cdot 5 \cdot 77.6 \cdot 9.81)^{-3} = 82.6\ kN$
G	$25.5 + 82.6 = 108.1\ kN$
Q	$2.5 \cdot 5 \cdot 5 = 62.5\ kN$

Table I.6: Input for the reliability analyses of Corner column (S1)

J

Resistance to Combination of Bending Moment and Axial Force

In the event that both a bending moment and an axial force are present, the possible effects of these on the bending moment resistance must be considered. In this case the normal force will be absorbed in the middle of the cross-section and the bending moment on the outside of the cross-section (see figure J.1). Based on the magnitude of the normal force, a certain height h_N is used for the normal force capacity. This can have consequences for the moment capacity and could lead to a reduction of it.

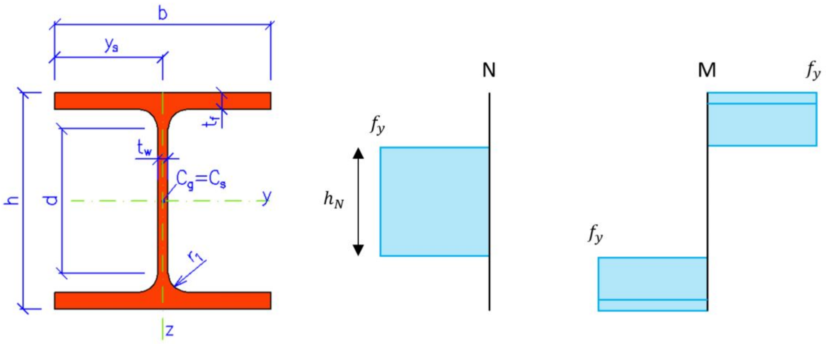

Figure J.1: Visual representation of combined bending moment and axial force on the cross-section

$$N_{Ed} = h_N \cdot t_w \cdot f_y \tag{J.1}$$

$$M_{y,Ed} = 2 \cdot b \cdot t_f \cdot \frac{h - t_f}{2} \cdot f_y + 2 \cdot t_w \cdot \frac{h - 2t_f - h_N}{2} \cdot \left(\frac{h - 2t_f - h - N}{4} + 0.5 \cdot h_N \right) \cdot f_y \tag{J.2}$$

The Eurocode takes this into account in the form of a number of formulas. In the case of class 1 and 2 cross-sections with double symmetrical I and H sections or other flanges sections the following formulas hold. However, first some checks if this reduction of the bending moment about the respectively $y - y$ or $z - z$ axis is needed.

If these criteria hold, no reduction effect of the axial force on the plastic bending moment about the $y - y$ axis:

$$N_{Ed} \leq 0.25 \cdot N_{pl,Rd} \tag{J.3}$$

$$N_{Ed} \leq \frac{0.5 \cdot h_w \cdot tw \cdot fy}{\gamma_{M0}} \tag{J.4}$$

If this criteria hold, no reduction effect of the axial force on the plastic bending moment about the $z-z$ axis:

$$N_{Ed} \leq \frac{h_w \cdot tw \cdot fy}{\gamma_{M0}} \tag{J.5}$$

In the case that a reduction is necessary, it is determined as follows:

$$M_{Ed} \leq M_{N,Rd} \tag{J.6}$$

$$M_{N,y,Rd} = M_{pl,y,Rd} \cdot \frac{1-n}{1-0.5 \cdot a} \leq M_{pl,y,Rd} \tag{J.7}$$

$$M_{N,z,Rd} = M_{pl,z,Rd} \quad (\text{if } n \leq a) \quad or \quad M_{N,z,Rd} = M_{pl,z,Rd} \cdot \left(1-\left(\frac{n-a}{1-a}\right)^2\right) \quad (\text{if } n > a) \tag{J.8}$$

Where:

$$n = \frac{N_{Ed}}{N_{pl,Rd}} \tag{J.9}$$

$$a = \frac{(A - 2 \cdot b \cdot t_f)}{A} \leq 0.5 \tag{J.10}$$